

PUBLICATIONS OF  
THE UNIVERSITY OF EASTERN FINLAND



UNIVERSITY OF  
EASTERN FINLAND

## **Dissertations in Health Sciences**

**SOILE TURUNEN**

# **DISEASE-DISCRIMINATING METHODS: ANALYTICAL AND SENSORY ANALYSIS WITH NON-INVASIVE SAMPLES**



**DISEASE-DISCRIMINATING METHODS:  
ANALYTICAL AND SENSORY ANALYSIS WITH  
NON-INVASIVE SAMPLES**



Soile Turunen

**DISEASE-DISCRIMINATING METHODS:  
ANALYTICAL AND SENSORY ANALYSIS WITH  
NON-INVASIVE SAMPLES**

To be presented by permission of the Faculty of Health Sciences,  
University of Eastern Finland for public examination in MD100  
Auditorium, Kuopio on June 14<sup>th</sup>, 2024, at 12 o'clock noon

Publications of the University of Eastern Finland  
Dissertations in Health Sciences  
No 830

School of Pharmacy, Faculty of Health Sciences  
University of Eastern Finland, Kuopio  
2024

## Series Editors

Research Director Jari Halonen, M.D., Ph.D., M.A. (education)  
Institute of Clinical Medicine, Surgery  
Faculty of Health Sciences

Professor Joonas Sirola, M.D., Ph.D.  
Institute of Clinical Medicine, Surgery  
Faculty of Health Sciences

University Researcher Toni Rikkonen, Ph.D.  
Institute of Clinical Medicine  
Faculty of Health Sciences

Professor Tarja Malm, Ph.D.  
A.I. Virtanen Institute for Molecular Sciences  
Faculty of Health Sciences

Lecturer Veli-Pekka Ranta, Ph.D.  
School of Pharmacy  
Faculty of Health Sciences

Lecturer Tarja Välimäki, Ph.D.  
Department of Nursing Science  
Faculty of Health Sciences

Printing office

Printing place, 2024

Distributor: University of Eastern Finland

Kuopio Campus Library

ISBN: 978-952-61-5227-1 (print)

ISBN: 978-952-61-5228-8 (PDF)

ISSNL: 1798-5706

ISSN: 1798-5706

ISSN: 1798-5714 (PDF)

Author's address: Faculty of Health Sciences, School of Pharmacy  
University of Eastern Finland  
KUOPIO  
FINLAND

Doctoral programme: Doctoral Programme in Drug Research

Supervisors: Professor Seppo Auriola, Ph.D.  
Faculty of Health Sciences, School of Pharmacy  
University of Eastern Finland  
KUOPIO  
FINLAND

Professor Jouko Vepsäläinen, Ph.D.  
Faculty of Health Sciences, School of Pharmacy  
University of Eastern Finland  
KUOPIO  
FINLAND

Docent Olli Kärkkäinen, D.Sc.  
Faculty of Health Sciences, School of Pharmacy  
University of Eastern Finland  
KUOPIO  
FINLAND

Reviewers: Docent Alex Dickens, DPhil  
Department of Chemistry and  
Turku Bioscience Centre  
University of Turku  
TURKU  
FINLAND

Docent Katriina Tiira, Ph.D.  
SmartDOG Oy  
RIIHIMÄKI  
FINLAND

Opponent:

Associate Professor Tiina Sikanen, Ph.D. (Pharm.)  
Faculty of Pharmacy  
University of Helsinki  
HELSINKI  
FINLAND



Turunen, Soile

Disease-discriminating methods: analytical and sensory analysis with non-invasive samples

Kuopio: University of Eastern Finland

Publications of the University of Eastern Finland

Dissertations in Health Sciences 830. 2024, 110 p.

ISBN: 978-952-61-5227-1 (print)

ISSNL: 1798-5706

ISSN: 1798-5706

ISBN: 978-952-61-5228-8 (PDF)

ISSN: 1798-5714 (PDF)

## **ABSTRACT**

Even though blood is the most widely used sample material in clinical diagnostics, the utilization of non-invasive samples, such as saliva and skin swabs, would confer advantages such as noninvasive ease of access and quick turnaround of sampling and testing. The pandemic due to the coronavirus disease which started in 2019 (COVID-19) revealed a major need for establishing rapid screening tests; one crucial aspect that emerged was that sample materials should be easily collected. Many metabolic processes within human cells respond to pathogens as well as exposures to toxic materials. These may result in homeostatic imbalances which change the composition or concentrations of many metabolites. For example, there can be changes in the amounts of small, soluble, or volatile, compounds that are produced, utilized, and discharged by cells and many of them can be detected in different kinds of sample materials, including saliva and skin swabs.

Today, a novel state-of-the-art technology called metabolomics can detect thousands of metabolites in a sample. Metabolomics can utilize high-resolution mass spectrometry-based analytics combined with high-performance separation techniques. Depending on the detection limit of the analytical method, relevant metabolites can be detected and examined,

and in this way, it may be possible to discover new biomarkers as well as obtaining novel, discriminative diagnostic tools for various pathological disorders.

It is well-known that the sense of smell is capable of recognizing and distinguishing volatile, odorous compounds and metabolites. In particular, the sense of smell of trained scent detection dogs is exquisitely sensitive; for example, these dogs currently help the police and customs officials to identify drugs, money, and explosives. In biomedical scent detection, the dogs' ability to recognize low blood sugar levels in diabetics, or different cancers, had been assessed before the emergence of COVID-19.

In this thesis, the suitability of liquid chromatography-mass spectrometry (LC-MS) for detecting human and dog saliva metabolites as well as the discriminative capabilities of a non-targeted metabolomics approach were assessed when the metabolites present in the saliva of Primary Sjögren's syndrome (pSS) patients were compared to those from healthy individuals. In addition, the scent detection threshold of dogs was tested with *Eucalyptus* hydrolat, and their ability to discriminate between healthy and individuals with COVID-19 based on the odor of skin swab samples was evaluated.

It was found that the non-targeted metabolomics analysis enabled the identification of more than two hundred metabolites that were present in human and dog saliva. When applied to pSS, differences in the metabolic profile of saliva were observed between the patients and healthy controls and individual metabolites were identified that were associated with the disease. The scent detection threshold of trained dogs was found to be very low, as the dogs recognized the smell of *Eucalyptus* even at a ratio of 1:10<sup>21</sup>. In addition, the dogs detected the COVID-19 infection with high accuracy in a validation study as well as in a real-life screening in the Helsinki-Vantaa airport.

In conclusion, this thesis shows that a high-resolution LC-MS method can analyze saliva metabolites and detect disease-related changes. Trained dogs are superb scent detectors, surpassing even advanced analytical techniques in their sensitivity and specificity. In the future, it is predicted that scent detection dogs may be utilized in screening against pathogens

as they offer many advantages, such as quick training and global availability. Non-invasive samples, like saliva and skin swabs, could be used to study and develop discriminative methods for diseases.

**Keywords:** saliva, odor, mass spectrometry, metabolomics, volatile organic compound, biomarker, scent detection dog, Sjögren's syndrome, COVID-19



Turunen, Soile

Sairauksia erottelevat menetelmät: analyttinen ja aistinvarainen analyysi sylki- ja ihopyyhintänäytteistä

Kuopio: Itä-Suomen yliopisto

Publications of the University of Eastern Finland

Dissertations in Health Sciences 830. 2024, 110 s.

ISBN: 978-952-61-5227-1(nid.)

ISSNL: 1798-5706

ISSN: 1798-5706

ISBN: 978-952-61-5228-8 (PDF)

ISSN: 1798-5714 (PDF)

## **TIIVISTELMÄ**

Kliinisen diagnostiikan käytetyin näytemateriaali on veri, mutta kajoamattoman näytteenottomenetelmänsä vuoksi esimerkiksi sylki- ja ihopyyhintänäytteiden kerääminen ja käyttäminen analytiikassa voisi olla helpompaa ja nopeampaa kuin verinäytteiden. Vuonna 2019 alkanut koronavirustaudin (COVID-19) aiheuttama pandemia toi esiin tarpeen kehittää nopeita seulontatestejä, joilla analysoitaisiin muitakin kuin nenänielu- ja verinäytteitä. Ihmisen solujen aineenvaihdunta reagoi taudinaiheuttajiin ja muihin haitallisiin tekijöihin, joka voi johtaa elimistön sisäisen tasapainon järkkymiseen. Tämä puolestaan voi muuttaa aineenvaihduntatuotteiden koostumusta tai pitoisuutta, kun solut tuottavat, käyttävät ja poistavat niitä poikkeavasti.

Aineenvaihduntatuotteet ovat pieniä, liukoisia tai haihtuvia yhdisteitä, joita voidaan havaita ja mitata erilaisista näytemateriaaleista mukaan lukien sylki- ja ihopyyhintänäytteet.

Aineenvaihduntatuotteiden mittauksessa voidaan yhdestä näytteestä havaita jopa tuhansia aineenvaihduntatuotteita nykyaikaisen huipputeknologian, metabolomiikan, menetelmillä. Näissä käytetään esimerkiksi korkean erottelukyvyn massaspektrometriaan perustuvaa analytiikkaa yhdistettynä korkean suorituskyvyn erotustekniikoihin, joka

mahdollistaa hyvin matalat havaitsemisrajat. Metabolomiikan avulla aineenvaihduntatuotteista voidaan tunnistaa sairauksille oleellisia yhdisteitä, mahdollisia uusia biomerkkiaineita ja näin edesauttaa kehittämään erottelevia, diagnostisia työkaluja erilaisiin sairauksiin.

Myös hajuaistin avulla pystytään havaitsemaan, tunnistamaan ja erottamaan haihtuvia kemiallisia yhdisteitä ja aineenvaihduntatuotteita. Erityisesti koulutettujen hajukoirien hajuaisti on hyvin herkkä, jonka vuoksi esimerkiksi poliisi ja tulliviranomaiset hyödyntävät niitä muun muassa huumeita, rahaa ja räjähteitä etsittäessä. Biolääketieteellisessä käytössä hajukoirien havaitsemiskykyä on arvioitu aiemmin muun muassa diabeetikon matalan verensokeritason ja erilaisten syöpien yhteydessä ennen COVID-19:n ilmaantumista.

Tässä väitöskirjatyössä arvioitiin nestekromatografia-massaspektrometrian (LC-MS) soveltuvuutta ihmisen ja koiran syljen aineenvaihduntatuotteiden havaitsemiseen sekä kohdentamattoman metabolomiikka-analyysin erottelukykyä, kun sylkinäytteitä verrattiin primaarista Sjögrenin oireyhtymää (pSS) sairastavien henkilöiden ja terveiden välillä. Lisäksi testattiin koulutettujen koirien hajuntunnistusherkkyyttä ja arvioitiin niiden kykyä erotella COVID-19 sairastuneet terveistä henkilöistä ihopyyhintänäytteiden perusteella.

Tutkimuksissa osoitettiin, että kohdentamaton metabolomiikka-analyysi mahdollisti yli kahdensadan aineenvaihduntatuotteen tunnistamisen ihmisen ja koiran syljestä. Syljen aineenvaihduntatuotteissa havaittiin eroja pSS potilaiden ja terveiden kontrollien välillä, ja tunnistettiin yksittäisiä yhdisteitä, jotka olivat yhteydessä tähän autoimmuunisairauteen. Väitöskirjan tulokset osoittavat myös, että koulutettujen koirien hajuntunnistusherkkyyks on erittäin korkea, sillä koirat tunnistivat eukalyptuksen tuoksun jopa laimennossuhteessa 1:10<sup>21</sup>. Koronakoirat havaitsivat COVID-19-tartunnan suurella tarkkuudella ihopyyhintänäytteistä niin validointitutkimuksessa kuin lentomatrustajien seulonnassa Helsinki-Vantaan lentoasemalla.

Yhteenvedona väitöskirjatyö osoittaa, että korkean erottelukyvyn LC-MS-menetelmällä voidaan analysoida syljen aineenvaihduntatuotteita ja havaita niissä sairauteen liittyviä muutoksia. Koirat ovat erinomaisia

ilmaisemaan niille opetettuja kohdehajuja, ja koirat päihittävät herkkyydessään ja tarkkuudessaan jopa edistyneet analyttiset tekniikat. Tulevaisuudessa hajukoiria voitaisiin hyödyntää maailmanlaajuisesti muidenkin infektiosairauksien kuin COVID-19 seulonnassa. Niin ikään kajoamattomia näytemateriaaleja, kuten sylki- ja ihopyyhintänäytteitä, voitaisiin käyttää sairauksia erottelevien menetelmien tutkimiseen ja kehittämiseen.

**Avainsanat:** sylki, haju, haihtuva orgaaninen yhdiste, biomerkkiaine, massaspektrometria, metabolomiikka, hajukoira, Sjögrenin syndrooma, COVID-19





## ACKNOWLEDGEMENTS

This thesis was carried out in the School of Pharmacy, Department of Health Sciences, University of Eastern Finland during 2018-2024. These studies were financially supported by Principal Jukka Mönkkönen's birthday gift fund, Trust of Matti ja Vappu Maukonen, Svenska Kulturfonden (138527), and Doctoral School of University of Eastern Finland. The LC-MS Metabolomics Center of the Biocentre Kuopio is acknowledged for the LC-MS resources used in the studies.

I would like to first thank my main supervisor Professor Seppo Auriola for taking care of the formalities of my studies. I am thankful to my co-supervisor Professor Jouko Vepsäläinen for introducing and choosing me to join the scent detection dog project. I owe my deepest gratitude to my second co-supervisor Docent Olli Kärkkäinen. You guided me through the maze of metabolomics already since I started the data-analysis for my master's thesis. All these years, you have given me the guidance and support whenever I needed it in my work, and you were encouraging and understanding during the time I felt blue. I would like to thank all my supervisors for being so flexible and supporting me in my choices and in my different life situations during these years. All these experiences brought me here, where and who I am now.

I warmly thank reviewers Docent Alex Dickens and Docent Katriiina Tiira for taking the time to read and evaluate my thesis and suggesting improving points. I am honored that Associate Professor Tiina Sikanen has agreed to act as an opponent in the public defense. I also thank Ewen MacDonald for reviewing the language of the thesis.

I would like to thank all my collaborators and co-authors who were working in these multidisciplinary projects. I want to express my deepest gratitude to Susanna Paavilainen, the owner and handler of the famous sniffer dog, Kössi. From day one when we started working with cancer sniffer dogs, there was a special bond between us. Working together has been easy and joyful and we have learned a lot from each other. You have supported me through the ups and downs during these years for which I

sincerely thank you from the bottom of my heart. Special thanks to Docent Anna Hielm-Björkman and Professor Anu Kantele from University of Helsinki for providing the opportunity to include scent detection dogs into my research expertise. I also warmly thank Professor Kati Hanhineva from the University of Turku for guidance in my early steps in the world of metabolomics. I have been honored to work for Afekta Technologies Ltd. since its early days. Professor Hannes Lohi and Dr. Jenni Puurunen from the University of Helsinki are thanked for novel insights in dog metabolomics as well as Professor Arja Kullaa and DDS Maria Herrala for providing me with an opportunity to participate to metabolomics research in a field of dentistry.

I am so thankful to my colleagues Miia Reponen, Maija Lahtela-Kakkonen and Topi Meuronen. Miia for teaching me the basics and tips of the lab work and hands-on mass spectrometry skills related to metabolomics as well as being “my person”. Maija for being my mentor. You have given me ideas, inspiration, support, comfort, and shared my joys and sorrows in those numerous hours in the car on the way to work and home. Topi for being there for me through all the emotions. Your character and sense of humor are what I have needed during this project. I highly appreciate your skills and knowledge and thank you for finding both the time and the patience for my problems, questions, and several topics of discussion during this journey. I am also thankful to my co-workers on the 3rd floor of Mediteknia at the School of Pharmacy and colleagues in Afekta Technologies Ltd.

I want to thank my friends, all three named Sanna. Sanna Willman for her interest towards my doctoral studies and thesis as well as for all the discussions over the phone. My best friends, the superwomen in my life, Sanna Nevalainen and Sanna Karvonen, for being there for me and providing other content to my life including nights in a hot tub, and dancing for hours.

I owe thanks to my mom Ritva and her husband Jorma for all their support during my studies. I also thank my 90-year-old grandparents Eila and Arvi for checking on me and asking how the thesis is progressing as well as my godmother Eija of sharing the feeling of the pain of a busy life. I

especially want to thank my children, Kaius, Venla and Tiitus. You are the lights of my life and the best I have ever created. I love you to the moon and back. Finally, I would like to thank my husband and soulmate Arto for all the support and love during these years. Thank you for being by my side and sharing our everyday life. There is nothing more important in life than family.

Outokumpu, 21 April 2024  
Soile Turunen



# LIST OF ORIGINAL PUBLICATIONS

This dissertation is based on the following original publications:

- I Turunen S, Puurunen J, Auriola S, Kullaa AM, Kärkkäinen O, Lohi H, Hanhineva K. Metabolome of canine and human saliva: a non-targeted metabolomics study. *Metabolomics* 16: 90, 2020.
- II Herrala M\*, Turunen S\*, Hanhineva K, Lehtonen M, Mikkonen JJW, Seitsalo H, Lappalainen R, Tjäderhane L, Niemelä RK, Salo T, Myllymaa S, Kullaa AM, Kärkkäinen O. Low-dose doxycycline treatment normalizes levels of some salivary metabolites associated with oral microbiota in patients with primary Sjögren's syndrome. *Metabolites* 11: 595, 2021.
- III Turunen S, Paavilainen S, Vepsäläinen J, Hielm-Björkman A. Scent detection threshold of trained dogs to *Eucalyptus* hydrolat. *Animals* 14: 1083, 2024.
- IV Kantele A, Paajanen J, Turunen S, Pakkanen SH, Patjas A, Itkonen L, Heiskanen E, Lappalainen M, Desquilbet L, Vapalahti O, Hielm-Björkman A. Scent dogs in detection of COVID-19: triple-blinded randomised trial and operational real-life screening in airport setting. *BMJ Global Health* 7: e008024, 2022.

\*Equal contribution.

The publications were adapted with the permission of the copyright owners.



# CONTENTS

<b>ABSTRACT</b> .....	<b>7</b>
<b>TIIVISTELMÄ</b> .....	<b>11</b>
<b>ACKNOWLEDGEMENTS</b> .....	<b>15</b>
<b>1 INTRODUCTION</b> .....	<b>25</b>
<b>2 REVIEW OF THE LITERATURE</b> .....	<b>29</b>
2.1 Mass spectrometry-based metabolomics.....	29
2.1.1 Fundamentals of mass spectrometry .....	29
2.1.2 Non-targeted mass spectrometry analysis of metabolites .	33
2.1.3 Discovery of disease biomarkers.....	38
2.2 Biomedical scent detection .....	42
2.2.1 The canine olfactory system .....	42
2.2.2 Canine detection of odor molecules .....	44
2.2.3 Disease-related human odor .....	45
<b>3 AIMS OF THE STUDY</b> .....	<b>49</b>
<b>4 SUBJECTS AND METHODS</b> .....	<b>51</b>
4.1 Study designs and participants .....	51
4.1.1 Study I .....	51
4.1.2 Study II .....	52
4.1.3 Study III .....	53
4.1.4 Study IV .....	56
4.2 Methods .....	62
4.2.1 LC-MS based non-targeted metabolomics .....	62
4.2.2 Odor discrimination.....	64
4.2.3 Quantitative H <sup>1</sup> NMR .....	67
4.2.4 Clinical laboratory tests for diagnosis of COVID-19 .....	68
4.2.5 Statistical methods .....	68
<b>5 RESULTS</b> .....	<b>71</b>
5.1 Non-targeted metabolomics of saliva .....	71
5.1.1 Saliva metabolome .....	71

5.1.2 Changes in saliva metabolite levels as disease response ...	72
5.2 Odor indication by scent detection dogs .....	76
5.2.1 Scent detection threshold .....	76
5.2.2 Screening the odor of a disease .....	78
<b>6 DISCUSSION .....</b>	<b>85</b>
<b>7 CONCLUSIONS AND FUTURE PROSPECTS .....</b>	<b>93</b>
<b>APPENDICES.....</b>	<b>111</b>



## ABBREVIATIONS

CI	Confidence interval	OR	Olfactory receptor
CID	Collision-induced dissociation	PC	Phosphatidylcholine
COVID-19	Coronavirus disease 2019	PCA	Principal Component Analysis
Da	Dalton	PLS-DA	Partial least squares-discriminant analysis
DDA	Data-dependent acquisition	pSS	Primary Sjögren's syndrome
DIA	Data-independent acquisition	Q-TOF	Quadrupole time-of-flight
ESI	Electrospray ionization	RP	Reversed-phase
GC	Gas chromatography	RT	Retention time
HILIC	Hydrophilic interaction liquid chromatography	RT-PCR	Reverse transcriptase polymerase chain reaction
LC-MS	Liquid chromatography-mass spectrometry	SARS-CoV-2	Severe acute respiratory syndrome coronavirus 2
LDD	Low dose doxycycline	Se	Sensitivity
m/z	Mass-to-charge ratio	Sp	Specificity
MS	Mass spectrometry	UHPLC	Ultra-high performance liquid chromatography
MS/MS	Tandem mass spectrometry	VNO	Vomer nasal organ
NMR	Nuclear magnetic resonance	VOC	Volatile organic compound



# 1 INTRODUCTION

Already in ancient Greece, Hippocrates recognized the altered body odor related to specific diseases (1). Today, it is known that the body emits volatile metabolites produced during cellular metabolism which can be detected using analytical methods, but also via olfaction i.e., with a sensory method (2-5). Today, physicians often use different kind of laboratory investigations or diagnostic procedures to determine the diagnosis, treat the disease, and monitor the prognosis or treatment response. Most analytical tests provide only non-specific information about the health status of patient. For example, elevations in the amounts of plasma C-reactive protein and alanine aminotransferase are encountered in numerous diseases (6, 7). In clinical practice all around the world, a vast number of different invasive samples are taken by highly trained professionals, e.g., biopsies, punctures, blood samples, and nasopharyngeal swabs. An invasive procedure means that they require an actual penetration of some part of the body, being possibly uncomfortable, even painful in some patients (8-10). Because of this, sampling procedures can be a stressful and anxiety-provoking experience.

Alternatively, different non-invasive sample types like sweat, saliva, and breath represent a means to develop new non-invasive diagnostic methods that can be quick, easy-to-use, and possibly less expensive (11-13). For example, these kind of diagnosis methods based on non-invasive specimens could reduce the number of unnecessary samples taken and costs related to sampling. This would be especially crucial in preventing the spread of viruses in times of pandemics and epidemics, but also in the early detection of diseases since an early diagnosis often improves the patient's prognosis. It has become evident in recent years that the rapid diagnosis of contagious viral infections can prevent the spread of the infection and thus protect human lives, reduce the burden on healthcare and allow society to function with some degree of normality.

Diseases trigger changes in cellular metabolism which are reflected in the secretions that can be sampled in a non-invasive way (14). The small

compounds produced in cellular biochemical processes are called metabolites and the entity of all metabolites in a biological system is called the metabolome (15). These metabolites can be measured and identified using different kinds of analytical methods, e.g., mass spectrometry (MS) or nuclear magnetic resonance (NMR) spectroscopy. These approaches can be applied for distinguishing of metabolic profiles and identifying the specific compounds that are behind the difference seen in the phenotypes. In the upstream analysis, the specific compounds are subsequently identified as potential biomarkers for the disease or biological response. In addition, the metabolic profile of a sample can be used to differentiate between healthy and diseased individuals, as well as to understand, follow-up and predict treatment responses and to monitor disease progression (16-18).

Although, the analytical methods have replaced the nose of Hippocrates in clinical diagnostics, the olfaction properties of dogs' (*Canis lupus familiaris*) have long been utilized for many purposes, e.g., tracking down wounded animals and searching for lost people. It was not until about 40 years ago, when the hypothesis was born that dogs could possibly detect the unique odors emitted by malignant tumors (19). Since then, the ability of dogs to discriminate samples between healthy and diseased individuals has been studied in a variety of diseases (20, 21). The scent discrimination performed by a dog means that the animal is trained to choose a specific scent or scent signature i.e., the target in preference to other smells. The idea of "choice" is learned by the dog as it is rewarded whenever he/she makes the "right choice" between the alternatives. When the target is a scent of disease, the dog's "right choice" discriminates between the samples of healthy and diseased individuals. The dog's indication behavior for the "right choice" is also trained whereas the dog-handler is responsible for the interpretation of the behavior.

In this thesis, two discriminative methods have been used to distinguish healthy and diseased individuals based on non-invasive samples. In a mass spectrometry-based method, human saliva was the target sample material of interest with Primary Sjögren's Syndrome (pSS) being chosen as the study disease. pSS is a chronic autoimmune disease belonging to the

family of rheumatic diseases (22). The characteristic feature of pSS is a chronic inflammation of exocrine glands, such as the salivary and lacrimal glands. While the most common symptoms of the disease are dry eyes and dry mouth, patients may also experience other symptoms such as fatigue and joint pain. Because of the pathological impact on the salivary glands and the production of saliva, it was hypothesized that it would potentially be possible to detect metabolic differences in saliva using mass spectrometry-based methods. Here, a non-targeted metabolomics approach was applied with ultra-high performance liquid chromatography coupled to mass spectrometry (UHPLC-MS) to investigate the saliva metabolome and altered levels of saliva metabolites in patients with pSS as compared to healthy subjects.

In another part of this project when the COVID-19 pandemic struck Finland in early 2020, scent detection dogs were trained to recognize people infected with severe acute respiratory syndrome coronavirus 2 (SARS-CoV-2). As sweat and skin secretions emit volatile organic compounds (VOCs), non-invasive and quick skin swaps were chosen as specimens with which to detect a COVID-19 infection as an alternative to testing with the polymerase chain reaction (PCR) from nasopharyngeal swabs, a technique with poor real-time feasibility in terms of capacity as well as being expensive and slow. The scent detection threshold of trained dogs was tested using *Eucalyptus* hydrolat as a target scent and the diagnostic accuracy of the dogs was defined in the identification of people infected with SARS-CoV-2 from skin swab samples.



## 2 REVIEW OF THE LITERATURE

### 2.1 MASS SPECTROMETRY-BASED METABOLOMICS

#### 2.1.1 Fundamentals of mass spectrometry

MS is an analytical technique that measures the mass-to-charge ratio ( $m/z$ , the mass divided by charge number) of ions (23). MS methods can be tailored for quantitative measurements of targeted compounds or they can be semi-quantitative measurements for all ions detected in a sample (i.e., non-targeted analysis) (15). An MS analysis can involve the detection of a range of molecular weights, from very small molecules having  $m/z$  values around of 20 Daltons (Da) to large protein complexes with  $m/z$  values up to 3.5 MDa (24). Today, the  $m/z$  of a compound can be determined with high resolution and with very high mass accuracy ( $< 1$  part per million) which makes it possible not only to measure the mass up to at least five decimal places with isotope information but also to reveal the chemical composition of the compound (25). The sensitivity of mass spectrometric detection is compound dependent, and in routine multi-component serum analysis with an UPLC-MS system the low limit of quantitation varies from picomolar to nanomolar concentrations (26-28). However, with specific MS instrumentation, markedly lower detection limits can be achieved, which makes possible single cell metabolomics (29).

An MS apparatus has three main components: an ion source, a mass analyzer, and a detector. When a sample is put into the mass spectrometer, it is first ionized in the ion source. The mass analyzer sorts the ions based on their  $m/z$  ratios. Lastly, the detector measures the  $m/z$  of the ions and displays the results as a mass spectrum. These mass spectra are collected over time and combined into a chromatogram. A wide repertoire of sample preparation methods as well as techniques for introducing the sample into the ion source have been developed depending on the sample; these can range from a single, pure compound

to complex mixture of molecules in the solid, liquid or gas phases (Figure 1).

The origins of MS can be traced back to the early 20<sup>th</sup> century when isotopes were detected using mass spectrometry (30). In the 1940s, the time-of-flight (TOF) MS procedures were introduced followed by the development of the quadrupole MS in the 1950s. The 1970s and 1980s saw the introduction of soft ionization techniques, such as electrospray ionization (ESI) and matrix-assisted laser desorption ionization which revolutionized the analysis of biomolecules like nucleic acids and proteins. From the 1990s to the present, different kinds of hybrid instruments and integrations of MS with chromatographic techniques, such as liquid chromatography (LC) and gas chromatography (GC) have expanded the applicability of MS techniques in various fields of modern scientific research (31). Today, several MS analyzers such as modern ion traps combined with different ionization sources can produce high-resolution data with accurate mass measurements and enhanced sensitivities (32).

For example, an ESI-Q-TOF (electrospray ionization-quadrupole time-of-flight) analysis begins by introducing a sample in the form of a fine spray through an ESI source where the molecules are ionized under high voltage into either positively or negatively charged ions (Figure 2) (33). The formed charged droplets are evaporated by the countercurrent of the heated dry gas (like nitrogen gas). Desolvation continues until the ions in the droplets turn into gas phase ions.

The generated ions are then delivered into the quadrupole mass filter which consists of a combination of direct current and radiofrequency voltages in four parallel metal rods through which the ions are guided (34). In a full scan, all the ions are allowed to travel forward and enter a collision cell whereas in tandem mass spectrometry (MS/MS) only the selected ions with a targeted  $m/z$  ratio are directed into the collision cell. Here, the selected ions are collided with a collision gas (typically nitrogen or argon) and fragments (i.e., daughter ions) of the precursor ion (i.e., the parent ion) are produced.



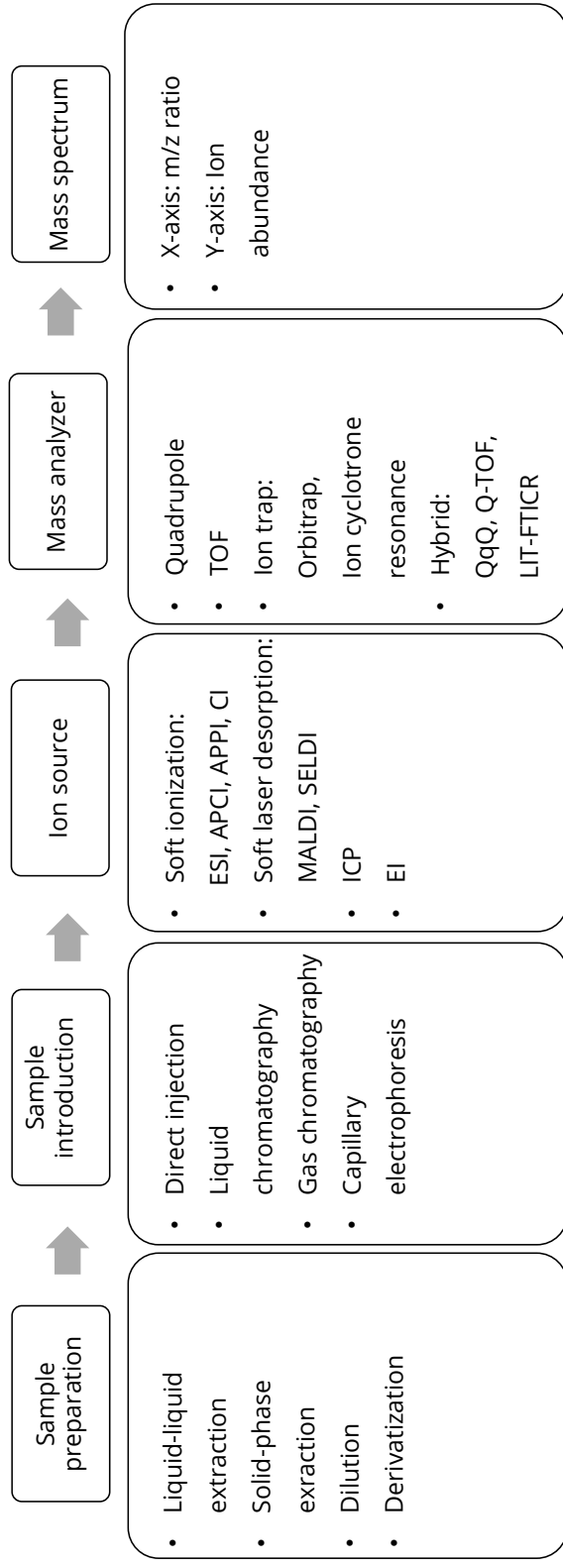


**Figure 1.** Flow chart of mass spectrometry analysis. Today, several options exist for each step of the analysis. The choice of methods is influenced by the sample type, the properties of the measured compounds as well as required accuracy and sensitivity (23, 35-37). APCI; atmospheric pressure chemical ionization; APPI, atmospheric pressure photoionization; CI, chemical ionization; EI, electron ionization; ESI, electrospray ionization; ICP, inductively coupled plasma; LIT-FTICR, linear ion trap-Fourier transform ion cyclotron resonance; MALDI, matrix-assisted laser desorption ionization; m/z, mass-to-charge ratio; QqQ, triple quadrupole; Q-TOF, quadrupole time-of-flight; SELDI, surface-enhanced laser desorption ionization; TOF, time-of-flight.

After the collision cell, the ions are accelerated via a pulser into the flight tube using an electric field where they are reflected into the detector. The flight time of the ions is directly proportional to their  $m/z$  values. Lighter ions with a small  $m/z$  ratio arrive in the detector earlier than heavier ones with larger  $m/z$  values. Finally, the detector converts the ions into electrons after which the signal is passed to be electronically handled.

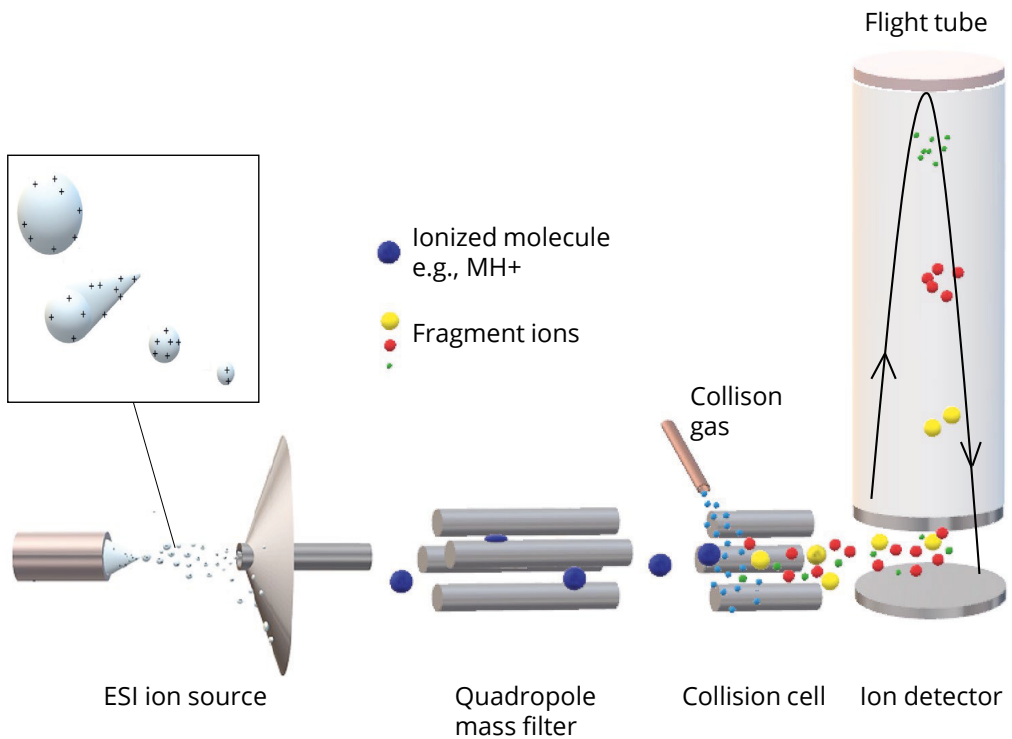


**Figure 2.** The schematic diagram of ESI-Q-TOF mass spectrometry. Ions are formed from charged liquid droplets in the ionization process in the ion source. In the full scan mode, all ions in a mass range of interest are directed into the flight tube without collision-induced dissociation (CID) providing signals from the molecular features of the measured sample. In the MS/MS mode, selected precursor ions pass through the quadrupole into the collision cell where CID produces molecule specific fragment ions which are used to identify the compounds.

The produced mass spectrum displays the  $m/z$  ratio of the detected ion and their abundance (i.e., intensity) yielding semi-quantitative data. In MS/MS, the result is a product ion spectrum which provides structural information about the precursor molecule. Reference ions are introduced in parallel with a sample to ensure continuous mass axis correction and in this way to ensure high mass accuracy. Those are stable ions which are formed from molecules with defined elemental formulas and known structures such as purine, trifluoroacetic acid, and hexakis (38).

The advantage of ESI-Q-TOF in the non-targeted measurement of small molecules is that it combines the capabilities of gently ionizing the intact molecules with quadrupole mass filtering and TOF mass analysis. For example, this enables the use of broad mass ranges, high mass resolution and a high dynamic range (31).

### **2.1.2 Non-targeted mass spectrometry analysis of metabolites**

Metabolites are molecules participating in cellular biochemical processes, and the entire collection of metabolites is called the metabolome. The human metabolome comprises thousands of metabolites i.e., amino acids, lipids, organic acids, nucleotides etc. Metabolites are typically small molecules that have molecular weights under 1500 Da (39). Given the vast differences in their concentrations which span a range from the picomolar to millimolar, and with their diverse physicochemical properties, such as polarity, acidity, and volatility, metabolites present a complex chemical landscape, posing challenges for non-targeted MS analysis (15). Often LC is coupled to MS to enhance the objective of non-targeted analysis, but also shot-gun methods have been used. The aim in metabolomics is to extract, separate, ionize, and measure as many compounds as technologically feasible that are present in the sample. The process is always a compromise because at each step some metabolites will be lost. A typical non-targeted metabolomics workflow is depicted in Figure 3.

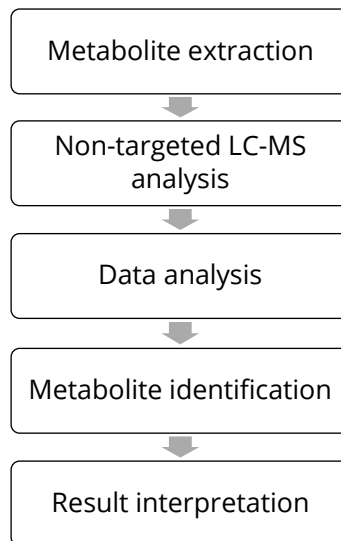


**Figure 3.** Simplified overview of non-targeted metabolomics workflow using LC-MS.

The aim of the extraction of metabolites is to recover as many different metabolites as possible, to stabilize the sample, and to precipitate the proteins to clean the sample for chromatographic separation (15). Different kinds of sample preparation methods can be applied, but often the simplest ones are favored to enable high-throughput platforms with short protocols where the key factor is repeatability (15, 40). These include, but are not limited to, liquid-liquid extraction and solid-phase extraction as well as the dilution of samples. A commonly used liquid-liquid extraction technique is to mix a sample with an organic solvent such as methanol, ethanol, acetonitrile, isopropanol, or mixtures of solvents although sometimes it involves only mixing with water. In solid-phase extraction, on the other hand, there are a variety of solid sorbent materials commercially available.

LC is tailored for compounds that are non-volatile and thermally labile, i.e., sensitive to heat. The chemical properties of the chromatographic column dictate the selectivity of the separation (41). For instance, reversed-phase (RP) chromatography is adept at isolating less polar compounds,

while hydrophilic interaction chromatography (HILIC) excels at separating polar metabolites by applying a gradient elution of an organic solvent. As the stationary phase retains and releases metabolites according to their polarity during the chromatographic gradient, a metabolite-specific record, retention time (RT), is obtained to assist in metabolite identification. Furthermore, the used organic solvents end up in the ion source, and the quality of these solvent impact on the produced data. If the quality requirements are not fulfilled, additional adducts or high background ion levels may occur leading to false or missed information in the downstream analysis (42).

In a non-targeted metabolomics analysis, both full scan MS and MS/MS spectra are acquired for high level of spectral information. Fragments from precursor ions are scanned with either data-dependent (DDA) or data-independent acquisition (DIA) methods (43). DDA performs a full scan analysis to determine  $m/z$  ratios and the intensities of the precursor ions, and this is followed by MS/MS scans of those ions that fulfill user-specified criteria. For example, the four most abundant precursor ions are fragmented in a selected time frame producing a good match between the precursors and fragments. In contrast, DIA methods induce the fragmentation of all ions within a selected  $m/z$  range and thus they produce complex fragmentation spectra with a poor match with precursor ions. DIA, on the other hand, offers advantages over DDA when applied in the field of proteomics (44).

Since the aim of a non-targeted metabolomics analysis is to gain as wide a view as possible from the whole metabolome of the sample, different techniques can be combined to increase the coverage of the measured metabolites. For example, the application of both ionization polarities, positive and negative, as well as different column chemistries, e.g., RP and HILIC, has a higher coverage of molecular features which when combined with fragmentation data, can aid in compound identification, and achieve better results than can be acquired by any single method alone.

The non-targeted LC-MS analysis is considered as a semi-quantitative procedure as the abundances of measured ions are comparable between samples, but exact concentrations are not calculated. This means that the

changes in metabolite levels between samples can be statistically calculated as estimates of the levels, but it is not possible to make an accurate determination of their concentrations. In addition, the values of ion abundances are not comparable between different studies or compound classes.

The acquired MS and MS/MS spectra constitute untargeted raw data. A key step of any workflow is how this data is processed to gain biological insights. The spectral data is collected using a peak picking software selected by the user. These software packages utilize algorithmic decisions and require parametrization to allow them to pick individual peaks of a sample (mass accuracy, signal count) followed by aligning the peaks (mass accuracy and RT tolerance) across the analyzed samples (38). The extracted data is preprocessed; this can involve several steps depending on the sample type and the number of samples to be analyzed. Typical preprocessing includes steps like drift correction, missing value imputation and flagging low-quality features. Finally, the data matrix is produced which displays entities for  $m/z$ , RT, and either peak height or peak area as abundance values for each molecular feature that passed through to preprocessing.

The goal of the statistical analysis in a metabolomics study is to identify the molecular features that are associated with the relevant factors, such as diseases, exposure, and responses to treatment across different study groups. To achieve this goal, a broad spectrum of statistical methods is employed, encompassing both univariate (i.e., feature-wise) and multivariate analyses (38, 45). In univariate analysis, the researcher tests the relationship between a single molecular feature and one or more variables of interest, such as the study group or a time point. Typical techniques include t-tests, analysis of variance (ANOVA) along with their non-parametric alternatives, Mann-Whitney U-test and Kruskal-Wallis test as well as more flexible linear models, such as a linear mixed effects model that allows for the inclusion of covariates and non-independent observations, such as repeated measurements in the same subject. In addition to p-values, effect size metrics like fold-change or Cohen's  $d$  are often reported. Supervised multivariate analysis techniques like partial

least squares-discriminant analysis (PLS-DA) and random forests are often combined with univariate statistics for biomarker identification and molecular fingerprinting. These techniques can identify a combination of molecular features that are associated with a variable of interest, such as a study group. In these models, the molecular feature levels are used to predict the levels of the variable of interest. Random forests can also use interactions between molecular features in the prediction. An unsupervised multivariate analysis is applied to detect patterns and structures within the data, such as clusters of samples or drift and batch effects. The commonly used techniques include principal component analysis (PCA), hierarchical clustering and t-distributed stochastic neighbor embedding.

In non-targeted metabolomics, the combination of p-values and effect-sizes from univariate analyses and variable importance metrics are used to prioritize the molecular features for identification, i.e., annotation, since it is often not feasible to identify all of the molecular features. Metabolite identification is based on a combination of the accurate mass of a molecule, a specific fragmentation pattern and the retention time (46). The information is obtained either by analyzing chemical standards or gleaned from public spectral databases. Today, the Human Metabolome Database (HMDB) contains >200 000 metabolite entries (47), PubChem consists of 100 million compounds (48), METLIN Gen2 over 800 000 compounds (49) and LipidMaps 48 000 lipid structures (50). In addition, e.g., MassBank and MoNa (MassBank of North America) provide access to downloadable spectra for automatic annotation software like MZmine (51), MS-Dial (52) and XCMS (53). Still, the metabolite annotation requires a manual inspection to assess the confidence of compound identification. The current proposed minimum requirements for annotation have been graded to four levels (46). In level 1, all three measured parameters of a molecular feature correspond to the chemical standard. Level 2 requires the correspondence of two parameters with a chemical standard or with public spectral databases while in level 3 annotations only the chemical group is identified and in level 4, the molecular feature is not identified. The updated reporting of standards and confidence levels for metabolite

annotation are still under discussion awaiting the final consensus at the metabolomics community-level. Similarly, one challenge is the inconsistent nomenclature of metabolites in the literature and in databases, which hinders the biological interpretation of the results (54, 55).

### **2.1.3 Discovery of disease biomarkers**

The presence of a disease can be associated with changes in biological pathways leading to alterations in the phenotype of an individual and these changes can be observed in the metabolome. The flow of biological information is depicted in Figure 4. By using metabolomics techniques, researchers can identify disease-specific biomarkers and unique metabolic signatures. Since the metabolome is dynamic, metabolomics also enables the follow-up of disease progression or treatment responses.

A non-targeted approach is used to discover novel biomarker candidates and to formulate hypotheses whereas targeted methods focus on specific compounds as well as providing quantitative data for validation of possible biomarkers. Biomarkers have been measured with LC-MS methods using various sample types; plasma and serum have been the primary samples of choice as they reflect the metabolic state of the whole body (56). However, other samples like urine, saliva, tissue extracts and even more specialized samples such as amniotic fluid, cerebrospinal fluid, and different kind of aspirates, have been employed. The choice of sample is paramount when planning metabolomics research for the discovery of biomarkers. Non-invasive samples are easier and more convenient to collect and usually people are more likely to agree to provide these specimens when compared to invasive samples, the latter also require trained healthcare professionals for safe collection (57, 58). However, there are some limitations regarding non-invasive samples. Saliva, for instance, is affected by many factors, such as the health and hydration status of the individual, which reflects on the volume and osmolarity of the saliva as well as on the quantities of the metabolites (59). In addition, there is a diurnal variation in saliva secretion.



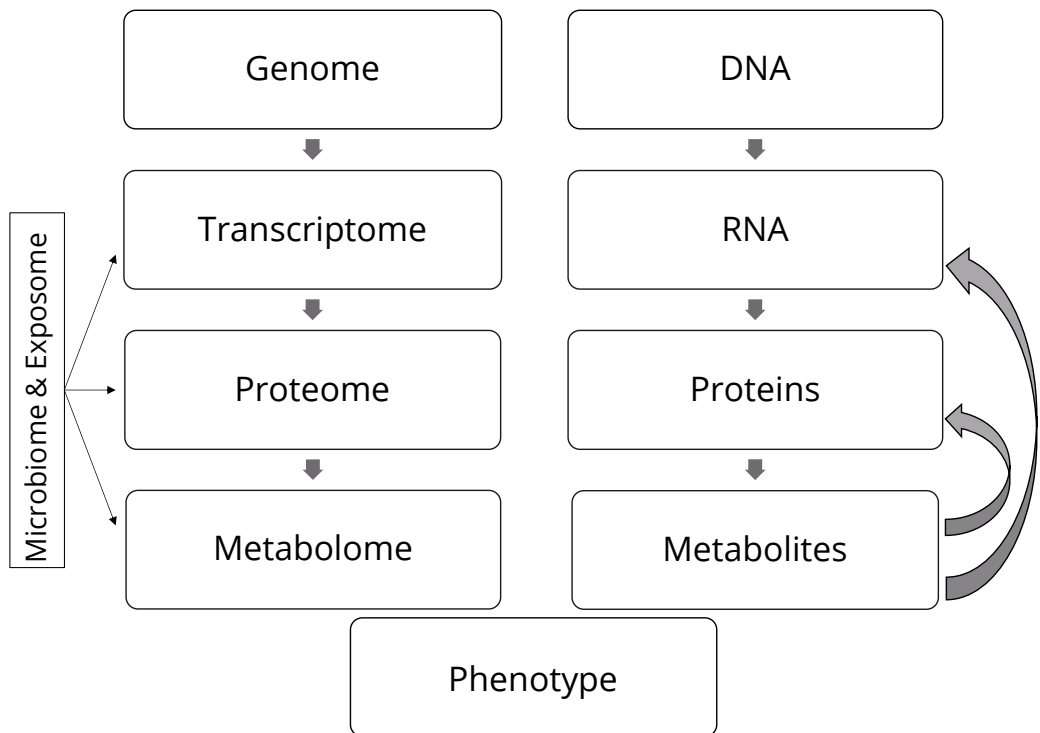
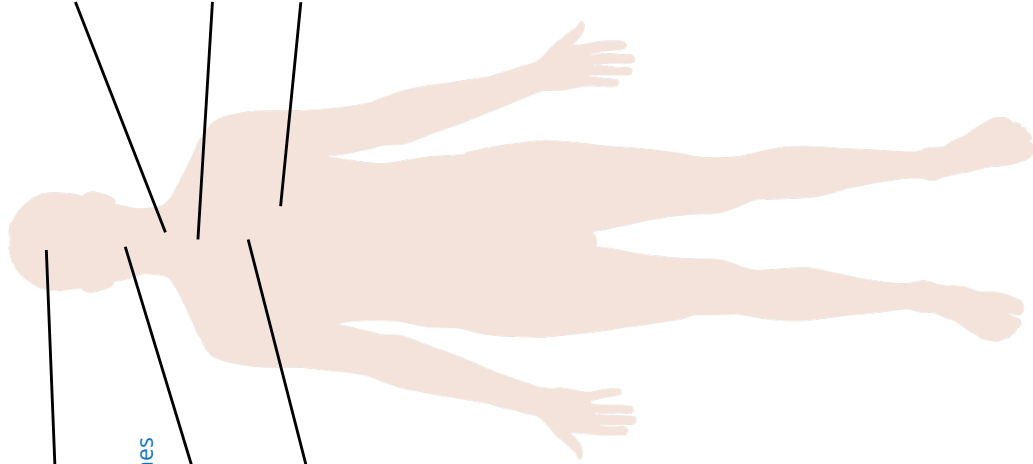


**Figure 4.** Simplified interactions in biological systems. Metabolites are acknowledged to be closest to the phenotype. In addition to systemic changes, the metabolome responds also to environmental exposures e.g., from diet, lifestyle choices, drugs, allergens, or air pollution (exposome), as well as to metabolites associated with favorable or hostile microbes (microbiome). In addition, metabolites have an active role in many cellular processes e.g., in cell signaling and growth, and have an effect even at the transcription level (60).

Despite of the limitations, it has been claimed that human saliva, being non-invasive and easy to collect, offers a promising alternative to traditional blood and urine samples in medical diagnostics (61-63). Saliva is primarily produced by acinar cells in the three pairs of the major salivary glands: the parotid, submandibular, and sublingual (58). There are also minor glands in other areas like the buccal, lingual, and palatine tissues that produce a thicker saliva (64). While comprising over 99% of water, saliva also contains electrolytes, proteins, cellular debris, and metabolites (59, 65, 66). Additionally, it can house bacteria, their by-products, food residues, and occasionally pathogens like viruses and fungi (58). Some of

saliva's components are filtered from the blood, but saliva has its own content of metabolites and thus there is only a weak correlation between metabolite levels in saliva and blood for most of the metabolites (67). There are exceptions, e.g., the concentration of steroids in saliva corresponds to the amount of active, free steroids in the blood that are not bound to proteins (68). Thus, measurement from saliva can be more informative than measuring the total (bound and unbound) steroid concentration in serum. Currently, this approach can be used to measure late-night salivary cortisol levels as a screening test for Cushing's syndrome (endogenous hypercortisolism) in clinics (69) and has been explored to help in the diagnoses of various illnesses from periodontal disease to systemic cancers as well as to Alzheimer's disease and COVID-19 to name just a few (61). Metabolomics studies of saliva have been widely reviewed elsewhere (61-63), but Figure 5 highlights some examples of the salivary metabolites associated with diseases which have been investigated using LC- or CE-MS-based metabolomics approaches.



**Alzheimer's disease**

phenylalanyl-proline, phenylalanyl-phenylalanine, urocanic acid, sum of 20 acyl-alkyl-phosphatidylcholines

**Periodontal disease**

phenylacetate, 3-phenylpropionate

**COVID-19**

leucine, phenylalanine, proline, tyrosine, valine, unknown C44H74N8O16

**Obesity in children**

creatinine, trans-4-hydroxyproline, 6 dipeptides, glycerol, N-acetylserine, erythronate, galactose

**Papillary thyroid carcinoma**

alanine, valine, proline, phenylalanine

**Barrett's esophagus**

glycolithocholic acid, chenodeoxycholic acid, glycocholic acid, glycochenodeoxycholic acid, glycodeoxycholic acid, hyocholic acid

**Breast cancer**

spermine, N1-acetylspermine, leucine, glycine, serine, spermidine, isoleucine, N1-acetylspermidine, cadaverine, butanoate

**Primary Sjögren's Syndrome**

O-phosphorylethanolamine, creatine, uridine monophosphate, uridine, cytidine 5'-monophosphate, serine, threonine, phenylalanine, alanine, lysine, glutamic acid, leucine/isoleucine, hypoxanthine, uric acid, lactic acid, malic acid, succinic acid, isovaleric acid, threitol, D-α-aminobutyric acid, GABA

**Figure 5.** Salivary metabolites differentiating between healthy and diseased individuals. Blue, level of metabolite lower in diseased compared to healthy; Red, level of metabolite higher in diseased compared to healthy. References for Alzheimer's disease (70, 71), Periodontal disease (72), COVID-19 (73), Obesity in children (74), Papillary thyroid carcinoma (75), Barrett's esophagus (76), Breast cancer (77), Primary Sjögren's Syndrome (78, 79). Original figure (Human body silhouette) modified from Wikimedia Commons.

## **2.2 BIOMEDICAL SCENT DETECTION**

### **2.2.1 The canine olfactory system**

The main anatomical structures associated with canine olfaction include the outer nose with the nares and nasal wings, nasal cavity, olfactory epithelium, vomeronasal organ (VNO), olfactory bulb and olfactory cortex (Figure 6) (80, 81). The nasal cavity is divided into two chambers which are separated by the nasal septum. Each chamber contains three turbinates; of these, the ethmoturbinate contains the olfactory epithelium (82). The size of the olfactory epithelium varies extensively from almost 170 cm<sup>2</sup> in German Shepherds down to 30 cm<sup>2</sup> in Pekinese (83). However, even small dogs can have an epithelium area that is ten times larger than that in humans (84). The olfactory epithelium is a mucous membrane which maintains the organ's humidity and traps odorants. The olfactory epithelium consists of olfactory receptor cells (ORCs), basal cells, supporting cells, and Bowman's glands (80, 81). Dogs have over 220 million expressed ORCs while humans have much fewer, 10-20 million (85-87). The cilia of ORCs are able to bind odorants via their receptors. One canine ORC has hundreds of cilia whereas humans have less than 30 cilia. One ORC expresses only one type of olfactory receptor (OR) (80, 88). ORs are G-protein-coupled receptors (GPCRs) that are grouped into Class I and Class II subgroups and are encoded by over 800 functional genes compared to about 400 functional genes in humans (89). OR genes are polymorphic, but a higher level of single nucleotide polymorphism and greater variation in

copy number have been reported in dogs (89-91). In addition, the number of inactive pseudogenes is less than in humans. The olfactory epithelium contains also trace amine-associated receptors (TAARs), but those have been much less extensively studied (92).

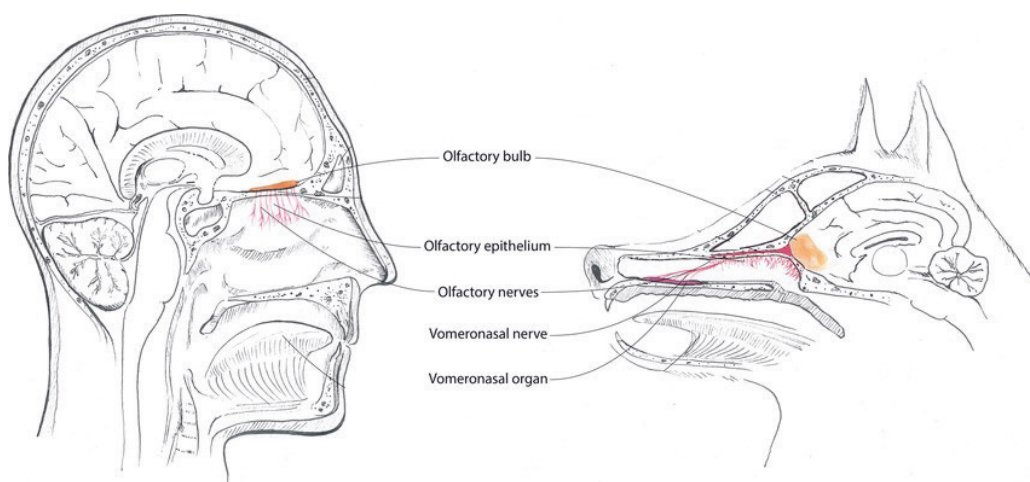


**Figure 6.** The anatomy of human and canine olfactory organs. Modified from (93). (Licensed under the CC-BY 4.0).

When an odorant molecule binds to the extracellular binding site of a specific OR, the stimulus-induced signal triggers the production of an action potential in primary sensory neurons to a specific glomerulus in the olfactory bulb (80, 88). One morphological study reported that on average the canine olfactory bulb is a region with a volume of  $0.18 \text{ cm}^3$  (versus human  $0.06 \text{ cm}^3$ ) of the forebrain (82) which, among other functions, acts as a relay station for neuronal signals. Axons of the mitral cells project to the olfactory cortex of the cerebrum which has two functional systems named neocortical and limbic (80, 88). The neocortical area regulates conscious odor perception whereas the limbic system combines several brain structures which together regulate behavior, motivation, memory as well as olfaction.

Moreover, dogs have an additional organ, the VNO, for sensing compounds. The VNO is located in the nasal septum; length is reported to be about 2.5 cm in Labrador retrievers and about 4.2 cm in Egyptian Baladi

dogs (94, 95). The VNO contains epithelium with one type of VNO receptor which reacts to signals that are sent from one animal to another (96). Those signals are generally thought to be pheromones. According to previous study, there are a broader group of molecules rather than simply being limited to pheromones, that are ligands of receptors in the VNO (97). Those are referred to semiochemicals and are sensed from a liquid source.

### **2.2.2 Canine detection of odor molecules**

Canines use active sniffing when they are detecting and analyzing odor molecules (98). Sniffing induces a unique nasal airflow that enables odorants to reach the olfactory epithelium whereas respiratory air has its own pathway. During sniffing, an average of 30 ml of air is inhaled into each nostril from the front (80). The right nostril is used for novel odors with the left nostril specializing in familiar odors as well as target odors to be identified by detection dogs. Only 12-13 percent of the air flow passes forward to the dorsal nasal cavity with high velocity (98). In the rear of the olfactory recess, the airflow changes direction by 180° and flows to the sensory epithelium of the ethmoturbinates inducing a unidirectional laminar flow during inhalation. During exhalation, no ventilation occurs in the olfactory structures which provides more time for odor detection. Finally, the airflow exits the organ via the nasopharynx.

The intranasal fluid dynamics provide efficient identification of odors as well as increasing the sensitivity. The detected odorant molecules by ORs in the ethmoturbinates are volatile or semi-volatile compounds with, but not limited to, organic, carbon-based structures (99). VOCs are described as low molecular weight chemical compounds which have a high vapor pressure, i.e., they evaporate at conditions of ambient temperature and normal pressure (100). However, inorganic molecules, such as ammonia (NH<sub>3</sub>), chlorine gas (Cl<sub>2</sub>) and hydrogen sulfide (H<sub>2</sub>S), have a smell (101). Furthermore, with the sense of smell, also some enantiomeric compounds can be distinguished, a feature that is difficult for analytical devices to detect (102).

In addition to their sensitive sensory system, motivation, behavior and cognitive abilities such as the ability to learn by operant conditioning, there appear to be even more important components of practical olfactory discrimination than neurochemical olfactory processes (103, 104). In operant conditioning, the dog's behavior is associated with a consequence (105). When the consequence is positive (e.g., food treats, playing with a toy, verbal praise, or petting) the dog increases the wanted behavior. This phenomenon is called positive reinforcement.

### **2.2.3 Disease-related human odor**

As a response to inflammation or a metabolic disorder due to a disease, the host's metabolism become altered and this induces a change in the composition and concentration of VOCs in various types of body fluids and tissues (106-108). This leads to the release of different VOC-patterns from the body which are detected and identified from different sample types e.g., breath, saliva, urine, feces, and blood.

The human body emits VOCs which are mainly secreted by the skin and sweat glands (109, 110). A recent systematic review summarized the identified skin VOCs of healthy individuals using different GC-MS methods including compounds from at least 32 different chemical classes (110). The most common VOCs were aldehydes (18%), carboxylic acids (12%), alkanes (12%), fatty alcohols (9%), ketones (7%), benzenes and derivatives (6%), alkenes (2%), and menthane monoterpenoids (2%).

In addition, the skin microbiome produces VOCs and contributes to the odor of a human being. The exposome associated with environment also has its own effect and thus, skin VOCs have an endogenous as well as an exogenous origin. Moreover, pathogens can release VOCs; specific VOC-patterns have been detected and identified from in vitro cell cultures of e.g., bacterial pathogens *Staphylococcus Aureus* and *Pseudomonas aeruginosa* (111) or viruses like Human rhinovirus and Influenza viruses (112).

The changes in chemical composition of skin VOCs due to the different diseases and conditions have been studied for decades. Changes in the

VOC-patterns have been linked to different conditions e.g., an infected skin, melanoma, visceral adenocarcinoma, as reviewed by Mitra et al. (2022). Likewise, distinctive VOC patterns have been identified in Parkinson's disease (5), tuberculosis (113), and a malaria infection (114).

Furthermore, the specific odor of a disease is also claimed to be identified by certain "super smeller" humans, as proven by Mrs. Joy Miller from the U.K. (115). Years before his diagnosis, she detected her husband's Parkinson's disease from his smell. After that, she has been helping researchers to identify biomarkers for Parkinson's, but she has also stated that "almost every disease has a unique odor" (116). To her, Alzheimer's smells faintly of vanilla, whereas cancer has an earthy, vegetable smell and tuberculosis has a particularly harsh smell.

The VOC-patterns recognized by medical detection dogs are still largely unknown, even though they are being investigated (117). At present, it has been shown that disease-specific changes in VOC-pattern can be detected by trained dogs. For example, prostate (118) and lung cancers (119), as well as *Clostridium difficile* (120) and malaria infections (121) among many others, have been identified by dogs with varying levels of accuracy from urine, feces, and clothes as a source of the VOCs, respectively.

Dogs have also been trained to discriminate between healthy and diseased individuals from the odor of sweat or skin samples as well as directly from the skin. Diabetes-alert dogs are one of the best known medical detection dogs; these animals are trained to detect hypoglycemia (122). Other conditions that the dogs have been reported to recognize are based on changes in the skin's odor e.g., in the presence of epileptic seizure (123, 124), stress (125) or Parkinson's disease (126). In addition, in a survey, many dog owners reported that their dogs were able to alert their owners to multiple conditions e.g., anxiety and migraine (127).

The latest exploitation of medical detection dogs relates to the SARS-CoV-2 virus infection, where the specimens with a body or sweat odor have been the most widely used sample types (128). The specific VOCs of COVID-19 infection in sweat and skin swab samples have been investigated to reveal the odor signal that is indicative of the presence of the disease to a scent detection dog. A previous study measured the VOCs from overnight-



worn T-shirts using headspace-solid phase microextraction-GC-MS and used dogs to discriminate between the diseased and the healthy controls (3). The VOC pattern distinguished between the study groups, but also revealed pet hair as a contaminant source for analytical measurement meanwhile the dogs did not respond to the odor of pets. Another research group collected armpit sweat onto cotton balls and sterile compresses which were subjected to dog detection and GC-MS analysis of COVID-19 (57). They also found a different VOC pattern between SARS-CoV-2 positive and negative samples and were able to putatively identify about 20 VOCs. In addition to dogs, Guest et al. utilized the data from a COVID-19 breath analysis conducted using GC-ion mobility spectrometry and used organic semi-conducting sensors aiming at detecting specific ketone and aldehyde compounds to spot the presence of SARS-CoV-2 infection from the socks worn by SARS-CoV-2 positive and negative participants (129). The sensor array was able to discriminate between infected and uninfected samples with 98% specificity (Sp) and 99% sensitivity (Se) confirming that the virus infection had generated a VOC pattern which was detectable from the individual's sweat.



### 3 AIMS OF THE STUDY

The general aim of this dissertation was to explore the ability of two sensitive detection methods, mass spectrometry and scent detection dogs, to differentiate between healthy individuals and diseased in non-invasive sample materials.

The specific aims were:

1. To explore the saliva metabolome of dogs and humans (Study I)
2. To apply a salivary metabolomics approach to identify metabolites with altered levels in the saliva of individuals with Primary Sjögren's syndrome (Study II)
3. To investigate the scent detection threshold of trained dogs (Study III)
4. To determine the diagnostic accuracy of scent detection dogs to screen SARS-CoV-2 infections from skin swabs (Study IV)



## 4 SUBJECTS AND METHODS

### 4.1 STUDY DESIGNS AND PARTICIPANTS

#### 4.1.1 Study I

Study I explored the metabolome of human and dog saliva. Voluntary human participants were recruited from the dental education clinic of Kuopio University Hospital. The inclusion criteria were healthy individuals with normal excretion of saliva. The exclusion criteria were as follows: smokers, removable dentures, systemic disease or treatment history of cancer, medication, and incapability of communication. As none of the examined males fulfilled the above mentioned criteria, 14 healthy, non-smoking females were recruited, aged between 30 and 70 years (mean 53 years, SD 11). All participants had good oral health having no gingivitis, missing or broken teeth nor caries as observed by a dentist. The study was conducted according to the Declaration of Helsinki and was approved by the Research Ethics Committee of the Northern Savo Hospital District (82/2014; 745/2018). A written consent was obtained from every participant. Stimulated saliva samples were collected by first chewing a 1g piece of paraffin wax for 30 s and then collecting the saliva for five minutes. Samples were collected between 9 and 11 a.m. after a minimum of 1 hour's fasting.

In the collection of the canine saliva samples, voluntary private dog owners were recruited in the North Karelia region. Saliva was collected from a total of 13 dogs (5 males, 6 females, and 2 neutered females). The dogs were reported as being healthy by their owners with one exception of an eye disease, cataract. No dogs were receiving any medication. The breeds were Belgian sheepdog (n = 2), Belgian Tervueren (n = 2), flat-coated retriever (n = 2), golden retriever (n = 2), Rottweiler (n = 3) and Weimaraner (n = 2), aged between 1 to 9 years (mean 5.5 years, SD 2.5). No specific oral or dental examination was done before saliva collection. The

study was conducted in accordance with institutional guidelines and in compliance with national and regional legislation. The study was approved by the Finnish National Animal Experiment Board (ESAVI/7482/04.10.07/2015). A written consent was obtained from every dog owner. Stimulated saliva samples were collected straight into a microcentrifuge tube from the dogs' mouth. Salivation was stimulated with the prospect of treats. Samples were collected between 9 and 11 a.m. after 12-hour's fasting.

#### **4.1.2 Study II**

Study II investigated altered salivary metabolites in patients with pSS. The study was conducted according to the Declaration of Helsinki and was approved by the Oulu University Hospital Ethical Committee (EETTMK: 116/2000; 36/2012) and the Research Ethics Committee of the Northern Savo Hospital District (82/2014; 745/2018).

The included participants had a diagnosis of pSS that fulfilled the criteria of the European Community guidelines. Exclusion criteria were smoking, and oral or systemic diseases other than pSS. Saliva samples were collected in the Training Clinic, Department of Dentistry, University of Oulu. Samples from 15 female patients (age 28-68 years, mean 48.6 years) were used in the study which comprised baseline samples (n=10) collected before low dose doxycycline (LDD, Periostat<sup>®</sup>, 20 mg doxycycline, 2 times/day) treatment and samples collected after one week of LDD treatment (n=15). By the time of saliva collection, participants had good oral health having no gingivitis, missing or broken teeth nor caries as observed by a dentist.

Healthy saliva donors were recruited to create a control group. The exclusion criteria were as follows: smokers, chronic disease, medication, or other treatment to affect the results. A total of 14 samples from age-matched females (age 28-68 years, mean 49.8 years), were used in the study. Written consent was obtained from every participant. From both groups, pSS and healthy controls, stimulated whole mouth saliva samples were collected according to the standard technique by first chewing a 1g

piece of paraffin wax for 30 s and then collecting the saliva for five minutes. Samples were collected between 10 and 12 a.m. after a minimum of 1 hour's fasting.

### 4.1.3 Study III

Study III determined the scent detection threshold of dogs to in-house made *Eucalyptus* hydrolat. According to Finnish research ethics, the particular experimental setup did not require an ethical statement from the ethics committee as the scent product was harmless and no data were collected from human participants i.e., dog-handlers.

The three-part study tested a total of 15 scent detection dogs in double-blinded, and randomized setting. Voluntary dog-handlers were recruited among trainers of a dog scent training sport called "nose work" as well as among cancer sniffing dogs. Study parts 1 and 2 were conducted in the Wise Nose dog training center (Helsinki, Finland) in June 2017 and study part 3 in the Vainuvoima scent training center (Loimaa, Finland) in April 2018. Part 1 tested 11 nose work sport dogs and one cancer sniffing dog (Figure 7). Most of the recruited dogs had experience with different target scents but the main target for the nose work sport dogs was eucalyptus hydrolat. Details of the dogs are presented in Table 1. In part 2, a cancer sniffing dog was re-tested to confirm the result of part 1. Part 3 included a training phase with three other dog and dog-handler pairs prior to the test day. The training period was four months and included 14 training sessions applying positive reinforcement method, i.e., the correct indication of the diluted solution was marked with a sound of a clicker and dogs were immediately rewarded with treats. The dogs were trained to discriminate the target scent of in-house made *Eucalyptus* hydrolat dilutions in decreasing concentrations (for details see Study III). In addition, study part 3 tested again the same cancer sniffing dog but this time in another location under different circumstances and with different apparatus compared to parts 1 and 2.

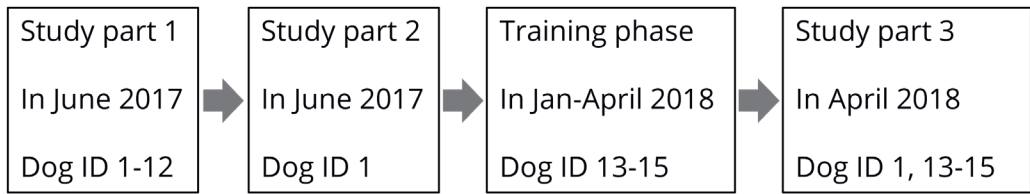


**Figure 7.** Flowchart of Study III. Characteristics of the tested dogs with identifiers (Dog ID) are depicted in Table 1.



Table 1. Characteristics of the dogs.

Dog ID	Breed	Age	Sex	Neutered status	Trained target scents	Level in Nose work Sports
1	Spanish Galgo mix	5y	M	Y	bedbugs, tracking of rats, molds, floor carpet glue residues, cancer	None
2	Parson Russell terrier	1y 9m	F	N	eucalyptus	H
3	Parson Russell terrier	2y 7m	M	Y	eucalyptus, bay leaf, lavender, pieces of Kong toy	C
4	Beagle	2y 2m	M	Y	eucalyptus, bay leaf, lavender, chanterelle, tracking of blood, human and dog scents	C
5	Cavalier King Charles spaniel	5y 2m	M	N	eucalyptus, bay leaf, lavender	H
6	Giant schnauzer	8y 5m	F	Y	eucalyptus, bay leaf, lavender	H
7	French bulldog	2y 6m	M	N	eucalyptus, bay leaf	H
8	Mittelspitz	6y 6m	F	N	eucalyptus	C
9	Shepard mix	4y 0m	F	N	eucalyptus, human scent	H
10	Parson Russell terrier	5y 10m	F	N	eucalyptus, chanterelle	H
11	Dogo Argentino	5y 0m	F	N	eucalyptus, tracking of human scent, district heating water	H
12	Long-haired Dutch shepherd	4y 2m	M	NA	eucalyptus	H
13	rough collie	5y 7m	M	N	eucalyptus	H
14	Danish-Swedish farm dog	5y 4m	F	Y	cancer	None
15	Australian kelpie	5y 7m	F	Y	eucalyptus, bay leaf, lavender	H

C, Contestant; F, Female; H, Hobbyist; ID, Identifier; M, Male; m, Months; N, No; NA, Not available; Y, Yes; y, Years.

#### **4.1.4 Study IV**

Study IV investigated if scent detection dogs could be trained to identify SARS-CoV-2 infected individuals and to determine the diagnostic accuracy of scent detection dogs to identify people with COVID-19 in comparison with reverse transcriptase polymerase chain reaction (RT-PCR). The three-arm study included dog training, a triple-blinded randomised validation study, and a real-life cohort at Helsinki-Vantaa International Airport, Finland. The operational real-life screening at the airport was conducted during the period of 23 September 2020 to 30 April 2021. The study was approved by the Helsinki University Hospital's ethics committee (HUS/1238/2020) and was part of a larger COVID-19 research protocol. A research permit was obtained from the local authorities at HUH (HUS/157/2020) and Vantaa City (VD/8473/13.00.00/2020). Written consent was obtained from every participant.

#### **Scent detection dogs**

The initial dog training was conducted at the scent detection dog training center Wise Nose (Vantaa, Finland). Nine dogs performed the identification at the minimum level of 80% in detecting SARS-CoV-2 positive samples in the training phase and continued their training in a purpose-built cubicle at the Helsinki-Vantaa International Airport. Four dogs were tested in the validation study, all of them had had previous experience of scent work. Three of the dogs were Labrador retrievers (6-year female worked with narcotics, 5-year and 8-year males worked with dangerous goods) and one White Shepherd (4-year female worked with canine cancer samples). The real-life study was based on the performance of the four validated dogs.

#### **Human participants**

The participants with a RT-PCR test result within 72 hours were recruited among hospitalized patients in Helsinki University Hospital (HUH), outpatients and healthy individuals in Helsinki contacted by the study team via phone call or those who enrolled through an advertisement posted at PCR sampling stations as well as incoming flight passengers and personnel

at Helsinki-Vantaa International Airport. Participants conducted skin swab sampling and filled in the questionnaire. No restrictions were established regarding the participants' age, sex, nationality, concurrent diseases or for individuals with an asymptomatic SARS-CoV-2 infection. Exclusion criteria were incomplete questionnaire and/or missing information in the RT-PCR result. Further information was collected via personal interviews by telephone as well as from electronic medical records of hospitalized patients. Table 2 summarizes the study design and the measurements conducted. The number of sniffed skin swab samples in different parts of the study with the main characteristics of participants are described in Table 3. In brief, the validation study consisted of 420 skin swab samples from which 306 individuals were tested as RT-PCR negative and 114 were revealed to be RT-PCR positive. In the real-life screening at the airport, a total of 303 samples were sniffed by the four validated dogs during their operational work. From those samples, 300 were collected from individuals tested as being RT-PCR negative and three tested positive with RT-PCR. In addition, the dogs screened 155 RT-PCR positive spike samples.

**Table 2.** Study IV design and measurements for parts 2 and 3.

	<b>Part 2 Validation study</b>	<b>Part 3 Real-life screening</b>	
Study design	-420 samples were randomized into four parallel test sets for each validated dog -A total of 140 three-sample line-ups were prepared -Triple-blinded tests were conducted in seven sessions where 20 three-sample line-ups were tested in one session	303 samples were screened during the operational work	155 positive spike samples were additionally screened during the operational work
Measurements	Diagnostic accuracy on all 420 samples and by virus type	Diagnostic accuracy on all 303 samples	Diagnostic accuracy on all 303 samples + 155 spike samples

**Table 3.** Participant and sample characteristics in Study IV part 2 and 3. For part 1 (Dog training), no sample data are available.

Characteristics	Part 2 Validation study		Part 3 Real-life screening		
	Recruited inpatient, outpatient and healthy volunteers (n=420)		Incoming flight passengers (n=303)		Spike samples (n=155)
	RT-PCR Neg (n=306)	RT-PCR Pos (n=114)	RT-PCR Neg (n=300)	RT-PCR Pos (n=3)	RT-PCR Pos (n=155)
Age, median (IQR)	40 (23)	34 (18)	42 (23)	48 (NA)	33 (27)
Child, 0–12 years, n (%)	2 (0.7)	13 (11.4)	2 (0.7)	0 (0)	18 (11.6)
Sex, female, n (%)	168 (54.9)	58 (51.3)	191 (63.7)	1 (33.3)	83 (53.5)
male, n (%)	137 (44.8)	55 (48.7)	109 (36.3)	2 (66.7)	72 (46.5)
Sample obtained, n (%)					
Healthy screened	301 (98.3)	0 (0)	300 (100)	3 (100)	0 (0)
Hospitalised (Non-COVID respiratory disease)	2 (0.7)	0 (0)	0 (0)	0 (0)	0 (0)
Outpatient	3 (1.0)	114 (100)	0 (0)	0 (0)	155 (100)

Characteristics	Part 2 Validation study		Part 3 Real-life screening		
	Recruited inpatient, outpatient and healthy volunteers (n=420)		Incoming flight passengers (n=303)		Spike samples (n=155)
	RT-PCR Neg (n=306)	RT-PCR Pos (n=114)	RT-PCR Neg (n=300)	RT-PCR Pos (n=3)	RT-PCR Pos (n=155)
Sample delay from PCR-test, days, median (IQR)	0 (1)	2 (2)	0 (0)	0 (0)	4 (4)
Symptoms, n (%)					
Asymptomatic	297 (97.1)	7 (6.1)	291 (97)	2 (66.7)	12 (7.7)
Respiratory infection	9 (2.9)	107 (93.9)	9 (3)	1 (33.3)	143 (92.3)
SARS-CoV-2 variant, n (%)					
Wild-type	NA	62 (54.4)	NA	2 (66.7)	NA
Variant	NA	28 (24.6)	NA	1 (33.3)	NA
Alpha	NA	25 (21.9)	NA	1 (33.3)	NA
Beta	NA	1 (0.9)	NA	0	NA
Alpha or beta	NA	2 (1.8)	NA	0	NA
Unknown	NA	24 (21)	NA	0	NA

Characteristics	Part 2 Validation study		Part 3 Real-life screening		
	Recruited inpatient, outpatient and healthy volunteers (n=420)		Incoming flight passengers (n=303)		Spike samples (n=155)
	RT-PCR Neg (n=306)	RT-PCR Pos (n=114)	RT-PCR Neg (n=300)	RT-PCR Pos (n=3)	RT-PCR Pos (n=155)
Chronic disease, n (%)					
Asthma, allergy	16 (5.2)	12 (10.5)	18 (6)	1 (33.3)	22 (14.2)
Cancer	2 (0.7)	5 (4.4)	1 (0.3)	0 (0)	6 (3.9)
Hypertension	14 (4.6)	8 (0.7)	25 (8.3)	0 (0)	11 (7.1)
Diabetes	6 (2.0)	5 (4.4)	8 (2.7)	0 (0)	5 (3.2)
Migraine	2 (0.7)	1 (0.9)	3 (1)	0 (0)	4 (2.6)

IQR, Interquartile range; Neg, Negative; Pos, Positive; RT-PCR, Reverse transcriptase polymerase chain reaction.

## 4.2 METHODS

### 4.2.1 LC-MS based non-targeted metabolomics

Studies I and II utilized a non-targeted metabolomics approach to detect metabolites and small compounds from saliva samples. Both human and dog saliva samples, were processed as follows: Proteins were precipitated, and metabolites extracted by adding two volumes of acetonitrile per one volume of saliva (e.g., 200  $\mu$ l of saliva and 400  $\mu$ l of acetonitrile). After centrifugation (10 600  $\times$  g for 5 min at 4°C), the supernatants were filtered through 0.2  $\mu$ m syringe filters with polytetrafluoroethylene membrane into glass vials. Three quality control (QC) samples were prepared and named as human, dog, and mixed QC. An aliquot of 30  $\mu$ l of each supernatant of human saliva was pooled in one tube and filtered accordingly with the same being applied for dog saliva supernatant as well mixed QC including all human and the dog saliva supernatants.

The metabolic profiling was conducted using an Agilent 6540 UHD accurate-mass ESI-Q-TOF tandem mass spectrometry coupled to a 1290 Infinity Binary UHPLC system (Agilent Technologies, Waldbronn, Karlsruhe, Germany). A more detailed description is depicted in Study I article and Klåvus et al. (38). The RP separation was performed with Zorbax Eclipse XDB-C18 column (2.1  $\times$  100 mm, 1.8  $\mu$ m, Agilent Technologies, Palo Alto, CA, USA) using gradient elution with a varying mobile-phase composition of water (A) and methanol (B) both with 0.1% (v/v) formic acid during the 16.5-minute run. HILIC separation was performed with Acquity UPLC<sup>®</sup> BEH Amide column (2.1  $\times$  100 mm, 1.7  $\mu$ m, Waters Corporation, Milford, MA, USA) using a gradient elution with a varying mobile-phase composition of 50% (v/v) acetonitrile in water (A) or 90% (v/v) acetonitrile in water (B) both with 20 mM ammonium formate buffer during the 12.5-minute run. For each chromatographic run, an injection volume of 2  $\mu$ l was applied.

An Agilent Jet Stream ESI was used as an ion source for mass spectrometry. The acquisition of full scan MS data was conducted within the 50-1600 m/z range in both, positive and negative, ionization modes. For data-dependent acquisitions with the automatic fragment-ion, MS/MS



analyses, CID voltages were set to 10V, 20V and 40V. Quality assurance of the continuous mass axis calibration assured the operation at high mass accuracy (< 2 parts per million). In addition, a QC mixed sample was injected multiple times for equilibrating the column before the start of the sample analyses as well as after every 9 samples for possible drift correction in the data-analysis. A separately collected human saliva QC was injected before the human saliva samples for the acquisition of MS data and after for the MSMS data. The same procedure was applied with collected dog saliva QC before and after the dog saliva samples. MassHunter Acquisition B.05.01 software (Agilent Technologies) was used for raw data acquisition from four analytical modes named as follows: RP positive, RP negative, HILIC positive and HILIC negative.

When extracting the molecular feature data, the above-mentioned raw data were exported to Mass Hunter Qualitative Analysis B.07.00 (Agilent Technologies) for peak picking and peak alignment. The value for ion abundance was set to a minimum of 10,000 to increase the quality of the collected data by excluding the background noise. The yielded feature files were imported into Agilent Mass Profiler Professional (MPP) 13.1.1 software for compound alignment and molecular features were exported for use as the data matrix. To be included for metabolite identification, a feature had to be present in at least 50% of samples in either human, or dog saliva.

MS-DIAL (RIKEN PRIME, versions 2.66 to 3.12) was utilized for semi-automated metabolite identification. The converted MS/MS data files were imported to MS-DIAL and both, public databases (Metlin and MassBank of North America, MoNA) and an in-house spectral library, were downloaded. Lipid annotation was performed using the built-in MS-DIAL library. Identification was based on comparing the similarity of exact  $m/z$ , RT and MS/MS spectra between databases and MS/MS datafiles. Every annotated metabolite was manually inspected and ranked to identification level 1 or level 2 according to Sumner et al. 2007. Briefly, in level 1,  $m/z$ , the retention time and the fragmentation pattern matched with in-house spectral library based on reference standards. In level 2, the  $m/z$  and the fragmentation pattern were accord with the public spectral database. The identified

features were manually inspected and integrated using the targeted feature extraction of Mass Hunter Profinder B.08.00 (Agilent Technologies) to minimize the appearance of false negative features.

#### **4.2.2 Odor discrimination**

In Study III, a stock solution of *Eucalyptus* hydrolat was prepared from an essential oil of *Eucalyptus radiata* (Frantsila, Kyröskoski, Finland). The stock solution was diluted with ultra-pure water in ratios (*Eucalyptus* oil : water) from 1:10<sup>4</sup> (mL/mL) down to 1:10<sup>24</sup> (details of preparing the solutions are described in Supplementary table 1 and in Study III). The aliquots of *Eucalyptus* hydrolat dilutions with decreasing concentrations were introduced as target samples in a line with non-target samples containing only ultra-pure water. Each sample had a volume of one mL in a single-use PP-plastic cup which was placed into a mesh-covered metallic jar and positioned in a metallic scent track (in part 1 and 2) or into a glass jar and positioned in an individual plywood stand (in part 3) according to a computer-generated randomization list. Every tested line-up contained one target and two non-target samples for a three-alternative forced-choice task. The scent discrimination was conducted in a double-blind manner where the dog and the dog-handler were blinded about the sample status. Within every line-up, the dog-handler reported the dog's indication out loud. The indication was recorded as correct if the dog alerted a jar with the target sample, using its individual-specific alerting behavior (focused stare, nose freeze, sitting or lying down in front of the indicated jar, or pawing the jar). The test ended with the first false indication (i.e., alerting behavior for non-target sample) or if the dog did not indicate any of the samples (i.e., no alerting behavior to any of the samples). The preceding diluted sample that was correctly indicated by the dog, was recorded as a result. The study followed the principles of operational conditioning and positive reinforcement. An external controller followed the studies, and two registrars of the results were present.

In Study IV, the identification of SARS-CoV-2 infected individuals was based on scent discrimination from skin swab samples performed by scent detection dogs. The participants collected skin swabs using sterile gauze swabs as follows: The layers of gauze were opened for swabbing the skin with single layer gauze in the neck and throat area, forehead, and wrists. From five to 20 gauzes were used and stored either in double or triple zip lock bags placed inside each other to avoid cross-contamination and evaporation. When used for scent discrimination, one gauze was transferred from the zip lock bag using disinfected metallic forceps into a 1L plastic freezer bag placed in a metallic can. In the real-life setting, the participant placed one of the gauzes straight into a can lined with above-mentioned freezer bag to perform an immediate scent discrimination test for COVID-19 infection.

The scent detection dog training was conducted using operant conditioning with positive reinforcement. Skin swab samples were introduced to a dog in metallic cans which were positioned in a purpose-built metallic line-up. The training started from step one where positive (meaning SARS-CoV-2 RT-PCR positive) skin swab sample in a metallic can was introduced to a dog and the animal was taught how to alert and indicate the positive sample. In step 2, one negative (meaning SARS-CoV-2 RT-PCR negative) skin swab sample was introduced in parallel with the positive sample allowing the dog to distinguish the scent difference between the samples. Step 3 included several negative and positive samples to be added to the line-up to further enhance and reinforce the scent discrimination and the indication of the positive samples. The confounding samples collected from individuals with different ages and diseases (e.g., respiratory, and viral diseases, asthma, allergies, cancer, and diabetes) were included in step 4. In the final stage, the dog was able to detect and correctly indicate a minimum of 80% of SARS-CoV-2 positive samples allowing a dog and a trainee to enhance the discrimination skills in Helsinki-Vantaa International Airport in the test cubicle.

The triple-blinded validation study was conducted according to a specially designed protocol in the test cubicle at the airport. Four cameras recorded the test sessions, and an external controller followed the study to

confirm the study was being conducted in a triple-blinded manner. One rehearsal session and seven validation sessions (VAL 1-7) were executed on different days as follows: On the test day, the sixty novel samples were prepared in a separate location in the airport. Samples were positioned in 20 line-ups each containing three samples using a computer-generated randomization list. A total of 140 line-ups was introduced to each dog during validation including 26 (18.6%) line-ups that did not contain any positive samples as randomized. All sets of samples were identical to the dogs, where a single parallel swabbed gauze was used only once and for one dog. More details of the sample handling are described in Study IV article. Line-ups were transported to the cubicle using a trolley. Figure 8 shows the triple-blinded study setup.

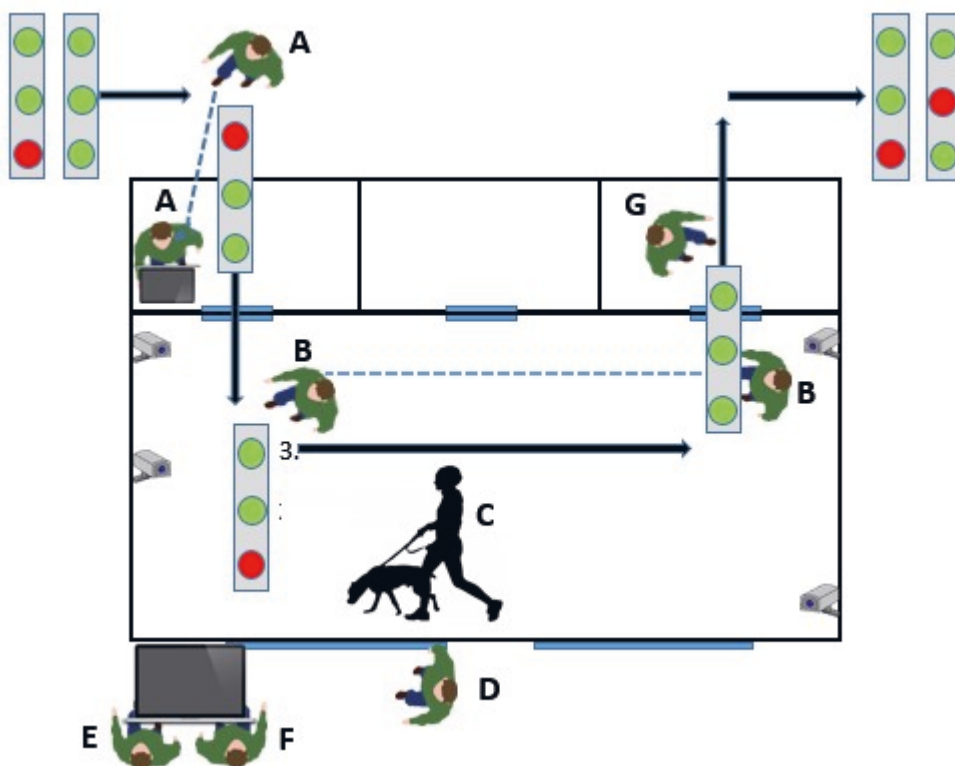


**Figure 8.** Triple-blinded validation study. The dog and the dog-handler (C) as well as assistants B, E and G were blinded about the sample's status. The line-up was imported through a hatch in the wall by assistant A to

assistant B who placed it on the floor. The dog performed the discrimination and the dog-handler reported out loud the result which was either approved or denied by assistant D from outside of the cubicle. The dog-handler rewarded the dog for a correct indication. The line-up was exported through a hatch in the wall by assistant B to assistant G. The external controller (E) and assistant F observed the validation process through video monitors. Figure from Study IV.

The real-life study to screen SARS-CoV-2 infected flight passengers and airport personnel was conducted in the purpose-built cubicle which had three sampling rooms with hatches on the walls for sample import into the test room. The scent detection dog performed the scent discrimination task in a line-up and a dog-handler interpreted the indication. A written result was given immediately to the participant.

#### **4.2.3 Quantitative H<sup>1</sup> NMR**

The proton nuclear magnetic resonance (H<sup>1</sup> NMR) spectra of the essential oil *Eucalyptus radiata* were measured and the detected compounds were quantified in the University of Eastern Finland in collaboration with Professor Jouko Vepsäläinen. Briefly, a spectrum of a sample in deuterium oxide D<sub>2</sub>O or methanol-d<sub>4</sub> (CD<sub>3</sub>OD) with an internal reference standard 3-(trimethylsilyl)-tetradeuteropropionic acid (TSP-d<sub>4</sub>) was measured using a 600 MHz Bruker NMR spectrometer coupled to a cryoprobe and an automatic sample changer. Compound identification was based on the spectra of reference compounds and concentrations were calculated based on quantitative reference standard TSP-d<sub>4</sub>. The lower limit of the quantitation was 0.01 millimolar (1 mg/L). A detailed description is depicted in Study III article.

#### **4.2.4 Clinical laboratory tests for diagnosis of COVID-19**

The scent discrimination result was compared to an RT-PCR assay detection of SARS-CoV-2 virus load from a nasopharyngeal swab. The participants reported the RT-PCR result in the study questionnaire.

When a contradictory result between scent discrimination and RT-PCR was encountered, the status of SARS-CoV-2 infection was clarified by analyzing serum SARS-CoV-2 antibodies against the spike glycoprotein (Spike IgG), and nucleocapsid protein using enzyme immunoassay in collaborating laboratories. The variant status of the virus was defined as follows: For the alpha variant, data of S gene target failure (SGTF) was used (SYNLAB for Diagnostics Centre of the Hospital District of Helsinki). For alpha or beta variants, TaqPath COVID-19 PCR *Kit* (Thermo Fisher Scientific, Waltham, Massachusetts, USA) and TipMolBiol *Kit* (Berlin, Germany) for the N501Y mutation in RT-PCR were performed in HUSLAB. According to epidemiological data from Finland, the first alpha variant cases were detected 18th December 2020 in Finland and the proportion of alpha and beta variants rapidly increased in week 2 of 2021. All collected samples before that timepoint were considered as the 'wild-type' strain (D614G Wuhan-like strain).

#### **4.2.5 Statistical methods**

##### **LC-MS based non-targeted metabolomics**

Univariate and multivariate analysis were exploited when assessing the metabolomics data. Univariate statistics were applied in Study I to depict the relative proportion of ion abundances of the identified metabolites between species (minimum, median, maximum) as well as to reveal the inter-individual and sample variation (mean, standard deviation). In Study II, Cohen's d was used to calculate effect sizes for measuring the difference between two group means, and Welch's t-test to calculate p-values from non-scaled ion abundance data.

In the multivariate analyses, PCA was exploited to identify possible associations among study variables in both studies. In addition, the variable importance in projection (VIP) values were obtained from PLS-DA

to reflect the relative importance of each X variable for each X variate in the prediction model in Study II. Multivariate analyses were done using SIMCA (version 15, Umetrics, Umea, Sweden).

### **Odor discrimination**

In the validation test in Study IV, a power calculation was conducted by Docent of Veterinary Medicine, Anna Hielm-Björkman (University of Helsinki, Finland). As described in Study IV article, the power calculation suggested a minimum of 108 RT-PCR positive and 108 negative samples to achieve Se and Sp of 90%. This sample size was expected to have an 80% probability of obtaining an estimated Se and Sp of which the lower boundary of the 95% confidence interval (CI) would be greater than the minimal value of 80% (calculated using <https://www.stat.ubc.ca/~rollin/stats/ssize/b1.html>).

Statistical analyses were performed by collaborative partner Professor Loic Desquilbet (Biostatistics and Clinical Epidemiology at the Ecole nationale vétérinaire d'Alfort, France) together with Docent of Veterinary Medicine, Anna Hielm-Björkman (University of Helsinki, Finland). Briefly, Se, Sp, positive predictive values and negative predictive values were calculated according to Trevethan (130). Se and Sp were calculated using two separate methods: First, the Se and Sp were calculated only for those samples that the dogs truly sniffed ( $Se_{sniff}$  and  $Sp_{sniff}$ ) and second, the Se and Sp were calculated for all the samples ( $Se_{all}$  and  $Sp_{all}$ ). With the latter approach, the assumption was that the dogs considered all un-sniffed samples as being negative, as they left them untouched. Additionally, the difference was determined between true positive (TP) (i.e., the dogs correctly identified an RT-PCR confirmed positive sample as positive) and false negative (FN) (i.e., the dogs did not mark a confirmed positive sample) indications done by any one of the four validated dogs during the validation. Furthermore, possibly associated descriptive or clinical variables with the TP/FN outcome variable were used as supplements in the evaluation. The following variables were included in the model: age; gender; concurrent chronic diseases (asthma, allergy, cancer, diabetes, or migraine); typical COVID-19 symptoms or not; time between symptom

onset and sample collections; time between RT-PCR test and sample collection and type of virus (wild type or alpha variant). The statistically significant variables left in the final model were reported and given as odds ratios with their confidence intervals and p-values. Excel (Microsoft Office, version 2016) and SPSS (SPSS statistics for Windows, version 27.0, IBM Corp, Armonk, NY) were used for the data analysis. More detailed information is provided in the Study IV article.



## 5 RESULTS

### 5.1 NON-TARGETED METABOLOMICS OF SALIVA

#### 5.1.1 Saliva metabolome

A total of 5468 out of 8375 metabolic features of saliva were accepted as the final data matrix which was utilized for metabolite identification in Study I. Human saliva contained 181 endogenous and exogenous compounds (Supplementary table 2) which were identified with verification level of 1 (n=64) or 2 (n=101) according Sumner et al. (2007). In addition, 16 other identified features were classified as chemical compounds. All the others were classified as follows: amino acids (n=15), amino acid derivatives (n=9), biogenic amines (n=7), lipids and carnitines (n=61), nucleic acid subunits (n=8), organic acids (n=5), small peptides (n=34) and other metabolites (n=26). Supplementary table 2 also illustrates the large variation observed in ion abundance between samples and between individuals along with descriptive statistics.

Furthermore, Study I characterized canine saliva and compared the results between species. In total, 171 metabolites were common between dogs and humans. On the contrary, 31 salivary metabolites were unique to dogs and nine to humans. Dog salivary metabolites included more lipid compounds (n=25) than their human counterparts. In addition, an amino acid derivative named phenylacetylglycine (level id 2), an organic acid designated as pyrocatechol sulfate (level id 2) and four other metabolites (quinaldic acid, sphingosine, usnic acid (level id 2) and sphinganine (level id 1) were only detected in dog saliva. Likewise, human saliva contained unique metabolites. Those were identified as dipeptides (n=8, level id 2) and gamma glutamylglutamic acid (level id 2). Similarly, as in human saliva, there was extensive variation in ion abundances within and between the identified metabolites observed in dog saliva samples. PCA (Figure 9) revealed the variation between saliva samples within the species, but also clearly separated the metabolic profiles of human and canine saliva.

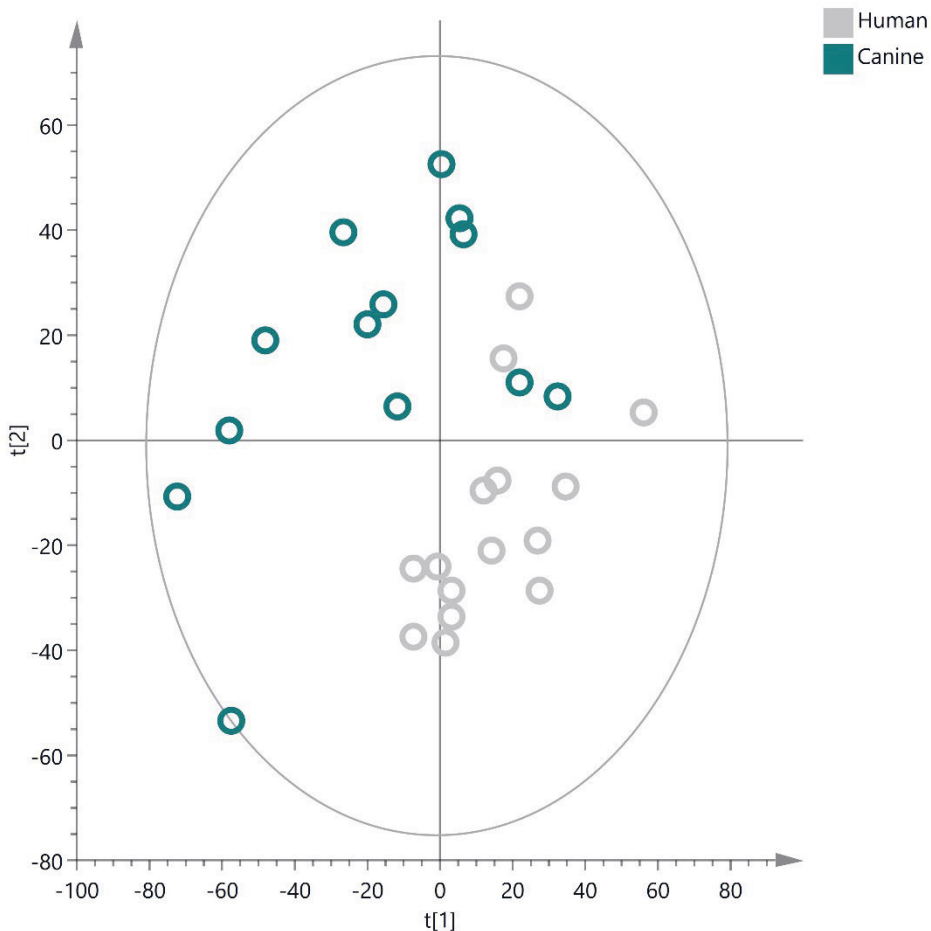


**Figure 9.** PCA of human and dog saliva metabolome in non-targeted LC-MS analysis. A separation of the species can be seen as well as the variation within the species.

### 5.1.2 Changes in saliva metabolite levels as disease response

Study II included patients with Primary Sjögren's Syndrome divided into two groups i.e. a group treated with the antibiotic LDD and a non-treated group. The third group consisted of healthy controls. An LC-MS based non-targeted metabolomics approach was applied to detect the changes in saliva metabolic profiles between the study groups.

After data preprocessing, a total of 4373 metabolic features were included in the data matrix. The multivariate analysis of the metabolomics data included PCA (Figure 10) which revealed that the metabolic profiles of saliva of pSS patients differed from that of healthy individuals. With LDD treatment, the profile was mixed between that of the diseased and healthy persons, but the analysis indicated that the treatment had changed the metabolic profiles of pSS patients towards a healthier one.

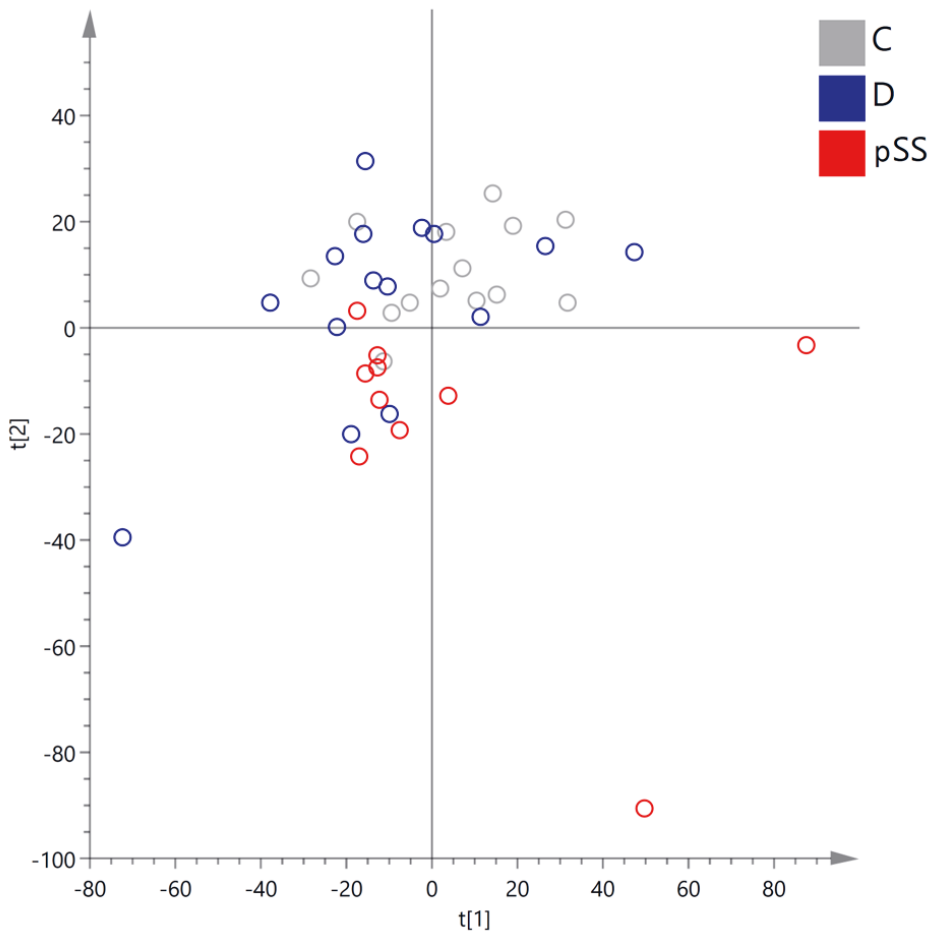


**Figure 10.** PCA of saliva metabolic profiles in non-targeted LC-MS analysis. C, control group (n=14); D, pSS patients with LDD treatment (n=15); pSS, pSS patients before LDD treatment (n=10).

After statistical analysis, including both univariate and multivariate analysis, the data matrix included 1380 metabolic features with  $p < 0.05$ . A total of 36 unique metabolites were identified at verification level 1 ( $n=15$ ) or 2 ( $n=11$ ) (Supplementary table 3) for example, being amino acids, peptides, lipids, and carnitines.

The mean ion abundance of 31 metabolites out of 36 was higher in the pSS patient group compared to healthy controls whereas 5 metabolites had lower mean ion abundance (Figure 11). Lysophosphatidylcholine 18:0 (LPC 18:0, level id 2) and lysophosphatidylethanolamine 18:0 (LPE 18:0, level id 2) were not observed in the control group but displayed higher abundance in the LDD group than present in pSS patients without LDD (difference not statistically significant D vs. pSS). In addition, pantothenic acid (vitamin B5, level id 1) was detected with low abundance in the control group and had significantly higher abundance in pSS group ( $p < 0.001$ ) as well as in LDD group ( $p < 0.01$ ). Pantothenic acid also exhibited the highest VIP value (2.46) in comparison between pSS group and healthy controls.

With respect to the four identified dipeptides (level id 2), three had a significantly higher abundance in the pSS group when compared to controls, whereas Arg-Ser had a significantly lower abundance. Phe-Ile, Tyr-Gln and Val-Leu corresponded to the LDD showing a decreased abundance after drug treatment which almost resembled the levels present in healthy controls. The abundances of five amino acids; glutamic acid (level id 1), isoleucine (level id 1), leucine (level id 2), phenylalanine (level id 1) and tryptophan (level id 1), were also significantly higher in the pSS groups in comparison to healthy controls. Of those, LDD treatment normalized the levels of phenylalanine very close to that of healthy controls, but not the other four.

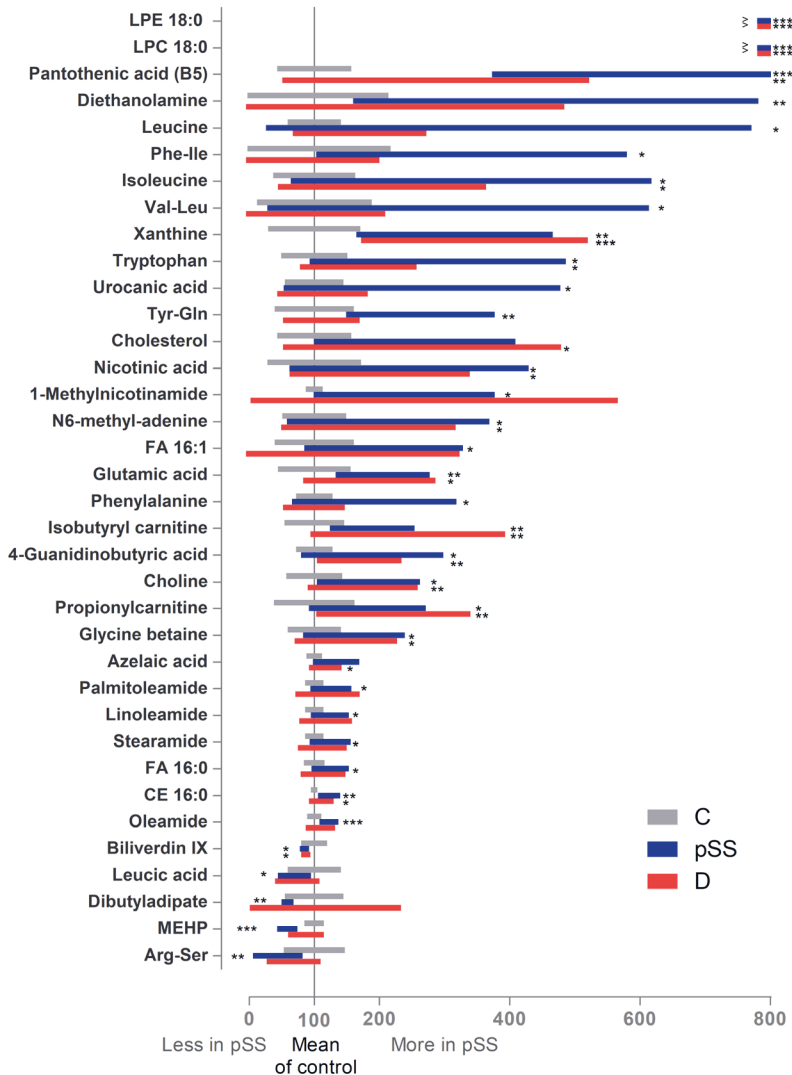


**Figure 11.** Forest Plot of identified salivary metabolites associated with pSS. Mean ion abundance of each metabolite with  $\pm$  standard deviation (SD) in pSS patients without LDD (pSS): red, or with LDD (D): blue, is compared to the corresponding values in the control group (C): grey and presented as percentage. Black asterisks show P-values \*  $< 0.05$ , \*\*  $< 0.01$  and \*\*\*  $< 0.001$  in comparison between pSS patients and healthy controls. Arg-Ser, arginine serine dipeptide; CE 16:0, Cholesteryl palmitic acid; FA, fatty acid; LPC, lysophosphatidylcholine; LPE, lysophosphatidylethanolamine; MEPH, Monoethylhexyl phthalic acid; Phe-Ile, phenylalanine isoleucine dipeptide; Tyr-Gln, tyrosine glutamine dipeptide; Val-Leu, valine leucine dipeptide.

## 5.2 ODOR INDICATION BY SCENT DETECTION DOGS

### 5.2.1 Scent detection threshold

The scent detection threshold of the trained dogs was tested using in-house made *Eucalyptus* hydrolat as a target odor in a three part study in Study III. The essential oil contained 4.12 mol/L of eucalyptol which was identified as the main component of the product by  $^1\text{H}$  NMR (details in Study III article).

In part 1 of the study, the maximum dilution ratio of *Eucalyptus* hydrolat which was correctly indicated by the nose work sport dogs, was  $1:10^{10}$  (2 out of 11 dogs) whereas three dogs indicated only the stock solution with highest concentration ( $1:10^4$ ) (Table 4). On the contrary, Dog 1 with no experience of nose work sports, correctly indicated all samples of dilutions from ratio  $1:10^4$  to  $1:10^{22}$ . When tested again in part 2 of the study, Dog 1 correctly indicated every sample of dilutions from stock solution down to the ratio  $1:10^{23}$ . After the training period in part 3, one of the three dogs reached the same result as Dog 1, indicating a dilution ration as high as  $1:10^{21}$ . In addition, two other dogs indicated very high dilution ratios of  $1:10^{19}$ , and  $1:10^{17}$ . The scent detection threshold is depicted in Figure 12. The amount of substance (n) and the number of eucalyptol molecules in prepared solutions are depicted in Supplementary table 1.

**Table 4.** The scent detection threshold of dogs to in-house *Eucalyptus* hydrolat. Dilution ratio of *Eucalyptus* oil in water is depicted.

Dog ID	Last ratio of <i>E. hydrolat</i> successfully indicated by a dog		
	Part 1	Part 2	Part 3
1	1:10 <sup>22</sup>	1:10 <sup>23</sup>	1:10 <sup>21</sup>
2	1:10 <sup>4</sup>		
3	1:10 <sup>6</sup>		
4	1:10 <sup>6</sup>		
5	1:10 <sup>8</sup>		
6	1:10 <sup>6</sup>		
7	1:10 <sup>8</sup>		
8	1:10 <sup>10</sup>		
9	1:10 <sup>10</sup>		
10	1:10 <sup>4</sup>		
11	1:10 <sup>4</sup>		
12	1:10 <sup>8</sup>		
13			1:10 <sup>19</sup>
14			1:10 <sup>17</sup>
15			1:10 <sup>21</sup>

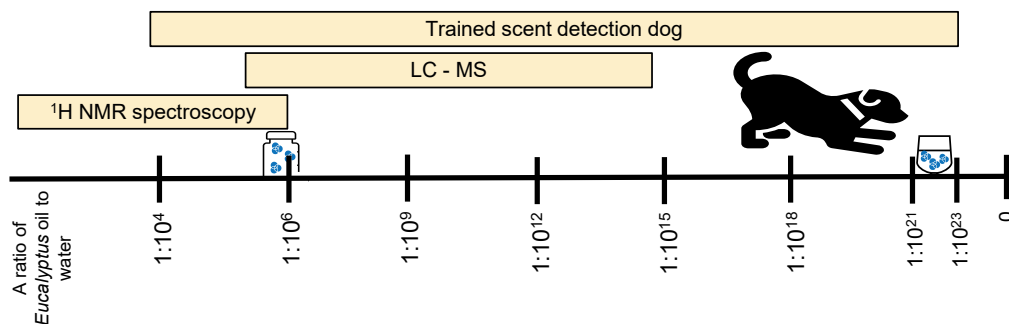


**Figure 12.** Trained scent detection dogs outperform common analytical techniques. In comparison to dogs, the quantitation limit of <sup>1</sup>H NMR spectroscopy was 1:10<sup>6</sup> in this study and in general, LC-MS methods can detect chemical compounds at ratio of 1:10<sup>15</sup>. Figure from Study III (not scaled).

### 5.2.2 Screening the odor of a disease

The diagnostic accuracy of trained scent detection dogs to identify and indicate people infected with SARS-CoV-2 was studied in a three part study setting comprising a training phase, a triple-blinded validation study and a real-life screening in Helsinki-Vantaa airport with more details given in Study IV. A total of nine dogs were further trained at the airport and four of them were selected for validation. Only one of the nine dogs showed poor working motivation for the scent detection at the test cubicle and was withdrawn to the training center.

In the validation study, the overall diagnostic accuracy, i.e., the probability that an individual will be correctly classified as SARS-CoV-2 infected, was 92% (95% CI 90-93%) for all sniffed samples when compared with the findings of RT-PCR. The diagnostic performance of the validated scent detection dogs is shown in Table 5. For all dogs, the combined sensitivity  $Se_{sniff}$  was 92% (95% CI 89-94%) with a specificity  $Sp_{sniff}$  value of 91% (95% CI 89-93%). The variation between the dogs was minor. The  $Se_{sniff}$  and  $Sp_{sniff}$  values for the lowest performance were 88% (95% CI 80-94%) and 90% (95% CI 85-93%), whereas the best performing dog achieved the values 93% (95% CI 85-96%) and 95% (95% CI 91-97%), respectively.



**Table 5.** The diagnostic performance of the dogs in the validation test.

Dog	Dogs' ind-ication	Sniffed RT-PCR pos samples	Sniffed RT-PCR neg samples	Sniffed samples/ all presented samples	Se <sub>sniff</sub> (95% CI)	Sp <sub>sniff</sub> (95% CI)	PPV <sub>sniff</sub> (95% CI)	NPV <sub>sniff</sub> (95% CI)	Se <sub>all</sub> (95% CI)	Sp <sub>all</sub> (95% CI)
Sijja	Pos	99	11	107 / 114	93 % (85-96)	95 % (91-97)	90 % (82-95)	96 % (92-98)	87 % (79-92)	96 % (93-98)
	Neg	8	206	217 / 306						
Rele	Pos	104	18	111 / 114	94 % (87-97)	92 % (87-95)	85 % (77-91)	97 % (93-98)	91 % (84-95)	94 % (91-96)
	Neg	7	197	215 / 306						
Kosti	Pos	99	23	107 / 114	93 % (85-96)	90 % (85-93)	81 % (73-87)	96 % (92-98)	87 % (79-92)	92 % (89-95)
	Neg	8	203	226 / 306						
E.T	Pos	90	23	102 / 114	88 % (80-94)	90 % (85-93)	80 % (71-86)	94 % (90-97)	79 % (70-86)	92 % (89-95)
	Neg	12	201	224 / 306						
All dogs	Pos	392	75	427 / 456	92 % (89-94)	91 % (89-93)	84 % (80-87)	96 % (94-97)	86 % (82-89)	94 % (92-95)
	Neg	35	807	882 / 1224						

CI, confidence interval; Neg, negative; NPV<sub>sniff</sub>, negative predictive value on sniffed samples; Pos, positive; PPV<sub>sniff</sub>, positive predictive value on sniffed samples; RT-PCR, reverse transcriptase polymerase chain reaction; Se<sub>all</sub>, sensitivity on all randomised samples; Se<sub>sniff</sub>, sensitivity on sniffed samples only; Sp<sub>all</sub>, specificity on all randomised samples; Sp<sub>sniff</sub>, specificity on sniffed samples only. PPV<sub>sniff</sub> and NPV<sub>sniff</sub> are based on the prevalence rate of COVID-19 positive samples in the data (27%).

In a total of 19/420 samples, there were discrepancies between the dogs' indications (at least two of the dogs) and the RT-PCR. Fifteen out of 19 samples (79%) were collected during late February and March 2021 and were included in two validation sessions (i.e., VAL 6-7). Eight of the 19 discrepant samples were RT-PCR positive with 11 samples being RT-PCR negative. After re-evaluation (including RT-PCR viral load, SARS-CoV-2 antibodies, symptoms, and time since symptom onset), those eight positive samples were further confirmed as SARS-CoV-2 positive including six alpha variants, one wild-type and one without information. Six out of 11 negative samples were confirmed as SARS-CoV-2 negative whereas four were uncertain and one was classified as a possible positive. Collected data for discrepancies are depicted in Study IV.

Validation sessions 1 and 2 (VAL 1-2) included only wild type SARS-CoV-2 positive samples while sessions from 3 to 7 included also alpha variants. The overall accuracy for SARS-CoV-2 wild type virus according to VAL 1-2 was 97% (95% CI 95-98%),  $Se_{sniff}$  99% (95% CI 96-100%) and  $Sp_{sniff}$  96% (95% CI 93-98%). As a result of all 114 SARS-CoV-2 positive samples, dogs indicated 30 false negative (FN) samples and 84 true positive (TP) samples. The associations of several variables with failure to identify positive samples were studied (for details see Study IV). Based on the odds ratio values with 95% CI, SARS-CoV-2 variant status was associated with a failure to identify positive samples (alpha vs wild-type, odds ratio=14.0, 95% CI 4.5-43.4). All four dogs correctly indicated 89% of the wild-type samples but only 36% of the alpha variant samples. In contrast, other studied variables (gender, concurrent chronic disease, time between symptom onset and sampling, time between PCR test and sampling, increasing age of the COVID-19 patients) were not associated with a failure to identify positive samples.

In the real-life study cohort, 97.7% of samples (296/303) of incoming passengers were correctly indicated by the dogs. The dogs discarded 296 samples as negative and indicated 4 samples as positive from 300 RT-PCR negative samples. From three RT-PCR positive samples, none was indicated as positive by the dogs. A total of seven discrepancies was observed; these were re-evaluated as earlier described. From the three RT-PCR positive

samples, one was determined afterward as SARS-CoV-2 negative, one as SARS-CoV-2 positive (alpha variant) and one as a likely postinfectious positive RT-PCR result whereas all RT-PCR negative samples were determined as SARS-CoV-2 negatives. The collected data for the discrepancies are depicted in Table 6.

In the real-life screening at the airport, the observed prevalence of COVID-19 positive samples was only 0.47 during the seven-month period. To maintain the screening skills for COVID-19 infection and the working motivation of the dogs, novel RT-PCR positive 'spike' samples were collected and imported into the cubicle. From a total of 155 spike samples, the dogs correctly indicated 98.7% as positive. Computationally, the  $Se$  and  $Sp$  would have been 97% (95% CI 92-99%) and 99% (95% CI 96-100%) if the spike samples had been part of the real-life cohort.

Table 6. Discrepancies between SARS-CoV-2 RT-PCR and dog indications in real-life cohort.

ID	Dog response	RT-PCR (viral load)	Symptoms	Time between symptom onset and skin swab / between RT-PCR test and skin swab	Antibody test result (time between RT-PCR test and antibody test, days)	Comment	SARS-CoV-2 infection status (variant, if available)
RL1	Neg	Pos (medium)	Asymptomatic	NA / 0	Neg (81)	Two additional neg PCR tests	Neg (wild-type)
RL2	Neg	Pos (high)	Muscle aches, headache, fever	1 / 0	Pos (57)		Pos (alpha)
RL3	Neg	Pos (medium)	Asymptomatic	-10 / 0	Pos (56)	Fever, cough, dyspnea, headache 10 days before tests	Post-infectious prolonged PCR positivity (wild-type)
RL4	Pos (two dogs)	Neg	Asymptomatic	NA / 0	Neg (178)	Neg scent dog test and PCR-test within 1 month	Neg

ID	Dog response	RT-PCR (viral load)	Symptoms	Time between symptom onset and skin swab / between RT-PCR test and skin swab	Antibody test result (time between RT-PCR test and antibody test, days)	Comment	SARS-CoV-2 infection status (variant, if available)
RL5	Pos/Neg (two dogs)	Neg	Asymptomatic	NA / 0	Neg (97)		Neg
RL6	Pos (two dogs)	Neg	Chest pain, cough, fever, tachycardia	1 / 0	Neg (113)	Second PCR test Neg 4 days after initial test	Neg
RL7	Pos	Neg	Sore throat	-5 / 0	Neg (55)		Neg

ID, Participant identifier; NA, Not available; Neg, Negative; Pos, Positive; RT-PCR, Reverse transcriptase polymerase chain reaction.



## 6 DISCUSSION

The primary objective of this doctoral research was to evaluate the discriminative capabilities of two very different methods, mass spectrometry and scent detection dogs, using non-invasive samples. Both methods were able to differentiate between healthy individuals and those with diseases using saliva and skin swab samples, respectively.

### **Metabolomics as a tool for analysis of saliva**

The research in one part of this thesis used UHPLC-Q-TOF MS to analyze the metabolites present in human saliva. This method provided high-resolution precursor data, and combined with tandem MS, made possible a reliable compound identification. As saliva is mostly water, also HILIC based chromatography was applied in addition to RP. Furthermore, both ionization modes, positive and negative, were utilized which increased the number of detected molecular features and further, were beneficial in identifying the metabolites. This non-targeted metabolomics approach captured data from a broad spectrum of small compounds of which around 200 could be identified. Normalization of saliva samples is a challenge in non-targeted metabolics studies. The properties of saliva, i.e, volume, osmolarity, viscosity, and concentration, vary. There is no method that is universally accepted as a reference for the normalization of saliva samples, in the way that the creatinine concentration is applied in urine metabolomics.

Furthermore, the analysis revealed notable differences in the metabolite profiles between pSS patients and healthy individuals, with most of the identified metabolites showing higher ion abundances in the saliva of the pSS patients. This proved that the method was suitable for characterizing saliva molecular signatures and for the discovery of potential biomarkers.

Already in 2015, the human saliva metabolome was extensively characterized by Dame et al. They identified 308 salivary metabolites using various methods including NMR, GC-MS, inductively coupled plasma-mass spectrometry coupled to MS, direct flow injection coupled to MS, and high-

performance LC (65). They completed the collection with literature-mining and acquired a total of 853 annotated saliva metabolites. With the LC-MS approach, they were able to identify 108 metabolites including amino acids, acylcarnitines, biogenic amines, glycerophospholipids, sphingolipids and vitamins (65). The LC-MS approach utilized in Study I identified 27 of them as well as 17 metabolites which Dame et al. had identified using one of the other platforms listed above. With respect to dog saliva, Study I was the first to reveal its metabolome, and in fact, only a few studies have been published afterwards. Those have described metabolic changes in dog saliva measured with a targeted LC-MS approach for amino acids, biogenic amines, polar and neutral lipids (131, 132).

There is no single analytical technique that can capture all of the small molecules present in a sample, i.e., the whole metabolome. Here, the LC-MS method used had its limitations; it detected those hydrophilic and hydrophobic compounds that are soluble in 80% (v/v) of methanol, ionize in ESI conditions, and have a mass range of  $m/z$  50-1600 Da. These criteria exclude many molecules e.g., saccharides or other carbohydrates as well as volatile short chain fatty acids, and thus they were not detected. Large molecular species like proteins were also not measured, as would be expected from our experimental setup. However, small peptides were evident in the saliva samples; these were identified primarily in human saliva. These peptides are known to originate from protein degradation and are consumed by oral bacteria. Dipeptides as well as single amino acid derivatives are also produced and modified by the oral microbiota (133). In relation to saliva samples, those compound classes might be interesting as microbiota derived metabolites of these compound classes might play an important role regarding the health of teeth and mouth and associated diseases (134, 135).

Moreover, a lipid analysis of human saliva was conducted in 2022; it identified large number of lipids (780 in all) of which 372 had been quantified using nanoflow UHPLC-ESI-MS/MS (136). The result highlights the need for special applications as only 85 lipids and lipid-like molecules were identified in Study I. Most of the non-polar lipids, i.e., neutral lipids, are not extracted in the methanol-based sample preparation protocol used



for saliva samples in Studies I and II since the focus was on polar lipids and water-soluble small molecules. Still, among the lipids, neutral fatty acids were predominant in human saliva whereas no polar phosphatidylcholines (PCs) were detected in human saliva in Study I, even though other investigators have described their presence (65, 137). Furthermore, the metabolomics method used in Study I could detect PCs as they were identified in dog saliva and different PCs have been reported e.g., in human plasma (138). In addition, fewer phosphatidylethanolamines, lysophosphatidylethanolamines, and lysophosphatidylcholines with lower ion signals were observed in human saliva than were evident in the dog saliva. These results are in line with a quantitative study using thin-layer chromatography conducted by Larsson et al. where lipids were detected only at low concentrations in human saliva (139). Furthermore, the whole human saliva was reported to contain more free fatty acids and neutral lipids e.g., di- and triglycerides than polar lipids such as PCs and phosphatidylethanolamines. Similar results have also been reported using a targeted LC-MS/MS method (140).

Furthermore, saliva contains exogenous compounds which originate from the environment, cosmetics, food, and drug intake etc. (141, 142). Here, for example, caffeine and theobromine were identified, being common metabolites originating from coffee and possibly from chocolate-based foods or pharmaceutical products, respectively. It was not surprising that different phthalates were identified as they are ubiquitous in the environment (143), or high levels of different amides which were considered here as contaminants of plastics (144).

The non-targeted metabolomics analysis further revealed significant differences in the saliva metabolite profiles of individuals with pSS when they were compared to healthy controls. The most significantly altered and identified metabolites had higher ion abundances in the saliva of pSS patients in comparison to healthy controls. Fifteen metabolites fulfilled the criteria of MSI (Metabolomics Standards Initiative) to be a potential biomarker whereas 21 should be further confirmed by analyzing the reference standards with the same analytical methods. Studies conducted with LC-MS methods have reported that certain dipeptides are associated

with pSS (79, 145) but the identified ones differed from those found in Study II. In addition, Hynne et al. identified creatine, vanillin, uridine monophosphate, cytidine monophosphate, and uridine at level 1 as the most significantly altered metabolites in pSS patients as compared to controls (79). In contrast, Li et al. reported 38 metabolites that could be used to significantly differentiate pSS patients from healthy controls, but they did not give more details of the level of identification (145). When using NMR and GC-MS, the analyzed saliva metabolites in pSS patients were partially overlapping with the compounds measured with LC-MS, e.g., amino acids but it is known that NMR also detects organic acids and GC-MS volatile compounds (146-148). It is evident that differences in study design, the usage of different analytical platforms followed by variations in upstream analysis including statistical methods, databases, and standard libraries, are responsible for the heterogeneity of the published studies.

Even though part of the metabolome remained uncharacterized, the number of detected molecular features was vast. Here, the data included thousands of molecular features achieving a high coverage of unknown and unidentified compounds. In a non-targeted metabolomics analysis, the identification of metabolites is invariably a challenge. Even with computer-aided approaches, the identification is only semi-automatic and manual inspection of the data is needed in order to make a confident identification, a process which is time-consuming and laborious. Most of the measured signals remained unidentified, although many of these signals likely originate from in-source fragments and adducts (149).

Moreover, a non-targeted approach is semi-quantitative and does not provide any information concerning the concentration of compounds of interest. The use of internal standards would have allowed the reliable quantitation of metabolites as well as an evaluation of the impact of the matrix effect and the yield of metabolites during the extraction step, but this poses challenges. A non-targeted metabolomics approach would have required a broad mix of standard analytes covering all classes of chemical compounds detected. For explorative research such as the ones conducted in this thesis, the benefits would have been limited, and outweighed by other factors for example in terms of costs. In addition, for the validation of

a biomarker, there would be a need to establish targeted LS-MS method. Still, the hypothesis-free nature of the method does give the opportunity to gain new insights and perspectives to be investigated in the future.

### **Scent detection as a tool for the analysis of skin swab samples**

While mass spectrometry provides a detailed analysis of the saliva metabolome, on the other hand, scent detection dogs possess a high-resolution sense of smell and can even outperform the state-of-the-art analytical methods in detecting certain compounds. Study III demonstrated that properly trained dogs could detect extremely low concentrations of a target scent. In comparison, while mass spectrometry can detect compounds at a ratio of 1:10<sup>15</sup>, the dogs detected the scent of eucalyptus in as low a ratio of 1:10<sup>21</sup>; at this level, there are calculated to be only 250 eucalyptol molecules per sniffed sample. Previous studies have reported olfactory thresholds as 1.5x10<sup>-12</sup> and 1.14x10<sup>-12</sup> for dogs using amyl acetate with a fruity odor as the target compound (150, 151). Concha et al. used a multi-choice carousel and mixed the compound with mineral oil whereas in the study of Walker et al., the dogs sniffed the odor of amyl acetate in a stream of air. However, the dogs' performance can vary based on training, motivation, personality, breed and genetic differences as seen also in the results of Study III and IV. For example, training could lead to physiological changes, since rodent studies have shown that training can increase the number of OR cells specific to the target scent molecule and increase the sensitivity towards this molecule (152, 153).

Even though the result was impressive, the study had some limitations. The target scent, in-house *Eucalyptus* hydrolat, originating from the essential oil of *Eucalyptus* which is known to be a mixture of soluble and volatile compounds (154). Quantitative NMR was used to measure the concentration of eucalyptol, the compound with an unambiguous scent which humans recognize as "eucalyptus", in the oil. The concentration of eucalyptol was rather high, and in contrast, no other compounds were detected. In contrast, NMR was limited to soluble molecules with a quantitation limit of 1 ppm and thus, the dilutions were not measured as such. For volatile molecules, GC-MS is needed to profile and quantify the

VOCs in a target scent. It is evident that for less concentrated soluble compounds, LC-MS could be applied since it is much more sensitive than NMR. There is one way to avoid the presence of a mixture of odorous molecules in a sample; a commercial chemical product of eucalyptol could be used as a source material. Conversely, the training part included as part 3 of this trial could be thought as one of its strengths. It allowed the dogs to become familiarized with the target scent and to have practice with the line-ups which improved the result significantly such that all participating dogs identified very low concentrations of the target scent.

When the SARS-CoV-2 virus emerged in Finland in 2020, scent detection dogs were trained to detect COVID-19 in various sample types. In order to achieve a rapid screening, skin swabs were preferable due to their non-invasive nature and ease of sampling. The dogs achieved a high accuracy rate when used to screen COVID-19 in skin swab samples. The validation tests achieved a sensitivity of 92% with a specificity of 91% when compared to RT-PCR. However, their detection rate for the alpha variant was lower, emphasizing the importance of training. A previous study also stated that the diagnostic performance of the dogs decreased towards the omicron variant when compared to the wild-type virus when masks were used as samples (155). The study design differs from others who have used mask samples (10 deep breaths in and out vs. 10 min (156) or 45min (157)). It is possible that too quick sampling may result in a lower overall accuracy (60-63%) when compared to other studies (87% and 97%, respectively). In contrast, Guest et al. claimed that the sensitivity of sniffer dogs was not reduced for the alpha variant when socks were used as a sample (129). In addition, Soggiu et al. reported that they did not observe any deterioration in the dogs' performance when sniffing people directly during the one-year period in 2021 even though the predominant SARS-CoV-2 variants had changed over time, but they lacked genotyping data about the virus (158). The other highlighted confounder studied was vaccination status which was uniformly stated not to affect the dogs' performance (57, 159, 160). In Finland, only 3.5% of the country's citizens had been vaccinated until end of the Study IV period (161) Thus, our study did not include this information.

In the real-life screening at Helsinki-Vantaa airport, the dogs detected nearly 99% of RT-PCR negative samples, but the real-life screening encountered challenges due to the low prevalence of the SARS-CoV-2 infection. The sensitivity could not be tested without positive spike samples and ad hoc analysis. During 2022-2023, a few other real-life scenarios have been published. These include reports from other scenarios e.g., concerts in Germany (160) and a hospital in Hawaii (162) where skin swabs were used as the sample material as well as pharmacy COVID-19 testing queues in North Italy (159) and elementary schools in California (163) where people were directly sniffed by dogs. The results in these studies were convincing, with sensitivity values ranging from 81.5% to 96% and specificity from 90% to 100%. These values exceed the minimum performance criteria of SARS-CoV-2 antigen-detecting rapid diagnostic tests ( $\geq 80\%$  Se and  $\geq 97\%$  Sp) and are even better than the values for antibody test kits ( $> 90\%$  Se and  $> 95\%$  Sp), and for RT-PCR based test kits ( $\geq 95\%$  Se and  $\geq 99\%$  Sp) set by the World Health Organization (WHO), and are convincing evidence that scent detection dogs can be used as a reliable screening tool in outbreaks of COVID-19 infections.

Even though the dogs have superior olfactory abilities for a wide range of chemical and biological detection applications, there is a lack of standardized protocols in the use and validation of detection dogs. Differences arise e.g., from the selection of dogs, the possibility of human bias, and from odor samples and odor delivery, to name just a few. This has been recognized among the canine researchers as proposals for SARS-CoV-2 canine detection standardization were published in 2020 to lay the ground for obtaining consensus for using medical detection dogs in future (128).



## 7 CONCLUSIONS AND FUTURE PROSPECTS

In conclusion, this thesis demonstrated that non-targeted, high-resolution LC-MS method can explore the salivary metabolome and identify changes in saliva metabolites related to a certain disease. Additionally, trained dogs can detect specific scents with high accuracy, outperforming even advanced analytical methods. Both methods proved effective in discriminative tasks when non-invasive sample materials were being tested. The specific conclusions for the aims are as follows:

1. The UHPLC-Q-TOF-MS method is feasible for studying salivary metabolites. The saliva metabolomes of humans and dogs were shown to contain a variety of metabolites within different chemical classes.
2. The non-targeted metabolomics analysis using the UHPLC-Q-TOF-MS method revealed significant differences in the saliva metabolite profiles of individuals with pSS when compared to healthy controls.
3. Trained scent detection dogs can indicate target scents at significantly smaller concentrations than previously reported and are even more sensitive than state-of-the art analytical detectors.
4. The high diagnostic accuracy of scent detection dogs is beneficial when screening skin swabs gathered from SARS-CoV-2 infected individuals. The study also highlights the importance of continuous retraining of dogs with SARS-CoV-2 positive samples as well as the regular inclusion of new emerging variants.

Mass spectrometers have been used for decades to discover novel biomarkers. Nonetheless, diagnostic separation methods based on mass spectrometer methods are of limited clinical use; they are challenging to set-up, and they are not suitable for rapid testing. In addition, they are expensive and limited by their size which means that they need to be located in specialized facilities. Instead, mass spectrometric methods can be used to study and resolve the pathology of different diseases by measuring and identifying changes in metabolic products. This aspect can

be very important in terms of drug development. For example, one option is first to use mass spectrometry-based methods to discover and validate a small molecule biomarker and then to develop easier, cheaper, and portable targeted tests for actual real-world clinical analysis.

While there is a need to continue basic research of non-communicable diseases, it is also evident that new applications are needed to allow the rapid and easy detection of contagious viral infections. Even though in early 2024, the COVID-19 disease caused by the SARS-CoV-2 corona virus is no longer classified in Finland as “a universally dangerous infectious disease”, it should be borne in mind that COVID-19 will not be the last pandemic to pose a threat to humanity. The rapid diagnosis of infectious viral diseases prevents the spread of the infection and therefore possibly protects human lives, reduces the burden on healthcare and can allow society to function in an almost normal manner. As a new application, scent detection dogs have several advantages. They can be trained in a fairly short time for a new target scent, they are transportable and exist globally. These can be considered as some of their key benefits when people need to be screened against pathogens in future pandemics.

Moreover, it is predicted that non-invasive sample materials will play an important role in fast and simple testing. For example, saliva samples, skin swabs or even sniffing the skin of a person represent ways of sampling and testing without the need for professional personnel. As an example, the dog scent test at the Helsinki-Vantaa airport took on average only three minutes from sampling to obtaining the result. This should be compared to the time required to obtain results from RT-PCR, which in the worst-case scenario in 2020, took several days and furthermore was an unpleasant experience for the subject being tested as the swab sample had to be taken from the nasopharynx. Globally, increasing numbers of scent detection dogs have been trained in recent years and the number of publications describing their pros and cons has expanded in the last three years, reflecting the interest towards using the dogs as one applicable discriminative method that is not limited to detecting COVID-19 infections.



## REFERENCES

1. Adams F. The genuine works of Hippocrates: W. Wood; 1886.
2. Gallagher M, Wysocki CJ, Leyden JJ, Spielman A, Sun X, Preti G. Analyses of volatile organic compounds from human skin. *British Journal of Dermatology*. 2008;159(4):780-91.
3. Gokool VA, Crespo-Cajigas J, Mallikarjun A, Collins A, Kane SA, Plymouth V, et al. The use of biological sensors and instrumental analysis to discriminate COVID-19 odor signatures. *Biosensors*. 2022;12(11):1003.
4. Mochalski P, Wiesenhofer H, Allers M, Zimmermann S, Güntner AT, Pineau NJ, et al. Monitoring of selected skin-and breath-borne volatile organic compounds emitted from the human body using gas chromatography ion mobility spectrometry (GC-IMS). *Journal of Chromatography B*. 2018;1076:29-34.
5. Trivedi DK, Sinclair E, Xu Y, Sarkar D, Walton-Doyle C, Liscio C, et al. Discovery of volatile biomarkers of Parkinson's disease from sebum. *ACS central science*. 2019;5(4):599-606.
6. Dyer EM, Waterfield T, Baynes H. How to use C-reactive protein. *Archives of Disease in Childhood-Education and Practice*. 2019;104(3):150-3.
7. Ioannou GN. Implications of elevated serum alanine aminotransferase levels: think outside the liver. *Gastroenterology*. 2008;135(6):1851-4.
8. Arıkan A, Esenay FI. Active and passive distraction interventions in a pediatric emergency department to reduce the pain and anxiety during venous blood sampling: a randomized clinical trial. *Journal of emergency nursing*. 2020;46(6):779-90.
9. Frazee BW, de la Guardia AR-H, Alter H, Chen CG, Fuentes EL, Holzer AK, et al. Accuracy and discomfort of different types of intranasal specimen collection methods for molecular influenza testing in emergency department patients. *Annals of emergency medicine*. 2018;71(4):509-17. e1.
10. Scotton WJ, Mollan SP, Walters T, Doughty S, Botfield H, Markey K, et al. Characterising the patient experience of diagnostic lumbar puncture in idiopathic intracranial hypertension: a cross-sectional online survey. *BMJ open*. 2018;8(5):e020445.

11. Kaloumenou M, Skotadis E, Lagopati N, Efstathopoulos E, Tsoukalas D. Breath Analysis: A Promising Tool for Disease Diagnosis&mdash;The Role of Sensors. *Sensors*. 2022;22(3):1238.
12. Nonaka T, Wong DT. Saliva diagnostics: Salivaomics, saliva exosomics, and saliva liquid biopsy. *The Journal of the American Dental Association*. 2023;154(8):696-704.
13. Tseng C-C, Kung C-T, Chen R-F, Tsai M-H, Chao H-R, Wang Y-N, et al. Recent advances in microfluidic paper-based assay devices for diagnosis of human diseases using saliva, tears and sweat samples. *Sensors and Actuators B: Chemical*. 2021;342:130078.
14. Spick M, Lewis HM, Frampas CF, Longman K, Costa C, Stewart A, et al. An integrated analysis and comparison of serum, saliva and sebum for COVID-19 metabolomics. *Sci Rep*. 2022;12(1):11867.
15. Dettmer K, Aronov PA, Hammock BD. Mass spectrometry-based metabolomics. *Mass spectrometry reviews*. 2007;26(1):51-78.
16. Hinton DJ, Vázquez MS, Geske JR, Hitschfeld MJ, Ho AMC, Karpnyak VM, et al. Metabolomics biomarkers to predict acamprosate treatment response in alcohol-dependent subjects. *Sci Rep*. 2017;7(1):2496.
17. Jääskeläinen T, Kärkkäinen O, Jokkala J, Klåvus A, Heinonen S, Auriola S, et al. A non-targeted LC-MS metabolic profiling of pregnancy: longitudinal evidence from healthy and pre-eclamptic pregnancies. *Metabolomics*. 2021;17(2):20.
18. Kärkkäinen O, Klåvus A, Voutilainen A, Virtanen J, Lehtonen M, Auriola S, et al. Changes in Circulating Metabolome Precede Alcohol-Related Diseases in Middle-Aged Men: A Prospective Population-Based Study With a 30-Year Follow-Up. *Alcohol Clin Exp Res*. 2020;44(12):2457-67.
19. Williams H, Pembroke A. Sniffer dogs in the melanoma clinic? *Lancet*. 1989;1(8640):734.
20. Cambau E, Poljak M. Sniffing animals as a diagnostic tool in infectious diseases. *Clinical Microbiology and Infection*. 2020;26(4):431-5.
21. Muppidi SS, Katragadda R, Lega J, Alford T, Aidman CB, Moore C. A review of the efficacy of a low-cost cancer screening test using cancer sniffing canines. *J Breath Res*. 2021;15(2).

22. Parisis D, Chivasso C, Perret J, Soyfoo MS, Delporte C. Current State of Knowledge on Primary Sjögren's Syndrome, an Autoimmune Exocrinopathy. *Journal of Clinical Medicine*. 2020;9(7):2299.
23. Glish GL, Vachet RW. The basics of mass spectrometry in the twenty-first century. *Nature Reviews Drug Discovery*. 2003;2(2):140-50.
24. Yin V, Devine PW, Saunders JC, Barendregt A, Cusdin F, Ristani A, et al. Stochastic assembly of biomacromolecular complexes: impact and implications on charge interpretation in native mass spectrometry. *Chemical Science*. 2023;14(35):9316-27.
25. Rojas-Chertó M, Kasper PT, Willighagen EL, Vreeken RJ, Hankemeier T, Reijmers TH. Elemental composition determination based on MS n. *Bioinformatics*. 2011;27(17):2376-83.
26. Henry H, Sobhi HR, Scheibner O, Bromirski M, Nimkar SB, Rochat B. Comparison between a high-resolution single-stage Orbitrap and a triple quadrupole mass spectrometer for quantitative analyses of drugs. *Rapid Communications in Mass Spectrometry*. 2012;26(5):499-509.
27. Häkkinen MR, Heinosalo T, Saarinen N, Linnanen T, Voutilainen R, Lakka T, et al. Analysis by LC-MS/MS of endogenous steroids from human serum, plasma, endometrium and endometriotic tissue. *Journal of Pharmaceutical and Biomedical Analysis*. 2018;152:165-72.
28. Ramsay E, Ruponen M, Picardat T, Tengvall U, Tuomainen M, Auriola S, et al. Impact of chemical structure on conjunctival drug permeability: adopting porcine conjunctiva and cassette dosing for construction of in silico model. *Journal of Pharmaceutical Sciences*. 2017;106(9):2463-71.
29. Liu R, Yang Z. Single cell metabolomics using mass spectrometry: Techniques and data analysis. *Analytica chimica acta*. 2021;1143:124-34.
30. Griffiths J. A brief history of mass spectrometry. *Anal Chem*. 2008;80(15):5678-83.
31. Arevalo Jr R, Ni Z, Danell RM. Mass spectrometry and planetary exploration: A brief review and future projection. *Journal of mass spectrometry*. 2020;55(1):e4454.
32. Nolting D, Malek R, Makarov A. Ion traps in modern mass spectrometry. *Mass spectrometry reviews*. 2019;38(2):150-68.

33. Wilm M. Principles of electrospray ionization. *Molecular & cellular proteomics*. 2011;10(7).
34. Glish GL, Goeringer DE. A tandem quadrupole/time-of-flight instrument for mass spectrometry/mass spectrometry. *Analytical Chemistry*. 1984;56(13):2291-5.
35. Forcisi S, Moritz F, Kanawati B, Tziotis D, Lehmann R, Schmitt-Kopplin P. Liquid chromatography–mass spectrometry in metabolomics research: Mass analyzers in ultra high pressure liquid chromatography coupling. *Journal of Chromatography A*. 2013;1292:51-65.
36. Theodoridis GA, Gika HG, Want EJ, Wilson ID. Liquid chromatography–mass spectrometry based global metabolite profiling: a review. *Analytica chimica acta*. 2012;711:7-16.
37. Yin P, Xu G. Current state-of-the-art of nontargeted metabolomics based on liquid chromatography–mass spectrometry with special emphasis in clinical applications. *Journal of Chromatography A*. 2014;1374:1-13.
38. Klåvus A, Kokla M, Noerman S, Koistinen VM, Tuomainen M, Zarei I, et al. “Notame”: Workflow for Non-Targeted LC–MS Metabolic Profiling. *Metabolites*. 2020;10(4):135.
39. Wishart DS, Tzur D, Knox C, Eisner R, Guo AC, Young N, et al. HMDB: the human metabolome database. *Nucleic acids research*. 2007;35(suppl\_1):D521-D6.
40. Ulaszewska MM, Weinert CH, Trimigno A, Portmann R, Andres Lacueva C, Badertscher R, et al. Nutrimetabolomics: an integrative action for metabolomic analyses in human nutritional studies. *Molecular nutrition & food research*. 2019;63(1):1800384.
41. Gika H, Virgiliou C, Theodoridis G, Plumb RS, Wilson ID. Untargeted LC/MS-based metabolic phenotyping (metabonomics/metabolomics): The state of the art. *Journal of Chromatography B*. 2019;1117:136-47.
42. Cajka T, Hricko J, Rudl Kulhava L, Paucova M, Novakova M, Fiehn O, et al. Exploring the Impact of Organic Solvent Quality and Unusual Adduct Formation during LC-MS-Based Lipidomic Profiling. *Metabolites*. 2023;13(9):966.

43. Defossez E, Bourquin J, von Reuss S, Rasmann S, Glauser G. Eight key rules for successful data-dependent acquisition in mass spectrometry-based metabolomics. *Mass Spectrom Rev.* 2023;42(1):131-43.
44. Bilbao A, Varesio E, Luban J, Strambio-De-Castillia C, Hopfgartner G, Müller M, et al. Processing strategies and software solutions for data-independent acquisition in mass spectrometry. *PROTEOMICS.* 2015;15(5-6):964-80.
45. Alonso A, Marsal S, Julià A. Analytical methods in untargeted metabolomics: state of the art in 2015. *Frontiers in bioengineering and biotechnology.* 2015;3:23.
46. Sumner LW, Amberg A, Barrett D, Beale MH, Beger R, Daykin CA, et al. Proposed minimum reporting standards for chemical analysis: chemical analysis working group (CAWG) metabolomics standards initiative (MSI). *Metabolomics.* 2007;3:211-21.
47. Wishart DS, Guo A, Oler E, Wang F, Anjum A, Peters H, et al. HMDB 5.0: the Human Metabolome Database for 2022. *Nucleic Acids Res.* 2022;50(D1):D622-d31.
48. Kim S, Chen J, Cheng T, Gindulyte A, He J, He S, et al. PubChem 2023 update. *Nucleic Acids Res.* 2023;51(D1):D1373-d80.
49. Xue J, Guijas C, Benton HP, Warth B, Siuzdak G. METLIN MS(2) molecular standards database: a broad chemical and biological resource. *Nat Methods.* 2020;17(10):953-4.
50. Conroy MJ, Andrews RM, Andrews S, Cockayne L, Dennis Edward A, Fahy E, et al. LIPID MAPS: update to databases and tools for the lipidomics community. *Nucleic Acids Research.* 2023.
51. Katajamaa M, Orešič M. Processing methods for differential analysis of LC/MS profile data. *BMC bioinformatics.* 2005;6:1-12.
52. Tsugawa H, Cajka T, Kind T, Ma Y, Higgins B, Ikeda K, et al. MS-DIAL: data-independent MS/MS deconvolution for comprehensive metabolome analysis. *Nat Methods.* 2015;12(6):523-6.
53. Tautenhahn R, Patti GJ, Rinehart D, Siuzdak G. XCMS Online: a web-based platform to process untargeted metabolomic data. *Anal Chem.* 2012;84(11):5035-9.

54. Koistinen V, Kärkkäinen O, Keski-Rahkonen P, Tsugawa H, Scalbert A, Arita M, et al. Towards a Rosetta stone for metabolomics: recommendations to overcome inconsistent metabolite nomenclature. *Nature Metabolism*. 2023;5(3):351-4.
55. Kärkkäinen O, Koistinen V, Hanhineva K. Inconsistent nomenclature of microbiota-associated metabolites hampers progress of the field. *Nature Metabolism*. 2022;4(4):406-.
56. Álvarez-Sánchez B, Priego-Capote F, Luque de Castro MD. Metabolomics analysis I. Selection of biological samples and practical aspects preceding sample preparation. *TrAC Trends in Analytical Chemistry*. 2010;29(2):111-9.
57. Callewaert C, Pezavant M, Vandaele R, Meeus B, Vankrunkelsven E, Van Goethem P, et al. Sniffing out safety: canine detection and identification of SARS-CoV-2 infection from armpit sweat. *Frontiers in Medicine*. 2023;10.
58. Cuevas-Córdoba B, Santiago-García J. Saliva: A Fluid of Study for OMICS. *OMICS: A Journal of Integrative Biology*. 2014;18(2):87-97.
59. Humphrey SP, Williamson RT. A review of saliva: Normal composition, flow, and function. *The Journal of Prosthetic Dentistry*. 2001;85(2):162-9.
60. Figlia G, Willnow P, Teلمان AA. Metabolites Regulate Cell Signaling and Growth via Covalent Modification of Proteins. *Developmental Cell*. 2020;54(2):156-70.
61. Gardner A, Carpenter G, So P-W. Salivary Metabolomics: From Diagnostic Biomarker Discovery to Investigating Biological Function. *Metabolites*. 2020;10(2):47.
62. Hyvärinen E, Savolainen M, Mikkonen JJ, Kullaa AM. Salivary metabolomics for diagnosis and monitoring diseases: Challenges and possibilities. *Metabolites*. 2021;11(9):587.
63. Nijakowski K, Zdrojewski J, Nowak M, Gruszczynski D, Knoll F, Surdacka A. Salivary metabolomics for systemic cancer diagnosis: A systematic review. *Metabolites*. 2022;13(1):28.
64. Proctor GB. The physiology of salivary secretion. *Periodontol 2000*. 2016;70(1):11-25.

65. Dame ZT, Aziat F, Mandal R, Krishnamurthy R, Bouatra S, Borzouie S, et al. The human saliva metabolome. *Metabolomics*. 2015;11(6):1864-83.
66. Katsani KR, Sakellari D. Saliva proteomics updates in biomedicine. *Journal of Biological Research-Thessaloniki*. 2019;26(1):17.
67. Ferrari E, Gallo M, Spisni A, Antonelli R, Meleti M, Pertinhez TA. Human Serum and Salivary Metabolomes: Diversity and Closeness. *International Journal of Molecular Sciences*. 2023;24(23):16603.
68. Wood P. Salivary steroid assays—research or routine? *Annals of clinical biochemistry*. 2009;46(3):183-96.
69. Carroll T, Raff H, Findling JW. Late-Night Salivary Cortisol for the Diagnosis of Cushing Syndrome: a Meta-Analysis. *Endocrine Practice*. 2009;15(4):335-42.
70. Huan T, Tran T, Zheng J, Sapkota S, MacDonald SW, Camicioli R, et al. Metabolomics analyses of saliva detect novel biomarkers of Alzheimer's disease. *Journal of Alzheimer's Disease*. 2018;65(4):1401-16.
71. Marksteiner J, Oberacher H, Humpel C. Acyl-alkyl-phosphatidylcholines are decreased in saliva of patients with alzheimer's disease as identified by targeted metabolomics. *Journal of Alzheimer's Disease*. 2019;68(2):583-9.
72. Liebsch C, Pitchika V, Pink C, Samietz S, Kastenmüller G, Artati A, et al. The saliva metabolome in association to oral health status. *Journal of Dental Research*. 2019;98(6):642-51.
73. Frampas CF, Longman K, Spick M, Lewis H-M, Costa CD, Stewart A, et al. Untargeted saliva metabolomics by liquid chromatography—Mass spectrometry reveals markers of COVID-19 severity. *PLoS One*. 2022;17(9):e0274967.
74. Goodson JM, Hardt M, Hartman M-L, Schulte F, Tavares M, Mutawa A-S, et al. Identification of salivary and plasma biomarkers for obesity in children by non-targeted metabolomic analysis. *BioRxiv*. 2018:371815.
75. Zhang J, Wen X, Li Y, Li X, Qian C, Tian Y, et al. Diagnostic approach to thyroid cancer based on amino acid metabolomics in saliva by ultra-performance liquid chromatography with high resolution mass spectrometry. *Talanta*. 2021;235:122729.

76. Dosedělová V, Laštovičková M, Ayala-Cabrera JF, Dolina J, Konečný Š, Schmitz OJ, et al. Quantification and identification of bile acids in saliva by liquid chromatography-mass spectrometry: Possible non-invasive diagnostics of Barrett's esophagus? *Journal of Chromatography A*. 2022;1676:463287.
77. Murata T, Yanagisawa T, Kurihara T, Kaneko M, Ota S, Enomoto A, et al. Salivary metabolomics with alternative decision tree-based machine learning methods for breast cancer discrimination. *Breast cancer research and treatment*. 2019;177:591-601.
78. Bosman P, Pichon V, Acevedo AC, Modesto FM, Paula LM, Le Pottier L, et al. Identification of potential salivary biomarkers for Sjögren's syndrome with an untargeted metabolomic approach. *Metabolomics*. 2023;19(9):76.
79. Hynne H, Sandås EM, Elgstøen KBP, Rootwelt H, Utheim TP, Galtung HK, et al. Saliva metabolomics in dry mouth patients with head and neck cancer or Sjögren's syndrome. *Cells*. 2022;11(3):323.
80. Jenkins EK, DeChant MT, Perry EB. When the Nose Doesn't Know: Canine Olfactory Function Associated With Health, Management, and Potential Links to Microbiota. *Frontiers in Veterinary Science*. 2018;5.
81. Kokocińska-Kusiak A, Woszczyło M, Zybala M, Maciocha J, Barłowska K, Dziecioł M. Canine Olfaction: Physiology, Behavior, and Possibilities for Practical Applications. *Animals*. 2021;11(8):2463.
82. Kavoi B, Makanya A, Hassanali J, Carlsson H-E, Kiama S. Comparative functional structure of the olfactory mucosa in the domestic dog and sheep. *Annals of Anatomy - Anatomischer Anzeiger*. 2010;192(5):329-37.
83. Issel-Tarver L, Rine J. The Evolution of Mammalian Olfactory Receptor Genes. *Genetics*. 1997;145(1):185-95.
84. Fitzek M, Patel PK, Solomon PD, Lin B, Hummel T, Schwob JE, et al. Integrated age-related immunohistological changes occur in human olfactory epithelium and olfactory bulb. *J Comp Neurol*. 2022;530(12):2154-75.
85. Helwany M, Bordonni B. Neuroanatomy, cranial nerve 1 (olfactory). 2020.
86. Neuhaus W, Müller A. Das Verhältnis der Riechzellenzahl zur Rieschshwelle beim Hund. *Naturwiss* 1954;41.



87. Neuhaus W, Müller A. The relationship of the number of olfactory cells to the olfactory threshold in the dog. Translation done by CL Lust 1969.
88. Firestein S. How the olfactory system makes sense of scents. *Nature*. 2001;413(6852):211-8.
89. Quignon P, Kirkness E, Cadieu E, Touleimat N, Guyon R, Renier C, et al. Comparison of the canine and human olfactory receptor gene repertoires. *Genome biology*. 2003;4(12):1-9.
90. Robin S, Tacher S, Rimbault M, Vaysse A, Dréano S, André C, et al. Genetic diversity of canine olfactory receptors. *BMC genomics*. 2009;10(1):1-16.
91. Tacher S, Quignon P, Rimbault M, Dreano S, Andre C, Galibert F. Olfactory receptor sequence polymorphism within and between breeds of dogs. *Journal of Heredity*. 2005;96(7):812-6.
92. Quignon P, Rimbault M, Robin S, Galibert F. Genetics of canine olfaction and receptor diversity. *Mamm Genome*. 2012;23(1-2):132-43.
93. Jendryn P, Twele F, Meller S, Osterhaus A, Schalke E, Volk HA. Canine olfactory detection and its relevance to medical detection. *BMC Infect Dis*. 2021;21(1):838.
94. Mahdy EAA, El Behery El, Mohamed SKA. Comparative morpho-histological analysis on the vomeronasal organ and the accessory olfactory bulb in Balady dogs (*Canis familiaris*) and New Zealand rabbits (*Oryctolagus cuniculus*). *J Adv Vet Anim Res*. 2019;6(4):506-15.
95. Yilmaz B, Yildiz H, Akkoc C, Arican I. Vomeronasal organ in labrador retriever dog (*Canis familiaris*). *Bull Vet Inst Pulawy*. 2008;52:185-8.
96. Barrios AW, Sánchez-Quinteiro P, Salazar I. Dog and mouse: toward a balanced view of the mammalian olfactory system. *Frontiers in Neuroanatomy*. 2014;8.
97. McGlone JJ, Archer C, Henderson M. Interpretive review: Semiochemicals in domestic pigs and dogs. *Front Vet Sci*. 2022;9:967980.
98. Craven BA, Paterson EG, Settles GS. The fluid dynamics of canine olfaction: unique nasal airflow patterns as an explanation of macrosmia. *Journal of the Royal Society Interface*. 2010;7(47):933-43.

99. Goss K-U. The physical chemistry of odors—Consequences for the work with detection dogs. *Forensic Science International*. 2019;296:110-4.
100. Carroll GT, Kirschman DL. A Peripherally Located Air Recirculation Device Containing an Activated Carbon Filter Reduces VOC Levels in a Simulated Operating Room. *ACS Omega*. 2022;7(50):46640-5.
101. Genva M, Kenne Kemene T, Deleu M, Lins L, Fauconnier M-L. Is It Possible to Predict the Odor of a Molecule on the Basis of its Structure? *International Journal of Molecular Sciences*. 2019;20(12):3018.
102. Brookes JC, Horsfield AP, Stoneham AM. Odour character differences for enantiomers correlate with molecular flexibility. *J R Soc Interface*. 2009;6(30):75-86.
103. Hall NJ, Glenn K, Smith DW, Wynne CD. Performance of Pugs, German Shepherds, and Greyhounds (*Canis lupus familiaris*) on an odor-discrimination task. *Journal of Comparative Psychology*. 2015;129(3):237.
104. Moser AY, Brown WY, Bennett P, Taylor PS, Wilson B, McGreevy P. Defining the Characteristics of Successful Biosecurity Scent Detection Dogs. *Animals*. 2023;13(3):504.
105. Vieira de Castro AC, Araújo Â, Fonseca A, Olsson IAS. Improving dog training methods: Efficacy and efficiency of reward and mixed training methods. *Plos one*. 2021;16(2):e0247321.
106. Amann A, de Lacy Costello B, Miekisch W, Schubert J, Buszewski B, Pleil J, et al. The human volatilome: volatile organic compounds (VOCs) in exhaled breath, skin emanations, urine, feces and saliva. *Journal of breath research*. 2014;8(3):034001.
107. Angle C, Waggoner LP, Ferrando A, Haney P, Passler T. Canine detection of the volatilome: a review of implications for pathogen and disease detection. *Frontiers in veterinary science*. 2016;3:47.
108. Lamote K, Janssens E, Schillebeeckx E, Lapperre TS, De Winter BY, Van Meerbeeck J. The scent of COVID-19: viral (semi-) volatiles as fast diagnostic biomarkers? *Journal of breath research*. 2020;14(4).
109. Zou Z, Yang X. Skin volatile organic compound emissions from 14 healthy young adults under controlled conditions. *Building and Environment*. 2022;222:109416.

110. Mitra A, Choi S, Boshier PR, Razumovskaya-Hough A, Belluomo I, Spanel P, et al. The human skin volatolome: A systematic review of untargeted mass spectrometry analysis. *Metabolites*. 2022;12(9):824.
111. Dryahina K, Sovová K, Nemeč A, Španěl P. Differentiation of pulmonary bacterial pathogens in cystic fibrosis by volatile metabolites emitted by their in vitro cultures: *Pseudomonas aeruginosa*, *Staphylococcus aureus*, *Stenotrophomonas maltophilia* and the *Burkholderia cepacia* complex. *Journal of breath research*. 2016;10(3):037102.
112. McCartney MM, Linderholm AL, Yamaguchi MS, Falcon AK, Harper RW, Thompson GR, III, et al. Predicting Influenza and Rhinovirus Infections in Airway Cells Utilizing Volatile Emissions. *The Journal of Infectious Diseases*. 2021;224(10):1742-50.
113. Vishinkin R, Busool R, Mansour E, Fish F, Esmail A, Kumar P, et al. Profiles of volatile biomarkers detect tuberculosis from skin. *Advanced Science*. 2021;8(15):2100235.
114. Pulido H, Stanczyk NM, De Moraes CM, Mescher MC. A unique volatile signature distinguishes malaria infection from other conditions that cause similar symptoms. *Scientific Reports*. 2021;11(1):13928.
115. Morgan J. Joy of super smeller: sebum clues for PD diagnostics. *The Lancet Neurology*. 2016;15(2):138-9.
116. George A. The woman who can smell Parkinson's. *New Scientist*. 2019;241(3220):40-1.
117. Kane SA, Lee YE, Essler JL, Mallikarjun A, Preti G, Verta A, et al. Canine discrimination of ovarian cancer through volatile organic compounds. *Talanta*. 2022;250:123729.
118. Grizzi F, Bax C, Hegazi MA, Lotesoriere BJ, Zanoni M, Vota P, et al. Early Detection of Prostate Cancer: The Role of Scent. *Chemosensors*. 2023;11(7):356.
119. Mazzola SM, Pirrone F, Sedda G, Gasparri R, Romano R, Spaggiari L, et al. Two-step investigation of lung cancer detection by sniffer dogs. *Journal of Breath Research*. 2020;14(2):026011.
120. Taylor MT, McCready J, Broukhanski G, Kirpalaney S, Lutz H, Powis J, editors. Using dog scent detection as a point-of-care tool to identify

- toxigenic clostridium difficile in stool. *Open Forum Infectious Diseases*; 2018: Oxford University Press US.
121. Guest C, Pinder M, Doggett M, Squires C, Affara M, Kandeh B, et al. Trained dogs identify people with malaria parasites by their odour. *The Lancet Infectious Diseases*. 2019;19(6):578-80.
  122. Hardin DS, Anderson W, Cattet J. Dogs can be successfully trained to alert to hypoglycemia samples from patients with type 1 diabetes. *Diabetes Therapy*. 2015;6:509-17.
  123. Catala A, Grandgeorge M, Schaff J-L, Cousillas H, Hausberger M, Cattet J. Dogs demonstrate the existence of an epileptic seizure odour in humans. *Scientific reports*. 2019;9(1):4103.
  124. Maa E, Arnold J, Ninedorf K, Olsen H. Canine detection of volatile organic compounds unique to human epileptic seizure. *Epilepsy & Behavior*. 2021;115:107690.
  125. Wilson C, Campbell K, Petzel Z, Reeve C. Dogs can discriminate between human baseline and psychological stress condition odours. *Plos one*. 2022;17(9):e0274143.
  126. Gao CQ, Wang SN, Wang MM, Li JJ, Qiao JJ, Huang JJ, et al. Sensitivity of sniffer dogs for a diagnosis of Parkinson's disease: a diagnostic accuracy study. *Movement Disorders*. 2022;37(9):1807-16.
  127. Reeve C, Wilson C, Hanna D, Gadbois S. Dog Owners' Survey reveals Medical Alert Dogs can alert to multiple conditions and multiple people. *PLoS One*. 2021;16(4):e0249191.
  128. Meller S, Al Khatri MSA, Alhammadi HK, Álvarez G, Alvergnat G, Alves LC, et al. Expert considerations and consensus for using dogs to detect human SARS-CoV-2-infections. *Frontiers in Medicine*. 2022;9.
  129. Guest C, Dewhirst SY, Lindsay SW, Allen DJ, Aziz S, Baerenbold O, et al. Using trained dogs and organic semi-conducting sensors to identify asymptomatic and mild SARS-CoV-2 infections: an observational study. *Journal of Travel Medicine*. 2022;29(3).
  130. Trevethan R. Sensitivity, specificity, and predictive values: foundations, pliabilities, and pitfalls in research and practice. *Frontiers in public health*. 2017;5:307.

131. González-Arostegui LG, Rubio CP, Rubić I, Rafaj RB, Gotić J, Cerón JJ, et al. Changes in the salivary metabolome in canine hypothyroidism: A pilot study. *Research in Veterinary Science*. 2022;151:189-95.
132. Muñoz-Prieto A, Rubić I, Horvatić A, Rafaj RB, Cerón JJ, Tvarijonavičiute A, et al. Evaluation of Changes in Metabolites of Saliva in Canine Obesity Using a Targeted Metabolomic Approach. *Animals*. 2021;11(9):2501.
133. Liebsch C, Pitchika V, Pink C, Samietz S, Kastenmüller G, Artati A, et al. The Saliva Metabolome in Association to Oral Health Status. *J Dent Res*. 2019;98(6):642-51.
134. Barnes VM, Ciancio SG, Shibly O, Xu T, Devizio W, Trivedi HM, et al. Metabolomics reveals elevated macromolecular degradation in periodontal disease. *J Dent Res*. 2011;90(11):1293-7.
135. Rzeznik M, Triba MN, Levy P, Jungo S, Botosoa E, Duchemann B, et al. Identification of a discriminative metabolomic fingerprint of potential clinical relevance in saliva of patients with periodontitis using <sup>1</sup>H nuclear magnetic resonance (NMR) spectroscopy. *PLOS ONE*. 2017;12(8):e0182767.
136. Lee GB, Caner A, Moon MH. Optimisation of saliva volumes for lipidomic analysis by nanoflow ultrahigh performance liquid chromatography-tandem mass spectrometry. *Analytica Chimica Acta*. 2022;1193:339318.
137. Lee GB, Caner A, Moon MH. Optimisation of saliva volumes for lipidomic analysis by nanoflow ultrahigh performance liquid chromatography-tandem mass spectrometry. *Anal Chim Acta*. 2022;1193:339318.
138. Meuronen T, Lankinen MA, Kärkkäinen O, Laakso M, Pihlajamäki J, Hanhineva K, et al. FADS1 rs174550 genotype and high linoleic acid diet modify plasma PUFA phospholipids in a dietary intervention study. *Eur J Nutr*. 2022;61(2):1109-20.
139. Larsson B, Olivecrona G, Ericson T. Lipids in human saliva. *Archives of Oral Biology*. 1996;41(1):105-10.
140. Caterino M, Fedele R, Carnovale V, Castaldo A, Gelzo M, Iacotucci P, et al. Lipidomic alterations in human saliva from cystic fibrosis patients. *Sci Rep*. 2023;13(1):600.

141. Bentley MC, Abrar M, Kelk M, Cook J, Phillips K. Validation of an assay for the determination of cotinine and 3-hydroxycotinine in human saliva using automated solid-phase extraction and liquid chromatography with tandem mass spectrometric detection. *Journal of Chromatography B: Biomedical Sciences and Applications*. 1999;723(1-2):185-94.
142. Bessonneau V, Pawliszyn J, Rappaport SM. The saliva exposome for monitoring of individuals' health trajectories. *Environmental health perspectives*. 2017;125(7):077014.
143. Hauser R, Calafat A. Phthalates and human health. *Occupational and environmental medicine*. 2005;62(11):806-18.
144. Jug U, Naumoska K, Metličar V, Schink A, Makuc D, Vovk I, et al. Interference of oleamide with analytical and bioassay results. *Scientific Reports*. 2020;10(1):2163.
145. Li Z, Mu Y, Guo C, You X, Liu X, Li Q, et al. Analysis of the saliva metabolic signature in patients with primary Sjögren's syndrome. *Plos one*. 2022;17(6):e0269275.
146. Kageyama G, Saegusa J, Irino Y, Tanaka S, Tsuda K, Takahashi S, et al. Metabolomics analysis of saliva from patients with primary Sjögren's syndrome. *Clinical & Experimental Immunology*. 2015;182(2):149-53.
147. Mikkonen JJ, Herrala M, Soininen P, Lappalainen R, Tjäderhane L, Seitsalo H, et al. Metabolic profiling of saliva in patients with primary Sjögren's syndrome. *Metabolomics*. 2013;3(3):1.
148. Setti G, Righi V, Mucci A, Panari L, Bernardelli G, Tarentini E, et al. Metabolic Profile of Whole Unstimulated Saliva in Patients with Sjögren's Syndrome. *Metabolites*. 2023;13(3):348.
149. Domingo-Almenara X, Montenegro-Burke JR, Guijas C, Majumder EL-W, Benton HP, Siuzdak G. Autonomous METLIN-guided in-source fragment annotation for untargeted metabolomics. *Analytical chemistry*. 2019;91(5):3246-53.
150. Concha AR, Guest CM, Harris R, Pike TW, Feugier A, Zulch H, et al. Canine olfactory thresholds to amyl acetate in a biomedical detection scenario. *Frontiers in Veterinary Science*. 2019;5:345.

151. Walker DB, Walker JC, Cavnar PJ, Taylor JL, Pickel DH, Hall SB, et al. Naturalistic quantification of canine olfactory sensitivity. *Applied Animal Behaviour Science*. 2006;97(2-4):241-54.
152. Wang H-W, Wysocki CJ, Gold GH. Induction of olfactory receptor sensitivity in mice. *Science*. 1993;260(5110):998-1000.
153. Youngentob SL, Kent PF. Enhancement of odorant-induced mucosal activity patterns in rats trained on an odorant identification task. *Brain research*. 1995;670(1):82-8.
154. Ieri F, Cecchi L, Giannini E, Clemente C, Romani A. GC-MS and HS-SPME-GC× GC-TOFMS determination of the volatile composition of essential oils and hydrosols (By-products) from four Eucalyptus species cultivated in Tuscany. *Molecules*. 2019;24(2):226.
155. Ozgur-Buyukatalay E, Demirbas YS, Bozdayi G, Kismali G, Ilhan MN. Is diagnostic performance of SARS-CoV-2 detection dogs reduced-due to virus variation-over the time? *Applied Animal Behaviour Science*. 2023;258:105825.
156. Devillier P, Gallet C, Salvator H, Lecoq-Julien C, Naline E, Roisse D, et al. Biomedical detection dogs for the identification of SARS-CoV-2 infections from axillary sweat and breath samples. *Journal of Breath Research*. 2022;16(3):037101.
157. Mendel J, Frank K, Edlin L, Hall K, Webb D, Mills J, et al. Preliminary accuracy of COVID-19 odor detection by canines and HS-SPME-GC-MS using exhaled breath samples. *Forensic Science International: Synergy*. 2021;3:100155.
158. Soggiu F, Sabbatinelli J, Giuliani A, Benedetti R, Marchegiani A, Sgarangella F, et al. Sensitivity and specificity of in vivo COVID-19 screening by detection dogs: Results of the C19-Screendog multicenter study. *Heliyon*. 2023;9(5).
159. Pirrone F, Piotti P, Galli M, Gasparri R, La Spina A, Spaggiari L, et al. Sniffer dogs performance is stable over time in detecting COVID-19 positive samples and agrees with the rapid antigen test in the field. *Scientific Reports*. 2023;13(1):3679.

160. Ten Hagen NA, Twele F, Meller S, Wijnen L, Schulz C, Schoneberg C, et al. Canine real-time detection of SARS-CoV-2 infections in the context of a mass screening event. *BMJ global health*. 2022;7(11):e010276.
161. Rokotusten edistyminen sairaanhoitopiireissä viikoittain eri ikäryhmissä: Terveyden ja hyvinvoinnin laitos; [cited 2023 Dec 14]. Available from: [https://sampo.thl.fi/pivot/prod/fi/vaccreg/cov19cov/summary\\_cov19covareatime](https://sampo.thl.fi/pivot/prod/fi/vaccreg/cov19cov/summary_cov19covareatime).
162. Maurer M, Seto T, Guest C, Somal A, Julian C. Detection of SARS-CoV-2 by Canine Olfaction: A Pilot Study. *Open Forum Infectious Diseases*. 2022;9(7).
163. Glaser CA, Le Marchand CE, Rizzo K, Bornstein L, Messenger S, Edwards CA, et al. Lessons Learned From a COVID-19 Dog Screening Pilot in California K-12 Schools. *JAMA Pediatrics*. 2023;177(6):644-6.



# APPENDICES

### APPENDIX 1. SUPPLEMENTAL TABLE STUDY III

**Supplementary table 1.** Prepared dilutions in part 1 of Study III.

<b>solution</b>	<b>preparation of dilutions</b>	<b>dilution ratio</b>	<b>n(eucalyptol) mol</b>	<b>Number of eucalyptol molecules</b>	<b>Number of eucalyptol molecules/ml</b>
stock solution	0.1 ml <i>Eucalyptus</i> oil, ad 1000 ml H <sub>2</sub> O	1:10 <sup>4</sup>	4.12x10 <sup>-4</sup>	2.48x10 <sup>20</sup>	2.48x10 <sup>17</sup>
dilution 1	0.1 ml stock solution, ad 10 ml H <sub>2</sub> O	1:10 <sup>6</sup>	4.12x10 <sup>-8</sup>	2.48x10 <sup>16</sup>	2.48x10 <sup>15</sup>
dilution 2	0.1 ml of dilution 1, ad 10 ml H <sub>2</sub> O	1:10 <sup>8</sup>	4.12x10 <sup>-10</sup>	2.48x10 <sup>14</sup>	2.48x10 <sup>13</sup>
dilution 3	0.1 ml of dilution 2, ad 10 ml H <sub>2</sub> O	1:10 <sup>10</sup>	4.12x10 <sup>-12</sup>	2.48x10 <sup>12</sup>	2.48x10 <sup>11</sup>
dilution 4	0.1 ml of dilution 3, ad 10 ml H <sub>2</sub> O	1:10 <sup>12</sup>	4.12x10 <sup>-14</sup>	2.48x10 <sup>10</sup>	2.48x10 <sup>9</sup>
dilution 5	0.1 ml of dilution 4, ad 10 ml H <sub>2</sub> O	1:10 <sup>14</sup>	4.12x10 <sup>-16</sup>	2.48x10 <sup>8</sup>	2.48x10 <sup>7</sup>
dilution 6	0.1 ml of dilution 5, ad 10 ml H <sub>2</sub> O	1:10 <sup>16</sup>	4.12x10 <sup>-18</sup>	2.48x10 <sup>6</sup>	2.48x10 <sup>5</sup>
dilution 7	0.1 ml of dilution 6, ad 10 ml H <sub>2</sub> O	1:10 <sup>18</sup>	4.12x10 <sup>-20</sup>	2.48x10 <sup>4</sup>	2482
dilution 8	0.1 ml of dilution 7, ad 10 ml H <sub>2</sub> O	1:10 <sup>20</sup>	4.12x10 <sup>-22</sup>	248	25
dilution 9	0.1 ml of dilution 8, ad 10 ml H <sub>2</sub> O	1:10 <sup>22</sup>	4.12x10 <sup>-24</sup>	2.5	0.25
dilution 10	0.1 ml of dilution 9, ad 10 ml H <sub>2</sub> O	1:10 <sup>24</sup>	4.12x10 <sup>-26</sup>	0.025	0.0025

The measured concentration of eucalyptol was 4.12x10<sup>-4</sup> mol/L; one Liter contains 4.12x10<sup>-4</sup> moles. The numbers of molecules in prepared solutions are calculated as follows: n x the Avogadro constant = 4.12x10<sup>4</sup> moles x 6.022x10<sup>23</sup> molecules/mol. mol, mole; n, amount of substance.

## APPENDIX 2. SUPPLEMENTAL TABLE STUDY I

**Supplementary table 2.** Identified metabolites in human saliva samples presented with the relative proportions of ion abundance.

Metabolite	Level of ID	Min	Med	Max	Mean	SD	n
Amino acids							
alanine	1	13180	22480	40910	24230	8319	14
arginine	1	436614	1409422	2045075	1489431	447851	14
aspartic acid	1	66610	249145	399489	226772	102281	14
glutamic acid	1	92510	219896	477880	224739	92767	14
glutamine	1	85529	149544	318895	180241	76951	14
histidine	1	354376	488143	1069618	563633	238881	14
isoleucine	1	31420	140750	246619	147429	62886	14
leucine	2	20697	119312	196690	112620	46369	14
lysine	1	57367	321507	489095	318715	131502	14
phenylalanine	1	342100	592727	1013511	614751	174399	14
proline	1	261167	3878169	11401076	3976177	3076374	14
serine	2	<10000	37455	88258	44710	18924	12
threonine	1	11676	23103	58526	25260	12162	14
tryptophan	1	<10000	<10000	34288	22474	8173	5
tyrosine	1	79017	183192	412868	212325	92235	14
Amino acid derivatives							
1-methyl-histidine	1	11191	18643	50624	21900	10602	14

Metabolite	Level of ID	Min	Med	Max	Mean	SD	n
3-methyl-histidine	2	<10000	<10000	43698	19375	12606	6
5-aminovaleric acid betaine	1	39681	110597	561505	139903	126323	14
carnitine	1	810251	1485396	5209412	1917738	1102753	14
citrulline	1	148079	360197	665101	369305	145733	14
creatine	1	1070832	1599528	2560989	1700864	494218	14
gamma glutamylglutamic acid	2	<10000	23557	101558	33655	27037	13
glycinebetaine	1	450155	1191462	2241265	1241617	504031	14
ornithine	1	112063	199787	369461	204923	83444	14
Biogenic amines							
asymmetric dimethylarginine	2	12057	19586	34784	21326	7535	14
cadaverine	1	20062	106938	336618	133957	106304	14
carnosine	1	<10000	<10000	14069	14069		1
creatinine	1	<10000	1768218	2807040	2005721	372065	10
histamine	1	<10000	27233	213795	62439	65065	12
spermidine	1	0	346	1729	596	595	14
taurine	2	33028	62705	83051	59969	18544	14
Lipids and carnitines							
acetylcarnitine	1	<10000	192280	544614	209886	155149	12
acylcarnitine C18:0	1	235	1271	2876	1280	785	14
azelaic acid	1	37854	45207	56463	46004	5591	14
DAG 34:1	2	<10000	<10000	23115	14244	4913	6
DAG 34:2	2	<10000	<10000	15559	12893	2044	5

Metabolite	Level of ID	Min	Med	Max	Mean	SD	n
DAG 36:3	2	<10000	<10000	23245	18128	6431	3
DAG 36:4	2	<10000	<10000	20966	18895	2930	2
FA 15:0	2	37879	71890	127786	66323	24722	14
FA 16:0	2	1741092	1969314	2418832	2000694	183002	14
FA 16:1	2	84217	278554	769808	291295	177097	14
FA 17:0	1	68962	84249	158464	94333	27753	14
FA 17:1	2	14253	34183	68761	35190	16365	14
FA 18:0	1	1762724	2137965	2902604	2195405	326722	14
FA 18:1	1	303215	485606	1395954	583143	303394	14
FA 18:2	2	86616	245000	857574	279117	203476	14
FA 18:3	2	<10000	16226	73462	28859	18151	9
FA 20:0	1	19776	31424	55360	32248	10277	14
FA 20:1	2	13801	17572	37779	20803	7991	14
FA 20:2	2	<10000	16496	48413	19957	10024	13
FA 20:3	2	16123	33537	140139	42078	31377	14
FA 20:4	2	<10000	87885	479090	130923	118481	13
FA 20:5	2	<10000	11784	41867	20218	9928	7
FA 21:0	2	2349	3090	4398	3227	683	14
FA 22:0	2	<10000	10423	18567	12280	3097	10
FA 22:1	1	<10000	<10000	11683	11653	43	2
FA 22:2	2	1079	2239	4427	2361	1002	14
FA 22:3	2	1854	3440	8009	3691	1764	14

Metabolite	Level of ID	Min	Med	Max	Mean	SD	n
FA 22:4	2	<10000	<10000	38537	17823	10383	6
FA 24:1 (n-9)	1	1357	3363	7059	3616	1829	14
gamma-butyrobetaine	2	228851	711345	1685899	834362	488931	14
glycerophosphocholine	1	<10000	<10000	23768	23768		1
hydroxypalmitic acid	2	<10000	11255	17943	13525	2604	8
isobutryl carnitine	2	15871	45861	94737	50626	23350	14
isovaleryl carnitine	1	29009	62403	402540	88812	96779	14
leucic acid	2	26369	59768	105831	61064	25243	14
LPC 16:0	2	<10000	<10000	19228	13555	4181	4
LPC 18:0	2	<10000	<10000	41702	26734	12999	3
LPC 18:1	2	0	0	8504	1628	2640	14
LPC 18:2	2	673	1492	3643	1826	1036	14
LPE 16:0	2	1119	2268	7056	2670	1572	14
LPE 18:0	2	<10000	<10000	12287	12287		1
LPE 18:1	2	1050	3011	5784	3004	1390	14
panthenol	2	326	1009	7555	2178	2291	14
PC 38:5e (18:1e_20:4)	2	2370	4163	5414	4188	770	14
PE 30:0 (15:0_15:0)	2	92	514	1695	519	397	14
PE 32:1 (15:0_17:1)	2	<10000	<10000	14513	14513		1
PE 34:2 (16:1_18:1)	2	<10000	<10000	13358	13358		1
PE 36:2 (18:1_18:1)	2	<10000	<10000	19097	19097		1
PE 36:2e (18:1e_18:1)	2	<10000	<10000	16125	13880	3175	2

Metabolite	Level of ID	Min	Med	Max	Mean	SD	n
PE 36:3e (18:2e_18:1)	2	6967	10393	18368	10947	3231	14
PE 36:4e (16:0e_20:4)	2	<10000	<10000	17742	12711	4358	3
PE 36:5e (16:1e_20:4)	2	<10000	12316	25173	16982	5299	10
PE 38:4 (18:0_20:4)	2	2183	4915	11117	5457	2304	14
PE 38:4e (18:0e_20:4)	2	482	1733	3541	1794	814	14
PE 38:5e (18:1e_20:4)	2	<10000	13631	29876	18679	5241	8
PE 38:6e (18:2e_20:4)	2	<10000	<10000	13788	13180	407	4
propionylcarnitine	1	17116	69733	188291	91310	57056	14
sebacic acid	2	13812	16413	23916	17232	2818	14
suberic acid	2	10258	15860	18933	15539	2373	14
TAG 36:0	2	<10000	<10000	245965	82716	86496	6
TAG 38:0	2	<10000	<10000	72190	46535	31840	3
Nucleic acid subunits							
2'-deoxy-cytidine	2	<10000	<10000	12687	12157	750	2
adenine	1	25195	182329	736118	233338	235232	14
adenosine	1	<10000	<10000	71880	31839	26569	5
cytidine	1	<10000	12904	208364	82150	76581	7
cytosine	1	<10000	13350	113782	28117	31709	12
guanine	2	<10000	<10000	14927	13326	2264	2
inosine	1	<10000	28611	540480	137433	166688	9
N6-methyl-adenine	2	17787	50615	123176	55816	27354	14
Organic acids							

Metabolite	Level of ID	Min	Med	Max	Mean	SD	n
4-guanidinobutanoic acid	1	<10000	12942	25562	16864	4783	10
gamma-aminobutyric acid (GABA)	1	<10000	58789	576304	101765	144164	13
indoxyl sulfate	1	<10000	<10000	12160	12160		1
lactic acid	2	<10000	36476	86772	50945	21448	10
succinic acid	1	93984	476081	797934	447175	256345	14
Other metabolites							
1-methylnicotinamide	1	<10000	<10000	14391	11940	1594	6
2-amino-1-phenylethanol	2	106355	192183	325172	198721	63134	14
2-amino-2-methyl-1-propanol	2	<10000	<10000	38069	22366	10867	6
3-indoleacetic acid	1	<10000	39463	175354	55963	44570	12
4-hydroxybenzaldehyde	1	<10000	<10000	13761	13761		1
4-methylpyridine	2	<10000	22131	98581	44244	28406	9
5-aminovaleric acid	1	1149976	4817223	7408576	4334341	1914220	14
allantoin	1	34597	63745	264543	82260	57824	14
caffeine	1	234706	974548	1881117	1041892	622177	14
choline	2	<10000	5041236	8221382	5453217	2359520	13
hydroxyphenyllactic acid	1	16951	59103	99507	57885	23596	14
kynurenic acid	1	247	746	1533	782	406	14
N-acetylgalactosamine 4-sulfate	2	<10000	<10000	35013	27636	9649	4
N-acetylglucosamine	2	56943	458389	1675208	526247	416014	14
N-acetylneuraminic acid	1	99750	245418	1643564	485899	514042	14
nicotinic acid	1	<10000	23384	106513	43642	31275	11



Metabolite	Level of ID	Min	Med	Max	Mean	SD	n
pantothenic acid	1	2409	5289	<10000	5004	2443	11
paraxanthine	1	94530	398382	821307	419424	256939	14
phosphocholine	1	<10000	261633	1142184	358497	270997	13
purine	2	<10000	135236	186741	132732	35577	10
riboflavin	1	442	2112	<10000	1996	1069	13
theobromine	1	32249	82651	226896	88418	52465	14
trigonelline	1	10243	378399	1645666	646219	544769	14
urea	2	63048	104945	176103	107003	30822	14
urocanic acid	1	10900	40058	71136	36386	16273	14
xanthine	1	29150	158465	394638	173813	123732	14
Small peptides							
arg-ile	2	18331	341025	710052	320444	215988	14
arg-phe	2	250431	744952	1458725	781501	373392	14
arg-ser	2	166259	677600	1155202	653047	308815	14
gly-pro	2	59843	255965	656388	317455	177859	14
gly-tyr	2	10647	93537	242898	91261	64126	14
his-glu	2	22420	65996	203852	73938	55262	14
his-gly	2	14162	99402	279463	113059	83707	14
his-his	2	17697	45681	139994	53110	31105	14
his-ile/leu	2	<10000	11516	57709	33166	17330	8
his-ser	2	50783	251538	532871	279670	120578	14
ile-ser	2	<10000	34407	83363	40065	22717	13

<b>Metabolite</b>	<b>Level of ID</b>	<b>Min</b>	<b>Med</b>	<b>Max</b>	<b>Mean</b>	<b>SD</b>	<b>n</b>
leu-leu	2	65277	367415	1188286	405343	301780	14
leu-phe	2	45017	126515	254275	136678	72849	14
leu-tyr	2	<10000	49692	142071	69066	43098	13
lys-phe	2	64608	180533	350198	196044	88265	14
lys-pro	2	<10000	12059	127461	54790	46774	8
phe-his	2	49613	422751	760880	357211	214378	14
phe-ile/leu	2	<10000	12556	129260	35793	41934	7
phe-ile-arg	2	<10000	29575	177209	63662	52243	9
phe-phe	2	19985	27603	66633	32422	12970	14
phe-tyr	2	<10000	34889	233467	76610	69517	11
pro-leu	2	<10000	85454	282915	103586	86414	13
pyroglu-pro	2	<10000	22740	131784	41311	32980	11
ser-ala	2	<10000	74119	357110	144653	107199	10
ser-ala-arg	2	27032	236658	473215	236955	142975	14
ser-gln	2	16908	89025	194865	93367	47091	14
ser-leu	2	<10000	55009	187601	72616	49118	12
ser-pro	2	59218	230405	1034273	311551	266567	14
thr-phe	2	185038	350604	887569	413981	224576	14
tyr-arg	2	65635	183701	1127841	262863	270167	14
tyr-gly	2	50474	98522	256180	108972	52709	14
tyr-ile/leu	2	30825	72468	194831	84837	45972	14
val-arg	2	11757	34742	122268	40493	28688	14

Metabolite	Level of ID	Min	Med	Max	Mean	SD	n
val-leu	2	30689	206065	882780	320566	283561	14
Chemical compounds							
dibutyl adipate	2	47565	64526	172698	73783	33110	14
diethanolamine	1	<10000	33277	451781	147588	168396	13
diethylhexyl adipate	2	58058	101414	1556448	249685	403937	14
diisodecyl phthalate	2	208712	222322	247443	225726	9688	14
dioctyl phthalate	1	254467	269640	308677	277037	17334	14
dodecyl sulfate	2	225102	632151	25249152	3650004	7175356	14
dodecylbenzenesulfonic acid	2	15936	213023	566013	216457	141432	14
linoleamide	2	23231544	31221685	38207392	30287081	4290249	14
myristamide	2	2751050	4606192	5908500	4427290	838115	14
oleamide	2	72842344	85608764	100743984	85188588	7996398	14
palmitoleamide	2	9643438	12678565	16119980	12508377	1779147	14
pentaerythritol tetrakis(3,5-di-tert-butyl-4-hydroxyhydrocinamate)	2	52410	76586	156358	97419	36912	14
phthalic acid mono-2-ethylhexyl ester	2	106038	128498	163136	132858	18364	14
stearamide	2	7812933	10203003	12323552	10065816	1374684	14
triethanolamine	2	<10000	29260	223469	53520	57605	13
tris(hydroxymethyl)aminomethane	2	<10000	180882	239265	183391	36688	12

ID, Identification; Max, Maximum value; Med, Median value; Min, Minimum value; n, the total number of saliva samples containing the metabolite above limit of detection; SD, Standard deviation.

### APPENDIX 3. SUPPLEMENTAL TABLE STUDY II

**Supplementary table 3.** Identified, statistically significant, salivary metabolites in comparison between pSS patients and healthy controls.

Metabolite	Level of ID	Healthy controls (C)		Sjögren's syndrome (pSS)		pSS vs C		
		Mean	SD	Mean	SD	VIP	p	d
Amino acids, peptides, and analogues								
4-Guanidino-butyric acid	2	16864	4783	31881	18325	1.38	0.031	1.3
<b>Glutamic acid</b>	1	122045	67786	250491	87720	1.91	<b>0.001</b>	1.7
Glycine betaine	1	1241617	504031	1999692	964523	1.43	0.041	1
Isoleucine	2	48927	30704	166871	135723	1.54	0.023	1.4
Leucine	2	112620	46369	448733	419771	1.56	0.032	1.4
Phenylalanine	1	614751	174399	1180634	775776	1.41	0.048	1.2
Tryptophan	1	33773	17245	97779	66429	1.63	0.014	1.5
Arg-Ser	2	653047	308815	285658	248390	1.56	0.004	-1.3
Phe-Ile	2	35793	41934	122220	85371	1.55	0.04	1.4
<b>Tyr-Gln</b>	2	56858	34559	149463	64758	1.96	<b>0.001</b>	1.9
Val-Leu	2	320566	283561	1029040	940151	1.42	0.043	1.2
Lipids and carnitines								
FA 16:0	2	19113838	2988053	23755538	5398164	1.4	0.029	1.1
FA 16:1	2	291295	177097	601015	353046	1.46	0.025	1.2
Leucic acid	2	61064	25243	42491	15691	1.25	0.037	-0.9
CE 16:0	1	4277005	204081	5253366	726120	2.03	0.002	2.1

Metabolite	Level of ID	Healthy controls (C)		Sjögren's syndrome (pSS)			pSS vs C		
		Mean	SD	Mean	SD	VIP	p	d	
Cholesterol	1	42086	23976	107189	65001	1.66	0.118	1.5	
Propionylcarnitine	1	91310	57056	165515	81484	1.47	0.025	1.1	
<b>Isobutyrylcarnitine</b>	2	50626	23350	95837	32915	1.85	<b>0.002</b>	1.6	
<b>LPC 18:0</b>	2	0	0	24441	13129	0.01	<b>&lt;0.001</b>		
<b>LPE 18:0</b>	2	0	0	16498	8405	0.34	<b>&lt;0.001</b>		
<b>Oleamide</b>	2	9389628	1079571	11488697	1386541	1.85	<b>&lt;0.001</b>	1.7	
Linoleamide	2	30287081	4290249	37683667	8799870	1.41	0.03	1.1	
Palmitoleamide	2	12508377	1779147	15694049	3897803	1.41	0.033	1.1	
Other									
Choline	2	5453217	2359520	9987031	4308942	1.59	0.01	1.4	
<b>Pantothenic acid (B5)</b>	1	4289	2431	25186	9179	2.46	<b>&lt;0.001</b>	3.6	
<b>MEHP</b>	1	101276	15673	58944	15552	2.35	<b>&lt;0.001</b>	-2.7	
<b>Xanthine</b>	1	173813	123732	548441	260922	2.05	<b>0.001</b>	1.9	
Urocanic acid	1	36386	16273	96702	77360	1.47	0.037	1.3	
1-Methyl-nicotinamide	2	11940	1594	28433	16638	1.68	0.039	1.8	
Biliverdin IX	1	162101	31725	137588	11938	1.28	0.017	-1.1	
N6-methyl-adenine	2	55816	27354	119280	86943	1.35	0.049	1.1	
Nicotinic acid	1	43642	31275	107135	80169	1.37	0.049	1.1	
Diethanolamine	1	147588	168396	695458	459234	1.89	0.004	1.7	
Stearamide	2	10065816	1374684	12518622	3182570	1.35	0.042	1.1	

Metabolite	Level of ID	Healthy controls (C)		Sjögren's syndrome (pSS)		pSS vs C		
		Mean	SD	Mean	SD	VIP	p	d
Dibutyladipate	2	73783	33110	43796	6608	1.45	0.005	-1.5

Arg-Ser, Arginine serine dipeptide; CE 16:0, cholesteryl palmitic acid; d, Cohen's d effect size; FA, fatty acid; ID, Identification; LPC, lysophosphatidylcholine; LPE, lysophosphatidylethanolamine; MEPH, Monoethylhexyl phthalic acid; p, p-value from Welch's t-test; Phe-Ile, phenylalanine isoleucine dipeptide; SD, standard deviation; Tyr-Gln, Tyrosine glutamine dipeptide; Val-Leu, Valine leucine dipeptide; VIP, variable importance in projection (from PLS-DA). Identified metabolites with  $p < 0.05$  in comparison between pSS patients and healthy controls are shown. Bolded text, p-value below multiple comparison corrected  $\alpha$  ( $p < 0.002$ ).

## ORIGINAL PUBLICATIONS (I – IV)





I

**Metabolome of canine and human saliva: a non-targeted  
metabolomics study**

Turunen S, Puurunen J, Auriola S, Kullaa A M, Kärkkäinen O, Lohi H and  
Hanhineva K

Metabolomics 16: 90, 2020





# Metabolome of canine and human saliva: a non-targeted metabolomics study

Soile Turunen<sup>1</sup> · Jenni Puurunen<sup>2,3</sup> · Seppo Auriola<sup>1</sup> · Arja M. Kullaa<sup>4</sup> · Olli Kärkkäinen<sup>1</sup> · Hannes Lohi<sup>2,3</sup> · Kati Hanhineva<sup>5</sup>

Received: 20 February 2020 / Accepted: 13 August 2020  
© The Author(s) 2020

## Abstract

**Introduction** Saliva metabolites are suggested to reflect the health status of an individual in humans. The same could be true with the dog (*Canis lupus familiaris*), an important animal model of human disease, but its saliva metabolome is unknown. As a non-invasive sample, canine saliva could offer a new alternative material for research to reveal molecular mechanisms of different (patho)physiological stages, and for veterinary medicine to monitor dogs' health trajectories.

**Objectives** To investigate and characterize the metabolite composition of dog and human saliva in a non-targeted manner.

**Methods** Stimulated saliva was collected from 13 privately-owned dogs and from 14 human individuals. We used a non-targeted ultra-high-performance liquid chromatography-quadrupole time-of-flight mass spectrometry (UHPLC-qTOF-MS) method to measure metabolite profiles from saliva samples.

**Results** We identified and classified a total of 211 endogenous and exogenous salivary metabolites. The compounds included amino acids, amino acid derivatives, biogenic amines, nucleic acid subunits, lipids, organic acids, small peptides as well as other metabolites, like metabolic waste molecules and other chemicals. Our results reveal a distinct metabolite profile of dog and human saliva as 25 lipid compounds were identified only in canine saliva and eight dipeptides only in human saliva. In addition, we observed large variation in ion abundance within and between the identified saliva metabolites in dog and human.

**Conclusion** The results suggest that non-targeted metabolomics approach utilizing UHPLC-qTOF-MS can detect a wide range of small compounds in dog and human saliva with partially overlapping metabolite composition. The identified metabolites indicate that canine saliva is potentially a versatile material for the discovery of biomarkers for dog welfare. However, this profile is not complete, and dog saliva needs to be investigated in the future with other analytical platforms to characterize the whole canine saliva metabolome. Furthermore, the detailed comparison of human and dog saliva composition needs to be conducted with harmonized study design.

**Keywords** Saliva · Human · Dog · Lipid · Metabolomics · Liquid chromatography · Mass spectrometry

## Abbreviations

ala Alanine  
arg Arginine  
DAG Diacylglycerol

FA Fatty acid  
gln Glutamine  
glu Glutamic acid  
gly Glycine  
his Histidine  
ile Isoleucine  
leu Leucine

**Electronic supplementary material** The online version of this article (<https://doi.org/10.1007/s11306-020-01711-0>) contains supplementary material, which is available to authorized users.

✉ Soile Turunen  
soiru@uef.fi

<sup>1</sup> School of Pharmacy, Faculty of Health Sciences, University of Eastern Finland, Kuopio, Finland

<sup>2</sup> Department of Veterinary Biosciences, and Department of Medical and Clinical Genetics, University of Helsinki, Helsinki, Finland

<sup>3</sup> Folkhälsan Research Center, Helsinki, Finland

<sup>4</sup> Institute of Dentistry, School of Medicine, Faculty of Health Sciences, University of Eastern Finland, Kuopio, Finland

<sup>5</sup> Institute of Public Health and Clinical Nutrition, Faculty of Health Sciences, University of Eastern Finland, Kuopio, Finland

LPC	Lysophosphatidylcholine
LPE	Lysophosphatidylethanolamine
PC	Phosphatidylcholine
PE	Phosphatidylethanolamine
phe	Phenylalanine
pro	Proline
pyroglu	Pyroglutamic acid
ser	Serine
TAG	Triacylglycerol
thr	Threonine
tyr	Tyrosine
val	Valine

## 1 Introduction

Human saliva has been studied and characterized extensively in recent years. Most of the saliva is water (over 99%) containing a variety of electrolytes, different kinds of proteins as well as low molecular weight (< 1500 Da of mass) metabolites (Dame et al. 2015; Humphrey and Williamson 2001; Gardner et al. 2020). Mucus, epithelial and blood cells, food remainders and traces of medications or chemical products are also found in saliva (Aps and Martens 2005; Elmongy and Abdel-Rehim 2016). Moreover, biological material such as DNA and bacteria with their metabolites exist in saliva (Cuevas-Cordoba and Santiago-Garcia 2014).

Since saliva is rich in small molecules and given its role as “a mirror of the body”, there is a growing interest towards saliva usage as a non-invasive sample material for monitoring health trajectories to aid diagnosis or reveal the molecular mechanisms of disease pathologies. The same applies to domestic dogs which suffer from similar diseases to humans such as metabolic diseases, chronic inflammation, and cancers, manifested as diabetes (O’Kell et al. 2017), inflammatory bowel disease (Minamoto et al. 2015) and leukemia (Breen and Modiano 2008), respectively. Physiological similarity with humans and the large size of the canine have been reasons for the rise of these animals to one of the biomedical models alongside the rodents, for example in the study of genomics (Hytonen and Lohi 2016; van Steenbeek et al. 2016) and behavior (Puurunen et al. 2018). Despite the rising interest in dogs and saliva metabolomics, there is no data available for the canine saliva metabolome.

Humans share the same anatomy and salivary gland structure with dogs, except for dogs’ zygomatic glands. The basic functions of saliva, such as lubrication, maintenance of oral homeostasis and dental welfare as well as bactericidal effects against pathogens, resemble each other (Dame et al. 2015; de Sousa-Pereira et al. 2015; Humphrey and Williamson 2001). Moreover, dogs use panting and evaporative cooling as the major function when exposed to heat and/or exercise (Goldberg et al. 1981). Differences between human

and canine saliva have been revealed in the comparison of the proteome signature where, for example, cystatins with antimicrobial properties have been recognized in lower levels in the saliva of canines compared to saliva of humans (Sanguansermsri et al. 2018). In addition, different antimicrobial protein family members are identified in human and dog saliva, such as cathelicidin 1, cathelicidin antimicrobial peptide and CRISP1 in dog saliva, whereas cathelicidins were not detected in healthy humans but CRISP3 was (de Sousa-Pereira et al. 2015).

Several studies of the human salivary metabolome link it to various conditions, including oral and breast cancers (Sugimoto et al. 2010), type 2 diabetes (Barnes et al. 2014) and Sjögren’s syndrome (Mikkonen et al. 2013). Therefore, also the salivary metabolome of the dog could reflect the metabolic activity of canines’ oral cavity and total body. In this study, we compared the metabolome of dog and human saliva utilizing UHPLC-qTOF-MS -based non-targeted metabolomics approach. We aimed to identify a wide range of saliva metabolites to explore the metabolic profiles of both species and their overlap.

## 2 Materials and methods

### 2.1 Animals and human participants

Voluntary Finnish dog owners were recruited for the canine saliva donation. The saliva collection was conducted from 13 privately-owned dogs with the owners’ written consent and presence. The dogs were healthy referring no disease with one exception (cataract) and were not subjected to any drug treatment according to their owners. The breeds were Belgian Sheepdog (n=2), Belgian Tervueren (n=2), Weimaraner (n=2), Rottweiler (n=3), Golden Retriever (n=2) and Flat-Coated Retriever (n=2). The age of the dogs varied from 1.2 years to 9.3 years. The mean age was 5.5 years and SD 2.5 years. The number of males were 5 and females 8. Two of the female dogs were neutered.

Human saliva samples were collected from 14 healthy, non-smoking females, aged between 30 and 70 years (mean age 53 years, SD 11) who were recruited from the dental education clinic of Kuopio University Hospital. The volunteers had no recent history of systemic diseases or were not taking any medication. Inclusion criteria were healthy subjects, with normal excretion of saliva and no medications. Exclusion criteria were smokers, wearing removable dentures, having systemic diseases or medication, having a treatment history for cancer, or being incapable of communication. Out of all the patients examined, no males met these criteria. At the time of the study, every subject underwent an oral and dental examination performed by a dentist, and

their oral health were good, no gingivitis, missing/broken teeth or caries.

## 2.2 Collection of saliva samples

Canine saliva samples were collected between 9 to 11 a.m. by the same person at the dog's home. The dogs were fasted and rested 12 h before sampling. Saliva was collected without causing any stress or harm to dogs as follows. Salivation was stimulated with prospect of food, i.e. the dog could see or sniff the treat but was not allowed to eat it. Saliva was collected under the tongue and from the surface of the mucosal lining of lips and cheek straight to 1.5 ml Eppendorf tube. The maximum collection time was four minutes. No contaminations, e.g. hair and blood, were observed in visual inspection. Immediately after sampling, proteins were precipitated, and metabolites extracted with two volumes of acetonitrile mixed with 1 volume of saliva simultaneously mixing gently in vortex and finally at maximum speed 10 s. Samples were kept on ice during shipping and stored in  $-20\text{ }^{\circ}\text{C}$  3–5 days prior to metabolomics analysis.

Human saliva samples were collected at least one hour after eating and drinking between 9 and 11 a.m. Stimulated saliva was collected using the standard technique according to Navazesh (1993) as follows. The saliva flow was stimulated by chewing a paraffin wax (1 g; Orion Diagnostica, Espoo, Finland) for 30 s, followed by the collection of the produced saliva into a glass cup for five minutes. Saliva samples were transported to the laboratory on ice, and then clarified by centrifugation ( $3000\times g$ , 20 min,  $+4\text{ }^{\circ}\text{C}$ ). The supernatants were stored at  $-20\text{ }^{\circ}\text{C}$  for later use.

## 2.3 Sample preparation

Dog and human saliva samples were thawed on ice. Human saliva samples were precipitated and extracted similarly as dog saliva (200  $\mu\text{L}$  of saliva and 400  $\mu\text{L}$  of acetonitrile). All samples were centrifuged ( $10,600\times g$ , 5 min,  $+4\text{ }^{\circ}\text{C}$ ), and the supernatants were filtrated through 0.2  $\mu\text{m}$  Acrodisc® Syringe Filters with a PTFE membrane (PALL Corporation, Ann Arbor, MI) prior subjecting to the LC–MS analyses. Quality control (QC) samples were made separately from dog and human samples by mixing aliquots of 30  $\mu\text{L}$  from every dog or human supernatant to one tube. QC mixed sample contained aliquots from every dog and human sample mixed into one tube.

HPLC-grade acetonitrile (VWR Chemicals, Fontenay-sous-Bois, France) was used for sample preparation. LC–MS grade methanol (Riedel-de Haën™, Honeywell, Seelze, Germany), HPLC-grade acetonitrile (VWR Chemicals, Fontenay-sous-Bois, France), LC–MS grade formic acid (Fluka™, Honeywell, Seelze, Germany), ammonium formate (Fluka™, Honeywell, Seelze, Germany) and class 1

ultra-pure water (ELGA Purelab ultra Analytical, UK) were used for mobile phase eluents in RP and HILIC chromatographic separation.

## 2.4 UHPLC-qTOF-MS analysis

The samples were analyzed by a 1290 LC system coupled to a 6540 UHD accurate-mass qTOF spectrometer (Agilent Technologies, Waldbronn, Karlsruhe, Germany) using electrospray ionization (ESI, Jet Stream) in positive (+) and negative (–) polarity. Separation was performed using reversed phase (RP) chromatography with a Zorbax Eclipse XDB-C18 column ( $2.1\times 100\text{ mm}$ , 1.8  $\mu\text{m}$ , Agilent Technologies, Palo Alto, CA, USA). The column temperature was  $50\text{ }^{\circ}\text{C}$  and flow rate 0.4 ml/min. Mobile phase consisted either water (A) or methanol (B) both with 0.1% (v/v) formic acid. The gradient was as follows: 2% B followed by a gradient to 100% B in 10 min, an isocratic step at 100% B for 4.5 min and 2% B for 2 min. Hydrophilic interaction (HILIC) chromatographic separation was performed on Acquity UPLC® BEH Amide column ( $2.1\times 100\text{ mm}$ , 1.7  $\mu\text{m}$ , Waters Corporation, Milford, MA). The column temperature was  $45\text{ }^{\circ}\text{C}$  and flow rate 0.6 ml/min. Mobile phase consisted of 50% v/v acetonitrile in water (A) or 90% v/v acetonitrile in water (B) both with 20 mM ammonium formate buffer. The gradient was as follows: 100% B for 2.5 min followed by a gradient to 0% B in 10 min and 100% B for 2.5 min. The sample volume of 2.0  $\mu\text{L}$  was injected for each chromatographic run.

The ESI source operated using the following conditions: capillary voltage 3500 V, nozzle voltage 1000 V, fragmentor voltage 100 V, skimmer 45 V, nebulizer pressure 45 psi, drying gas temperature  $325\text{ }^{\circ}\text{C}$  and flow 10 l/min and sheath gas temperature  $350\text{ }^{\circ}\text{C}$  and flow 11 l/min. Mass data were acquired with scan time of 600 ms over a 50–1600 m/z range. For automatic MS/MS analyses, four ions with the highest intensities were selected for fragmentation from every precursor scan cycle where precursor isolation width was set to 1.3 Da. Selected precursor ions were excluded after two product ion spectra and released after a 0.25-min hold. Precursor scan time either ended at 20,000 counts or after 500 ms, depending on the ion intensity. Product ion scan time was 500 ms. Collision energies were 10 V, 20 V and 40 V. Continuous internal calibration was performed during analyses to assure the desired mass accuracy. The reference ions from infusion solution were m/z 121.05087300 and 922.00979800 for positive mode and m/z 112.985587 and 966.000725 for negative mode. For the quality assurance of the chromatographic and mass spectrometry runs, QC mixed sample were injected at the beginning of the analysis and after every 9 samples. Separate dog QC and human QC samples were analyzed in the beginning of the corresponding analysis to provide the MS data, and used for the automatic data-dependent

MS/MS analyses. The data acquisition was accomplished with MassHunter Acquisition B.05.01 software (Agilent Technologies).

## 2.5 Non-targeted metabolomics data preprocessing

The LC–MS raw data from four different analytical modes (RP+, RP–, HILIC+, HILIC–) was exported to MassHunter Qualitative Analysis B.07.00 (Agilent Technologies, USA) for feature extraction and peak picking combined with chromatographic alignment across all data files per mode. To remove the redundant and non-specific information considered as background noise, peaks with ion abundance less than 10,000 were excluded from further analysis. The feature files were imported as compound exchange format (.cef-files) into Agilent Mass Profiler Professional software (MPP version 13.1.1, Agilent Technologies) for compound alignment yielding a peak list which was exported to Microsoft Excel 2016. Altogether, 8375 molecular features were collected in the four analytical modes. Out of those, molecular features that were present in at least 50% of the samples in either of the sample groups (5468 features) were considered for metabolite identification. Principal component analysis was performed using SIMCA (version 15, Umetrics).

## 2.6 Metabolite identification

The putative metabolite identification was performed using an open-source software, MS-DIAL (RIKEN PRIME). Collected MS/MS data was converted as.abf-files using Analysis Base File Converter program (Reifycs Inc.) and converted files were imported to MS-DIAL (versions 2.66 to 3.12). Public databases, Metlin and MassBank of North America (MoNA), and in-house LC–MS/MSMS standard library were downloaded to MS-DIAL for utilization of retention time, accurate mass, isotope ratio and MS/MS spectrum information for peak and metabolite identification. The built-in MS-DIAL library was utilized for lipid identification. Each matched spectrum was manually inspected. The guidelines from Sumner et al. (2007) were used for ranking metabolite identifications as follows: Compounds in identification level 1 were verified by comparing exact mass, retention time and MS/MS fragmentation spectra with in-house LC–MS/MSMS standard library. Compounds in level 2 were matched with exact mass and MSMS spectra from public databases mentioned above. MassHunter Profinder B.08.00 software (Agilent Technologies) was applied for targeted feature extraction to minimize the appearance of false negative features implemented with the manual inspection and integration of the targeted feature.

## 3 Results

With the aim to explore salivary metabolite composition in dog and human, we focused on 5468 metabolic features collected with four analytical modes using a non-targeted metabolomics approach. A total of 211 metabolites were identified (Table 1) including both endogenous and exogenous compounds. Among those, 31 metabolites (14.6%) were found only in dog saliva, and 9 metabolites (4.2%) only in human saliva (Fig. 1). The identities of 69 metabolites were verified as level 1 identification (Sumner et al. 2007) whereas 142 metabolites were in identification level 2. Characteristics and reference spectra for all identified metabolites in human and dog saliva are given as supplementary material (S1). The identified metabolites were classified as amino acids, amino acids derivatives, biogenic amines, lipids and carnitines, nucleic acid subunits, organic acids, small peptides, chemicals, and other metabolites.

The major difference between the human and dog saliva metabolites was observed in the lipid group. Dog saliva contained 25 lipids or lipid-like molecules (i.e. carnitines), which were absent in the human saliva, including 11 phosphatidylcholines (PC), 6 phosphatidylethanolamines (PE), 3 lysophosphatidylethanolamines (LPE), 2 lysophosphatidylcholines (LPC), 1 diacylglycerol (DAG) and 2 acylcarnitines. In contrast, small peptides, including mostly dipeptides, were more prevalent in human when compared to canine saliva. Dogs were completely lacking eight of the 34 identified small peptides, and in total, 13 dipeptides had minor ion abundance in the dog saliva.

Both the dog and human saliva contained 15 of the 20 generic amino acids. However, asparagine, cysteine, glycine, methionine and valine were not detected from the saliva of both species. The group of amino acid derivatives included ten metabolites. Among those, gamma glutamylglutamic acid was detected only in humans, and phenylacetyl glycine only in canines. Besides amino acids and their derivatives, asymmetric dimethylarginine (ADMA), cadaverine, carnosine, creatinine, histamine, spermidine and taurine were identified as biogenic amines. Those seven metabolites and eight different nucleic acid subunits were detected in both species. Furthermore, canine saliva contained also one unique organic acid which was identified as pyrocatechol sulfate, and four other compounds named quinaldic acid, sphinganine, sphingosine and usnic acid.

The entity of identified metabolites in canine and human saliva indicate partially comprised species-specific metabolic profiles (Table 1). In addition, a large variation in ion abundance within and between the identified saliva metabolites were observed in both species. Inter-individual variation and sample variation is shown with descriptive statistics in the supplementary material (S2). Furthermore,

**Table 1** Identified metabolites in dog and human saliva in the non-targeted LC-MS analysis

Compound ID	Level of ID	Dog			Human		
		Min	Median	Max	Min	Median	Max
<b>Amino acids</b>							
alanine	1	11621	37378	60490	13180	22480	40910
arginine	1	<10000	214558	654257	436614	1409422	2045075
aspartic acid	1	<10000	19530	56048	66610	249145	399489
glutamic acid	1	45808	352114	795587	92510	219896	477880
glutamine	1	172434	636094	1025305	85529	149544	318895
histidine	1	18000	509729	1065260	354376	488143	1069618
isoleucine	1	13531	324410	752675	31420	140750	246619
leucine	2	24612	286748	458104	20697	119312	196690
lysine	1	<10000	58618	144231	57367	321507	489095
phenylalanine	1	10952	279868	517735	342100	592727	1013511
proline	1	51145	296961	501040	261167	3878169	11401076
serine	2	10401	131521	203482	<10000	37455	88258
threonine	1	<10000	108277	173863	11676	23103	58526
tryptophan	1	<10000	44538	64061	<10000	<10000	34288
tyrosine	1	<10000	25757	41843	79017	183192	412868
<b>Amino acid derivatives</b>							
1-methyl-histidine	1	<10000	60565	129019	11191	18643	50624
3-methyl-histidine	2	<10000	23990	73519	<10000	<10000	43698
5-aminovaleric acid betaine	1	12428	100529	346778	39681	110597	561505
carmitine	1	167694	1081252	1965566	810251	1485396	5209412
citrulline	1	18649	480638	774749	148079	360197	665101
creatine	1	779746	2402765	4766552	1070832	1599528	2560989
gamma glutamylglutamic acid	2	0	0	0	<10000	23557	101558
glycinebetaine	1	3641697	10717865	21103608	450155	1191462	2241265
ornithine	1	<10000	53746	268798	112063	199787	369461
phenylacetylglucine	2	19069	98686	382722	0	0	0
<b>Biogenic amines</b>							
asymmetric dimethylarginine	2	<10000	93638	192806	12057	19586	34784
cadaverine	1	<10000	<10000	70675	20062	106938	336618
carnosine	1	<10000	77531	345281	<10000	<10000	14069
creatinine	1	<10000	3595432	10086481	<10000	1768218	2807040
histamine	1	<10000	<10000	20555	<10000	27233	213795
spermidine	1	<10000	41291	474831	0	346	1729
taurine	2	11922	112591	221966	33028	62705	83051
<b>Lipids and carnitines</b>							
acetylcarnitine	1	65986	876765	2350521	<10000	192280	544614
acylcarnitine C16:0	1	<10000	70459	131534	0	0	0
acylcarnitine C18:0	1	20847	108243	224379	235	1271	2876
acylcarnitine C18:1	2	12269	83360	151949	0	0	0
azelaic acid	1	55255	142717	327229	37854	45207	56463
DAG 34:1	2	<10000	205691	822295	<10000	<10000	23115
DAG 34:2	2	65044	190939	862855	<10000	<10000	15559
DAG 36:3	2	73002	525301	2066243	<10000	<10000	23245
DAG 36:4	2	27386	236542	1097107	<10000	<10000	20966
DAG 38:4	2	52681	237655	907217	0	0	0
FA 15:0	2	42503	381984	1221547	37879	71890	127786
FA 16:0	2	1904573	2225850	2935780	1741092	1969314	2418832
FA 16:1	2	99647	947405	5787185	84217	278554	769808
FA 17:0	1	83142	124843	303479	68962	84249	158464
FA 17:1	2	24010	114688	419195	14253	34183	68761
FA 18:0	1	1906062	2265398	3147739	1762724	2137965	2902604
FA 18:1	1	496478	1830159	3901249	303215	485606	1395954
FA 18:2	2	122906	697812	1022533	86616	245000	857574
FA 18:3	2	<10000	65541	148335	<10000	16226	73462
FA 20:0	1	14102	46432	65739	19776	31424	55360
FA 20:1	2	29563	163202	441862	13801	17572	37779

Table 1 (continued)

Compound ID	Level of ID	Dog			Human		
		Min	Median	Max	Min	Median	Max
FA 20:2	2	16807	179383	325995	<10000	16496	48413
FA 20:3	2	25837	130995	271927	16123	33537	140139
FA 20:4	2	126220	1012611	1694682	<10000	87885	479090
FA 20:5	2	29051	82854	228736	<10000	11784	41867
FA 21:0	2	<10000	18796	125634	2349	3090	4398
FA 22:0	2	15540	28550	48955	<10000	10423	18567
FA 22:1	1	35515	120940	233114	<10000	<10000	11683
FA 22:2	2	<10000	57428	130210	1079	2239	4427
FA 22:3	2	<10000	43436	173654	1854	3440	8009
FA 22:4	2	17392	101471	180448	<10000	<10000	38537
FA 24:1 (n-9)	1	40284	90624	201122	1357	3363	7059
gamma-butyrobetaine	2	14949	248812	751914	228851	711345	1685899
glycerophosphocholine	1	24233	328573	928629	<10000	<10000	23768
hydroxypalmitic acid	2	77734	193115	445803	<10000	11255	17943
isobutyril carnitine	2	13086	115881	874317	15871	45861	94737
isovalerylcarnitine	1	12599	141423	341344	29009	62403	402540
leucic acid	2	<10000	25422	41427	26369	59768	105831
LPC 16:0	2	95458	648254	16030733	<10000	<10000	19228
LPC 16:1	2	<10000	54524	138021	0	0	0
LPC 18:0	2	113515	455793	4515596	<10000	<10000	41702
LPC 18:1	2	<10000	373385	2099599	0	0	8504
LPC 18:2	2	23760	215712	639442	673	1492	3643
LPE 16:0	2	14886	57102	335617	1119	2268	7056
LPE 16:1	2	<10000	62830	486427	0	0	0
LPE 18:0	2	113221	315339	529906	<10000	<10000	12287
LPE 18:1	2	44841	229410	516071	1050	3011	5784
LPE 18:2	2	21575	100444	298766	0	0	0
LPE 20:4	2	32446	110101	456484	0	0	0
panthenol	2	<10000	45107	229860	326	1009	7555
PC 32:1 (16:0_16:1)	2	125717	433195	1881012	0	0	0
PC 32:1e (16:0e_16:1)	2	156372	808574	1960968	0	0	0
PC 34:1 (16:0_18:1)	2	<10000	959665	2183143	0	0	0
PC 34:2 (16:0_18:2)	1	527876	1679345	3151504	0	0	0
PC 34:2e (16:0e_18:2)	2	<10000	1311992	2878498	0	0	0
PC 34:3 (16:1_18:2)	2	<10000	132082	1016841	0	0	0
PC 36:2 (18:1_18:1)	2	<10000	1048913	2627064	0	0	0
PC 36:3 (18:1_18:2)	2	<10000	1427006	5155045	0	0	0
PC 36:4	2	<10000	247531	2210703	0	0	0
PC 38:4 (18:0_20:4)	2	<10000	853419	1552674	0	0	0
PC 38:5 (18:1_20:4)	2	<10000	448002	1111031	0	0	0
PC 38:5e (18:1e_20:4)	2	<10000	1129401	3377601	2370	4163	5414
PE 28:0 (13:0_15:0)	2	<10000	119668	317171	0	0	0
PE 30:0 (15:0_15:0)	2	<10000	107950	559716	92	514	1695
PE 32:1 (15:0_17:1)	2	37852	204677	437195	<10000	<10000	14513
PE 32:2 (16:1_16:1)	2	19175	158878	338527	0	0	0
PE 33:2 (15:0_18:2)	2	<10000	104006	234261	0	0	0
PE 34:2 (16:1_18:1)	2	<10000	315200	587195	<10000	<10000	13358
PE 36:2 (18:1_18:1)	2	59997	134283	299542	<10000	<10000	19097
PE 36:2e (18:1e_18:1)	2	51929	93390	246276	<10000	<10000	16125
PE 36:3 (18:1_18:2)	2	141166	230330	330667	0	0	0
PE 36:3e (18:2e_18:1)	2	131863	424557	1203428	6967	10393	18368
PE 36:4 (16:0_20:4)	2	77210	222944	387097	0	0	0
PE 36:4e (16:0e_20:4)	2	205650	378956	912821	<10000	<10000	17742
PE 36:5e (16:1e_20:4)	2	101753	176899	409725	<10000	12316	25173
PE 38:4 (18:0_20:4)	2	155607	393155	748449	2183	4915	11117
PE 38:4e (18:0e_20:4)	2	89687	307156	675664	482	1733	3541
PE 38:5 (18:1_20:4)	2	100884	296574	671320	0	0	0



Table 1 (continued)

Compound ID	Level of ID	Dog			Human		
		Min	Median	Max	Min	Median	Max
PE 38:5e (18:1e_20:4)	2	408052	780956	1966641	<10000	13631	29876
PE 38:6e (18:2e_20:4)	2	267091	877130	1714394	<10000	<10000	13788
propionylcarnitine	1	29989	305075	652985	17116	69733	188291
sebacic acid	2	17955	29244	53705	13812	16413	23916
suberic acid	2	18493	36830	71278	10258	15860	18933
TAG 36:0	2	<10000	46413	325421	<10000	<10000	245965
TAG 38:0	2	<10000	16567	278288	<10000	<10000	72190
<b>Nucleic acid subunits</b>							
2'-deoxy-cytidine	2	11574	121793	664924	<10000	<10000	12687
adenine	1	30862	546767	1140050	25195	182329	736118
adenosine	1	1165584	3535798	5904123	<10000	<10000	71880
cytidine	1	19218	341518	1218546	<10000	12904	208364
cytosine	1	<10000	26965	91078	<10000	13350	113782
guanine	2	<10000	36689	189630	<10000	<10000	14927
inosine	1	14277	433451	867561	<10000	28611	540480
N6-methyl-adenine	2	<10000	13774	50640	17787	50615	123176
<b>Organic acids</b>							
4-guanidinobutanoic acid	1	269089	1392982	6177370	<10000	12942	25562
gamma-aminobutyric acid (GABA)	1	<10000	33837	64474	<10000	58789	576304
indoxyl sulfate	1	<10000	47357	305682	<10000	<10000	12160
lactic acid	2	<10000	122285	225557	<10000	36476	86772
pyrocatechol sulfate	2	113205	1745700	3459574	0	0	0
succinic acid	1	45409	140947	229175	93984	476081	797934
<b>Other metabolites</b>							
1-methylnicotinamide	1	10128	161587	389096	<10000	<10000	14391
2-amino-1-phenylethanol	2	<10000	40291	103424	106355	192183	325172
2-amino-2-methyl-1-propanol	2	<10000	107208	587120	<10000	<10000	38069
3-indoleacetic acid	1	<10000	14938	37641	<10000	39463	175354
4-hydroxybenzaldehyde	1	<10000	29604	186914	<10000	<10000	13761
4-methylpyridine	2	481	2233	8898	<10000	22131	98581
5-aminovaleric acid	1	102880	508819	1371563	1149976	4817223	7408576
allantoin	1	91518	228324	647239	34597	63745	264543
caffeine	1	<10000	<10000	24719	234706	974548	1881117
choline	2	2836825	16398828	27260268	<10000	5041236	8221382
hydroxyphenyllactic acid	1	<10000	47289	118171	16951	59103	99507
kynurenic acid	1	42796	326080	961407	247	746	1533
N-acetylgalactosamine 4-sulfate	2	<10000	56180	126171	<10000	<10000	35013
N-acetylglucosamine	2	<10000	<10000	30449	56943	458389	1675208
N-acetylneuraminic acid	1	<10000	47849	176244	99750	245418	1643564
nicotinic acid	1	<10000	75651	175443	<10000	23384	106513
pantothenic acid	1	<10000	41614	103199	2409	5289	<10000
paraxanthine	1	<10000	<10000	36642	94530	398382	821307
phosphocholine	1	<10000	<10000	91148	<10000	261633	1142184
purine	2	82881	1493615	3907676	<10000	135236	186741
quinaldic acid	2	<10000	34591	195869	0	0	0
riboflavin	1	<10000	24184	66906	442	2112	<10000
sphinganine	1	23812	68181	122139	0	0	0
sphingosine	2	34958	188907	233951	0	0	0
theobromine	1	393	3354	<10000	32249	82651	226896
trigonelline	1	<10000	64859	226093	10243	378399	1645666
urea	2	<10000	<10000	172306	63048	104945	176103
urocanic acid	1	<10000	414615	588379	10900	40058	71136
usnic acid	2	<10000	41140	575241	0	0	0
xanthine	1	<10000	43955	117175	29150	158465	394638
<b>Small peptides</b>							
arg-ile	2	<10000	22196	34949	18331	341025	710052
arg-phe	2	<10000	45418	297897	250431	744952	1458725

Table 1 (continued)

Compound ID	Level of ID	Dog			Human		
		Min	Median	Max	Min	Median	Max
arg-ser	2	109	1955	4214	166259	677600	1155202
gly-pro	2	921	7991	24520	59843	255965	656388
gly-tyr	2	0	0	0	10647	93537	242898
his-glu	2	0	0	0	22420	65996	203852
his-gly	2	110	1394	3470	14162	99402	279463
his-his	2	0	0	0	17697	45681	139994
his-ile/leu	2	<10000	11735	16672	<10000	11516	57709
his-ser	2	0	714	1540	50783	251538	532871
ile-ser	2	223	1249	3180	<10000	34407	83363
leu-leu	2	<10000	16538	44365	65277	367415	1188286
leu-phe	2	<10000	<10000	12514	45017	126515	254275
leu-tyr	2	0	609	2477	<10000	49692	142071
lys-phe	2	523	2711	5132	64608	180533	350198
lys-pro	2	0	0	0	<10000	12059	127461
phe-his	2	109	692	3021	49613	422751	760880
phe-ile/leu	2	892	2475	5046	<10000	12556	129260
phe-ile-arg	2	0	0	0	<10000	29575	177209
phe-phe	2	0	643	2844	19985	27603	66633
phe-tyr	2	<10000	17609	74288	<10000	34889	233467
pro-leu	2	0	0	0	<10000	85454	282915
pyroglu-pro	2	0	1647	5592	<10000	22740	131784
ser-ala	2	3800	8553	13588	<10000	74119	357110
ser-ala-arg	2	0	0	0	27032	236658	473215
ser-gln	2	0	0	0	16908	89025	194865
ser-leu	2	<10000	<10000	13591	<10000	55009	187601
ser-pro	2	<10000	14358	31931	59218	230405	1034273
thr-phe	2	0	313	1132	185038	350604	887569
tyr-arg	2	<10000	<10000	19613	65635	183701	1127841
tyr-gly	2	236	635	1812	50474	98522	256180
tyr-ile/leu	2	0	1734	4178	30825	72468	194831
val-arg	2	<10000	<10000	34841	11757	34742	122268
val-leu	2	<10000	14638	37038	30689	206065	882780
<b>Chemical compounds</b>							
dibutyl adipate	2	45845	106927	655818	47565	64526	172698
diethanolamine	1	18671	63434	135897	<10000	33277	451781
diethylhexyl adipate	2	145957	1520708	7535913	58058	101414	1556448
diisodecyl phthalate	2	99927	277741	1640341	208712	222322	247443
dioctyl phthalate	1	434106	1873771	7066364	254467	269640	308677
dodecyl sulfate	2	145172	1097399	2697976	225102	632151	25249152
dodecylbenzenesulfonic acid	2	287702	873888	1751253	15936	213023	566013
linoleamide	2	11863390	30840156	60906180	23231544	31221685	38207392
myristamide	2	1686252	3648810	9409145	2751050	4606192	5908500
oleamide	2	48130344	91514384	132632448	72842344	85608764	100743984
palmitoleamide	2	5279505	12170688	23845604	9643438	12678565	16119980
pentaerythritol tetrakis(3,5-di-tert-butyl-4-hydroxyhydrocinnamate)	2	34593	76145	213762	52410	76586	156358
phthalic acid mono-2-ethylhexyl ester	2	60347	74071	107216	106038	128498	163136
stearamide	2	3478602	9423142	19570576	7812933	10203003	12323552
triethanolamine	2	<10000	117186	4144601	<10000	29260	223469
tris(hydroxymethyl)aminomethane	2	<10000	175962	348895	<10000	180882	239265

Level of identification (ID) based on Sumner et al. (2007).

Ion abundance  
Color

0 - &lt;10000

10000-99999

100000-999999

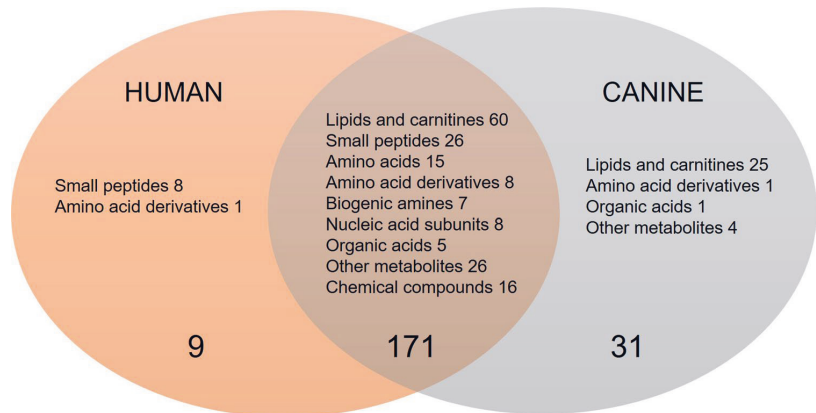
&gt;1000000

Minimum, median and maximum abundances are shown.

the principal component analysis clearly separated the different species, however large variation was also observed within species (supplementary material S3). Example total

ion chromatograms of salivary samples of dog and humans from all four analytical modes are shown in the supplementary material (S4).

**Fig. 1** Venn diagram displaying the shared and unique salivary metabolites by classes among the two species. Metabolite was annotated as unique when the ion abundance was confirmed as zero in all samples per study group. Unique metabolites with zero ion abundance were confirmed with the manual inspection and integration of the targeted feature using MassHunter Profinder B.08.00 software (Agilent Technologies)



#### 4 Discussion

This study provides the first characterization of canine saliva metabolome and compares its content to the human saliva. We identified altogether 211 metabolites in 13 dog and 14 human saliva samples. Dog saliva contained 31 unique metabolites that were mostly lipids and lipid-like molecules. This study demonstrates the feasibility of UHPLC-qTOF-MS in canine and human salivary metabolomics. Exploitation of both, high-resolution precursor and fragmentation data in MS/MS, enables the identification of metabolites that typically exist in lower amounts in saliva than in serum.

Comparison of the content of canine and human saliva revealed differences in the salivary lipids and lipid-like molecules. PCs were not detected in our current analysis in the human saliva, and in addition, eight out of 18 PEs were absent or found with low ion abundance in the human saliva. However, previous studies have reported on PCs in human saliva (Dame et al. 2015). Likewise, our analytical method is capable of detecting PCs, as we have reported them earlier from e.g. human plasma, and therefore most likely other than methodological issues are the reason why they were not detected in the current analysis from human saliva. PCs and PEs are major phospholipids of the plasma membranes in animal cells. This result may indicate the presence of epithelial cell membranes from the oral cavity in the dog saliva samples. Other identified lipids also had lower ion abundance in the human saliva samples when compared with the canine samples. An exception was observed with the most abundant fatty acids in tissues, FA 16:0, FA 18:0 and FA 18:1, which were present with high ion signals also in the human samples. These findings agree with a quantitative study conducted by Larsson et al. (1996) where lipids were detected only in low concentrations in human saliva. Instead, the whole saliva was found to contain more free fatty acids

and neutral lipids like di- and triglycerides than polar lipids, such as PCs or PEs (Larsson et al. 1996).

In contrast to lipids, small peptides were found predominantly in human saliva. Canine saliva included only 13 clear signals from di- and tripeptides, whereas 34 were found from human samples. Small peptides in saliva originate from protein degradation induced by host and bacterial proteases (Liebsch et al. 2019). Thus, oral health status, and especially periodontitis, can affect the salivary dipeptides. In the present study, human participants were healthy, and according to dog owners', the dogs were not reported to have any diseases with one exception (cataract). It is unclear if the different fasting time (12 h for dogs versus minimum of one hour for human participants) and/or oral health, combined with the differences in antimicrobial and homeostatic protein compositions between species, affect to peptide levels observed in this study. In addition, the differences in sample collection (e.g. using paraffin wax) and handling may have had an effect.

We identified six additional metabolites, which were present only in the canine saliva. Those included sphingosine and its derivative sphinganine, which are the major bases of the sphingolipids in mammals. Metabolites included also phenylacetylglycine (amino acid derivative) and pyrocatechol sulfate (organic acid) which are reported to be normal human metabolites. Previously, pyrocatechol sulfate was detected in our platform not only in human plasma but also in dog plasma (Hanhineva et al. 2015; Puurunen et al. 2016). Moreover, we putatively identified usnic acid in dog saliva. Usnic acid originates from lichens and might be a trace from a dog food. On the contrary to endogenous metabolites, exogenous compounds in saliva are traces from, for example, food, cosmetics, drug intake and environment (Dame et al. 2015). We identified 16 chemical compounds in both species, including phthalates, which are used as plasticizers. Furthermore, we identified two surfactants, dodecyl

sulfate and dodecylbenzenesulfonic acid, which are used in cosmetics and foods. In addition, fatty acid amides myristamide, palmitoleamide, stearamide, oleamide and linoleamide, were found with high ion abundance in both species. Although these compounds are recognized as endogenous plasma metabolites (Kim et al. 2019), the identified fatty acid amides are also known as lubricants, detergents and softeners which we have found to be derived from the filters used in sample preparation (data not shown). Thus, they are considered as contaminants in this study.

The identified metabolites in dog and human saliva were characterized by inter-individual variation. Several factors, such as diurnal variation, oral health status, physiological condition, gender, age and nutrition are known to have an influence on the metabolite composition of human saliva (Kawanishi et al. 2019; Liebsch et al. 2019; Mikkonen et al. 2013). These factors should be investigated in dogs when the potential of saliva as a sample material for research and diagnostics is discussed as the differences in saliva metabolites between dog breeds, age and sex remain unsolved in this study. Those above-mentioned factors have been identified as affecting the dog plasma metabolome (Lloyd et al. 2016, 2017) and saliva proteome (Pasha et al. 2018). Nevertheless, saliva provides information from several organs and its utility as “the new blood” for the diagnosis and monitoring of human systemic diseases has been studied through omics (Cuevas-Cordoba and Santiago-Garcia 2014). This could also be a case for dogs and veterinary medicine after overcoming the sampling problems and conducting metabolic profiling with larger sample size.

There are some limitations in our study. Firstly, there is no standard operation procedure for collecting dog saliva. In this study, we designed the canine saliva sampling protocol according to the reviewed literature (Elmongy and Abdel-Rehim 2016; Lensen et al. 2015) which aimed to be the most appropriate for the LC–MS analysis. We observed that, even though the dogs were trained for showing their teeth and to cooperate with their owners, the collection of saliva was still tricky to execute due to the characteristic features of saliva being elastic and mucous. Therefore, alternative sampling techniques that are comfortable for the dogs and easy to perform, and which provide enough sample material, need to be developed. Secondly, the non-targeted LC–MS method yields semi-quantitative data suitable for identification and sample-wise comparison but does not provide exact quantities for the detected compounds in saliva. Therefore, when exact quantities are required, other analytical approaches, such as nuclear magnetic resonance spectroscopy (NMR) or targeted LC–MS methods should be applied. However, the low sensitivity of NMR compared to MS limits the detection of the salivary metabolites identified in this study with NMR technique. Furthermore, metabolite identification was focused to the

compounds that were classified into identification level 1 and level 2 according Sumner et al. (2007). A wide range of unidentified metabolites still exist in the canine saliva. This is evident according to our data, where in total over 8000 molecular features were detected providing a couple of hundred identifications. The identification of the metabolites behind these molecular features remains a challenge, and only small fraction of measured molecular features can usually be identified in a non-targeted metabolomics study. In addition, the applied LC–MS method does not capture the whole canine saliva metabolome. Characterization of the whole canine saliva metabolome would require use of more diverse set of methods (e.g. NMR and GC–MS) (Dame et al. 2015). Thirdly, our human subjects were all women. For comparing the metabolomes between species, both genders should be included to the study populations despite studies reporting only quantitative differences in salivary metabolites between men and women (Okuma et al. 2017; Takeda et al. 2009). Moreover, more restricted age range could have reduced variation seen in the canine samples. Finally, comparability between human and canine salivary metabolite profiles would improve if more aspects of the study design including sampling protocol could be harmonized between the species.

In conclusion, we were able to identify 211 metabolites in the dog and human saliva using non-targeted metabolite profiling. This study provides novel information that encourages the continuation of the studies with larger cohorts. The results demonstrate the potential of dog saliva metabolome to be used in understanding, for example, disease pathology or changes in metabolism due to xenobiotics or nutrition. Furthermore, saliva could be a source of specific biomarkers also for canines’ oral health problems as well as other diseases, but further research is needed to establish and validate the canine saliva biomarkers. Understanding the differences between dogs and humans will then allow the results to be extrapolated to human health.

**Acknowledgements** Mrs. Miia Reponen is acknowledged for her help with sample preparation and with the LC-MS analyses. The dog owners are thanked for participation.

**Author contributions** ST, HL, KH and JP conceived and designed the research of dog saliva. AK designed the research of human saliva. ST conducted canine saliva sample collection and preparation of both canine and human saliva samples. ST performed LC–MS analysis and data analysis with compound identification. OK supervised compound identification. ST drafted the manuscript which was reviewed, edited and approved by all authors.

**Funding** JP and HL were partially supported by the Academy of Finland (308887) and the Jane and Aatos Erkko Foundation. KH was supported by Academy of Finland (277986). The LC–MS unit at the School of Pharmacy received support from Biocentre Finland. Open

access funding provided by University of Eastern Finland (UEF) including Kuopio University Hospital.

**Data availability** The datasets generated during and/or analysed during the current study are available from the corresponding author on reasonable request.

**Code availability** Not applicable.

## Compliance with ethical standards

**Conflict of interest** The authors declare that they have no conflict of interest. OK and KH are founders of Afekta Technologies Ltd., a metabolomics analysis service company.

**Ethical approval** Human samples: The study was approved by the Research Ethics Committee of the Northern Savo Hospital District (82/2014; 745/2018). The investigation was conducted according to the Declaration of Helsinki. An informed consent to provide saliva for research purposes was given by every donor and a written consent was obtained from every participant. Dog samples: The study was approved by the Finnish national Animal Experiment Board (ESAVI/7482/04.10.07/2015), and the canine saliva samples were collected in accordance with institutional guidelines and in compliance with national and regional legislation. An informed consent to provide canine saliva for research purposes was given by every dog owner and a written consent was obtained from dogs' owners.

**Informed consent** All authors have approved the version to be published.

**Open Access** This article is licensed under a Creative Commons Attribution 4.0 International License, which permits use, sharing, adaptation, distribution and reproduction in any medium or format, as long as you give appropriate credit to the original author(s) and the source, provide a link to the Creative Commons licence, and indicate if changes were made. The images or other third party material in this article are included in the article's Creative Commons licence, unless indicated otherwise in a credit line to the material. If material is not included in the article's Creative Commons licence and your intended use is not permitted by statutory regulation or exceeds the permitted use, you will need to obtain permission directly from the copyright holder. To view a copy of this licence, visit <http://creativecommons.org/licenses/by/4.0/>.

## References

- Aps, J. K. M., & Martens, L. C. (2005). Review: The physiology of saliva and transfer of drugs into saliva. *Forensic Science International*, *150*(2–3), 119–131.
- Barnes, V. M., Kennedy, A. D., Panagakos, F., Devizio, W., Trivedi, H. M., Jonsson, T., et al. (2014). Global metabolomic analysis of human saliva and plasma from healthy and diabetic subjects, with and without periodontal disease. *PLoS ONE*, *9*, e105181.
- Breen, M., & Modiano, J. F. (2008). Evolutionarily conserved cytogenetic changes in hematological malignancies of dogs and humans—man and his best friend share more than companionship. *Chromosome Research*, *16*, 145–154.
- Cuevas-Cordoba, B., & Santiago-Garcia, J. (2014). Saliva: A fluid of study for OMICS. *OMICS: A Journal of Integrative Biology*, *18*, 87–97.
- Dame, Z. T., Aziat, F., Mandal, R., Krishnamurthy, R., Bouatra, S., Borzouie, S., et al. (2015). The human saliva metabolome. *Metabolomics*, *11*, 1864–1883.
- de Sousa-Pereira, P., Cova, M., Abrantes, J., Ferreira, R., Trindade, F., Barros, A., et al. (2015). Cross-species comparison of mammalian saliva using an LC-MALDI based proteomic approach. *Proteomics*, *15*, 1598–1607.
- Elmongy, H., & Abdel-Rehim, M. (2016). Saliva as an alternative specimen to plasma for drug bioanalysis: A review. *Trac-Trends in Analytical Chemistry*, *83*, 70–79.
- Gardner, A., Carpenter, G., & So, P. W. (2020). Salivary metabolomics: From diagnostic biomarker discovery to investigating biological function. *Metabolites*, *10*, 47.
- Goldberg, M. B., Langman, V. A., & Taylor, C. R. (1981). Panting in dogs: Paths of air flow in response to heat and exercise. *Respiration Physiology*, *43*, 327–338.
- Hanhineva, K., Lankinen, M. A., Pedret, A., Schwab, U., Kolehmainen, M., Paananen, J., et al. (2015). Nontargeted metabolite profiling discriminates diet-specific biomarkers for consumption of whole grains, fatty fish, and bilberries in a randomized controlled trial. *Journal of Nutrition*, *145*, 7–17.
- Humphrey, S. P., & Williamson, R. T. (2001). A review of saliva: Normal composition, flow, and function. *Journal of Prosthetic Dentistry*, *85*, 162–169.
- Hytonen, M. K., & Lohi, H. (2016). Canine models of human rare disorders. *Rare Disease*, *4*, e1241362.
- Kawanishi, N., Hoshi, N., Masahiro, S., Enomoto, A., Ota, S., Kaneko, M., et al. (2019). Effects of inter-day and intra-day variation on salivary metabolomic profiles. *Clinica Chimica Acta*, *489*, 41–48.
- Kim, M., Snowden, S., Suvitaival, T., Ali, A., Merkler, D. J., Ahmad, T., et al. (2019). Primary fatty amides in plasma associated with brain amyloid burden, hippocampal volume, and memory in the European Medical Information Framework for Alzheimer's Disease biomarker discovery cohort. *Alzheimers & Dementia*, *15*, 817–827.
- Larsson, B., Olivecrona, G., & Ericson, T. (1996). Lipids in human saliva. *Archives of Oral Biology*, *41*, 105–110.
- Lensen, C. M. M., Moons, C. P. H., & Diederich, C. (2015). Saliva sampling in dogs: How to select the most appropriate procedure for your study. *Journal of Veterinary Behavior-Clinical Applications and Research*, *10*, 504–512.
- Liebsch, C., Pitchika, V., Pink, C., Samietz, S., Kastenmuller, G., Artati, A., et al. (2019). The saliva metabolome in association to oral health status. *Journal of Dental Research*, *98*, 642–651.
- Lloyd, A. J., Beckmann, M., Tailliant, K., Brown, W. Y., Draper, J., & Allaway, D. (2016). Characterisation of the main drivers of intra- and inter-breed variability in the plasma metabolome of dogs. *Metabolomics*, *12*, 72.
- Lloyd, A. J., Beckmann, M., Wilson, T., Tailliant, K., Allaway, D., & Draper, J. (2017). Ultra high performance liquid chromatography-high resolution mass spectrometry plasma lipidomics can distinguish between canine breeds despite uncontrolled environmental variability and non-standardized diets. *Metabolomics*, *13*, 15.
- Mikkonen, J. J. W., Herrala, M., Soininen, P., Lappalainen, R., Tjäderhane, L., Seitsalo, H., et al. (2013). Metabolic profiling of saliva in patients with primary sjögren's syndrome. *Metabolomics*, *3*, 128.
- Minamoto, Y., Otoni, C. C., Steelman, S. M., Buyukleblebici, O., Steiner, J. M., Jergens, A. E., et al. (2015). Alteration of the fecal microbiota and serum metabolite profiles in dogs with idiopathic inflammatory bowel disease. *Gut Microbes*, *6*, 33–47.
- Navazesh, M. (1993). Methods for collecting saliva. *Annals of the New York Academy of Sciences*, *694*, 72–77.
- O'Kell, A. L., Garrett, T. J., Wasserfall, C., & Atkinson, M. A. (2017). Untargeted metabolomic analysis in naturally occurring canine diabetes mellitus identifies similarities to human Type 1 Diabetes. *Science Reports*, *7*, 9467.

- Okuma, N., Saita, M., Hoshi, N., Soga, T., Tomita, M., Sugimoto, M., et al. (2017). Effect of masticatory stimulation on the quantity and quality of saliva and the salivary metabolomic profile. *PLoS ONE*, *12*, e0183109.
- Pasha, S., Inui, T., Chapple, I., Harris, S., Holcombe, L., & Grant, M. M. (2018). The saliva proteome of dogs: Variations within and between breeds and between species. *Proteomics*, *18*, 1700293.
- Puurunen, J., Tiira, K., Lehtonen, M., Hanhineva, K., & Lohi, H. (2016). Non-targeted metabolite profiling reveals changes in oxidative stress, tryptophan and lipid metabolisms in fearful dogs. *Behavioral and Brain Functions*, *12*, 7.
- Puurunen, J., Tiira, K., Vapalahti, K., Lehtonen, M., Hanhineva, K., & Lohi, H. (2018). Fearful dogs have increased plasma glutamine and gamma-glutamyl glutamine. *Science Reports*, *8*, 15976.
- Sanguanserm, P., Jenkinson, H. F., Thanasak, J., Chairatvit, K., Roytrakul, S., Kittisenachai, S., et al. (2018). Comparative proteomic study of dog and human saliva. *PLoS ONE*, *13*, e0208317.
- Sugimoto, M., Wong, D. T., Hirayama, A., Soga, T., & Tomita, M. (2010). Capillary electrophoresis mass spectrometry-based saliva metabolomics identified oral, breast and pancreatic cancer-specific profiles. *Metabolomics*, *6*, 78–95.
- Sumner, L. W., Amberg, A., Barrett, D., Beale, M. H., Beger, R., Daykin, C. A., et al. (2007). Proposed minimum reporting standards for chemical analysis Chemical Analysis Working Group (CAWG) Metabolomics Standards Initiative (MSI). *Metabolomics*, *3*, 211–221.
- Takeda, I., Stretch, C., Barnaby, P., Bhatnager, K., Rankin, K., Fu, H., et al. (2009). Understanding the human salivary metabolome. *Nmr in Biomedicine*, *22*, 577–584.
- van Steenbeek, F. G., Hytonen, M. K., Leegwater, P. A., & Lohi, H. (2016). The canine era: The rise of a biomedical model. *Animal Genetics*, *47*, 519–527.

**Publisher's Note** Springer Nature remains neutral with regard to jurisdictional claims in published maps and institutional affiliations.

## II

### **Low-dose doxycycline treatment normalizes levels of some salivary metabolites associated with oral microbiota in patients with primary Sjögren's syndrome**

Herrala M\*, Turunen S\*, Hanhineva K, Lehtonen M, Mikkonen J J W, Seitsalo H, Lappalainen R, Tjäderhane L, Niemelä R K, Salo T, Myllymaa S, Kullaa A M and Kärkkäinen O

Metabolites 11: 595, 2021

\*Equal contribution





## Article

# Low-Dose Doxycycline Treatment Normalizes Levels of Some Salivary Metabolites Associated with Oral Microbiota in Patients with Primary Sjögren's Syndrome

Maria Herralá <sup>1,2,3,\*</sup>, Soile Turunen <sup>4,†</sup>, Kati Hanhineva <sup>5,6</sup>, Marko Lehtonen <sup>4</sup>, Jopi J. W. Mikkonen <sup>2,7</sup>, Hubertus Seitsalo <sup>8</sup>, Reijo Lappalainen <sup>7</sup>, Leo Tjäderhane <sup>3,9</sup>, Raija K. Niemelä <sup>10</sup>, Tuula Salo <sup>9,11,12,13</sup>, Sami Myllymaa <sup>7,14</sup>, Arja M. Kullaa <sup>1,2,15</sup> and Olli Kärkkäinen <sup>4</sup>

- <sup>1</sup> Research Group of Oral Health Sciences, Faculty of Medicine, Oulu University Hospital, University of Oulu, 90220 Oulu, Finland; arja.kullaa@uef.fi
  - <sup>2</sup> Institute of Dentistry, Faculty of Health Sciences, University of Eastern Finland, 70211 Kuopio, Finland; jopi.mikkonen@uef.fi
  - <sup>3</sup> Medical Research Center Oulu, Oulu University Hospital, University of Oulu, 90014 Oulu, Finland; leo.tjaderhane@helsinki.fi
  - <sup>4</sup> School of Pharmacy, University of Eastern Finland, 70210 Kuopio, Finland; soile.turunen@uef.fi (S.T.); marko.lehtonen@uef.fi (M.L.); olli.karkkainen@uef.fi (O.K.)
  - <sup>5</sup> Institute of Public Health and Clinical Nutrition, University of Eastern Finland, 70211 Kuopio, Finland; kati.hanhineva@uef.fi
  - <sup>6</sup> Department of Life Technologies, Food Chemistry and Food Development Unit, University of Turku, 20014 Turku, Finland
  - <sup>7</sup> Department of Applied Physics, University of Eastern Finland, 70211 Kuopio, Finland; reijo.lappalainen@uef.fi (R.L.); sami.myllymaa@uef.fi (S.M.)
  - <sup>8</sup> Private Dental Clinic Hammas&Hammas, 00130 Helsinki, Finland; hubertus.seitsalo@hammashammas.fi
  - <sup>9</sup> Department of Oral and Maxillofacial Diseases, Faculty of Medicine, University of Helsinki, 00014 Helsinki, Finland; tuula.salo@oulu.fi
  - <sup>10</sup> Department of Rheumatology, Oulu University Hospital, 90220 Oulu, Finland; Raija.Niemela@ppshp.fi
  - <sup>11</sup> Translational Immunology Research Program (TRIMM), University of Helsinki, 00014 Helsinki, Finland
  - <sup>12</sup> Department of Pathology, Faculty of Medicine, University of Helsinki, Helsinki University Hospital, 00014 Helsinki, Finland
  - <sup>13</sup> Cancer and Translational Medicine Research Unit, University of Oulu, 90014 Oulu, Finland
  - <sup>14</sup> Diagnostic Imaging Center, Kuopio University Hospital, 70029 Kuopio, Finland
  - <sup>15</sup> Educational Dental Clinic, Kuopio University Hospital, 90220 Kuopio, Finland
- \* Correspondence: marherra@student.oulu.fi; Fax: +358-8-537-5560  
† Equal contribution.



**Citation:** Herralá, M.; Turunen, S.; Hanhineva, K.; Lehtonen, M.; Mikkonen, J.J.W.; Seitsalo, H.; Lappalainen, R.; Tjäderhane, L.; Niemelä, R.K.; Salo, T.; et al. Low-Dose Doxycycline Treatment Normalizes Levels of Some Salivary Metabolites Associated with Oral Microbiota in Patients with Primary Sjögren's Syndrome. *Metabolites* **2021**, *11*, 595. <https://doi.org/10.3390/metabo11090595>

Academic Editor: Daniel Globisch

Received: 29 June 2021

Accepted: 28 August 2021

Published: 3 September 2021

**Publisher's Note:** MDPI stays neutral with regard to jurisdictional claims in published maps and institutional affiliations.



**Copyright:** © 2021 by the authors. Licensee MDPI, Basel, Switzerland. This article is an open access article distributed under the terms and conditions of the Creative Commons Attribution (CC BY) license (<https://creativecommons.org/licenses/by/4.0/>).

**Abstract:** Saliva is a complex oral fluid, and plays a major role in oral health. Primary Sjögren's syndrome (pSS), as an autoimmune disease that typically causes hyposalivation. In the present study, salivary metabolites were studied from stimulated saliva samples ( $n = 15$ ) of female patients with pSS in a group treated with low-dose doxycycline (LDD), saliva samples ( $n = 10$ ) of non-treated female patients with pSS, and saliva samples ( $n = 14$ ) of healthy age-matched females as controls. Saliva samples were analyzed with liquid chromatography mass spectrometry (LC-MS) based on the non-targeted metabolomics method. The saliva metabolite profile differed between pSS patients and the healthy control (HC). In the pSS patients, the LDD treatment normalized saliva levels of several metabolites, including tyrosine glutamine dipeptide, phenylalanine isoleucine dipeptide, valine leucine dipeptide, phenylalanine, pantothenic acid (vitamin B5), urocanic acid, and salivary lipid cholesteryl palmitic acid (CE 16:0), to levels seen in the saliva samples of the HC. In conclusion, the data showed that pSS is associated with an altered saliva metabolite profile compared to the HC and that the LDD treatment normalized levels of several metabolites associated with dysbiosis of oral microbiota in pSS patients. The role of the saliva metabolome in pSS pathology needs to be further studied to clarify if saliva metabolite levels can be used to predict or monitor the progress and treatment of pSS.

**Keywords:** saliva; Sjögren's syndrome; metabolomics; hyposalivation; doxycycline

## 1. Introduction

Saliva is an essential biofluid in the oral cavity, and its composition and volume are important factors in oral health. Saliva is secreted from three pairs of major salivary glands and several minor salivary glands, and the autonomic nervous system is involved in the control of salivary secretion [1] (pp. 27–29). Many factors, including systemic diseases, can affect salivary production. Sjögren’s syndrome (SS) is a disease that affects salivary glands, manifesting as hyposalivation and abnormal levels of salivary components [2]. Sjögren’s syndrome can be classified as primary (pSS) or secondary (sSS) forms. The focus of this article is pSS. SS has a wide range of clinical manifestations and symptoms, from affecting salivary or lacrimal glands to multi-organ symptoms and, potentially, a high risk of malignant lymphomas [3,4]. Patients with pSS usually have to wait a long time for a diagnosis, during which the disease progresses. Hauck et al. 2013 [5] noted a diagnosis delay of four years (median) between onset and diagnosis (range 0–28 years) in a Canadian population. There is an urgent need to study and develop new tools for the diagnosis and monitoring of pSS.

The metabolic profile of saliva can provide an early diagnosis of pSS and monitoring of its progress [6]. SS is associated with alterations in the metabolite profile of saliva; for example, elevated levels of choline, taurine, and alanine have been reported [6,7]. Recent developments in instrumentation have led to new spectrometric platforms for metabolomics, which employ state-of-the-art analytical techniques, such as different mass spectrometry methods in conjunction with either high-performance liquid chromatography (HPLC-MS) or two-dimensional gas chromatography (2DGC-MS) and nuclear magnetic resonance (NMR) spectroscopy [8]. In our previous study, 24 salivary metabolites were identified using  $^1\text{H}$  NMR spectroscopy [9].

Gardner et al. 2020 [10] listed numerous diseases that have been studied using metabolomic techniques, for which potential salivary biomarkers have been found. These include oral cancer, oral leukoplakia, breast cancer, prostate cancer, periodontal disease (common, aggressive, and chronic), dental caries, pSS, dementia, Alzheimer’s disease, mild cognitive impairment, Parkinson’s disease, celiac disease, sarcoidosis, recurrent aphthous ulceration, untreated and treated HIV, hepatitis B, medication-related osteonecrosis of the jaw, parotid gland tumor, adult and pediatric obesity, and external apical root resorption in orthodontic therapy. There is new knowledge indicating that dysbiotic oral microbiota can invade the ductal cells, providing new insights into the etiopathogenesis of pSS [11].

Matrix metalloproteinases (MMPs) have been studied as a potential target of interest in the treatment plan of pSS. Low-dose doxycycline (LDD) has been suggested to help pSS patients’ symptoms by decreasing MMP activity. LDD also has an antimicrobial effect [12]. In Seitsalo et al. [12], data suggested that LDD medication did not relieve pSS patients’ symptoms.

The present study aimed to measure changes in the saliva metabolite profile associated with pSS and to investigate if LDD treatment can normalize some of these changes. We used non-targeted LC-MS-based metabolomics methods to measure saliva metabolite profiles from samples collected from healthy controls (HC) and pSS patients with or without LDD treatment.

## 2. Results

The salivary flow rate was  $0.14 \pm 0.06$  mL/min (mean  $\pm$  SD) before medication and  $0.15 \pm 0.07$  mL/min after one week of medication. No statistically significant difference was observed between salivary flow rates. All identified metabolites with *p*-values below 0.05 are reported in Table 1. The multivariate analysis results are shown in Figure 1. The PCA showed the separation of the untreated pSS patients’ saliva metabolite profile from the saliva metabolite profile of the HC. pSS patients with LDD treatment were mixed with

the first two groups in the PCA, indicating that the doxycycline treatment shifted the saliva metabolite profile closer to that seen in the HC compared to the untreated pSS patients.

Good predictability is seen in the PLS-DA model between the saliva metabolite profiles of the HC and the untreated pSS patients (PLS-DA model with three components,  $Q^2$  (cumulative) = 0.77), indicating a clear separation of the saliva metabolite profiles, in line with the PCA results. In contrast, the predictability was decreased in the PLS-DA models between the LDD-treated pSS patients' salivary metabolite profiles compared to the HC ( $Q^2$  (cum) = 0.67) and the untreated pSS patients ( $Q^2$  (cum) = 0.39). However, the results also show that, even after the LDD treatment, the saliva metabolite profile of pSS patients is different from that of HC.

Identified metabolites that were significantly different between the saliva samples of patients with pSS and HC are reported in Table 1. The results of the univariate analyses were mostly in line with the results of the multivariate analysis. The exceptions were lysophosphatidylethanolamide 18:0 (LPE 18:0) and lysophosphatidylcholine 18:0 (LPC 18:0), which were not observed in the samples from HC, but were seen in most of the samples from patients with pSS. VIP values from PLS-DA, and  $p$ -values and Cohen's  $d$  effect sizes, are reported in Table 1. In the univariate analysis, there were 912, 767, and 223 molecular features with  $p$ -values below 0.05 when comparing untreated pSS patients to controls, LDD-treated pSS patients to controls, and untreated pSS patients to treated pSS patients, respectively. However, we were not able to identify most of these molecular features, which is typical for a non-targeted metabolomics study. In the pathway analysis, four pathways had  $p$ -values below 0.05: aminoacyl-tRNA biosynthesis ( $p = 0.0013$ ); valine, leucine, and isoleucine biosynthesis ( $p = 0.0082$ ); nicotinate and nicotinamide metabolism ( $p = 0.0286$ ); and histidine metabolism ( $p = 0.0323$ ) when the pSS group was compared to the controls. However, none of these results survived correction for multiple testing (Supplementary Table S1).

In the pSS patients, the LDD treatment normalized saliva levels of some metabolites, namely, tyrosine glutamine dipeptide, phenylalanine isoleucine dipeptide, valine leucine dipeptide, phenylalanine, pantothenic acid (vitamin B5), urocanic acid, and cholesteryl palmitic acid (CE 16:0), to levels seen in the saliva samples of the HC (Figure 2). Here, the results of multivariate and univariate analyses are also in line.

Table 1. Identified salivary metabolites associated with Sjögren's syndrome.

Metabolite	ID	Healthy Controls, HC (C)		Sjögren's Syndrome (pSS) without LDD		Sjögren's Syndrome (pSS) with LDD (D)		pSS vs. C		D vs. C		D vs. pSS						
		Mean	SD	Mean	SD	Mean	SD	VIP	p	d	VIP	p	d	VIP	p	d		
Amino acids, peptides, and analogues																		
4-Guaminobutyric acid	2	16,864	4783	31,881	18,325	28,463	10,929	1.38	0.031	1.3	1.83	0.004	1.5	0.39	0.612	0.612	-0.2	
Glutamic acid	1	122,045	67,786	250,491	87,720	225,246	124,395	1.91	0.001	1.7	1.48	0.010	1.1	0.72	0.558	0.558	-0.2	
Glycine betaine	1	1241,617	504,031	1,999,692	964,523	1,849,530	974,498	1.43	0.041	1.0	1.31	0.045	0.8	0.33	0.708	0.708	-0.2	
Isoleucine	2	48,927	30,704	166,871	135,723	99,906	78,292	1.54	0.023	1.4	1.28	0.037	0.9	1.00	0.184	0.184	-0.6	
Leucine	2	112,620	46,369	448,733	419,771	190,974	115,700	1.56	0.032	1.4	1.37	0.026	1.0	1.54	0.088	0.088	-1.0	
Phenylalanine	1	614,751	174,399	1,180,634	775,776	612,765	291,252	1.41	0.048	1.2	0.53	0.982	0.0	1.58	0.050	0.050	-1.1	
Tryptophan	1	33,773	17,245	97,779	66,429	56,455	30,196	1.63	0.014	1.5	1.32	0.021	1.0	1.32	0.091	0.091	-0.9	
Arg-Ser	2	653,047	308,815	285,658	248,390	447,258	269,746	1.56	0.004	-1.3	1.10	0.072	-0.7	1.49	0.145	0.145	0.6	
Phe-Ile	2	35,793	41,934	122,220	85,371	33,595	37,875	1.55	0.040	1.4	0.39	0.923	-0.1	1.81	0.037	0.037	-1.4	
Tyr-Gln	2	56,858	34,559	149,463	64,758	63,153	33,558	1.96	0.001	1.9	0.48	0.641	0.2	2.23	0.002	0.002	-1.8	
Val-Leu	2	320,566	283,561	1,029,040	940,151	300,576	370,401	1.42	0.043	1.2	0.47	0.871	-0.1	1.61	0.040	0.040	-1.1	
Lipids and carnitines																		
FA 16:0	2	19,113,838	2,988,053	23,755,538	5,398,164	21,707,731	6,550,119	1.40	0.029	1.1	1.01	0.181	0.5	0.58	0.403	0.403	-0.3	
FA 16:1	2	291,295	177,097	601,015	353,046	406,038	534,487	1.46	0.025	1.2	0.64	0.442	0.3	0.91	0.283	0.283	-0.4	
Azelaic acid	1	46,004	5591	61,345	16,287	54,030	11,500	1.67	0.161	1.4	1.27	0.025	0.9	0.95	0.238	0.238	-0.5	
Leucic acid	2	61,064	25,243	42,491	15,691	45,390	20,708	1.25	0.037	-0.9	1.00	0.089	-0.7	1.23	0.706	0.706	0.2	
CE 16:0	1	4,277,005	204,081	5,253,366	726,120	4,751,349	817,147	2.03	0.002	2.1	1.23	0.045	0.9	1.02	0.122	0.122	-0.7	
Cholesterol	1	42,086	23,976	107,189	65,001	111,790	89,827	1.66	0.118	1.5	1.50	0.010	1.2	0.45	0.883	0.883	0.1	
Propionylcarnitine	1	91,310	57,056	165,515	81,484	202,565	108,289	1.47	0.025	1.1	1.73	0.002	1.3	0.62	0.340	0.340	0.4	
Isobutyryl carnitine	2	50,626	23,350	95,837	32,915	123,268	75,870	1.85	0.002	1.6	1.80	0.004	1.5	0.77	0.244	0.244	0.5	
LPC 18:0	2	0	0	24,441	13,129	71,932	99,287	0.01	<0.001		0.68	<0.001		0.84	0.170	0.170	0.8	
LPE 18:0	2	0	0	16,498	8405	17,072	8133	0.34	<0.001		0.25	<0.001		0.35	0.941	0.941	0.1	
Oleamide	2	9,389,628	1,079,571	11,488,697	1,386,541	10,258,327	2,115,434	1.85	<0.001	1.7	0.96	0.174	0.5	1.03	0.092	0.092	-0.7	
Linoleamide	2	30,287,081	4,290,249	37,683,667	8,799,870	35,644,986	12,192,656	1.41	0.030	1.1	1.04	0.140	0.7	0.44	0.639	0.639	-0.2	
Palmitoleamide	2	12,508,377	1,779,147	15,694,049	3,897,803	15,115,575	6,193,420	1.41	0.033	1.1	1.04	0.137	0.7	0.20	0.777	0.777	-0.1	
Other																		
Choline	2	5,453,217	2,359,520	9,987,031	4,308,942	9,524,364	4,603,084	1.59	0.010	1.4	1.60	0.009	1.2	0.31	0.804	0.804	-0.1	
Pantothenic acid (B5)	1	4289	2431	25,186	9179	12,290	10,088	2.46	<0.001	3.6	1.53	0.009	1.3	1.81	0.003	0.003	-1.3	
MEHP	1	101,276	15,673	58,944	15,552	88,751	27,838	2.35	<0.001	-2.7	0.87	0.146	-0.6	1.77	0.002	0.002	1.4	
Xanthine	1	173,813	123,732	548,441	260,922	601,704	302,916	2.05	0.001	1.9	2.15	<0.001	2.0	0.41	0.644	0.644	0.2	
Uroacnic acid	1	36,386	16,273	96,702	77,360	40,992	25,246	1.47	0.037	1.3	0.41	0.572	0.2	1.55	0.052	0.052	-1.1	

Table 1. Cont.

Metabolite	ID	Healthy Controls, HC (C)		Sjögren's Syndrome (pSS) without LDD		Sjögren's Syndrome (pSS) with LDD (D)		pSS vs. C		D vs. C		D vs. pSS				
		Mean	SD	Mean	SD	Mean	SD	VIP	p	VIP	p	VIP	p	d		
1-Methylnicotinamide	2	11,940	1594	28,433	16,638	33,923	33,704	1.68	0.039	1.8	1.27	0.069	1.2	0.42	0.664	0.2
Biliverdin IX	1	162,101	31,725	137,588	11,938	140,733	11,422	1.28	0.017	-1.1	1.33	0.030	-1.0	0.46	0.519	0.3
N6-methyl-adenine	2	55,816	27,354	119,280	86,943	102,200	74,734	1.35	0.049	1.1	1.35	0.037	0.9	0.39	0.618	-0.2
Nicotinic acid	1	43,642	31,275	107,135	80,169	87,564	60,411	1.37	0.049	1.1	1.34	0.029	1.0	0.71	0.541	-0.3
Diethanolamine	1	147,588	168,396	695,458	459,234	219,384	495,663	1.89	0.004	1.7	0.56	0.628	0.2	1.56	0.027	-1.0
Stearamide	2	10,065,816	1,374,684	12,518,622	3,182,570	11,313,506	3,775,837	1.35	0.042	1.1	0.94	0.247	0.5	0.56	0.399	-0.3
Dibutyladipate	2	73,783	33,110	43,796	6608	86,324	85,921	1.45	0.005	-1.5	0.54	0.606	0.2	1.10	0.077	0.9

Legend: Bolded text, *p*-values below multiple comparison corrected  $\alpha$  ( $p < 0.002$ ); Arg-Ser, Arginine serine dipeptide; CE 16:0, cholesteryl palmitic acid; d, Cohen's d effect size; FA, fatty acid; ID, level of identification (1 = verified by comparing exact mass, retention time, and MS/MS fragmentation spectra with in-house standard library, 2 = matched with exact mass and MSMS spectra from public databases); LPC, lysophosphatidylcholine; LPE, lysophosphatidylethanolamine; MEFH, Monoethylhexyl phthalic acid; Phe-Ile, phenylalanine isoleucine dipeptide; SD, standard deviation; Tyr-Gln, Tyrosine glutamine dipeptide; Val-Leu, Valine leucine dipeptide; VIP, variable importance to projection (from PLS-DA); *p*, *p*-value from Welch's *t*-test; Mean ion abundance is shown; Identified metabolites with  $p < 0.05$  in comparison between patients with pSS and HC are shown.

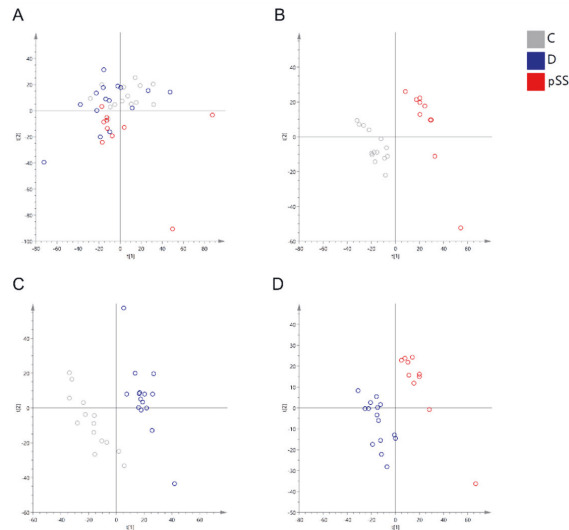


**Figure 1.** Results of principal component analysis of the metabolomics data. In the principal component analysis (PCA), a separation of the groups can be seen, in which the metabolite profile of the saliva samples from the Sjögren's syndrome patients before drug treatment (pSS) are separated from the metabolite profile of saliva samples from the HC (C), whereas Sjögren's syndrome patients with LDD treatment (D) are mixed with the first two groups (A). Partial least sum of squares (PLS-DA) models between the controls and the Sjögren's syndrome patients without drug treatment ((B): Three components, R2Y (cumulative) = 0.99, Q2 (cumulative) = 0.77), between the controls and Sjögren's syndrome patients with low-dose doxycycline treatment ((C): Four components, R2Y (cum) = 0.99, Q2 (cum) = 0.67), and Sjögren's syndrome patients with and without drug treatment ((D): Two components, R2Y (cum) = 0.94, Q2 (cum) = 0.39).

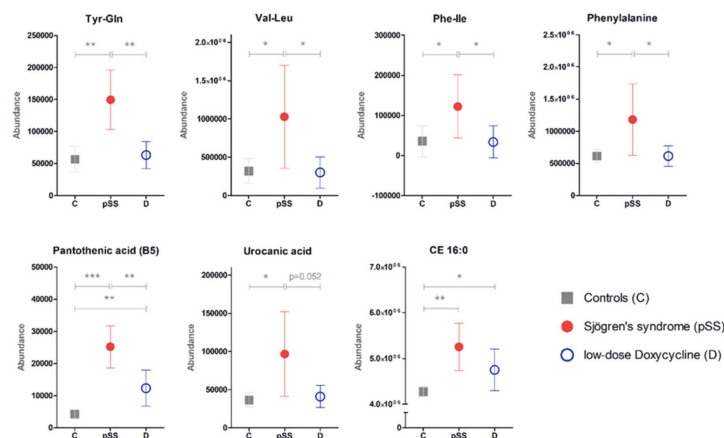


**Figure 2.** LDD treatment normalized levels of metabolites in the saliva samples of patients with Sjögren's syndrome. Several metabolites were altered in the saliva samples of patients with pSS when compared to the saliva samples from HC. LDD treatment normalized levels of some, but not all, of these metabolites closer to levels seen in HC. Mean ion abundance with 95% confidence intervals is shown. Legend: CE 16:0, cholesteryl palmitic acid; Phe-Ile, phenylalanine isoleucine dipeptide; Tyr-Gln, Tyrosine glutamine dipeptide; Val-Leu, Valine leucine dipeptide; \*,  $p < 0.05$ ; \*\*,  $p < 0.01$ ; \*\*\*,  $p < 0.001$ .

### 3. Discussion

In the present study, we observed that the saliva metabolite profile was different between pSS patients and HC. Moreover, we found out that the LDD treatment reversed some, but not all, of these changes.

We observed high levels of dipeptides, namely, tyrosine glutamine dipeptide, phenylalanine isoleucine dipeptide, and valine leucine dipeptide, and phenylalanine, in the saliva samples of patients with pSS. Previous reports have shown that pSS patients have dysbiosis in oral microbiota in bacterial species (e.g., *Prevotella* and *Porphyromonas* species) that can degrade proteins into smaller peptides and further into amino acids, such as phenylalanine [11,13–17]. Moreover, high levels of dipeptides and phenylalanine in saliva have been associated with dysbiosis of oral microbiota in other oral pathologies, such as periodontitis [15,18]. Therefore, high levels of dipeptides and phenylalanine in the saliva of pSS patients are likely to be associated with dysbiosis in the oral microbiota composition.

Moreover, high pantothenic acid (vitamin B5) levels were observed in saliva samples of pSS patients. Oral microbiota can synthesize pantothenic acid, which is needed to form coenzyme-A (CoA), an essential cofactor of cellular metabolism [19–21]. Pantothenic acid has been associated with the release of cytokines, and appears to have antibacterial properties towards some bacteria, such as mycobacteria [22,23]. Urocanic acid can also be degraded by bacteria [24]. Therefore, high levels of pantothenic acid and urocanic acid in the saliva of pSS patients may also be associated with dysbiosis in the oral microbiota composition.

Furthermore, LDD treatment normalized levels of several metabolites associated with dysbiosis of the oral microbiota (Figure 2). In the present study, we analyzed masticatory stimulated saliva, which is verified as an adequate alternative to unstimulated saliva for microbiome-related studies [25]. LDD treatment did not show a statistically significant difference for salivary flow. However, it is unclear how or if dysbiosis is connected to pSS. Therefore, it appears likely that LDD treatment normalized the dysbiosis of oral microbiota seen in pSS patients, a hypothesis that needs further investigations.

Moreover, cholesteryl palmitic acid (CE 16:0) is an ester of cholesterol found in saliva, in addition to cell membranes and blood [26]. Salivary lipids are important for the flexibility, fluidity, and permeability of oral cellular membranes, and levels of salivary lipids, including cholesteryl esters, are altered in SS patients [27,28]. Therefore, LDD appears to normalize the levels of some salivary lipids, i.e., CE 16:0 in this study, but not all in pSS patients.

The pathway analysis indicated that four pathways, namely aminoacyl-tRNA biosynthesis; valine, leucine, and isoleucine biosynthesis; nicotinate and nicotinamide metabolism; and histidine metabolism, were altered in the saliva samples from the pSS group when compared to the controls, indicating alterations in the amino acid metabolism. However, these results should be considered preliminary and be verified with a larger cohort of patients.

It should be noted that the LDD treatment appears to only normalize the saliva metabolite profile in some patients with pSS (Figure 1). Unfortunately, the present study had limited statistical power, due to a relatively small sample size. Therefore, we were not able to conduct subgroup analyses to compare those who responded well to LDD treatment to those who did not. With a larger sample size, this kind of pharmacometabolomics analysis may reveal new predictive biomarkers to recognize, before treatment, those individuals who are most likely to benefit from the LDD treatment. In Seitsalo et al. [12], LDD did not affect pSS patients' clinical symptoms.

In conclusion, we observed that pSS is associated with an altered saliva metabolite profile when compared to HC. Furthermore, we showed that the LDD treatment normalized levels of several metabolites associated with dysbiosis of oral microbiota in patients with pSS. Further study is needed to better understand the role of the saliva metabolome in pSS pathology and to investigate if saliva metabolite levels can be used to predict patients who are likely to benefit from doxycycline treatment.

## 4. Materials and Methods

### 4.1. Ethical Statement

This study was designed within the recommendations of the Declaration of Helsinki and the Oulu University Hospital Ethical Committee gave a favorable opinion regarding all plans of the study (EETTMK: 116/2000 and 36/2012). For the mass spectroscopy component of the study, ethical permission for the research was granted by The Hospital District of Northern Savo, Kuopio, Finland (745/2018; (82/2014). As stated in the Declaration of Helsinki, all participants give their written consent to participate in this study.

### 4.2. Participants

The pSS group consisted of 15 female patients who were aged 28–68 years (mean age 48.6 years). Diagnostic criteria for Sjogren's syndrome were based on those of the European Community guidelines [29,30]. Smoking habit, and oral or systemic diseases other than pSS, were exclusion criteria; more detailed information is provided in Niemelä et al., (2004). The control group consisted of 14 healthy females, aged between 28 and 68 years (mean age 49.8 years). The control subjects did not have chronic diseases, were non-smoking, and were not receiving treatment to affect the results.

### 4.3. Collection of Salivary Samples

Both stimulated and unstimulated saliva samples from the pSS patients were collected as described in Seitsalo et al. [12]. When saliva samples were collected, no periodontal diseases or carious lesions were present. Because patients typically suffer from hyposalivation, some samples were not sufficient for analysis with LC-MS or were poor quality. Saliva flow rates (mL/min) were calculated immediately after collection, as described previously (Herrala et al., (2021)). The Wilcoxon signed ranks test was used to analyze the salivary flow rate between the pre-medication and one week medication samples. Therefore, from a total of 25 stimulated saliva samples of pSS patients were analyzed: 10 before LDD treatment and 15 after treatment with LDD (Periostat<sup>R</sup>, 20 mg doxycycline), which was given twice per day for one week. The control group saliva samples ( $n = 14$ ) were collected only once at the medical campus of the University of Oulu, Finland.

The saliva sample collection followed the protocols proposed in the study of Navazesh 1993 [31]. All the saliva samples were collected considering the circadian rhythm (between 10 am and 12 am). Eating and drinking were not allowed a minimum of one hour before the saliva sample collection. After collection, the saliva samples were immediately centrifuged and the supernatants were stored and transported as described in [6,9]. We demonstrate this study design in Figure 3.

### 4.4. Metabolomics Analysis

The metabolomics analysis pipeline and the saliva sample metabolomics analysis have been previously described in detail [32,33]. Briefly, the saliva samples were thawed on ice. Saliva samples were precipitated and extracted in the ratio of 200  $\mu$ L of saliva and 400  $\mu$ L of acetonitrile. All samples were centrifuged (10,600  $\times$  g, 5 min, +4  $^{\circ}$ C), and the supernatants were filtered through 0.2  $\mu$ m Acrodisc<sup>®</sup> Syringe Filters with a PTFE membrane (PALL Corporation, Ann Arbor, MI, USA) prior to the LC-MS analyses. The quality control (QC) sample contained 30  $\mu$ L aliquots from all experimental samples mixed in one tube.

HPLC-grade acetonitrile (VWR Chemicals, Fontenay-sous-Bois, France) was used for sample preparation. LC-MS grade methanol (Riedel-de Haën<sup>™</sup>, Honeywell, Seelze, Germany), HPLC-grade acetonitrile (VWR Chemicals, Fontenay-sous-Bois, France), LC-MS grade formic acid (Fluka<sup>™</sup>, Honeywell, Seelze, Germany), ammonium formate (Fluka<sup>™</sup>, Honeywell, Seelze, Germany), and class 1 ultra-pure water (ELGA Purelab ultra Analytical, High Wycombe, UK) were used for mobile phase eluents in reverse phase (RP) and hydrophilic interaction (HILIC) liquid chromatography separation.

The samples were analyzed by a 1290 LC system coupled to a 6540 UHD accurate-mass Q-ToF spectrometer (Agilent Technologies, Waldbronn, Karlsruhe, Germany) using



electrospray ionization (ESI, Jet Stream) in both positive and negative polarity, and using both RP and HILIC.

For the quality assurance of the chromatographic and mass spectrometry runs, QC samples were injected at the beginning of the analysis and after every 9 samples. The QC samples were used for the automatic data-dependent MS/MS analyses. The data acquisition was accomplished with MassHunter Acquisition B.05.01 software (Agilent Technologies).

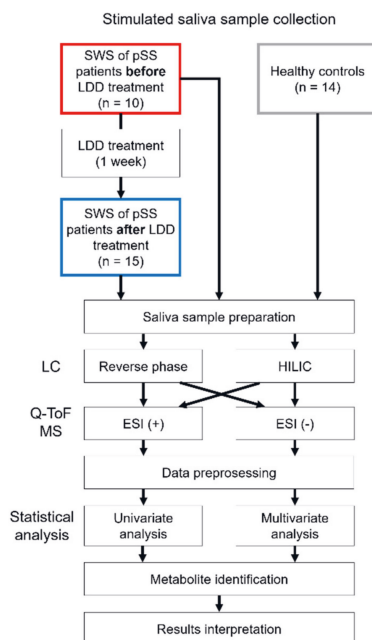


**Figure 3.** Workflow of the non-targeted metabolomics analysis. Stimulated whole saliva (SWS) samples were collected from patients with primary Sjögren’s syndrome (pSS) before and after low-dose doxycycline (LDD) treatment (20 mg twice per day for one week) and from healthy controls. Saliva samples with low quantity or low quality were removed from the analysis. Details of the non-targeted metabolomics analysis of saliva samples has been previously described [32]. Briefly, after sample preparation, the samples were analyzed with four different analytical methods: using both reverse phase and hydrophilic interaction (HILIC) liquid chromatography (LC) separation, followed with both positive and negative electrospray ionization (ESI). After data preprocessing, we used both multivariate and univariate statistical methods to identify molecular features of interest, from which identification of metabolites was undertaken using both in-house and publicly available databases.

The LC-MS raw data from four different analytical modes (RP+, RP−, HILIC+, HILIC−) was exported to MassHunter Qualitative Analysis B.07.00 (Agilent Technologies, Santa Clara, CA, USA) for feature extraction and peak picking, combined with chromatographic alignment across all data files per mode. To remove the redundant and non-specific information considered to be background noise, peaks with ion abundance less than 10,000 were excluded from further analysis. The feature files were imported as compound exchange format (.cef) files into Agilent Mass Profiler Professional software (MPP version 13.1.1, Agilent Technologies) for compound alignment to yield a peak list.

Multivariate analyses, principal component analysis (PCA), and partial least sum of squares discriminant analysis (PLS-DA) were performed to mean centered and autoscaled data using SIMCA (version 15, Umetrics, Umea, Sweden). For univariate analysis, we used

Cohen's  $d$  to calculate effect sizes and Welch's  $t$ -test to calculate  $p$ -values from non-scaled ion abundance data. Because of the correlated nature of metabolomics data, we adjusted the  $\alpha$  level by the number of latent components needed to explain 95% of the variance in the metabolomics data in the PCA to account for multiple testing. Here, 32 latent components were needed to explain 95% of the data and the new  $\alpha$  was set to 0.002.

The metabolite identification was performed using open-source software, MS-DIAL (RIKEN PRIME). Collected MS/MS data was converted to .abf files using the Analysis Base File Converter program (Reifycs Inc., Tokyo, Japan) and converted files were imported into MS-DIAL (versions 2.66 to 3.90). Public databases, Metlin and MassBank of North America (MoNA), and an in-house standard library were used. The guidelines from Sumner et al. [34] were used for ranking metabolite identifications as follows: Compounds in identification level 1 were verified by comparing exact mass, retention time, and MS/MS fragmentation spectra with the in-house standard library. Compounds in level 2 were matched with exact mass and MSMS spectra from the public databases mentioned above. We used MetaboAnalyst (version 5.0, [35]) to undertake a pathway analysis of identified metabolites with a  $p$ -value below 0.05. We used KEGG pathways for humans as a reference metabolic pathway.

**Supplementary Materials:** The following are available online at <https://www.mdpi.com/article/10.3390/metabo11090595/s1>, Table S1: Results of the pathway analysis.

**Author Contributions:** Conceptualization, M.H., S.T., H.S., L.T., R.K.N., T.S., A.M.K. and O.K.; methodology, H.S., T.S., L.T., M.H., K.H., O.K., S.T. and A.M.K.; software, O.K., K.H., M.L. and S.T.; validation, O.K., M.H. and A.M.K.; formal analysis, M.L., J.J.W.M., K.H., S.M. and O.K.; investigation, M.H., J.J.W.M., A.M.K., S.T. and O.K.; resources, O.K., S.M., K.H., M.L., M.H. and A.M.K.; data curation, M.L., O.K., S.T., J.J.W.M. and K.H.; writing—original draft preparation, O.K., M.H., T.S., L.T. and A.M.K.; writing—review and editing, M.H., S.M., A.M.K. and O.K.; visualization, O.K. and J.J.W.M.; supervision, A.M.K., R.L., T.S., L.T., S.M., M.L. and K.H.; project administration, A.M.K., K.H. and O.K.; funding acquisition, M.H., T.S., L.T. and A.M.K. All authors have read and agreed to the published version of the manuscript.

**Funding:** The Finnish Funding Agency for Technology and Innovation (Tekes), a project called Oraldent (2186/31/2010), and Oral Cancer (52/31/2014) funded part of this study. M.H. received a personal grant from the Finnish Dental Society, Apollonia.

**Institutional Review Board Statement:** The study was conducted according to the guidelines of the Declaration of Helsinki and approved by the Oulu University Hospital Ethical Committee gave a favorable opinion regarding all plans of the study (EETTMK: 116/2000 and 36/2012) and for the mass spectroscopy part of the study the ethical permission for the research was granted by The Hospital District of Northern Savo, Kuopio, Finland (745/2018; (82/2014).

**Informed Consent Statement:** Informed consent was obtained from all subjects involved in the study.

**Data Availability Statement:** The data presented in this study are available in [Supplementary Table S1].

**Acknowledgments:** We thank Miia Reponen for technical assistance with the mass spectrometry analyses, and Biocenter Finland and Biocenter Kuopio for supporting the core LC-MS laboratory facility.

**Conflicts of Interest:** O.K. and K.H. are founders of Afekta Technologies Ltd., a company providing metabolomics analysis services. The other authors have no potential conflict of interest to declare.

## References

1. Wong, D. *Salivary Diagnostics*; Wiley-Blackwell: Ames, IA, USA, 2008; pp. 27–29.
2. Jazzar, A.A.; Shirlaw, P.J.; Carpenter, G.H.; Challacombe, S.J.; Proctor, G.B. Salivary S100A8/A9 in Sjögren's syndrome accompanied by lymphoma. *J. Oral Pathol. Med.* **2018**, *47*, 900–906. [[CrossRef](#)]
3. Cecchetti, A.; Finamore, F.; Ucciferri, N.; Donati, V.; Mattii, L.; Polizzi, E.; Ferro, F.; Sernissi, F.; Mosca, M.; Bombardieri, S.; et al. Phenotyping multiple subsets in Sjögren's syndrome: A salivary proteomic SWATH-MS approach towards precision medicine. *Clin. Proteom.* **2019**, *16*, 26. [[CrossRef](#)]

4. Zoukhri, D.; Rawe, I.; Singh, M.; Brown, A.; Kublin, C.L.; Dawson, K.; Haddon, W.F.; White, E.L.; Hanley, K.M.; Tusé, D.; et al. Discovery of putative salivary biomarkers for Sjögren's syndrome using high resolution mass spectrometry and bioinformatics. *J. Oral Sci.* **2012**, *54*, 61–70. [[CrossRef](#)] [[PubMed](#)]
5. Hauck, T.S.; Douglas, S.C.; Bookman, A. Sjogren's syndrome in Canada: Diagnosis, treatment and patient perspectives. *Connections* **2013**, *7*.
6. Herrala, M.; Mikkonen, J.J.; Pesonen, P.; Lappalainen, R.; Tjäderhane, L.; Niemelä, R.K.; Seitsalo, H.; Salo, T.; Myllymaa, S.; Kullaa, A.M. Variability of salivary metabolite levels in patients with Sjögren's syndrome. *J. Oral Sci.* **2021**, *63*, 22–26. [[CrossRef](#)] [[PubMed](#)]
7. Kageyama, G.; Saegusa, J.; Irino, Y.; Tanaka, S.; Tsuda, K.; Takahashi, S.; Sendo, S.; Morinobu, A. Metabolomics analysis of saliva from patients with primary Sjögren's syndrome. *Clin. Exp. Immunol.* **2015**, *182*, 149–153. [[CrossRef](#)]
8. Spratlin, J.L.; Serkova, N.J.; Eckhardt, S.G. Clinical applications of metabolomics in oncology: A review. *Clin. Cancer Res.* **2009**, *15*, 431–440. [[CrossRef](#)]
9. Mikkonen, J.J.; Herrala, M.; Soininen, P.; Lappalainen, R.; Tjäderhane, L.; Seitsalo, H.; Niemelä, R.; Salo, T.; Kullaa, A.M.; Myllymaa, S. Metabolic profiling of saliva in patients with primary Sjögren's syndrome. *Metabolomics* **2013**, *3*, 1.
10. Gardner, A.; Carpenter, G.; So, P.W. Salivary Metabolomics: From Diagnostic Biomarker Discovery to Investigating Biological Function. *Metabolites* **2020**, *10*, 47. [[CrossRef](#)]
11. Alam, J.; Lee, A.; Lee, J.; Kwon, D.I.; Park, H.K.; Park, J.H.; Jeon, S.; Baek, K.; Lee, J.; Park, S.H.; et al. Dysbiotic oral microbiota and infected salivary glands in Sjögren's syndrome. *PLoS ONE* **2020**, *15*, e0230667. [[CrossRef](#)]
12. Seitsalo, H.; Niemelä, R.K.; Marinescu-Gava, M.; Vuotila, T.; Tjäderhane, L.; Salo, T. Effectiveness of low-dose doxycycline (LDD) on clinical symptoms of Sjögren's syndrome: A randomized, double-blind, placebo controlled cross-over study. *J. Negat. Results Biomed.* **2007**, *6*, 11. [[CrossRef](#)] [[PubMed](#)]
13. Rusthen, S.; Kristoffersen, A.K.; Young, A.; Galtung, H.K.; Petrovski, B.É.; Palm, Ø.; Enersen, M.; Jensen, J.L. Dysbiotic salivary microbiota in dry mouth and primary Sjögren's syndrome patients. *PLoS ONE* **2019**, *14*, e0218319. [[CrossRef](#)] [[PubMed](#)]
14. Singh, M.; Teles, F.; Uzel, N.G.; Papas, A. Characterizing Microbiota from Sjögren's Syndrome Patients. *JDR Clin. Transl. Res.* **2020**. [[CrossRef](#)] [[PubMed](#)]
15. Takahashi, N. Oral Microbiome Metabolism: From "Who Are They?" to "What Are They Doing?". *J. Dent. Res.* **2015**, *94*, 1628–1637. [[CrossRef](#)]
16. Van der Meulen, T.A.; Harmsen, H.J.; Bootsma, H.; Liefers, S.C.; Vich Vila, A.; Zhernakova, A.; Fu, J.; Wijmenga, C.; Spijkervet, F.K.; Kroese, F.G.; et al. Dysbiosis of the buccal mucosa microbiome in primary Sjögren's syndrome patients. *Rheumatology* **2018**, *57*, 2225–2234. [[CrossRef](#)]
17. van der Meulen, T.A.; Harmsen, H.J.; Vila, A.V.; Kurilshikov, A.; Liefers, S.C.; Zhernakova, A.; Fu, J.; Wijmenga, C.; Weersma, R.K.; de Leeuw, K.; et al. Shared gut, but distinct oral microbiota composition in primary Sjögren's syndrome and systemic lupus erythematosus. *J. Autoimmun.* **2019**, *97*, 77–87. [[CrossRef](#)]
18. Liebsch, C.; Pitchika, V.; Pink, C.; Samietz, S.; Kastenmüller, G.; Artati, A.; Suhre, K.; Adamski, J.; Nauck, M.; Völzke, H.; et al. The Saliva Metabolome in Association to Oral Health Status. *J. Dent. Res.* **2019**, *98*, 642–651. [[CrossRef](#)]
19. Czumaj, A.; Szrok-Jurga, S.; Hebanowska, A.; Turyn, J.; Swierczynski, J.; Sledzinski, T.; Stelmanska, E. The Pathophysiological Role of CoA. *Int. J. Mol. Sci.* **2020**, *21*, 9057. [[CrossRef](#)]
20. Hill, M.J. Intestinal flora and endogenous vitamin synthesis. *Eur. J. Cancer Prev. Off. J. Eur. Cancer Prev. Organ. (ECP)* **1997**, *6* (Suppl. S1), S43–S45. [[CrossRef](#)]
21. Lassalle, F.; Spagnoletti, M.; Fumagalli, M.; Shaw, L.; Dyble, M.; Walker, C.; Thomas, M.G.; Bamberg Migliano, A.; Balloux, F. Oral microbiomes from hunter-gatherers and traditional farmers reveal shifts in commensal balance and pathogen load linked to diet. *Mol. Ecol.* **2018**, *27*, 182–195. [[CrossRef](#)] [[PubMed](#)]
22. Gheita, A.A.; Gheita, T.A.; Kenawy, S.A. The potential role of B5: A stitch in time and switch in cytokine. *Phytother. Res.* **2020**, *34*, 306–314. [[CrossRef](#)]
23. He, W.; Hu, S.; Du, X.; Wen, Q.; Zhong, X.P.; Zhou, X.; Zhou, C.; Xiong, W.; Gao, Y.; Zhang, S.; et al. Vitamin B5 Reduces Bacterial Growth via Regulating Innate Immunity and Adaptive Immunity in Mice Infected with Mycobacterium tuberculosis. *Front. Immunol.* **2018**, *9*, 365. [[CrossRef](#)]
24. Hug, D.H.; Dunkerson, D.D.; Hunter, J.K. The degradation of L-histidine and trans- and cis-urocanic acid by bacteria from skin and the role of bacterial cis-urocanic acid isomerase. *J. Photochem. Photobiol. B* **1999**, *50*, 66–73. [[CrossRef](#)]
25. Belstrøm, D.; Holmstrup, P.; Bardow, A.; Kokaras, A.; Fiehn, N.E.; Paster, B.J. Comparative analysis of bacterial profiles in unstimulated and stimulated saliva samples. *J. Oral Microbiol.* **2016**, *8*, 30112. [[CrossRef](#)]
26. Larsson, B.; Olivecrona, G.; Ericson, T. Lipids in human saliva. *Arch. Oral Biol.* **1996**, *41*, 105–110. [[CrossRef](#)]
27. Matczuk, J.; Żendzian-Piotrowska, M.; Maciejczyk, M.; Kurek, K. Salivary lipids: A review. *Adv. Clin. Exp. Med. Off. Organ Wroc. Med. Univ.* **2016**, *26*, 1021–1029. [[CrossRef](#)]
28. Slomiany, B.L.; Kosmala, M.; Nadziejko, C.; Murty, V.L.; Gwozdziński, K.; Slomiany, A.; Mandel, I.D. Lipid composition and viscosity of parotid saliva in Sjögren syndrome in man. *Arch. Oral Biol.* **1986**, *31*, 699–702. [[CrossRef](#)]
29. Vitali, C.; Bombardieri, S.; Jonsson, R.; Moutsopoulos, H.M.; Alexander, E.L.; Carsons, S.E.; Daniels, T.E.; Fox, P.C.; Fox, R.I.; Kassan, S.S.; et al. Classification criteria for Sjögren's syndrome: A revised version of the European criteria proposed by the American-European consensus group. *Ann. Rheum. Dis.* **2002**, *61*, 554–558. [[CrossRef](#)]

30. Niemela, R.K.; Takalo, R.; Paakko, E.; Suramo, I.; Paivansalo, M.; Salo, T.; Hakala, M. Ultrasonography of salivary glands in primary Sjogren's syndrome. A comparison with magnetic resonance imaging and magnetic resonance sialography of parotid glands. *Rheumatology* **2004**, *43*, 875–879. [[CrossRef](#)]
31. Navazesh, M. Methods for collecting saliva. *Ann. N. Y. Acad. Sci.* **1993**, *694*, 72–77. [[CrossRef](#)] [[PubMed](#)]
32. Turunen, S.; Puurunen, J.; Auriola, S.; Kullaa, A.M.; Kärkkäinen, O.; Lohi, H.; Hanhineva, K. Metabolome of canine and human saliva: A non-targeted metabolomics study. *Metabolomics* **2020**, *16*, 90. [[CrossRef](#)] [[PubMed](#)]
33. Klävus, A.; Kokla, M.; Noerman, S.; Koistinen, V.M.; Tuomainen, M.; Zarei, I.; Meuronen, T.; Häkkinen, M.R.; Rummukainen, S.; Farizah Babu, A.; et al. "Notame": Workflow for Non-Targeted LC-MS Metabolic Profiling. *Metabolites* **2020**, *10*, 135. [[CrossRef](#)] [[PubMed](#)]
34. Sumner, L.W.; Amberg, A.; Barrett, D.; Beale, M.H.; Beger, R.; Daykin, C.A.; Fan, T.W.; Fiehn, O.; Goodacre, R.; Griffin, J.L.; et al. Proposed minimum reporting standards for chemical analysis Chemical Analysis Working Group (CAWG) Metabolomics Standards Initiative (MSI). *Metabolomics* **2007**, *3*, 211–221. [[CrossRef](#)] [[PubMed](#)]
35. Pang, Z.; Chong, J.; Zhou, G.; Morais, D.; Chang, L.; Barrette, M.; Gauthier, C.; Jacques, P.E.; Li, S.; Xia, J. MetaboAnalyst 5.0: Narrowing the gap between raw spectra and functional insights. *Nucl. Acids Res.* **2021**, *49*, W388–W396. [[CrossRef](#)]

III

**Scent detection threshold of trained dogs to *Eucalyptus hydrolat***

Turunen S, Paavilainen S, Vepsäläinen J and Hielm-Björkman A

Animals 14:1083, 2024





Article

# Scent Detection Threshold of Trained Dogs to *Eucalyptus* Hydrolat

Soile Turunen <sup>1</sup>, Susanna Paavilainen <sup>2,3</sup>, Jouko Vepsäläinen <sup>1</sup> and Anna Hielm-Björkman <sup>4,\*</sup>

<sup>1</sup> School of Pharmacy, Faculty of Health Sciences, University of Eastern Finland, 70211 Kuopio, Finland; soile.turunen@uef.fi (S.T.); jouko.vepsalainen@uef.fi (J.V.)

<sup>2</sup> Wise Nose-Finnish Odor Separation Association, 00790 Helsinki, Finland; susanna.paavilainen@noseacademy.fi

<sup>3</sup> Nose Academy Ltd., 70780 Kuopio, Finland

<sup>4</sup> DogRisk Research Group, Department of Equine and Small Animal Medicine, Faculty of Veterinary Medicine, University of Helsinki, 00014 Helsinki, Finland

\* Correspondence: anna.hielm-bjorkman@helsinki.fi; Tel.: +358-443270462

**Simple Summary:** Dogs have an extraordinary sense of smell that is far superior to humans', thanks to their unique anatomy and physiology. This remarkable ability allows them to detect and differentiate between very low concentrations of odor molecules, but the threshold seems to depend on the target odor. This study focused on determining the lowest concentration of *Eucalyptus* hydrolat that would be detectable by trained dogs. This substance was selected for the study as it is used in a dog scent training sport called "nose work". The research involved testing dogs with progressively diluted concentrations of this hydrolat until they could no longer identify it, thus determining their scent detection threshold. When dogs were trained to respond to the *Eucalyptus* hydrolat at decreasing concentrations, they successfully detected the scent even when it was diluted to ratios between 1:10<sup>17</sup> and 1:10<sup>21</sup>. The study also used analytical spectroscopy to analyze the contents of ten commercial *Eucalyptus* hydrolats, revealing variations in their ingredients. The findings highlight two key points. First, with appropriate training, dogs can learn to identify very low concentrations of *Eucalyptus* hydrolat. Second, the consistency of the scent source is crucial in training a dog, not only in canine sport competitions, but also in olfactory research.

**Abstract:** Dogs' (*Canis lupus familiaris*) sense of smell is based on a unique anatomy and physiology that enables them to find and differentiate low concentrations of odor molecules. This ability is exploited when dogs are trained as search, rescue, or medical detection dogs. We performed a three-part study to explore the scent detection threshold of 15 dogs to an in-house-made *Eucalyptus* hydrolat. Here, decreasing concentrations of the hydrolat were tested using a three-alternative forced-choice method until the first incorrect response, which defined the limit of scent detection for each tested dog. Quantitative proton nuclear magnetic resonance spectroscopy was used to identify and measure the contents of ten commercial *Eucalyptus* hydrolats, which are used in a dog scent training sport called "nose work". In this study, the dogs' limit of detection initially ranged from 1:10<sup>4</sup> to 1:10<sup>23</sup> but narrowed down to 1:10<sup>17</sup>–1:10<sup>21</sup> after a training period. The results show that, with training, dogs learn to discriminate decreasing concentrations of a target scent, and that dogs can discriminate *Eucalyptus* hydrolat at very low concentrations. We also detected different concentrations of eucalyptol and lower alcohols in the hydrolat products and highlight the importance of using an identical source of a scent in training a dog for participation in canine scent sport competitions and in olfactory research.

**Keywords:** canine; olfaction; eucalyptol; hydrolat; nose work; line-up



**Citation:** Turunen, S.; Paavilainen, S.; Vepsäläinen, J.; Hielm-Björkman, A. Scent Detection Threshold of Trained Dogs to *Eucalyptus* Hydrolat. *Animals* **2024**, *14*, 1083. <https://doi.org/10.3390/ani14071083>

Received: 26 January 2024

Revised: 25 March 2024

Accepted: 2 April 2024

Published: 3 April 2024



**Copyright:** © 2024 by the authors. Licensee MDPI, Basel, Switzerland. This article is an open access article distributed under the terms and conditions of the Creative Commons Attribution (CC BY) license (<https://creativecommons.org/licenses/by/4.0/>).

## 1. Introduction

It is well-known that dogs have an excellent sense of smell [1]. The anatomy and physiology of the nasal structures of dogs lend themselves especially well to conveying the airflow to the olfactory epithelium of the nose [2]. The nasal epithelium contains olfactory receptor (OR) cells which possess ORs coded by a wide repertoire of polymorphic OR genes [3]. Compared to humans, dogs have more OR coding genes, but fewer of them are dormant [4]. The nerve signal is triggered by odor molecules after they bind to the specific ORs. The signal projects into the olfactory bulb, which is more predominant in dogs than in humans [5]. Due to these special characteristics, it is possible for dogs to detect odor molecules at very low concentrations.

Conventionally, dogs' superior ability for odor discrimination is employed for many purposes, e.g., by the police and customs officials, as they train service dogs to detect substances such as narcotics [6], semen stains [7], ignitable liquids [8], explosives [9], etc. Dogs can detect the target scents even in very demanding conditions, such as in varying temperatures and humidities, as well as with other distractors [10,11]. This skill is widely utilized, e.g., when rescue, search, and hunting dogs seek and trace their targets, dead or alive, on/in/under water, soil, or snow. Despite some technical and ethical challenges, there has been considerable interest in medical scent detection dogs regarding SARS-CoV-2 detection [12–16]. The usage of disease scent dogs has been also studied in connection with cancer [17–21], Parkinson's disease [22], malaria [23], *E-Coli*-bacteriuria [24], and *Clostridium difficile* infection detection [25], among others.

In addition to service and medical scent detection dogs, several other canine scent detection alternatives have become popular. Dogs have been trained to detect many scents, e.g., truffles in the ground [26], mold in houses [27], and bed bugs in apartments and hotels [28]. Both a dog sport and a hobby, nose work was developed in the USA in 2006. In this scent training sport, dogs are trained to detect and indicate the scents of birch, anise, and cloves from various search areas [29]. In Finland, nose work dogs detect three alternative target scents, namely Eucalyptus, bay leaf, and lavender [30]. In nose work sports, the scents are usually presented to the dogs using commercial hydrolats. These are obtained as a by-product during the steam distillation of a target plant when producing its essential oil [31]. These hydrolats are reported to contain water and dissolved natural compounds.

As dogs and their scent-detecting capabilities are widely used, there is an increasing interest to quantify the thresholds of their olfactory sensitivity. Walker et al. used a “find the target” method, where they built an olfactometer to determine accurately the olfactory threshold of two dogs to amyl acetate, a compound which has a banana-like odor, from the air [1,32]. Olfactometers were also used when determining dogs' threshold to detect the Spotted Lantern fly (a foreign species in the USA) [33], and when evaluating dogs' generalization and discrimination across isoamyl acetate concentrations [34]. In addition, different kinds of apparatus are nowadays applied in scent detection training and testing that present target odors using scent tracks, scent line-ups, cones, carousels, and other scent wheels. In these, the target odors or samples are placed in open or mesh-covered jars, where the odor molecules are transferred into the air by passive diffusion and with the help of the dog's sniffing. Concha et al. tested dogs' olfactory threshold with amyl acetate using an eight-choice carousel [35], whereas DeChant et al. selected isoamyl acetate as a target for a three-alternative forced-choice test in a scent line-up device [36]. Other studies conducted in applied animal science and forensic science have used scent line-ups or carousels when investigating dogs' olfactory threshold to other targets, e.g., tuatara and gecko scents [37], koi carp [38], or ignitable liquids [8], as well as when studying olfactory properties of dogs and wolves in detecting raw food [39]. Detection thresholds for odors can be determined using different kinds of methods in both humans and dogs [40]. Studies in canine olfactory threshold research exploiting a staircase procedure have recently been reported in conjunction with a step-down procedure [33,36]. Whereas step-down procedures include one or several exposures to each concentration of a target odor before



introducing the next lower concentration of the target, the staircase procedure applies pre-defined steps where the concentration of a target odor is either increased or decreased according to the dog's failure or success to indicate the target, respectively.

The aim of this study was to determine the scent detection threshold of trained dogs to an in-house-made *Eucalyptus* hydrolat, a source of an unambiguous scent, eucalyptol. The dog's threshold for the target scent was determined by using a three-alternative forced-choice procedure applying scent line-ups. Each target sample was presented in a descending concentration order. A total of 15 dogs were tested in double-blinded, randomized sample settings where the last correct indication was recorded as the individual threshold.

## 2. Materials and Methods

### 2.1. Preparation of In-House *Eucalyptus* Hydrolat

A pure (100%) essential oil of *Eucalyptus radiata* (Frantsila, Kyröskoski, Finland) was purchased as the source of the target scent. To prepare the stock solution (i.e., in-house *Eucalyptus* hydrolat) the *Eucalyptus* oil was diluted with class 1 ultra-pure water (Elga Purelab Ultra Analytical, High Wycombe, UK). The stock solution contained the ratio of 1:10,000 (1:10<sup>4</sup>) oil in water (0.1 mL:999.9 mL), mimicking the average concentration of the *Eucalyptus* hydrolats used in dog nose work sports. The stock solutions were prepared in a laboratory in the School of Pharmacy of the University of Eastern Finland with clean laboratory glassware into a one-liter volumetric flask and transported to the test site at room temperature. The above-mentioned class 1 ultra-pure water was used for further dilutions and for non-target samples.

### 2.2. Preparation of In-House *Eucalyptus* Hydrolat Dilutions

The stock solution was diluted in the test sites to prepare the odor samples as follows: Researcher 1 was responsible for diluting the solutions as described in Table 1 and Supplementary Tables S1 and S2 in a space separate from the testing room. Every diluted solution utilized a glass graduated pipette to exactly measure 0.1 mL or 1.0 mL of the previous diluted solution into a 20 mL transparent glass bottle, in which 9.9 mL or 9.0 mL of class 1 ultra-pure water was added, respectively. The bottle was capped, inverted, and shaken to obtain a homogenous solution. For the non-target samples, parallel bottles were filled with 10.0 mL of the class 1 ultra-pure water. Disposable powder-free nitrile gloves were used when preparing the dilutions. A new pair of gloves was changed when starting to prepare the next solution.

**Table 1.** Prepared dilutions using the in-house-made *Eucalyptus* hydrolat, i.e., stock solution and water, in Study 1. Dilution ratios of *Eucalyptus* oil in water are depicted as the value of a volume fraction.

Solution	Dilution Ratio
stock solution	1:10 <sup>4</sup>
dilution 1	1:10 <sup>6</sup>
dilution 2	1:10 <sup>8</sup>
dilution 3	1:10 <sup>10</sup>
dilution 4	1:10 <sup>12</sup>
dilution 5	1:10 <sup>14</sup>
dilution 6	1:10 <sup>16</sup>
dilution 7	1:10 <sup>18</sup>
dilution 8	1:10 <sup>20</sup>
dilution 9	1:10 <sup>22</sup>
dilution 10	1:10 <sup>24</sup>

### 2.3. Preparation of Target and Non-Target Samples

A vortex mixer was used to mix the prepared-in-house *Eucalyptus* hydrolat dilutions. A one milliliter (1.0 mL) sample of the diluted solution, i.e., the target sample, as well as 1.0 mL of the class 1 pure water, i.e., the non-target sample, were transferred from their

glass bottles into single-use PP-plastic cups (ABENA drinking cup, 200 mL, white PP, Denmark) using their designated graduated pipettes. Researcher 1 transferred the target and non-target samples into the plastic cups immediately before testing each scent line-up to ensure uniformity of sample processing for each tested dog.

#### 2.4. Scent Line-Up Tracks for a Three-Alternative Forced-Choice Method

Researcher 2 was responsible for placing the samples prepared by Researcher 1 as follows: one target and two non-target samples were placed into clean mesh-covered metallic jars (stainless-steel, 85 mm high and 70 mm in diameter, Figure 1) or clean glass jars (clear glass, 98 mm high and 67 mm in diameter, Figure 2). The jars were transferred to the test room and placed in the scent track according to a computer-generated randomization list ([www.sealedenvelope.com](http://www.sealedenvelope.com), accessed on 31 May 2017). A total of three jars were placed in a metallic scent track with nine holes for the metallic jars (in Study 1 and 2, Figure 1), or in three individual plywood stands holding the glass jars (in Study 3, Figure 2). These three jars constituted a scent track for line-up odor discrimination using a three-alternative forced-choice method. Disposable powder-free nitrile gloves were used and changed between every tested scent line-up. Mesh covers and metallic and glass jars were used only once, i.e., for one sample, during each test day.

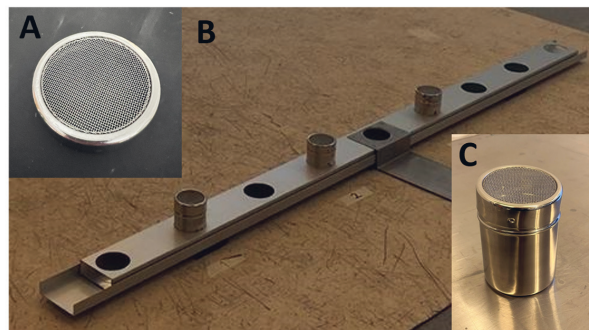


**Figure 1.** A metallic scent track was used as an apparatus for a three-alternative forced-choice task in Studies 1 and 2 (A); mesh cover (B); scent track with three metallic jars placed on every second place from the left (C); mesh-covered metallic jar containing the plastic cup with target or non-target sample.



**Figure 2.** Individual plywood stands were used in Study 3 as a three-alternative forced-choice device (A); glass jar (B); glass jars containing the plastic cup with target or non-target sample.

#### 2.5. Test Protocol

The dilutions were presented in descending order starting from the strongest concentration (stock solution, 1:10,000). The indication was recorded as correct if the dog alerted a jar with the target sample, using its individual-specific alerting behavior (focused stare, nose freeze, sitting or lying down in front of the indicated jar, or pawing the jar) for a

minimum of two seconds. The indication was recorded as incorrect if the dog indicated a jar with the non-target sample by alerting as mentioned above. A lack of indication was recorded if the dog did not indicate any of the three samples, but simply left all three jars without making any alerting behavior. Distractor scents were not used because the study aim was not to test the specificity of the dogs towards *Eucalyptus* hydrolat, but to determine the threshold of the lowest ratio in aqueous solution that individual dogs could discriminate from pure water.

One dog at a time performed the discrimination test in a double-blind manner, i.e., neither the dog nor the handler knew the status of the samples in the scent line-up. Handlers were instructed to give their dogs a signal to start the discrimination test and then to report the dog's target indication (sample number 1, 2, or 3) out loud. The handler received feedback of the result (vocally YES/NO) and rewarded the dog with verbal praise or a clicker paired with treats for the correct indication.

Two people kept notes of the handlers' reporting and one external assessor observed the tests in the test room. Only the external assessor was blinded to the sample status. The test results were interpreted as follows: All consecutive indications had to be correct. An incorrect indication or lack of indication led to a termination of the test. As the threshold value for each tested dog, the lowest correctly indicated concentration of diluted in-house-made *Eucalyptus* hydrolat was reported as a value of the volume fraction, i.e., ratio of *Eucalyptus* oil to water (mL:mL).

### 2.6. Study 1

This study aimed to determine the scent detection threshold of nose work sport dogs to an in-house-made *Eucalyptus* hydrolat. Eleven dogs training nose work sports, and one dog with no sporting experience of nose work but an ability to identify several other target scents, were recruited for Study 1 with their handlers. Details of the dogs are presented in Table 2. All recruited nose work sports dogs were either hobbyists or contestants of the sport in Finland. They had been trained with different commercial *Eucalyptus* hydrolats, which are used as sources of the scent of *Eucalyptus* by the Finnish Nose Work Club. As none of these dogs had encountered the produced-in-house *Eucalyptus* hydrolat before the test day, their handlers were allowed to familiarize the dog with the target scent as follows: The dogs were allowed to sniff one mL of the stock solution from a jar, followed by a clicker sound and a treat for positive reinforcement training of the target sample, for a maximum of five times. Handlers were solely responsible for deciding whether to conduct the familiarization procedure or not. The test started a few minutes after the familiarization process had been completed.

In the test, handlers were allowed to estimate and determine the strength of the correct indication. If the dog's indication was correct and stated as strong, the test proceeded. If the indication was stated as weak, the dog was allowed to search the same samples again in a new order up to four times. The jars were re-arranged in the line-up by Researcher 2 out of sight of the dog handler pair. This seemingly subjective decision was not used as an assessment method, as the first incorrect or lack of indication ended the test for the dog. Instead, repetition was used as a means of reinforcing the alerting behavior to the target sample after a weak indication.

One dog with no prior experience of nose work sports (Dog 1) had a brief training session before the trial. First, Dog 1 was allowed to sniff 1 mL of stock solution from a jar, followed by a clicker sound and a treat for positive reinforcement training of the target sample, for a total five times. Second, five training scent line-ups were performed mimicking the test protocol, and again, Dog 1 was rewarded with a clicker and treats for the correct Indication of stock solution. Study 1 was conducted at the Wise Nose dog training center in Viikki, Finland in June 2017.

Table 2. Demographics and results of the dogs in Studies 1–3.

Dog	Breed	Age	Sex	Neutered Status	Trained Target Scents	Level in Nose Work Sports	Last Ratio of <i>E. hydrolat</i> Successfully Indicated by Dog		
							Study 1	Study 2	Study 3
1	Spanish Galgo mix	5 y	M	Y	bedbugs, tracking of rats, molds, floor carpet glue residues, cancer eucalyptus	no experience	1:10 <sup>22</sup>	1:10 <sup>23</sup>	1:10 <sup>21</sup>
2	Parson Russell terrier	1 y 9 m	F	N	eucalyptus, bay leaf, lavender, pieces of Kong toy	hobbyist	1:10 <sup>4</sup>		
3	Parson Russell terrier	2 y 7 m	M	Y	eucalyptus, bay leaf, lavender, chanterelle, tracking of blood, human, and dog scents	contestant	1:10 <sup>6</sup>		
4	Beagle	2 y 2 m	M	Y	eucalyptus, bay leaf, lavender	contestant	1:10 <sup>6</sup>		
5	Cavalier King Charles spaniel	5 y 2 m	M	N	eucalyptus, bay leaf, lavender	hobbyist	1:10 <sup>8</sup>		
6	Giant schnauzer	8 y 5 m	F	Y	eucalyptus, bay leaf, lavender	hobbyist	1:10 <sup>6</sup>		
7	French bulldog	2 y 6 m	M	N	eucalyptus, bay leaf	hobbyist	1:10 <sup>8</sup>		
8	Mittelspitz	6 y 6 m	F	N	eucalyptus	contestant	1:10 <sup>10</sup>		
9	Shepherd mix	4 y 0 m	F	N	eucalyptus, human scent	hobbyist	1:10 <sup>10</sup>		
10	Parson Russell terrier	5 y 10 m	F	N	eucalyptus, chanterelle	hobbyist	1:10 <sup>4</sup>		
11	Dogo Argentino	5 y 0 m	F	N	ID tracking of human, district heating water, eucalyptus	hobbyist	1:10 <sup>4</sup>		
12	Long-haired Dutch shepherd	4 y 2 m	M	NA	eucalyptus	hobbyist	1:10 <sup>8</sup>		
13	rough collie	5 y 7 m	M	N	eucalyptus	hobbyist			1:10 <sup>19</sup>
14	Danish-Swedish farm dog	5 y 4 m	F	Y	cancer	no experience			1:10 <sup>17</sup>
15	Australian kelpie	5 y 7 m	F	Y	eucalyptus, bay leaf, lavender	hobbyist			1:10 <sup>21</sup>

y, years; m, months; M, male; F, female; Y, yes (sterilized); N, no (not sterilized); NA, not available; hobbyist, dog has participated in nose work sports exercises but not competed yet; contestant, dog has participated in an official nose work sports competition in Finland.

### 2.7. Study 2

Study 2 was conducted to re-test and verify Dog 1's surprisingly low threshold to the in-house *Eucalyptus* hydrolat recorded in Study 1. The same test protocol was applied as described in Study 1. Here, Dog 1 was again allowed to sniff a 1 mL sample of the stock solution from a jar, followed by a clicker sound and a treat for positive reinforcement training of the target sample, for a total five times before starting the test. Study 2 was conducted at the Wise Nose dog training center in Viikki, Finland in June 2017.

### 2.8. Study 3

Based on the results from Studies 1 and 2, the aim of this study was first to train the dogs to discriminate the in-house *Eucalyptus* hydrolat in decreasing concentrations from the pure water and then to conduct the testing. Dog 1 was included to test his scent detection threshold in another location under different circumstances and with a different apparatus compared to Studies 1 and 2. Three new dog handler pairs were recruited for Study 3 (Table 2), with the dogs being trained by their handlers in the Vainuvoima scent training center a total of 14 times during a four-month period. In the training, the stock solution was diluted as described in the study protocol and in Supplementary Table S2. One training session comprised of an average of 20 scent line-ups per dog where one line-up contained 0 or 1 target sample of diluted solution and 3 to 5 non-target samples. Several different concentrations were used in one training session. Their training was based on the positive reinforcement method, i.e., the dogs were rewarded with a clicker and treats when they correctly indicated the diluted solutions. The dogs were tested similarly as described in Study 1. For these dogs, no prior training occurred on the test day of Study 3. Dog 1 was again allowed to sniff a 1 mL sample of the stock solution from a jar, followed by a clicker sound and a treat for positive reinforcement training of the target, for a total of five times. The study was conducted in the Vainuvoima scent training center in Loimaa, Finland in April 2018.

### 2.9. Ethics Statement

This research does not include the kind of experimental setup that would demand applying for an ethical statement from the ethics committee, according to Finnish research ethics. Voluntary participants were recruited for tests conducted with a harmless scent product and no data was collected from dog owners and/or dog handlers.

### 2.10. NMR Analysis of the *Eucalyptus* Oil and Hydrolats

Essential *Eucalyptus* oil, as well as ten different *Eucalyptus* hydrolat solutions used in nose work sports training and competitions, were purchased from online stores. The content of the oil and hydrolats were measured using the nuclear magnetic resonance (NMR) technique as follows:  $^1\text{H}$  NMR spectra were measured using a 600 MHz Bruker NMR spectrometer equipped with a cryoprobe (Bruker Prodigy TCI 600 S3 H&F-C/N-D-05 Z) and an automatic SampleJet sample changer. Prior to the NMR measurements, 100  $\mu\text{L}$  of a sample was transferred to a 5 mm NMR tube, followed by  $\text{D}_2\text{O}$  (425  $\mu\text{L}$ ) containing 1.0 mM 3 (trimethylsilyl)-propionic- $d_4$  acid (TSP) as an internal standard of known concentration. The *Eucalyptus* oil was measured as  $\text{CD}_3\text{OD}$ . Compounds were identified by using separately measured reference compounds.  $^1\text{H}$  NMR spectra were collected using the zg automation program with the following parameters:  $90^\circ$  pulse angle, total relaxation delay 13 s, and 32 scans at 300 K. The concentrations of the identified compounds (X) from the NMR spectrum are calculated using the equation:

$$c(X) = (A(X)/A(Y) \times N(Y)/N(X) \times c(Y))$$

where N is the number of protons producing the signal and A is the area of the signal. Y is the reference compound with the known concentration, for example, TSP. Typically,  $^1\text{H}$  NMR detection limits depend on measuring time and the compound's structure. In this

study, a measuring time of approximately 6 min with 32 scans was used, making it possible to detect 0.002 millimolar and to quantify 0.01 millimolar (i.e., 1 mg/L) concentrations of small molecules (molecular weight < 500 g/mol).

### 3. Results

#### 3.1. Scent Detection Threshold

In Study 1, two of the 11 nose work sports dogs indicated the diluted-in-house *Eucalyptus* hydrolat at a ratio of  $1:10^{10}$ , whereas three of the dogs only indicated the stock solution at the highest concentration of  $1:10^4$  (Table 2). The rest of the nose work sports dogs indicated other concentrations in between these levels. Dog 1 was the only animal that indicated all dilutions between the dilution ratios of  $1:10^4$  and  $1:10^{22}$ . In the second study (2), all tested dilution ratios from  $1:10^4$  to  $1:10^{23}$  were indicated by Dog 1. In the third study (3), two dogs indicated samples up to a dilution ratio of  $1:10^{21}$  (Dogs 1 and 15), one to a ratio of  $1:10^{19}$  (Dog 13) and one to a ratio of  $1:10^{17}$  (Dog 14). The results are presented in Table 2. The scent detection thresholds of trained dogs to *Eucalyptus* hydrolat are illustrated in Figure 3.

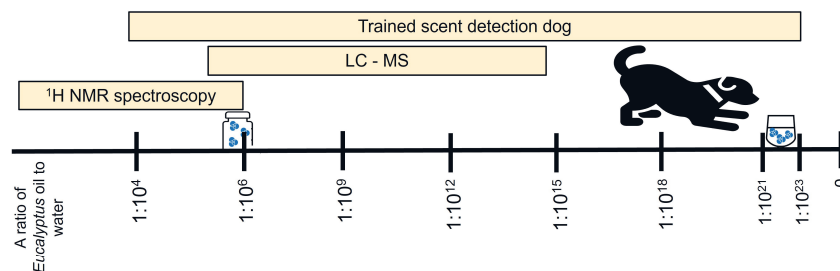


**Figure 3.** The olfactory threshold of the trained dogs outperforms typical analytical techniques. While trained sniffer dogs needed a minimum of only  $1:10^{21}$ – $1:10^{23}$  of *Eucalyptus* oil in an aqueous solution for odor indication, the detection limit of  $^1\text{H}$  NMR spectroscopy was  $2:10^6$  in this study. For comparison, it should be noted that basic mass spectrometry methods coupled with liquid chromatography detect common chemical compounds in liquids at  $1:10^{15}$  levels, but this technique was not utilized here. The figure is not scaled.  $^1\text{H}$  NMR, proton nuclear magnetic resonance; LC-MS, liquid chromatography-mass spectrometry.

#### 3.2. NMR Detection and Identification of Compounds

When the content of the essential *Eucalyptus* oil and the ten purchased *Eucalyptus* hydrolats were measured using NMR spectroscopy, the analysis revealed a large variation in the concentration of eucalyptol between the different products. The oil contained 4.12 mol/L of eucalyptol, which was identified as the main compound of the oil (Figure 4A). On the contrary, some of the hydrolats contained less eucalyptol than the limit of detection (C(eucalyptol) min. < 0.01 mmol/L, max. 5.05 mmol/L) (Figure 4B–F). In addition, three alcohols with varying concentrations were identified in the hydrolats: ethanol (min. < 0.01 mmol/L, max. 32.72 mmol/L), methanol (min. < 0.01 mmol/L, max. 1.15 mmol/L), and benzyl alcohol (min. < 0.01 mmol/L, max. 42.68 mmol/L). Some of the identified ingredients included acetic acid and formic acid (for detailed information, see Supplementary Table S3). Examples of the NMR spectra of different *Eucalyptus* hydrolats and the *Eucalyptus* oil used in this study are presented in Figure 4 and Supplementary Figure S1.

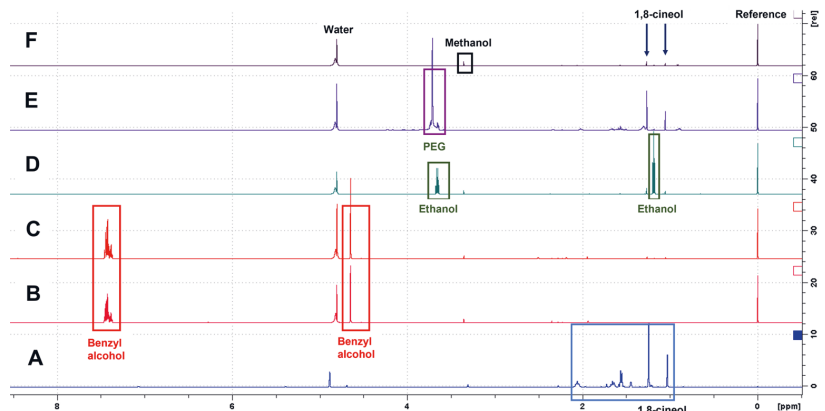


**Figure 4.**  $^1\text{H}$  NMR spectra revealed the existence of different ingredients in the *Eucalyptus* hydrolats. (A) The spectrum shows the typical signals of eucalyptol (blue box) in the sample of the 100% essential oil of *Eucalyptus radiata* (Frantsila, Kyröskoski, Finland). The quantified concentration of eucalyptol was 4.12 mol/L. (B–F) The spectra show signals from benzyl alcohol (red boxes), ethanol (green boxes), polyethylene glycol (PEG, purple box), and methanol (black box) in different *Eucalyptus* hydrolats. In addition, signals of water and the standard compound TSP (Reference) are named, and the two characteristic signals of eucalyptol (1,8-cineol) are highlighted with arrows.

#### 4. Discussion

The results of this study indicate that it is possible to train dogs with decreasing concentrations of a target scent to improve their olfactory threshold. Here, eleven nose work sport dogs were tested using an in-house-prepared *Eucalyptus* hydrolat in Study 1. Though the dogs had previously been training for nose work with commercial *Eucalyptus* hydrolat products and some of them were even competing in nose work sports, these dogs were able to indicate only substantially higher concentrations of the in-house *Eucalyptus* hydrolat in comparison to the dogs in Study 3. In contrast to Study 1, the three dogs in Study 3 were trained with diluted target scent solutions, and when tested, all of them successfully indicated very low concentrations of the in-house *Eucalyptus* hydrolat.

The difference between the results of Study 1 and Study 3 can partially be explained by the prior training with the descending concentrations of the target scent in Study 3. DeChant et al. reported that training at lower concentrations of the target odor improved the dogs' threshold to isoamyl acetate as compared to dogs that were trained with only one concentration [36]. Our findings are in agreement with DeChant et al., i.e., that training with ever-decreasing concentrations of a target scent might have enhanced the dogs' generalization to the *Eucalyptus* hydrolat, possibly by changing the physiology of the olfactory system. Rodent studies have suggested that training may be able to increase the number of OR cells specific to a target scent molecule and increase the sensitivity towards the molecule [41,42], but for dogs, this remains a research question for the future. The second methodological aspect is that we conducted this study utilizing the three-alternative forced-choice scent line-up method, using scent tracks and jars for samples. The scent line-up method has been used in several studies, e.g., to test dogs' olfactory threshold to isoamyl acetate [36] and ignitable liquid [8], as well as in SARS-CoV-19 detection [15]. However, some of the nose work sport dogs in Study 1 were not familiar with this method. Instead, they were accustomed to finding hidden target scents in various environments which greatly differ from working with a scent line-up. This was overcome in Study 3, where the scent line-up method was applied already in the training period, ensuring that the dogs were prepared for the test.

The third technical consideration emerges from the NMR measurements of the ten commercial *Eucalyptus* hydrolat products. The NMR spectra revealed the presence of sev-



eral substances in the purchased *Eucalyptus* hydrolats, e.g., the presence of lower alcohols such as ethanol and benzyl alcohol, which were not detected in the essential *Eucalyptus* oil. In addition, the concentrations of these lower alcohols varied substantially between the products. According to the literature, a steam distillation process does not involve lower alcohols. Instead, ethanol and propylene glycol are used to remove unstable terpenes from essential oils to obtain more flavor and increase the product's shelf life [43]. In addition to these alcohols, the concentration of eucalyptol, the compound with a characteristic smell of eucalyptus, differed between the analyzed products by up to more than 500-fold. Three out of the ten hydrolat products contained less than the quantification limit, 0.01 mmol/L of eucalyptol, according to the NMR analysis. This is evidence that the hydrolats used in nose work sport training and competitions are not standardized. These hydrolats also differed from the target scent used in Study 1. In fact, hydrolat products from different manufacturers might lead to totally different odor patterns for dogs due to their different amounts of volatile organic compounds (VOCs). The VOCs are affected by the ingredients and their concentrations. As a possible consequence, problems may arise in nose work sporting competitions when a dog searches for a scent of *Eucalyptus* hydrolat that differs from the one(s) with which he/she has been trained. In the case of nose work, a sport in which national and international competitions are held, it would be extremely important for the scent products to be standardized, both in terms of ingredients and concentrations.

Additionally, one dog (Dog 1) was tested three times within this project. He had been trained to discriminate between several different target odors using the scent line-up method before participating in the studies. However, this 5-year-old neutered male dog had no prior training with any *Eucalyptus* hydrolats (i.e., no experience of nose work sports), but the handler trained him quickly to detect the target scent before testing him in each of the three trials. In Study 1, he already achieved an astonishing threshold of 1:10<sup>22</sup>. When he was re-tested in Study 2, he could discriminate the in-house-made *Eucalyptus* hydrolat at the lowest ratio recorded in this study (1:10<sup>23</sup>). In Study 3, he reached the ratio of 1:10<sup>21</sup>, showing reproducible results. We assume that this dog was successful because he had a very highly developed sense of smell, he was quick at learning new targets, and he had already mastered several different odor targets, including early-stage cancers. In fact, research has shown that dogs with more trained targets tend to learn a new one more easily [44,45], and only 2 to 3 exposures are needed for such dogs to learn to respond to a novel target odor [46]. Individual differences between the scent detection dogs, as seen here in our study, have been observed in most studies. Several reasons have been proposed to explain this phenomenon, including the personality of the dog and its training and motivation [35]. In addition, there are differences in the anatomy and physiology of the olfactory organs of different breeds of dogs. Dogs have been bred from different genetic backgrounds, leading to different sizes of the olfactory epithelium, as well as the number and type of ORs present in an individual dog's epithelium [47,48]. The large OR gene repertoire (1094 genes for dogs) and the high level of polymorphism in canine OR genes have been discussed alongside signal transduction and brain processing when trying to find an explanation for the extremely sensitized sense of smell of these animals [47].

There are several limitations to this study. The criterion of "first incorrect response" was chosen as indicating the dogs' threshold for *Eucalyptus* hydrolat, which did not allow us to statistically determine the true and absolute threshold. As dogs make errors for a variety of behavioral and situational reasons by performing a repetition of every concentration, it would have allowed a statistical estimate of threshold variability for each individual dog. Thresholds for odors can be studied using different kinds of methods in both humans and dogs: both the step-down and the staircase method usually involve several exposures to each concentration, allowing for calculations of performance metrics [40]. In addition, we chose a three-alternative forced-choice procedure, whereas at least four or five alternatives would have achieved a more satisfactory measurement of the threshold. Wise et al. described the three-alternative forced-choice method with ascending concentrations (FC-AML) where the individual concentration was presented only once, but this made it



impossible to calculate estimates of correct proportions for any given concentration [40]. However, FC-AML has been suggested to be a valid tool for characterizing both average threshold and individual differences. We applied these FC-AML method criteria in a post hoc analysis for our results as follows: Firstly, the dog responded correctly in the last three consecutive trials with the descending concentration of the target scent; secondly, the handler was sure that the dog's last indication was correct. A total of nine out of 15 tested dogs met these criteria when the dilution ratio of 1:10<sup>8</sup> was the target in the third trial, whereas all dogs in Study 3 were able to indicate the target odor in a minimum of seven and a maximum of nine consecutive trials where the probability of correctly indicating the consecutive tracks was 0.333<sup>7</sup> ( $p = 0.00045$ ) for seven trials and 0.333<sup>9</sup> ( $p = 0.00005$ ) for nine trials. However, these values should be interpreted with caution because no power analysis was made to determine the effect size. In addition, it is essential to consider the context as well as potential biases when interpreting results with a  $p$ -value less than 0.05.

The usage of a liquid dilution in threshold testing might produce inconsistency between the solutions compared to air dilution [36]. Here, we used the same dilution method across all three studies and transferred the target and non-target samples into plastic cups and jars just before presenting them to a dog. We estimated that this procedure made no temporal difference in how the target odor evaporated and equilibrated in the jar between the trials for a dog, but that it harmonized the study set-up between the dogs. In addition, the volatile compounds from a liquid sample would be transferred into the air by passive diffusion. The active sniffing by the dog causes the odor molecules to gain access to the dog's nasal olfactory epithelium [10]. Thus, the significance of using a liquid dilution is considered to be minor. Moreover, the testing procedures were performed indoors during June 2017 (Studies 1 and 2 were in the Wise Nose training center) and April 2018 (Study 3 was in the Vainuvoima training center). The humidity and the temperature of the room were not recorded, except for Study 2 (humidity 39% and temperature 22 °C). We presume that for Study 1 and 3 the values would have been similar to those present in Study 2, but we do acknowledge that the humidity and temperature should be recorded when studying scent detection capabilities of dogs.

The final limitation was that the essential *Eucalyptus* oil used in these three studies was not identical to the commercial *Eucalyptus* hydrolat products that were analyzed in this study. The essential *Eucalyptus* oil is a mix of several substances. Studies conducted with gas chromatography-mass spectrometry (GC-MS) have identified VOCs, e.g., monoterpene hydrocarbons such as limonene, and other oxygenated monoterpenes such as  $\alpha$ -terpineol in *Eucalyptus* oils [49,50]. In general, the same VOCs are also found in *Eucalyptus* hydrolats. These are natural compounds originating from *Eucalyptus* tree leaves and stems, and they are likely also part of the VOC pattern detected by the dogs. Nevertheless, we chose to use the essential oil, as we hypothesized that its aqueous dilutions would be the best way to simulate the *Eucalyptus* hydrolats. In addition, the concentration of the main component of the *Eucalyptus* oil, eucalyptol, was high enough to conduct a serial dilution; further, eucalyptol is miscible in 3500 mg/L water (at 21 °C) [51]. However, the diluted target solutions were not measured using the NMR spectroscopy technique, as such low concentrations cannot be detected with this kind of analytical technique (see text of Figure 3). In the future, when studying dogs' threshold to detect the pure odor of eucalyptol, it would be preferable to utilize a commercial product of 99% of eucalyptol (synonym 1,8 cineol) instead of an essential oil. In addition, GC-MS could be applied to investigate the VOC pattern and to quantify the main scent-producing compounds present in the sample down to the detection limit of the analytical technique.

## 5. Conclusions

In conclusion, dogs can be trained to indicate extremely low concentrations of compounds vaporizing from aqueous samples, concentrations clearly below the detection threshold of sophisticated analytical instruments used today, as well as far below what has

previously been reported for dogs. The contents of *Eucalyptus* hydrolats are highly variable, which may result in inequality when these are used in nose work sports.

**Supplementary Materials:** The following supporting information can be downloaded at: <https://www.mdpi.com/article/10.3390/ani14071083/s1>, Figure S1: Expansion of methyl region of <sup>1</sup>H NMR spectra shows the structure of eucalyptol, the main compound in *Eucalyptus* oil; Table S1: Prepared dilutions in Study 2; Table S2: Prepared dilutions in Study 3; Table S3: Concentrations of identified compounds in <sup>1</sup>H NMR analysis of ten commercial *Eucalyptus* hydrolat products.

**Author Contributions:** Conceptualization, S.P., A.H.-B. and J.V.; methodology, S.P., A.H.-B. and J.V.; formal analysis, S.T. and J.V.; investigation, S.P., A.H.-B. and J.V.; resources, S.P., A.H.-B. and J.V.; data curation, S.T.; writing—original draft preparation, S.T.; writing—review and editing, S.T., A.H.-B., J.V. and S.P.; visualization, S.T. and J.V.; supervision, A.H.-B. and J.V.; project administration, A.H.-B.; funding acquisition, A.H.-B. All authors have read and agreed to the published version of the manuscript.

**Funding:** S.T. was funded by Svenska Kulturfonden, grant number 138527. Open access funding provided by University of Helsinki.

**Institutional Review Board Statement:** Ethical review and approval were waived for this study because the research does not include the kind of experimental setup that would require applying for an ethical statement from the ethics committee, according to Finnish research ethics. Voluntary participants were recruited for tests conducted with a harmless scent product, and no data was collected from dog owners and/or dog handlers.

**Informed Consent Statement:** Informed consent was obtained from all the owners of the animals involved in the study.

**Data Availability Statement:** The original contributions presented in the study are included in the article and Supplementary Material. Further inquiries can be directed to the corresponding author.

**Acknowledgments:** The authors thank Maritta Salminkoski for laboratory assistance, dog owners and handlers Miira Hellsten, Kirsi Suominen, Outi Uljas, Mia Laurinen, Sonja Lunkka, Johanna Kuusi, Anna Loimaranta, Minna Lepistö, Erkkü Jussinheimo and their dogs for participation, as well as Ilkka Hormila and Hannele Koskinen for acting as external assessors.

**Conflicts of Interest:** A.H.-B. declare no conflicts of interest. S.V. and J.P. are founders of Nose Academy Ltd., a company providing product development for canine scent detection, as well as research and design services. S.T. is an employee of Afekta Technologies Ltd., a company providing metabolomics analysis services. The funder or the companies had no role in the design of the study; in the collection, analyses, or interpretation of data; in the writing of the manuscript; or in the decision to publish the results.

## References

1. Walker, D.B.; Walker, J.C.; Cavnar, P.J.; Taylor, J.L.; Pickel, D.H.; Hall, S.B.; Suarez, J.C. Naturalistic quantification of canine olfactory sensitivity. *Appl. Anim. Behav. Sci.* **2006**, *97*, 241–254. [[CrossRef](#)]
2. Craven, B.A.; Paterson, E.G.; Settles, G.S. The fluid dynamics of canine olfaction: Unique nasal airflow patterns as an explanation of macrosmia. *J. R. Soc. Interface* **2010**, *7*, 933–943. [[CrossRef](#)] [[PubMed](#)]
3. Tacher, S.; Quignon, P.; Rimbault, M.; Dreano, S.; Andre, C.; Galibert, F. Olfactory receptor sequence polymorphism within and between breeds of dogs. *J. Hered.* **2005**, *96*, 812–816. [[CrossRef](#)] [[PubMed](#)]
4. Quignon, P.; Kirkness, E.; Cadieu, E.; Touleimat, N.; Guyon, R.; Renier, C.; Hitte, C.; André, C.; Fraser, C.; Galibert, F. Comparison of the canine and human olfactory receptor gene repertoires. *Genome Biol.* **2003**, *4*, R80. [[CrossRef](#)] [[PubMed](#)]
5. Kavoi, B.M.; Jameela, H. Comparative Morphometry of the Olfactory Bulb, Tract and Stria in the Human, Dog and Goat. *Int. J. Morphol.* **2011**, *29*, 939–946. [[CrossRef](#)]
6. Jezierski, T.; Adamkiewicz, E.; Walczak, M.; Sobczyńska, M.; Górecka-Bruzda, A.; Ensminger, J.; Papet, E. Efficacy of drug detection by fully-trained police dogs varies by breed, training level, type of drug and search environment. *Forensic Sci. Int.* **2014**, *237*, 112–118. [[CrossRef](#)]
7. van Dam, A.; Schoon, A.; Wierda, S.F.; Heeringa, E.; Aalders, M.C.G. The use of crime scene detection dogs to locate semen stains on different types of fabric. *Forensic Sci. Int.* **2019**, *302*, 109907. [[CrossRef](#)] [[PubMed](#)]
8. Abel, R.J.; Lunder, J.L.; Harynuk, J.J. A novel protocol for producing low-abundance targets to characterize the sensitivity limits of ignitable liquid detection canines. *Forensic Chem.* **2020**, *18*, 100230. [[CrossRef](#)]

9. Gazit, I.; Goldblatt, A.; Grinstein, D.; Terkel, J. Dogs can detect the individual odors in a mixture of explosives. *Appl. Anim. Behav. Sci.* **2021**, *235*, 105212. [[CrossRef](#)]
10. Jenkins, E.K.; DeChant, M.T.; Perry, E.B. When the Nose Doesn't Know: Canine Olfactory Function Associated with Health, Management, and Potential Links to Microbiota. *Front. Vet. Sci.* **2018**, *5*, 56. [[CrossRef](#)]
11. Jinn, J.; Connor, E.G.; Jacobs, L.F. How Ambient Environment Influences Olfactory Orientation in Search and Rescue Dogs. *Chem. Senses* **2020**, *45*, 625–634. [[CrossRef](#)] [[PubMed](#)]
12. D'Aniello, B.; Pinelli, C.; Varcamonti, M.; Rendine, M.; Lombardi, P.; Scandurra, A. COVID Sniffer Dogs: Technical and Ethical Concerns. *Front. Vet. Sci.* **2021**, *8*, 669712. [[CrossRef](#)] [[PubMed](#)]
13. Grandjean, D.; Sarkis, R.; Lecoq-Julien, C.; Benard, A.; Roger, V.; Levesque, E.; Bernes-Luciani, E.; Maestracci, B.; Morvan, P.; Gully, E.; et al. Can the detection dog alert on COVID-19 positive persons by sniffing axillary sweat samples? A proof-of-concept study. *PLoS ONE* **2020**, *15*, e0243122. [[CrossRef](#)] [[PubMed](#)]
14. Jendrym, P.; Schulz, C.; Twele, F.; Meller, S.; von Köckritz-Blickwede, M.; Osterhaus, A.D.M.E.; Ebbers, J.; Pilchová, V.; Pink, I.; Welte, T.; et al. Scent dog identification of samples from COVID-19 patients—A pilot study. *BMC Infect. Dis.* **2020**, *20*, 536. [[CrossRef](#)] [[PubMed](#)]
15. Kantele, A.; Paajanen, J.; Turunen, S.; Pakkanen, S.H.; Patjas, A.; Itkonen, L.; Heiskanen, E.; Lappalainen, M.; Desquilbet, L.; Vapalahti, O.; et al. Scent dogs in detection of COVID-19: Triple-blinded randomised trial and operational real-life screening in airport setting. *BMJ Glob. Health* **2022**, *7*, e008024. [[CrossRef](#)] [[PubMed](#)]
16. Meller, S.; Caraguel, C.; Twele, F.; Charalambous, M.; Schoneberg, C.; Chaber, A.L.; Desquilbet, L.; Grandjean, D.; Mardones, F.O.; Kreienbrock, L.; et al. Canine Olfactory Detection of SARS-CoV-2-Infected Humans—A Systematic Review. *Ann. Epidemiol.* **2023**, *85*, 68–85. [[CrossRef](#)]
17. Willis, C.M.; Church, S.M.; Guest, C.M.; Cook, W.A.; McCarthy, N.; Bransbury, A.J.; Church, M.R.T.; Church, J.C.T. Olfactory detection of human bladder cancer by dogs: Proof of principle study. *BMJ* **2004**, *329*, 712. [[CrossRef](#)] [[PubMed](#)]
18. McCulloch, M.; Jezierski, T.; Broffman, M.; Hubbard, A.; Turner, K.; Janecki, T. Diagnostic Accuracy of Canine Scent Detection in Early- and Late-Stage Lung and Breast Cancers. *Integr. Cancer Ther.* **2006**, *5*, 30–39. [[CrossRef](#)]
19. Junqueira, H.; Quinn, T.A.; Biringer, R.; Hussein, M.; Smeriglio, C.; Barrueto, L.; Finizio, J.; Huang, X.Y. Accuracy of Canine Scent Detection of Non-Small Cell Lung Cancer in Blood Serum. *J. Osteopath. Med.* **2019**, *119*, 413–418. [[CrossRef](#)]
20. Taverna, G.; Tidu, L.; Grizzi, F.; Torri, V.; Mandressi, A.; Sardella, P.; La Torre, G.; Cocciolone, G.; Seveso, M.; Giusti, G.; et al. Olfactory system of highly trained dogs detects prostate cancer in urine samples. *J. Urol.* **2015**, *193*, 1382–1387. [[CrossRef](#)]
21. Muppidi, S.S.; Katragadda, R.; Lega, J.; Alford, T.; Aidman, C.B.; Moore, C. A review of the efficacy of a low-cost cancer screening test using cancer sniffing canines. *J. Breath Res.* **2021**, *15*, 024001. [[CrossRef](#)]
22. Gao, C.; Wang, S.; Wang, M.; Li, J.; Qiao, J.; Huang, J.; Zhang, X.; Xiang, Y.; Xu, Q.; Wang, J.; et al. Sensitivity of sniffer dogs for a diagnosis of Parkinson's disease: A diagnostic accuracy study. *Mov. Disord.* **2022**, *37*, 1807–1816. [[CrossRef](#)] [[PubMed](#)]
23. Guest, C.; Pinder, M.; Doggett, M.; Squires, C.; Affara, M.; Kandeh, B.; Dewhirst, S.; Morant, S.V.; D'Alessandro, U.; Logan, J.G.; et al. Trained dogs identify people with malaria parasites by their odour. *Lancet Infect. Dis.* **2019**, *19*, 578–580. [[CrossRef](#)] [[PubMed](#)]
24. Maurer, M.; McCulloch, M.; Willey, A.M.; Hirsch, W.; Dewey, D. Detection of Bacteriuria by Canine Olfaction. *Open Forum Infect. Dis.* **2016**, *3*, ofw051. [[CrossRef](#)]
25. Taylor, M.T.; McCready, J.; Broukhanski, G.; Kirpalaney, S.; Lutz, H.; Powis, J. Using Dog Scent Detection as a Point-of-Care Tool to Identify Toxigenic *Clostridium difficile* in Stool. *Open Forum Infect. Dis.* **2018**, *5*, ofy179. [[CrossRef](#)]
26. Büntgen, U.; Bagi, I.; Fekete, O.; Molinier, V.; Peter, M.; Splivallo, R.; Vahdatzadeh, M.; Richard, F.; Murat, C.; Tegel, W.; et al. New Insights into the Complex Relationship between Weight and Maturity of Burgundy Truffles (*Tuber aestivum*). *PLoS ONE* **2017**, *12*, e0170375. [[CrossRef](#)]
27. Kauhainen, E.; Harri, M.; Nevalainen, A.; Nevalainen, T. Validity of detection of microbial growth in buildings by trained dogs. *Environ. Int.* **2002**, *28*, 153–157. [[CrossRef](#)]
28. Pfister, M.; Koehler, P.G.; Pereira, R.M. Ability of bed bug-detecting canines to locate live bed bugs and viable bed bug eggs. *J. Econ. Entomol.* **2008**, *101*, 1389–1396. [[CrossRef](#)] [[PubMed](#)]
29. National Association of Canine Scent Work®. About Us, Trial Rule Book. 2022. Available online: <https://www.nacsw.net/> (accessed on 24 February 2024).
30. Finnish Kennel Club. The Rule Book of Finnish Kennel Club for Official Nose Work Test. 2020. Available online: <https://www.kennelliitto.fi/koiraharrastukset/kokeet-ja-kilpailut/nose%20work/nose%20work-kokeen-jarjestajalle> (accessed on 24 February 2024).
31. Paolini, J.; Leandri, C.; Desjobert, J.M.; Barboni, T.; Costa, J. Comparison of liquid-liquid extraction with headspace methods for the characterization of volatile fractions of commercial hydrolats from typically Mediterranean species. *J. Chromatogr. A* **2008**, *1193*, 37–49. [[CrossRef](#)]
32. Chemical Datasheet, N-Amyl Acetate. Available online: <https://cameochemicals.noaa.gov/chemical/2465> (accessed on 13 March 2024).
33. Aviles-Rosa, E.O.; Kane, S.A.; Mizuho, N.; Feuerbacher, E.; Hall, N.J. Olfactory threshold of dogs (*Canis lupus familiaris*) to cold-killed spotted lantern fly eggs. *Appl. Anim. Behav. Sci.* **2023**, *261*, 105880. [[CrossRef](#)]

34. DeChant, M.T.; Bunker, P.C.; Hall, N.J. Stimulus Control of Odorant Concentration: Pilot Study of Generalization and Discrimination of Odor Concentration in Canines. *Animals* **2021**, *11*, 326. [CrossRef] [PubMed]
35. Concha, A.R.; Guest, C.M.; Harris, R.; Pike, T.W.; Feugier, A.; Zulch, H.; Mills, D.S. Canine Olfactory Thresholds to Amyl Acetate in a Biomedical Detection Scenario. *Front. Vet. Sci.* **2018**, *5*, 345. [CrossRef] [PubMed]
36. DeChant, M.T.; Hall, N.J. Training with varying odor concentrations: Implications for odor detection thresholds in canines. *Anim. Cogn.* **2021**, *24*, 889–896. [CrossRef] [PubMed]
37. Browne, C.M.; Stafford, K.J.; Fordham, R.A. The detection and identification of tuatara and gecko scents by dogs. *J. Vet. Behav.* **2015**, *10*, 496–503. [CrossRef]
38. Collins, M.A.; Browne, C.M.; Edwards, T.L.; Ling, N.; Tempero, G.W.; Gleeson, D.M.; Crockett, K.; Quaipe, J. How low can they go: A comparison between dog (*Canis familiaris*) and environmental DNA detection of invasive koi carp (*Cyprinus rubrofuscus*). *Appl. Anim. Behav. Sci.* **2022**, *255*, 105729. [CrossRef]
39. Polgár, Z.; Kinnunen, M.; Újváry, D.; Miklósi, Á.; Gácsi, M. A Test of Canine Olfactory Capacity: Comparing Various Dog Breeds and Wolves in a Natural Detection Task. *PLoS ONE* **2016**, *11*, e0154087. [CrossRef] [PubMed]
40. Wise, P.M.; Bien, N.; Wysocki, C.J. Two rapid odor threshold methods compared to a modified method of constant stimuli. *Chem. Percept.* **2008**, *1*, 16–23. [CrossRef]
41. Wang, H.-W.; Wysocki, C.J.; Gold, G.H. Induction of Olfactory Receptor Sensitivity in Mice. *Science* **1993**, *260*, 998–1000. [CrossRef] [PubMed]
42. Youngentob, S.L.; Kent, P.F. Enhancement of odorant-induced mucosal activity patterns in rats trained on an odorant identification task. *Brain Res.* **1995**, *670*, 82–88. [CrossRef]
43. Health, H.B. *Source Book of Flavours*, 2nd ed.; Aspen Publishers, Inc.: Gaithersburg, MD, USA, 1999.
44. Williams, M.; James, M.J. Training and maintaining the performance of dogs (*Canis familiaris*) on an increasing number of odor discriminations in a controlled setting. *Appl. Anim. Behav. Sci.* **2002**, *78*, 55–65. [CrossRef]
45. Reeve, C.; Wilson, C.; Hanna, D.; Gadbois, S. Dog Owners' Survey reveals Medical Alert Dogs can alert to multiple conditions and multiple people. *PLoS ONE* **2021**, *16*, e0249191. [CrossRef] [PubMed]
46. Moser, A.Y.; Brown, W.Y.; Bizo, L.A.; Andrew, N.R.; Taylor, M.K. Biosecurity Dogs Detect Live Insects after Training with Odor-Proxy Training Aids: Scent Extract and Dead Specimens. *Chemical Senses.* **2020**, *45*, 179–186. [CrossRef] [PubMed]
47. Quignon, P.; Rimbault, M.; Robin, S.; Galibert, F. Genetics of canine olfaction and receptor diversity. *Mamm. Genome* **2012**, *23*, 132–143. [CrossRef] [PubMed]
48. Robin, S.; Tacher, S.; Rimbault, M.; Vaysse, A.; Dréano, S.; André, C.; Hitte, C.; Galibert, F. Genetic diversity of canine olfactory receptors. *BMC Genom.* **2009**, *10*, 21. [CrossRef] [PubMed]
49. Ieri, F.; Cecchi, L.; Giannini, E.; Clemente, C.; Romani, A. GC-MS and HS-SPME-GCxGC-TOFMS Determination of the Volatile Composition of Essential Oils and Hydrosols (By-Products) from Four Eucalyptus Species Cultivated in Tuscany. *Molecules* **2019**, *24*, 226. [CrossRef]
50. Campos, J.F.; Berteina-Raboin, S. Eucalyptol, an All-Purpose Product. *Catalysts* **2022**, *12*, 48. [CrossRef]
51. Drugbank Online. Eucalyptol. 2021. Available online: <https://go.drugbank.com/drugs/DB03852> (accessed on 24 February 2024).

**Disclaimer/Publisher's Note:** The statements, opinions and data contained in all publications are solely those of the individual author(s) and contributor(s) and not of MDPI and/or the editor(s). MDPI and/or the editor(s) disclaim responsibility for any injury to people or property resulting from any ideas, methods, instructions or products referred to in the content.

## IV


### **Scent dogs in detection of COVID-19: triple-blinded randomised trial and operational real-life screening in airport setting**

Kantele A, Paajanen J, Turunen S, Pakkanen S H, Patjas A, Itkonen L, Heiskanen E, Lappalainen M, Desquilbet L, Vapalahti O and Hielm-Björkman A

BMJ Global Health 7: e008024, 2022



# Scent dogs in detection of COVID-19: triple-blinded randomised trial and operational real-life screening in airport setting

Anu Kantele <sup>1,2</sup>, Juuso Paaajanen,<sup>3</sup> Soile Turunen,<sup>4,5</sup> Sari H Pakkanen,<sup>1,2</sup> Anu Patjas,<sup>1,2</sup> Laura Itkonen,<sup>6</sup> Elina Heiskanen,<sup>6</sup> Maija Lappalainen,<sup>7</sup> Loic Desquilbet,<sup>8</sup> Olli Vapalahti,<sup>7,9</sup> Anna Hielm-Björkman<sup>6</sup>

**To cite:** Kantele A, Paaajanen J, Turunen S, *et al*. Scent dogs in detection of COVID-19: triple-blinded randomised trial and operational real-life screening in airport setting. *BMJ Global Health* 2022;7:e008024. doi:10.1136/bmjgh-2021-008024

**Handling editor** Seye Abimbola

AK and JP contributed equally.

Received 16 November 2021  
Accepted 14 March 2022

## ABSTRACT

**Objective** To estimate scent dogs' diagnostic accuracy in identification of people infected with SARS-CoV-2 in comparison with reverse transcriptase polymerase chain reaction (RT-PCR). We conducted a randomised triple-blinded validation trial, and a real-life study at the Helsinki-Vantaa International Airport, Finland.

**Methods** Four dogs were trained to detect COVID-19 using skin swabs from individuals tested for SARS-CoV-2 by RT-PCR. Our controlled triple-blinded validation study comprised four identical sets of 420 parallel samples (from 114 individuals tested positive and 306 negative by RT-PCR), randomly presented to each dog over seven trial sessions. In a real-life setting the dogs screened skin swabs from 303 incoming passengers all concomitantly examined by nasal swab SARS-CoV-2 RT-PCR. Our main outcomes were variables of diagnostic accuracy (sensitivity, specificity, positive predictive value, negative predictive value) for scent dog identification in comparison with RT-PCR.

**Results** Our validation experiments had an overall accuracy of 92% (95% CI 90% to 93%), a sensitivity of 92% (95% CI 89% to 94%) and a specificity of 91% (95% CI 89% to 93%) compared with RT-PCR. For our dogs, trained using the wild-type virus, performance was less accurate for the alpha variant (89% for confirmed wild-type vs 36% for alpha variant, OR 14.0, 95% CI 4.5 to 43.4). In the real-life setting, scent detection and RT-PCR matched 98.7% of the negative swabs. Scent airport prevalence (0.47%) did not allow sensitivity testing; our only SARS-CoV-2 positive swab was not identified (alpha variant). However, ad hoc analysis including predefined positive spike samples showed a total accuracy of 98% (95% CI 97% to 99%).

**Conclusions** This large randomised controlled triple-blinded validation study with a precalculated sample size conducted at an international airport showed that trained scent dogs screen airport passenger samples with high accuracy. One of our findings highlights the importance of continuous retraining as new variants emerge. Using scent dogs may present a valuable approach for high-throughput, rapid screening of large numbers of people.

## WHAT IS ALREADY KNOWN ON THIS TOPIC

⇒ Previous data suggest that scent dogs can discriminate between samples from individuals infected with SARS-CoV-2 and controls.

## WHAT THIS STUDY ADDS

⇒ Scent dogs showed high diagnostic accuracy in a randomised, controlled, triple-blinded validation test with sample size based on power calculations.  
⇒ Scent dogs trained with wild-type SARS-CoV-2 virus also mastered identification of other variants, although less accurately, revealing their robust discriminatory power and indicating a need for continual training to deal with emerging new variants of concern.

## HOW THIS STUDY MIGHT AFFECT RESEARCH, PRACTICE AND/OR POLICY

⇒ Scent dog detection can serve as a prescreening method to save time and resources or even as the sole testing method when other approaches are not yet available—for example, at the early stages of a pandemic.  
⇒ Scent dogs trained to screen SARS-CoV-2 carriers at a public international airport, and other similar mass gatherings, can provide a valuable tool to contain the pandemic.



© Author(s) (or their employer(s)) 2022. Re-use permitted under CC BY-NC. No commercial re-use. See rights and permissions. Published by BMJ.

For numbered affiliations see end of article.

**Correspondence to**  
Dr Anu Kantele;  
anu.kantele@hus.fi

## INTRODUCTION

Containment of the COVID-19 pandemic necessitates rapid large-scale identification of infected individuals. Most patients with SARS-CoV-2 disease are either asymptomatic or have only mild symptoms, but can be contagious.<sup>1</sup> The test-and-isolate strategy has largely relied on the modern reverse transcriptase-polymerase chain reaction (RT-PCR) technique. Its practicality is hampered by inadequate availability, restricted testing capacity, high costs, long turnaround time, and prolonged positivity after infection.<sup>2,3</sup> Rapid



screening methods, such as antigen tests are already in use.<sup>4</sup> A fascinating screening strategy consists of detection by trained scent dogs, an approach not confined to laboratories, enabling large sample numbers with results in real time.<sup>5,6</sup>

Dogs have an extremely sensitive olfactory system: their limit of detection reaches as low as one part per trillion concentrations,<sup>7</sup> exceeding the instruments currently available.<sup>8</sup> Dogs are presumed to detect distinct volatile organic compounds (VOCs)<sup>9</sup> released by their hosts' metabolic processes in various conditions.<sup>5</sup> Indeed, dogs have been reported to identify distinct VOCs elicited by various bacterial, viral and parasitic infections.<sup>10–12</sup>

During the current pandemic, scent detection dogs have been trained to identify samples from hospitalised patients with COVID-19<sup>13–17</sup> (online supplemental table 1). The preliminary data suggest that dogs can be trained within weeks to detect samples from SARS-CoV-2-infected individuals with an accuracy comparable to standard RT-PCR. However, stronger evidence is needed with power calculated sample sizes, better defined control groups, and above all, randomised double/triple-blinded research designs including previously unsniffed samples from the actual target population, outpatients. While proof-of-concept studies have been encouraging, scent dogs need to be taken from laboratory settings to real-life conditions.

The scent dog approach appears particularly appealing for screening SARS-CoV-2-infected individuals in public places and among masses of travellers at airports and harbours. In the spring 2020, we started training dogs to see whether they could identify samples from SARS-CoV-2-infected individuals and, in the autumn, started operational scent work at the Helsinki-Vantaa International Airport. Here, we present the results of a three-faceted study comprising (1) the dogs' training, (2) a prospective, randomised triple-blind validation study using four dogs and (3) a real-life prospective study using the same dogs in daily screening of incoming passengers at the airport, comprising a simultaneous scent detection dog test and nasopharyngeal SARS-CoV-2 RT-PCR.

## METHODS

### Study design

We explored whether scent dogs can be trained to identify humans with SARS-CoV-2 infection. The study was conducted at the scent detection dog training centre Wise Nose, Vantaa, Finland; University of Helsinki, Finland (Veterinary Faculty and Departments of Equine and Small Animal Medicine and Veterinary Biosciences and the DogRisk/Helsinki One Health and Medical Faculty, Department of Virology) and Meilahäti Vaccine Research Centre, MeVac and Helsinki University Hospital Laboratory (HUSLAB), Helsinki University Hospital (HUH), Finland.

At the Helsinki-Vantaa International Airport, the study was conducted in a specifically designed cubicle



**Figure 1** The purpose-built cubicle at the Helsinki-Vantaa International Airport. (A) The cubicle from the outside with the doors into the three sampling rooms. (B) Sampling room with a hatch for handing in the sample for the scent detection dog test. (C) A room for scent detection dog testing, showing two of the three hatches to the right. (D) White Shepherd, E.T., inside the test room, indicating the sample in the middle (No 2) as positive. During the validation, only three of the five scent track holes had cans with samples.

(figure 1A) built at the arrivals terminal. The cubicle setting was used in the dogs' final training, in the validation and as an area where the dogs screened incoming travellers in the real-life study. The cubicle had three sampling rooms for passengers' skin swab sampling (figure 1B), a working area for the dogs and sliding hatches on walls for samples and tracks (figure 1C).

### Patient and public involvement

The participants were recruited from among the following groups: (1) inpatients in HUH, (2) outpatients and healthy individuals who were contacted by telephone or who contacted the study team in response to advertisements posted at PCR testing stations around Helsinki and (3) incoming flight passengers and personnel at Helsinki-Vantaa International Airport. For all inpatients and outpatients, a recent RT-PCR result was available at the time of recruitment. At the airport, recruited passengers were tested concomitantly by RT-PCR and a scent detection dog. Those with a pretravel negative RT-PCR test less than 72 hours old were not retested. For inclusion of airport employees, a RT-PCR test result within 72 hours was required.

All the volunteers gave written informed consent. They completed questionnaires on demographics, symptoms and PCR test results. If their results were not available at the time of form filling, these were obtained later. In addition, electronic medical records of hospitalised patients and personal interviews were used, when needed.

Individuals with incomplete questionnaires and/or non-availability of RT-PCR results were excluded. There were no restrictions of age, sex, nationality or concurrent diseases. In addition, samples from individuals



with asymptomatic or typical COVID-19 symptoms were included in all three arms of the study.

### Skin swab sampling and specimen handling

All volunteers collected the skin swabs themselves using a sterile package containing five gauze eight ply swabs (Mölnlycke Healthcare AB, Göteborg, Sweden). They were instructed to separate the layers of the gauze and use a single layer to swab the skin of their neck, throat area, forehead, and wrists. They swabbed 5–20 gauze samples and, to avoid evaporation and cross-contamination during storage, they placed them in the smallest of three plastic zip lock bags (volumes 0.5 L, 1 L and 2 L) each of which they placed inside the next, larger one (Minigrip; Suominen Joustopakkauset Oy, Ikaalinen, Finland).

The outpatient samples to be used in the training, validation and as spike samples in the real-life cohort were collected from the volunteers at their homes shortly after their RT-PCR tests. The courier left the sampling kit at the front door, and after sampling, returned the samples to the dog training facility. All samples, positive and negative samples separated, were stored in plastic boxes (Smart Store; Orthex Sweden AB, Tingsryd, Sweden) in a dark place at 21°C–23°C until used. Samples with an unknown infection status were stored separately until the status was confirmed. The storage time for the validation samples was 0–5 months.

At the airport, in the sampling room (figure 1B), the gauze swab was placed in a 1 L plastic freezer bag (Pirkka; HP Rani Plast Ab, Teerijärvi, Finland) and then placed inside a metallic stainless steel can (85 mm high and 70 mm in diameter). Four extra swabbed gauze samples were placed in a 0.5 L plastic zip lock bag (Minigrip; Suominen Joustopakkauset Oy, Ikaalinen, Finland), enclosed in a 1 L zip lock bag and stored as previously described.

For each validation session, the scent tracks with samples were prepared in a separate location at the airport on the validation day. Sixty cans were prepared for each dog as follows: The zip lock bag containing the sample was opened, and a single gauze was transferred with sterile metallic tweezers into a can lined with a 1 L plastic freezer bag. To avoid sample odour contamination, the positive and negative samples were prepared on separate tables. The cans were loaded onto the scent tracks according to

a computer-generated randomisation list, and a trolley with the tracks transported to the cubicle.

The study team used adequate personal protective equipment, including a mask and powder-free nitrile gloves, when handling the study specimens.

### Confirmation of a COVID-19 diagnosis

A COVID-19 diagnosis was based on a positive RT-PCR of a nasopharyngeal swab. Discrepancies in the validation results (at least two dogs giving a response different from that of the RT-PCR test) and in the real-life study were resolved by serum SARS-CoV-2 antibody test analysed by nucleocapsid protein and Spike IgG enzyme immunoassays, as described previously.<sup>18</sup> When serum samples could not be obtained, viral load, symptoms and information about SARS-CoV-2 exposure were used to estimate the infection status.

The variant status of SARS-CoV-2 was determined by the SYNLAB for Diagnostics Centre of the Hospital District of Helsinki using data of S gene target failure (SGTF) for the alpha variant, HUSLAB using TaqPath COVID-19 PCR (Thermo Fisher Scientific, Waltham, Massachusetts, USA) and TipMolBiol (Berlin, Germany) using N501Y mutation RT-PCR, which detects alpha or beta variants. The initial RT-PCR samples were subjected to genomic sequencing and bioinformatics analysis as previously described.<sup>19</sup> Based on epidemiological data,<sup>20</sup> all samples obtained before 6 January 2020 were considered 'wild-type,' with reference to the D614G Wuhan-like strain.

### Animals

All the dogs included in this study had previous experience of scent work (table 1).

### Part I: Dog training

The initial training, aiming to provide the dogs with a clear scent picture of COVID-19, was carried out by skilled canine scent detection trainers using operant conditioning, with a clicker and treats used for positive reinforcement. In brief, first, the dogs were exposed to cans containing positive samples and taught to indicate a can with a positive sample. Second, they were introduced to a negative sample in parallel with a positive sample to allow scent discrimination. Third, the number of negative and positive samples was increased in the scent track to reinforce discrimination between positive

**Table 1** The dogs' characteristics, working history and indication behaviours

Dog name	Breed	Age	Sex	Alert response for positive sample	Working history
Silja	Labrador retriever	6	F	Pawing	Narcotics
Rele	Labrador retriever	5	M	Sits	Dangerous goods
Kosti	Labrador retriever	8	M	Sits	Dangerous goods
E.T.	White Shepherd	4	F	Nose freeze + one paw	Canine cancer

E.T. was initially trained to discriminate SARS-CoV-2 infection using urine samples and later, skin swab samples, while the other three were directly trained by skin swabs from patients with COVID-19 in the acute stage of the disease.

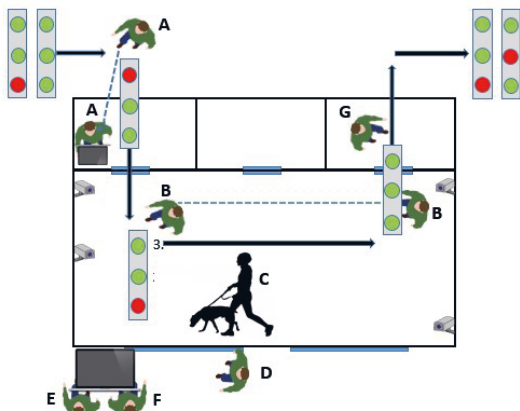


**Figure 2** Triple-blinded study. Assistant A gives the track through a hatch in the wall to assistant B, who places it on the floor and, after the dog and dog handler C have completed their work, gives it to assistant G. The dog handler C announces the result to data recorder D, who instructs whether to reward the dog. The external evaluator E and assistant F follow the setup from a video screen (four cameras inside the cubicle) and verify the triple-blinded study conduct. Blinded: the dog, handler C, assistants B, E, G. Circles: red, SARS-CoV-2 reverse transcriptase-polymerase chain reaction positive; green, negative sample.

and negative samples. Finally, confounding samples, including samples obtained from volunteers with other respiratory and viral diseases and samples from children, seniors or individuals with underlying diseases, such as asthma or allergies, cancer or diabetes, were introduced as controls. Once the dog and dog handler pair achieved a success rate of higher than 80% in detecting SARS-CoV-2 positive samples, the dog continued its training at Helsinki-Vantaa International Airport in the purpose-built working cubicle described earlier (figure 1A–D). The training was performed during a period when novel virus variants had not yet emerged in Finland.

The training was conducted using two different types of purpose-built metallic scent tracks each with either five or nine holes for the cans and/or triangular shaped metallic single can-holders. Cans used for positive samples were not mixed with cans used for negative samples. The cans and can-holders were washed in an industrial dishwasher at a temperature of around 85°C between every exercise.

## Part II: Triple-blinded validation study at Helsinki-Vantaa International Airport

The validation study was conducted according to the Helsinki University triple-blind validation protocol, as described in detail in the online supplemental notes; for the design and execution see figure 2. In total, six investigators and one external controller were present at all validation sessions. Prior to the first validation day, the validation team and the dogs were familiarised with the study conditions and the protocol in a rehearsal session

identical to a validation session, here also introducing 60 novel samples. This was followed by seven validation sessions (VAL1–7). In these sessions, four parallel samples from the 420 individuals were randomised (samples: n=1680; dogs: n=4) into tracks of three samples, with 20 tracks in each of the seven sessions. Thus, each dog was exposed to 140 scent tracks. To allow comparisons between dogs, all four dogs received an identical set of samples. Thus, each parallel sample was used only once and for only one dog. The samples were assigned to the sessions (VAL1–7) in chronological order, the ones collected first in the VAL1 session and last in the VAL7 session. The order of the sample collection and the order of the validation sessions per dog are shown in online supplemental table 2).

The dogs were rewarded for each positive result immediately after the correct indication. If a dog immediately selected the positive sample and skipped sniffing the other samples, the result was still recorded as successful.

The validation stage of the study was recorded using four cameras set up at different angles. A retired police sergeant from the Finnish K-9 police dog school was present during all the validation sessions as an external controller, confirming that the validations followed the predetermined protocol.

## Part III: Real-life cohort

The operational activity at Helsinki-Vantaa International Airport took place between 23 September 2020 and 30 April 2021. In total, 10 119 travellers (83.2%) and airport employees (16.8%) took part in the scent detection dog test, resulting in 48 (0.47%) samples indicated as positive. Part of these were recruited to the validation or the real-life study.

For collection of the skin swabs, see description above. The can with the sample was passed through a hatch to an assistant in the dogs' working space (figure 1C). The dog handler then placed the can in the five-hole scent track, together with a variable number of control samples (figure 1D). The dog handler interpreted the dog's indications as positive or negative for SARS-CoV-2 and a written test result was given to the participant.

## Statistical analysis

The power calculation suggested a minimum of 108 RT-PCR positive and 108 negative samples to achieve sensitivity (Se) and specificity (Sp) of 90%. This sample size was expected to have an 80% probability of obtaining an estimated Se and Sp of which the lower bound of the 95% CI would be greater than the minimal value of 80% (calculated using <https://www.stat.ubc.ca/~rollin/stats/ssize/b1.html>).<sup>21</sup>

Se and Sp were calculated according to Trevethan.<sup>22</sup> To cover incidences where the dogs directly marked a positive sample and skipped sniffing one or both of the other samples in the same track, Se and Sp were calculated using two separate methods. First, we calculated the

Se and Sp only for those samples the dogs truly sniffed ( $Se_{sniff}$  and  $Sp_{sniff}$ ). Second, we calculated the Se and Sp for all the samples ( $Se_{all}$  and  $Sp_{all}$ ). In this approach, we assumed that the dogs considered all un-sniffed samples negative, as they left them untouched. Positive predictive values (PPVs) and negative predictive values (NPVs) were calculated based on our data and on hypothetical prevalence scenarios<sup>23</sup>: 40% reflecting a high prevalence setting such as a pandemic time hospital, and 1% reflecting a low prevalence setting such as an airport.

We also investigated whether some epidemiological/clinical variables were possibly associated with failure to identify positive samples. To do so, we restricted the calculations to include only positive samples. Positive samples were defined as a true positive (TP) if all four dogs correctly marked them, and as a false negative (FN) if even a single dog did not mark the sample. The candidate variables potentially associated with the outcome (FN) were: age, gender, concurrent chronic diseases (asthma, allergy, cancer, diabetes, migraine), presence of typical COVID-19 symptoms, duration of symptoms (time in days between symptom onset and sample collections), time between RT-PCR test and sample collection and type of virus (wild type vs alpha variant). Univariate logistic regression models were performed and ORs with their corresponding 95% confidence intervals (95% CI) were provided. For quantitative variables (such as age, duration of symptoms and time between RT-PCR test and sample collection), the linearity of the association was investigated using restricted cubic spline (RCS) functions with three knots located at the 5th, 50th, and 95th centiles of

the quantitative variable.<sup>24</sup> When the association with the outcome (on the log scale) was not considered as linear, the quantitative variable was included in the model with the RCS functions, and ORs were provided for arbitrary values. Because of the low number of FN samples, multivariate models could not be performed. However, in order to rule out the possible confounding effects of the candidate variables, bivariate logistic regression models were performed, exploring one by one each candidate variable as a potential confounder together with the variable of interest. ORs were considered significant (type-I error set at 0.05) when their corresponding 95% CI did not include the number 1. To obtain Se and Sp values for wild-type only samples, we used for calculations VAL1–2 (where no alpha variants had yet emerged). SAS University Edition (SAS Institute Inc., Cary, North Carolina, USA) was used for the statistical data analysis.

## RESULTS

### Participant and sample characteristics

For research design and number of samples in the three studies, see flowchart in figure 3. The particulars of the volunteers who provided samples for the validation and real-time studies are presented in table 2.

#### Part I: Dog training

The initial training relied on a positive reinforcement approach and predefined positive and negative samples. Having completed that phase at a training centre (qualifying by sensitivity and specificity exceeding 80%) and,

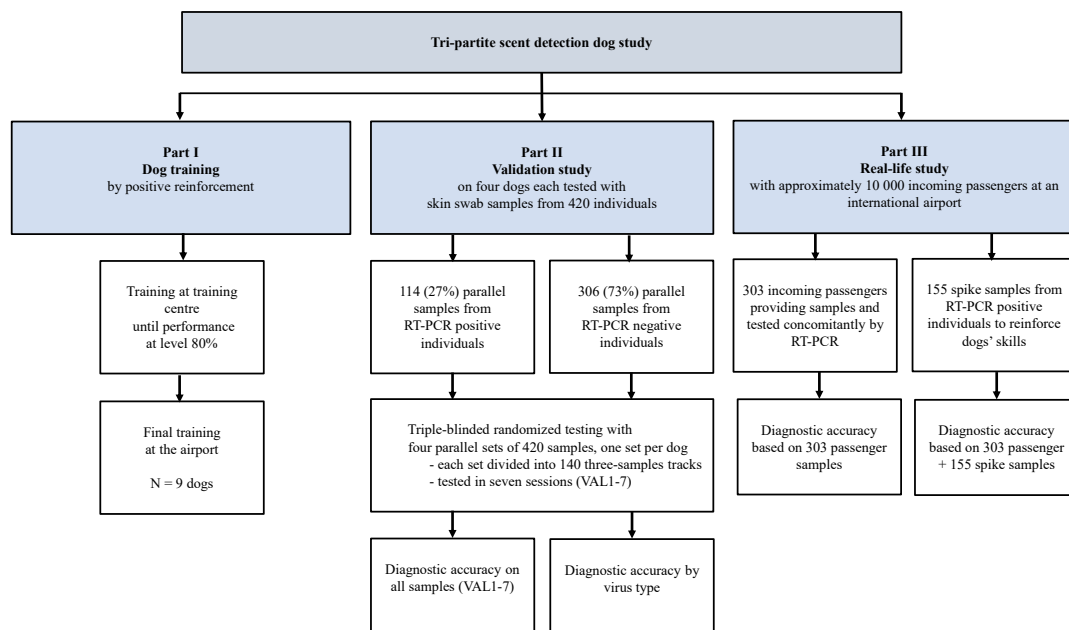


Figure 3 Flow chart of the study conduct.

**Table 2** Data of volunteers providing skin swab samples with concomitant reverse transcriptase-polymerase chain reaction (RT-PCR) verification

Characteristics	Skin swab samples used in the validation study			Skin swab samples sniffed by the validated dogs during operational work		
	Overall (n=420)	RT-PCR negative (n=306)	RT-PCR positive (n=114)	Overall (n=303)	RT-PCR negative (n=300)	RT-PCR positive (n=3)
Age, median (IQR)	38 (21)	40 (23)	34 (18)	42 (22)	42 (23)	48 (NA)
Child, 0–12 years, n (%)	15 (3.6)	2 (0.7)	13 (11.4)	2 (0.7)	2 (0.7)	0 (0)
Sex, female, n (%)	226 (53.8)	168 (54.9)	58 (50.9)	192 (63.4)	191 (63.7)	1 (33.3)
Male, n (%)	192 (45.7)	137 (44.8)	55 (48.2)	111 (36.6)	109 (36.3)	2 (66.7)
Sample obtained, n (%)						
Healthy screened	301 (71.7)	301 (98.3)	0 (0)	303 (100)	300 (100)	3 (100)
Hospitalised (non-COVID respiratory disease)	2 (0.5)	2 (0.7)	0 (0)	0 (0)	0 (0)	0 (0)
Outpatient	117 (27.9)	3 (1.0)	114 (100)	0 (0)	0 (0)	0 (0)
Days between PCR test and sampling, days, median (IQR)	0 (2)	0 (1)	2 (1)	0 (0)	0 (0)	0 (0)
Symptoms, n (%)						
Asymptomatic	304 (72.4)	297 (97.1)	7 (6.1)	293 (96.7)	291 (97.0)	2 (66.7)
Respiratory infection	116 (27.6)	9 (2.9)	107 (93.9)	10 (3.3)	9 (3.0)	1 (33.3)
Days between start of symptoms and sampling, days, median (IQR)	4 (3)	3 (17)	4 (3)	NA	NA	NA
SARS-CoV-2 variant*, n (%)						
Wild-type†	62 (14.8)	NA	62 (54.4)	2 (0.7)	NA	2 (66.7)
Variant	28 (6.7)	NA	28 (24.6)	1 (0.4)	NA	1 (33.3)
Alpha	25 (6.0)	NA	25 (21.9)	1 (0.4)	NA	1 (33.3)
Beta	1 (0.2)	NA	1 (0.9)	0	NA	0
Alpha or beta	2 (0.5)	NA	2 (1.8)	0	NA	0
Unknown	24 (5.7)	NA	24 (21.1)	0	NA	0
Chronic disease, n (%)						
Asthma, allergy	28 (6.7)	16 (5.2)	12 (10.5)	19 (6.3)	18 (6.0)	1 (33.3)
Cancer	7 (1.7)	2 (0.7)	5 (4.4)	1 (0.3)	1 (0.3)	0 (0)
Hypertension	22 (5.2)	14 (4.6)	8 (7.0)	25 (8.3)	25 (8.3)	0 (0)
Diabetes	11 (2.6)	6 (2.0)	5 (4.4)	8 (2.6)	8 (2.7)	0 (0)
Migraine	3 (0.7)	2 (0.7)	1 (0.9)	3 (1.0)	3 (1.0)	0 (0)

\*SARS-CoV-2 variant status was determined using S-Gene Target Failure (for alpha), N501Y Mutation PCR (for alpha or beta) and/or gene sequencing (for beta and some alphas) combined with epidemiological information (first alpha variant cases were detected 18 December in Finland).  
†Wild-type refers to Wuhan-like lineages.

before starting operational work, the dogs were further coached in the purpose-built cubicle at the Helsinki-Vantaa International Airport (figure 1).

## Part II: Validation

For the validation study, we selected the four dogs working at the airport during the study period. The conduct followed the detailed Helsinki University Scent detection validation protocol (online supplemental notes). Each dog was presented with an identical set of 420 parallel novel randomised samples, including 114 positives (27%) and 306 negatives (73%; table 2), in 140 fixed three-sample tracks, provided over seven validation trial sessions (VAL1–7). Of the 140 tracks, 26 (18.6%)

were randomised as not containing positive samples. The session and track order were not disclosed to personnel and varied by dog.

Overall, the diagnostic accuracy of all samples sniffed was 92% (95% CI 90% to 93%). The combined sensitivity  $Se_{sniff}$  and specificity  $Sp_{sniff}$  for all four dogs was 92% (95% CI 89% to 94%) and 91% (89%–93%), respectively (for un-sniffed samples and positive and negative predictive values, see table 3). Only minor variation was seen between the dogs: the best performance reached 93% (95% CI 85% to 96%) for  $Se$  and 95% (91% to 97%) for  $Sp$ , and the lowest 88% (80% to 94%) and 90% (85% to 93%), respectively. To obtain  $Se$  and  $Sp$  values for

**Table 3** The diagnostic performance of the scent dogs in the triple-blind validation test

Dog	Dogs' indication	Sniffed RT-PCR positive samples	Sniffed RT-PCR negative samples	Sniffed samples/all presented samples	Sniffed samples (% from all samples)	Se <sub>sniff</sub> * (95% CI)	Sp <sub>sniff</sub> † (95% CI)	PPV <sub>sniff</sub> ‡ (95% CI)	NPV <sub>sniff</sub> § (95% CI)	Se <sub>all</sub> ¶ (95% CI)	Sp <sub>all</sub> ‡ (95% CI)
Sija	Positive	998	11	107/114	324 (77)	93% (85% to 96%)	95% (91% to 97%)	90% (82% to 95%)	96% (92% to 98%)	87% (79% to 92%)	96% (93% to 98%)
	Negative	206	206	217/306							
Rele	Positive	1047	18	111/114	326 (78)	94% (87% to 97%)	92% (87% to 95%)	85% (77% to 91%)	97% (93% to 98%)	91% (84% to 95%)	94% (91% to 96%)
	Negative	197	197	215/306							
Kosti	Positive	998	23	107/114	333 (79)	93% (85% to 96%)	90% (85% to 93%)	81% (73% to 87%)	96% (92% to 98%)	87% (79% to 92%)	92% (89% to 95%)
	Negative	203	203	226/306							
E.T.	Positive	90	23	102/114	326 (78)	88% (80% to 94%)	90% (85% to 93%)	80% (71% to 86%)	94% (90% to 97%)	79% (70% to 86%)	92% (89% to 95%)
	Negative	12	201	224/306							
All dogs	Positive	392	75	427/456	1309 (78)	92% (89% to 94%)	91% (89% to 93%)	84% (81% to 87%)	96% (94% to 97%)	86% (82% to 89%)	94% (92% to 95%)
	Negative	35	807	882/1224							

\*Se<sub>sniff</sub>, sensitivity on sniffed samples only.  
 †Sp<sub>sniff</sub>, specificity on sniffed samples only.  
 ‡PPV<sub>sniff</sub>, positive predictive value on sniffed samples. Based on the prevalence rate of COVID-19 positive samples in our data (27%).  
 §NPV<sub>sniff</sub>, negative predictive value on sniffed samples. Based on the prevalence rate of COVID-19 positive samples in our data (27%).  
 ¶Se<sub>all</sub>, sensitivity on all randomised samples; 10. Sp<sub>all</sub>, specificity on all randomised samples.  
 ‡RT-PCR, reverse transcriptase-polymerase chain reaction.

detecting wild-type samples only, we used the data from VAL1–2 where no alpha variants had emerged, separately: the overall accuracy was 97% (95% CI 95% to 98%), the Se 99% (96% to 100%) and the Sp 96% (93% to 98%). The figures for each dog's individual validation session are provided in online supplemental table 2).

Discrepancies (at least two dogs' results differing from the RT-PCR) were observed for 19/420 samples (table 4), 79% of them in VAL6–7, with samples gathered in late February–March 2021. Eight of the 19 samples were RT-PCR positive. Our re-evaluation of sample status (based on RT-PCR viral load, symptoms, time since symptom onset and antibody data) confirmed all these eight as SARS-CoV-2 positive, of which six were alpha variants, one not known, and one was wild-type. Of the 11 RT-PCR negative samples detected as positive by the dogs, six were confirmed as SARS-CoV-2 negative, four as uncertain and one as a possible positive.

Based on the prevalence rate of COVID-19 positive samples in our data (27%), the overall PPV and NPV were 83.9% (95% CI 80.8% to 86.7%) and 95.8% (94.4% to 96.9%), respectively (table 3). In a population with 40% prevalence, the PPV and NPV were calculated as 87.8% (95% CI 85.3% to 90.0%) and 94.4% (92.4% to 95.8%), respectively. In a population with a prevalence of 1% the PPV and NPV were 9.8% (8.1% to 12.0%) and 99.91% (99.88% to 99.93%), respectively.

Of the 114 positive COVID-19 samples, 30 were FN and 84 were TP. Failure to identify a COVID-19 positive sample was associated with the SARS-CoV-2 variant status (alpha vs wild-type; OR=14.0; 95% CI, 4.5 to 43.4; table 5): the dogs indicated correctly 89% of the confirmed wild-type samples but only 36% of the alpha variant samples. Based on the OR values with the 95% CI, gender, concurrent chronic disease, time between start of symptoms and sampling, time since PCR test and increasing age of patients were found not to be associated with failure to identify a COVID-19 positive samples (table 5). None of the ORs presented in table 5 were modified in bivariate analyses (data not shown).

### Part III: Real-life cohort

The dog identification and the RT-PCR result matched for 296/303 (97.7%) of the real-life samples of incoming passengers. The dogs correctly identified the samples as negative for 296/300 (98.7%) RT-PCR negative swabs. Table 6 provides details of the seven discrepant results. The dogs indicated three RT-PCR positive cases as negative. After re-evaluation with clinical and serological data, one was judged as SARS-CoV-2 negative, one as SARS-CoV-2 positive and one as a likely postinfectious positive RT-PCR result. Similarly, the dogs indicated four RT-PCR negative cases as positive. These were all judged as SARS-CoV-2 negative.

To maintain the dogs' screening skills in this low prevalence (0.47%) setting, a total of 155 novel RT-PCR positive 'spike' samples were provided to the dogs during working days (online supplemental table 3). They correctly indicated 98.7% of them as positive. Had the spike samples been calculated as part of the real-life study, the dogs' performance

**Table 4** Validation participants with a discrepancy between SARS-CoV-2 RT-PCR and the response from two dogs or more

Participants	Dog response	RT-PCR (viral load)	Symptoms	Time between symptom onset and skin swab/between RT-PCR test and skin swab, days	Antibody test (time between RT-PCR test and antibody test), days	Comment	SARS-CoV-2 infection status (variant*, if available)
VL1	Negative	Positive (medium)	Fever, rhinitis, diarrhoea	9/5	Positive (83)	Close relative PCR positive	Positive (alpha)
VL2	Negative	Positive (medium)	Headache, cough, muscle pain	4/3	NA†	Relative and close contact PCR positive	Positive (alpha)
VL3	Negative	Positive (low)	Asymptomatic	NA/5	NA	6-year-old child. Two relatives PCR positive	Positive (wild-type)‡
VL4	Negative	Positive (medium)	Fever, cough, loss of taste and smell, headache	9/5	Positive (48)	Relative PCR positive	Positive (alpha)
VL5	Negative	Positive (high)	Sore throat, headache fever	0/0	NA	11-year-old-child. Four relatives PCR positive	Positive (NA)
VL6	Negative	Positive (medium)	Cough, muscle pain, loss of taste and smell, headache	3/2	NA	Two relatives PCR positive	Positive (alpha)
VL7	Negative	Positive (medium)	Aches, tiredness, headache	3/2	Positive (108)	Close contact with PCR positive	Positive (alpha)
VL8	Negative	Positive (medium)	Tiredness, sore throat, muscle pain, headache, loss of taste and smell, diarrhoea	3/2	NA	Close contact with PCR positive	Positive (alpha)
VL9	Positive	Negative	Asymptomatic	NA/0	Positive (99)	Three PCR negative within 2 weeks	Possible positive
VL10	Positive	Negative	Asymptomatic	NA/3	NA	NA	Uncertain
VL11	Positive	Negative	Asymptomatic	NA/3	Negative (85)	Two PCR negative within 3 days	Negative
VL12	Positive	Negative	Asymptomatic	NA/0	Negative (72)	Three PCR negative within 5 days	Negative
VL13	Positive	Negative	Asymptomatic	NA/0	NA	PCR negative month after dog test.	Uncertain
VL14	Positive	Negative	Asymptomatic	NA/0	NA	NA	Uncertain
VL15	Positive	Negative	Asymptomatic	NA/0	NA	Two PCR tests negative within 3 days	Uncertain
VL16	Positive	Negative	Asymptomatic	NA/0	Negative (82)	Three PCR negative tests within 3 days	Negative
VL17	Positive	Negative	Asymptomatic	NA/0	Negative (95)	Two PCR negative tests within 3 days	Negative
VL18	Positive	Negative	Asymptomatic	NA/1	Negative (83)	Two PCR positive	Negative
VL19	Positive	Negative	Headache, cough	NA/2	Negative (68)	Two PCR positive	Negative

\*variant, SARS-CoV-2 variant status was determined using S-Gene Target Failure, N501Y Mutation PCR and/or gene sequencing combined with epidemiological information (first alpha variant cases were detected 18 December in Finland).  
 †NA, not available.  
 ‡Wild-type, refers to Wuhan like non-VoC lineages.  
 RT-PCR, reverse transcriptase-polymerase chain reaction.



**Table 5** Univariate analysis of associations between variables and failure to identify COVID-19 positive samples

Variables suspected to be associated with the dog's performance	OR*	95% CI†
Alpha variant (vs wild-type)	14.0	4.5 to 43.4
Presence of COVID-19 symptoms	2.2	0.3 to 19.3
Female (vs male)	0.8	0.3 to 1.8
Concurrent chronic disease	1.0	0.4 to 2.9
Days between start of symptoms and sampling (days)	1.0	0.8 to 1.2
Days between PCR test and sampling (days)	1.1	0.8 to 1.5
Age‡		
30	1.0	0.7 to 1.3
40 (reference)	1	
50	0.7	0.4 to 1.3
60	0.5	0.1 to 1.7

\*OR, Odds Ratio.  
 †CI, confidence interval, significant only when not including the number one.  
 ‡Age was included by using restricted cubic spline functions (see text for details).

would have reached a sensitivity of 97% (95% CI 92% to 99%) and a specificity of 99% (96% to 100%).

In the operational real-life setup, we also used five non-validated dogs. Their results closely accorded with those of the validated dogs (data not shown).

**DISCUSSION**

Our study demonstrates that, in comparison with RT-PCR, scent detection dogs can be trained to identify SARS-CoV-2-infected individuals from skin swab samples with high diagnostic accuracy. In our real-life setting with a very low prevalence, the performance in identifying negative samples was very good (98.7%). Unfortunately, because of a low number of confirmed positive cases, accuracy with respect to positive samples could not be reliably assessed. However, ad hoc analysis also calculating the positive spike swabs showed a real-life performance of 98.5% for detecting positive samples. Below we discuss separately each of the three parts of the study.

**Part I: Training of dogs**

To keep the training short, we used dogs with previous scent work experience. Unlike studies conducted only in laboratory settings,<sup>13-17</sup> we included two phases: initial training at a training centre, and—once the dogs were qualified—training in a challenging environment (Helsinki-Vantaa International Airport). Only one of nine dogs did not show high motivation for working in the test cubicle.

**Part II: Validation test**

Our validation experiment showed a high diagnostic accuracy with 92% sensitivity and 91% specificity. Several previous studies suggest that scent dogs can distinguish between samples from SARS-CoV-2-infected and uninfected individuals (reviewed in online supplemental table 1). However, although they demonstrate

**Table 6** Real-life cohort participants with a discrepancy between SARS-CoV-2 RT-PCR and dog response

Participants	Dog response	RT-PCR (viral load)	Symptoms	Time between symptom onset and skin swab/ between RT-PCR test and skin swab, days	Antibody test result (time between RT-PCR test and antibody test, days)	Comment	SARS-CoV-2 infection status (variant*, if available)
RL1	Negative	Positive (medium)	Asymptomatic	NA†/0	Negative (81)	Two additional negative PCR tests	Negative (wild-type)‡
RL2	Negative	Positive (high)	Muscle aches, headache, fever	1/0	Positive (57)		Positive (alpha)
RL3	Negative	Positive (medium)	Asymptomatic	-10/0	Positive (56)	Fever, cough, dyspnoea, headache 10 days before tests	Postinfectious prolonged PCR positivity (wild-type)
RL4	Positive (two dogs)	Negative	Asymptomatic	NA/0	Negative (178)	Negative scent dog test and PCR-test within 1 month	Negative
RL5	Positive/Negative (two dogs)	Negative	Asymptomatic	NA/0	Negative (97)		Negative
RL6	Positive (two dogs)	Negative	Chest pain, cough, tachycardia, fever	1/0	Negative (113)	Second PCR test negative 4 days after initial test	Negative
RL7	Positive	Negative	Sore throat	-5/0	Negative (55)		Negative

\*Variant, SARS-CoV-2 variant status was determined using S-Gene Target Failure, N501Y Mutation PCR and/or gene sequencing combined with epidemiological information (first alpha variant cases were detected 18 December in Finland).  
 †NA, not available.  
 ‡Wild-type, refers to Wuhan like non\_VoC lineages.  
 RT-PCR, reverse transcriptase-polymerase chain reaction.

the dogs' diagnostic accuracy, these previous proof-of-concept studies<sup>13–17</sup> had some limitations: small samples sizes,<sup>13 16 17</sup> repeated use of the same samples,<sup>15</sup> use of inactivated samples,<sup>13 14 16</sup> use of empty cans or clean gauze swabs as controls<sup>15 16</sup> and conducting validation tests only in laboratory settings.<sup>13–17</sup> Perhaps even more importantly, in those studies almost all samples were collected from hospitals,<sup>13 15–17</sup> failing to cover the actual target population, outpatients. Alternatively, positive samples were from hospitals and controls from outside hospitals—potentially misleading the dogs to identify hospital-associated odours as positive cues. Indeed, scent dog guidelines advise to watch out for systematic differences between positive and control samples.<sup>25</sup> Apart from these published proof-of-concept studies, some non-peer reviewed preprints provide further data<sup>26</sup>: Guest *et al* collected 400 odour samples from patients with asymptomatic or mild COVID-19 and demonstrated in a randomised double-blind trial under laboratory conditions with six dogs a sensitivity range of 82%–94% and a specificity range of 76%–92%.

Based on the overall Se and Sp (92% and 91%, respectively), we calculated PPV and NPV according to two infection probability scenarios reflecting the prevalence of 40% and 1%. For a population with a prevalence of 40%, we estimated a PPV of 87.8% and a NPV of 94.4%. This means that the information provided by the dog (marking or not marking) increases the chances of detection to around 90%. For a population with a prevalence of 1%, by contrast, we estimated a PPV of 9.8% and an NPV of 99.9%. In both scenarios, high NPV supports the use of dogs for screening to exclude individuals not needing RT-PCR. We therefore suggest that dogs could be used both in sites of high SARS-CoV-2 prevalence, such as hospitals (to prescreen patients and personnel), as well as in low prevalence sites such as airports or ports (to prescreen passengers). Such prescreening could save considerably both time and PCR testing resources.

Our study design overcomes some of the major limitations of the previous studies: our sample size was based on a power calculation, our validation experiment was conducted outside laboratory conditions and our samples were collected in a random fashion as four parallel swabs, each used only once. We collected positive and negative swabs from both asymptomatic and symptomatic outpatients, children and seniors, and those with non-communicable diseases, and included samples collected during early and late phases of the disease. Unlike the previous validation studies, we randomly included tracks with no positive samples. This mimics better the real-life situation in low-prevalence settings.

In univariate analysis, the only variable strongly associated with failure to identify COVID-19 positive samples was the alpha variant (table 5). Indeed, according with the epidemiological situation in our country,<sup>20</sup> the virus variants started to emerge only at the end of our validation sample collection period, with 59% of the positive samples in VAL6–7 confirmed to represent virus variants

(mostly alpha) and only 3% the wild-type virus (the virus type of the others remained unknown). Importantly, the dogs had only been trained to detect samples of patients infected by the wild-type virus. The emergence of the new variants presumably explains the less successful performance by the dogs towards the end of the study period. In the bivariate analyses, after adjustment for all other variables possibly associated with the dogs' performance, the association between variant type and detection failure remained as strong as in the univariate analysis. Naturally, we cannot rule out confounding effects of other variables than the ones we investigated. Interestingly, Guest *et al* also had a small amount of alpha variant samples in their dataset. Their dogs correctly identified 38/48 (79%) of the alpha variant samples, the rate remaining lower than for the wild-type virus.<sup>26</sup> The difference was not significant, yet as their study was not designed to investigate the variants, it might have lacked statistical power. In our investigation the difference was highly significant according to the OR and its 95% CI, as the dogs correctly indicated 55/62 (89%) of the confirmed wild-type samples, but only 9/25 (36%) of the alpha variant samples. Thus, while the dogs indicated the alpha variant samples, their performance was lower than with the wild-type virus. Indeed, this observation is remarkable as it proves the scent dogs' robust discriminatory power. The obvious implication is that training samples should cover all epidemiologically relevant variants. Our preliminary observations suggest that dogs primed with one virus type can in a few hours be retrained to detect its variants (data not shown).

Another aspect to discuss is the low number of asymptomatic sample donors, which could have hampered the evaluation of the scent dogs' performance with samples from such individuals. In fact, the performance related to asymptomatic subjects is of particular importance, since in a real-world screening most individuals are asymptomatic. However, as we collected four samples from each of the sample donors, we ended up with 28 tests with samples from asymptomatic individuals. Only one was incorrectly identified as negative and two were left unsniffed. Thus 25/28 (89.3%) were correctly identified as positive. In our analysis lack of symptoms was not associated with poorer performance.

Finally, since dogs may become tired or unfocused when working long hours, we ran the validation tests randomly in varying order over seven working days for each dog. Like in previous studies,<sup>14 15</sup> all dogs did not perform equally. The differences were surprisingly small, however, particularly considering that the dog with the lowest results, E.T, was diagnosed with parotitis during her validation study, yet also her less successful days prior to diagnosis were included in her data. The low inter-dog variability observed in our study originates most probably from the consistent high-quality training performed both in the training centre and at the airport.



### Part III: real-life air passenger study

While the validation experiment was successful, the real-life study at the airport met with some adversity. Although the dogs identified 98.7% of the negative samples as negative, they indicated four RT-PCR negatives as positives and did not identify three RT-PCR positive cases. Re-evaluations (the time span between symptom onset and sampling for RT-PCR, clinical symptoms, viral loads as cycle threshold counts and SARS-CoV-2 antibodies) of the RT-PCR positive cases suggested, however, that only one of the three represented the targeted group of early and potentially infectious cases. One of the RT-PCR positive individuals failed to seroconvert, suggesting a false-positive RT-PCR result. The samples of another three RT-PCR positive individuals had been collected as late as 10 days after symptom onset, presumably indicating a postinfectious positive RT-PCR result. Interestingly, the virus in the single verified case was identified as an alpha variant, possibly reflecting the dogs' lower sensitivity to detect it.

A major difference between the real-life and validation studies was seen in the rate of positive samples, which was over 50-fold lower in the real-life study than in validation (0.47% vs 27% of all samples)—that is, the dogs would have got only one positive sample to sniff each week at the most. Anticipating a low prevalence, the dogs' skills were kept up by providing them with a total of 155 novel (not sniffed by any dog), positive 'spike' samples over their shifts. Had these spike samples been included in the real-life study, the prevalence would have been 34%, not differing from that in the validation study, thus confirming the methods' potential for screening SARS-CoV-2 carriers. Similarly to any other diagnostic or screening tests, positive controls are needed to validate their accuracy. With the dogs, these spike samples serve as controls and also act as rewards, reinforcing the detection. In a low-prevalence setting, the use of spike samples needs to be preplanned before implementing scent dogs in the operational work. Of note, collection of spike samples from patients may no longer be needed in the future, as preliminary data suggest that spike material can be produced in the laboratory.<sup>27</sup>

### Limitations of the study

Some limitations deserve to be discussed. First, scent dogs previously trained to detect other substances such as drugs may also mark them, and the dog handler may record the marking falsely as positive for COVID-19. In this study, samples with false indications were not studied for narcotics and dangerous goods—that is, odours with which the three dogs were previously familiar.

Second, the age of the samples varied. The samples used in training and validation, as well as the 'spike' samples were older than in the real-life study, for they had to be verified before use: in the real-life operational setting, the samples were freshly collected and immediately presented to the dogs. We acknowledge that storage might have affected the VOCs.<sup>28</sup> Further studies have

been started to determine the precise nature of COVID-19-specific VOCs.

Third, the validation test also had some limitations. The low number of positive samples available led to a lack of tracks with multiple positive samples. This should not have had any greater effect on the results, as the dogs had practised both with blank tracks and tracks with multiple positive samples.

Finally, since variants did not emerge in Finland at the time of training, only wild-type samples were used. Many of the discrepant results were associated with the new variant. In the future, operational work skills should be kept up by simultaneous training with samples of emerging virus variants. Fortunately, once the dogs have received the basic training, retraining to cover new variants is expected to be easy as discussed above.

### CONCLUSION

Employing a triple-blinded validation study setup, we provided evidence that trained scent dogs can master detection of samples from individuals infected with SARS-CoV-2 with good diagnostic accuracy. Interestingly, trained using samples only from individuals who had contracted the wild-type virus, the dogs' performance declined with samples of the variant era. We also provided some evidence that dogs can be trained to work at an international airport where large-scale rapid screening of crowds in a short period of time is required. In the real-life setting, we verified the results from our validation study for negative samples, but the dogs' ability to detect positive samples could not be confirmed owing to low prevalence of positive individuals. Ad hoc analysis also taking into account the positive spike samples, however, yielded convincing accuracy among the real-life cohort.

### Author affiliations

<sup>1</sup>Meilahti Vaccine Research Center, MeVac, Department of Infectious Diseases, University of Helsinki and Helsinki University Hospital, Helsinki, Finland

<sup>2</sup>Human Microbiome Research Program, Faculty of Medicine, University of Helsinki, Helsinki, Finland

<sup>3</sup>Department of Pulmonary Medicine, Heart and Lung Center, Helsinki University Hospital and University of Helsinki, Helsinki, Finland

<sup>4</sup>School of Pharmacy, Faculty of Health Sciences, University of Eastern Finland, Kuopio, Finland

<sup>5</sup>Nose Academy Ltd, Kuopio, Finland

<sup>6</sup>Department of Equine and Small Animal Medicine, University of Helsinki, Helsinki, Finland

<sup>7</sup>HUS Diagnostic Center, HUSLAB, Clinical Microbiology, Helsinki University Hospital and University of Helsinki, Helsinki, Finland

<sup>8</sup>Department of Biostatistics and Clinical Epidemiology, Ecole nationale vétérinaire d'Alfort, Maisons-Alfort, France

<sup>9</sup>Departments of Virology and Veterinary Biosciences, University of Helsinki, Helsinki, Finland

**Acknowledgements** The authors thank all scent dogs, dog handlers, trainers and study personnel who contributed to the study, particularly Ville Saksa, Eliisa Kekäläinen, Jaakko Kulonpalo, Sointu Mero, Simo Miettinen, Taru Miller, Suvi Kuivainen from Helsinki University Hospital and UH; the dog-handlers and assistants at the airport, Susanna Paavilainen, Anette Kare, Terhi Käppi, Marika Nöjd, Heli Niuro, Oona Pyykkö, Egil Björkman, Tanja Tall and Johanna Laitsaari; those collecting and handling the samples at Wise Nose Tuomas Stenius, Annika Tiainen, Kristiina Luostarinen, Jon Mäkinen, Maiju Heikkinen, Ja Akkanen; as well as dog

trainer Tommy Wiren. We also thank the external controller Lauri Kanerva for his continuous participation in the validation trials. Finally, our most sincere thanks go to the scent dogs that we worked with in this project, and to all the volunteers who provided and delivered the samples used in the training, the validation test and the clinical application.

**Contributors** Study plan: AK, EH, LD, AH-B; ethics approval: AK, SHP, AP; sample acquisition: AK, JP, ST, SHP, AP, AH-B; laboratory analyses: OV, ML; statistical analysis: LD, AH-B; data curation: JP, ST, LI, EH, AH-B; funding acquisition: AK, OV, AH-B; supervision and project administration: AK, AH-B; writing of original draft: AK, JP, ST, AH-B; critical comments: OV; guarantor: AK, AH-B; review and approval of the final manuscript: AK, JP, ST, SHP, AP, LI, EH, LD, OV, AH-B.

**Funding** This study was supported by the veterinary clinic chain Evidensia, The Swedish Cultural Foundation in Finland (grant 138527), The Finnish Kennel Club, and The Finnish Cultural Foundation (grant 70287). The RT-PCR and antibody analyses were supported by the Finnish Cultural Foundation, the Finnish Governmental Subsidy for Health Science Research (TYH 2018322), the Finnish Medical Association, Jane and Aatos Erkkö Foundation and the Academy of Finland (grants 1336490, 336 439 and 335527). The open access funded by Helsinki University Library. The funders of the study had no role in study design, data collection, data analysis or writing of the report.

**Competing interests** All authors have completed the ICMJE uniform disclosure form at <http://www.icmje.org/disclosure-of-interest/> and declare: no support from any organisation for the submitted work; no financial relationships with any organisations that might have an interest in the submitted work in the previous 3 years; no other relationships or activities that could appear to have influenced the submitted work.

**Patient and public involvement** Patients and/or the public were not involved in the design, or conduct, or reporting, or dissemination plans of this research.

**Patient consent for publication** Not applicable.

**Ethics approval** The study was part of a larger COVID-19 research protocol approved by the Helsinki University Hospital ethics committee (HUS/1238/2020). A research permit was obtained from the local authorities at HUH (HUS/157/2020) and Vantaa City (VD/8473/13.00.00/2020). All the participants provided written informed consent.

**Provenance and peer review** Not commissioned; externally peer reviewed.

**Data availability statement** Data are available upon reasonable request. All data relevant to the study are included in the article or uploaded as supplementary information. All data relevant to the study are included in the article or uploaded as supplementary information. Additional data are available upon reasonable request. Films are available through a link provided in the manuscript.

**Supplemental material** This content has been supplied by the author(s). It has not been vetted by BMJ Publishing Group Limited (BMJ) and may not have been peer-reviewed. Any opinions or recommendations discussed are solely those of the author(s) and are not endorsed by BMJ. BMJ disclaims all liability and responsibility arising from any reliance placed on the content. Where the content includes any translated material, BMJ does not warrant the accuracy and reliability of the translations (including but not limited to local regulations, clinical guidelines, terminology, drug names and drug dosages), and is not responsible for any error and/or omissions arising from translation and adaptation or otherwise.

**Open access** This is an open access article distributed in accordance with the Creative Commons Attribution Non Commercial (CC BY-NC 4.0) license, which permits others to distribute, remix, adapt, build upon this work non-commercially, and license their derivative works on different terms, provided the original work is properly cited, appropriate credit is given, any changes made indicated, and the use is non-commercial. See: <http://creativecommons.org/licenses/by-nc/4.0/>.

#### ORCID ID

Anu Kantele <http://orcid.org/0000-0002-0004-1000>

## REFERENCES

- Sayampanathan AA, Heng CS, Pin PH, *et al*. Infectivity of asymptomatic versus symptomatic COVID-19. *Lancet* 2021;397:93–4.
- Surkova E, Nikolayevskyy V, Drobniewski F. False-positive COVID-19 results: hidden problems and costs. *Lancet Respir Med* 2020;8:1167–8.
- Woloshin S, Patel N, Kesselheim AS. False negative tests for SARS-CoV-2 Infection - challenges and implications. *N Engl J Med* 2020;383:e38.
- Tang Y-W, Schmitz JE, Persing DH, *et al*. Laboratory diagnosis of COVID-19: current issues and challenges. *J Clin Microbiol* 2020;58:1–9.
- Angle TC, Passler T, Waggoner PL, *et al*. Real-time detection of a virus using detection dogs. *Front Vet Sci* 2016;3:1–6.
- Jones RT, Guest C, Lindsay SW, *et al*. Could bio-detection dogs be used to limit the spread of COVID-19 by travellers? *J Travel Med* 2020;27:1–3.
- Walker DB, Walker JC, Cavnar PJ, *et al*. Naturalistic quantification of canine olfactory sensitivity. *Appl Anim Behav Sci* 2006;97:241–54.
- Angle C, Waggoner LP, Ferrando A, *et al*. Canine detection of the volatome: a review of implications for pathogen and disease detection. *Front Vet Sci* 2016;3:1–7.
- Abd El Qader A, Lieberman D, Shemer Avni Y, *et al*. Volatile organic compounds generated by cultures of bacteria and viruses associated with respiratory infections. *Biomed Chromatogr* 2015;29:1783–90.
- Maurer M, McCulloch M, Willey AM, *et al*. Detection of bacteriuria by canine olfaction. *Open Forum Infect Dis* 2016;3:1–6.
- Bomers MK, van Agtmael MA, Luijk H, *et al*. Using a dog's superior olfactory sensitivity to identify *Clostridium difficile* in stools and patients: proof of principle study. *BMJ* 2012;345:e7396–8.
- Guest C, Pinder M, Doggett M, *et al*. Trained dogs identify people with malaria parasites by their odour. *Lancet Infect Dis* 2019;19:578–80.
- Jendryn P, Schulz C, Twele F, *et al*. Scent dog identification of samples from COVID-19 patients - a pilot study. *BMC Infect Dis* 2020;20:1–7.
- Jendryn P, Twele F, Meller S, *et al*. Scent dog identification of SARS-CoV-2 infections in different body fluids. *BMC Infect Dis* 2021;21:1–14.
- Grandjean D, Sarkis R, Lecoq-Julien C, *et al*. Can the detection dog alert on COVID-19 positive persons by sniffing axillary sweat samples? A proof-of-concept study. *PLoS One* 2020;15:e0243122–19.
- Essler JL, Kane SA, Nolan P, *et al*. Discrimination of SARS-CoV-2 infected patient samples by detection dogs: a proof of concept study. *PLoS One* 2021;16:e0250158–14.
- Eskandari E, Ahmadi Marzaleh M, Roudgari H, *et al*. Sniffer dogs as a screening/diagnostic tool for COVID-19: a proof of concept study. *BMC Infect Dis* 2021;21:1–8.
- Rusanen J, Kareinen L, Levanov L, *et al*. A 10-minute "mix and read" antibody assay for SARS-CoV-2. *Viruses* 2021;13:143.
- Truong Nguyen PT, Plyusnin I, Sironen T, *et al*. HAVoC, a bioinformatic pipeline for reference-based consensus assembly and lineage assignment for SARS-CoV-2 sequences. *BMC Bioinformatics* 2021;22:373.
- Kant R, Nguyen PT, Blomqvist S, *et al*. Incidence trends for SARS-CoV-2 alpha and beta variants, Finland, spring 2021. *Emerg Infect Dis* 2021;27:3137–41.
- Rosner B. *Fundamentals of biostatistics*. 8th edn, 2016: 249–59.
- Trevethan R. Sensitivity, specificity, and predictive values: foundations, Pliabilities, and pitfalls in research and practice. *Front Public Health* 2017;5:p. 307.
- Altman DG, Bland JM. Diagnostic tests 2: predictive values. *BMJ* 1994;309:102.
- Desquilbet L, Mariotti F. Dose-response analyses using restricted cubic spline functions in public health research. *Stat Med* 2010;29:n/a–57.
- Edwards TL, Browne CM, Schoon A, *et al*. Animal olfactory detection of human diseases: guidelines and systematic review. *Journal of Veterinary Behavior* 2017;20:59–73.
- Guest C, Dewhurst SY, Allen DJ. Using trained dogs and organic semi-conducting sensors to identify asymptomatic and mild SARS-CoV-2 infections. Available: <https://www.ishtm.ac.uk/research/centres-projects-groups/using-dogs-to-detect-covid-19#results>
- Mendel J, Frank K, Edlin L, *et al*. Preliminary accuracy of COVID-19 odor detection by canines and HS-SPME-GC-MS using exhaled breath samples. *Forensic Sci Int Synerg* 2021;3:100155.
- Forbes SL, Rust L, Trebilcock K, *et al*. Effect of age and storage conditions on the volatile organic compound profile of blood. *Forensic Sci Med Pathol* 2014;10:570–82.





## **SOILE TURUNEN**

---

Diseases cause changes in the body's soluble and volatile metabolites which can be studied by analytical and sensory methods. This thesis aimed to explore the ability of these methods to differentiate between healthy individuals and diseased based on non-invasive samples. A mass spectrometry-based metabolomics revealed changes in salivary metabolites in patients with Primary Sjögren's Syndrome. Furthermore, scent detection dogs detected SARS-CoV-2 infected from skin swabs with high accuracy. Overall, this thesis demonstrates the effectiveness of both methods in the discriminative task using non-invasive samples.



UNIVERSITY OF  
EASTERN FINLAND

**uef.fi**

**PUBLICATIONS OF  
THE UNIVERSITY OF EASTERN FINLAND**  
Dissertations in Health Sciences

ISBN 978-952-61-5227-1  
ISSN 1798-5706